RELIABILITY-BASED INSPECTION PLANNING WITH APPLICATION TO DECK STRUCTURE THICKNESS MEASUREMENT OF CORRODED AGING TANKERS

by

Jinting Guo

A dissertation submitted in partial fulfillment
of the requirements for the degree of
Doctor of Philosophy
(Naval Architecture and Marine Engineering)
in The University of Michigan
2010

Doctoral Committee:

Associate Professor Anastassios N. Perakis, Chair
Professor Will Hansen
Professor Nickolas Vlahopoulos
Ge Wang, American Bureau of Shipping

To my parents
Fengkang Guo and Niane Cai
and my wife
Eeteng Khoo

ACKNOWLEDGEMENTS

First, I would like to thank the Department of Naval Architecture and Marine Engineering at the University of Michigan for providing a fellowship for the majority of this work. Without financial support, I would never have had the chance to pursue my doctoral degree in the United States of America.

I would like to give my grateful and sincere thanks to my advisor, Professor Anastassios N. Perakis, for his support, encouragement, and patience throughout this research and my graduate studies at the University of Michigan. His wisdom and expertise has made a deep impression on me. His inspiration will benefit me my whole life.

I owe special thanks to Dr. Ge Wang for giving me consistent guidance and advice during my research. The long hours he dedicated are highly appreciated. I also would like to thank Professor Will Hansen and Professor Nickolas Vlahopoulos, for being members of my committee for their technical help and expertise.

Many people from the American Bureau of Shipping have contributed to my work, either by providing guidance or support. I am very grateful to Dr. Lyuben Ivanov and Dr. Nianzhong Chen for their insightful comments. Thanks to Jim Speed, Donna Browning and Smarty John for improving the manuscript. Gratitude is also due to my colleagues in the Offshore Engineering Department and Corporate Operational Safety and Evaluation Department of the American Bureau of Shipping.

Also, I would like to acknowledge a number of my friends in Houston and at the University of Michigan. Thank you for giving me so many memorable moments.

Finally, I must express my deepest gratitude and warmest thanks to my parents, my wife, and my son. Without their love, encouragement, patience, and support, this dissertation would have never been completed.

TABLE OF CONTENTS

DEDICATION ……..……..ii

ACKNOWLEDGEMENTS iii

LIST OF FIGURES ix

LIST OF TABLES xiv

LIST OF ABBREVIATIONS xvii

LIST OF SYMBOLS xix

ABSTRACT ……..…….xxiii

CHAPTER 1 INTRODUCTION 1

1.1 Background 1

1.1.1 Current Practice of Hull Inspections 3

1.1.2 Reliability-Based Inspection Planning for Marine Structures 7

1.1.3 Structural Reliability Analysis on Ship Structures 8

1.1.4 Analyzed Deck Panels 11

1.2 Objective 13

1.3 Organization 14

CHAPTER 2 RELIABILITY-BASED INSPECTION PROCEDURE 17

2.1 Introduction 17

2.2 Evaluation of Time-Variant Reliability of a Tanker's Deck Panels 19

2.2.1 Limit State Function 20
2.2.2 Compressive Stress of Deck Panel 21
2.2.3 Ultimate Strength Prediction of the Deck Panels 23
2.2.4 Uncertainties and Their Measures 32
2.2.5 Time-Variant Evaluation 35
2.2.6 Prediction of Time-Variant Failure Probability 38
2.3 Target Levels of Failure Probability 43
2.4 Scheduling Thickness Measurements 49
2.5 Summary 53
CHAPTER 3 PROBABILISTIC CAPACITY PREDICTION FOR DECK PANELS OF TANKERS 54
3.1 Introduction 54
3.2 Previous Studies on Strength Model 54
3.2.1 Unstiffened Plate Panel 55
3.2.2 Stiffened Panel 57
3.3 Uncertainties of Ultimate Strength Prediction 60
3.3.1 General 60
3.3.2 Uncertainty Analysis 62
3.3.3 Results 65
3.4 Uncertainties in the Material Properties of Steels for Shipbuilding 67
3.4.1 Uncertainties in Young's Modulus 67
3.4.2 Uncertainties in Yield Stress 68
3.4.3 Uncertainties Due to Manufacturing Tolerance in Shipbuilding 70
3.5 Summary 73

CHAPTER 4 PROBABILISTIC MODELING OF LOADS ON DECK PANELS 74

4.1 Introduction 74

4.2 Modeling Still-Water Bending Moment 75

4.2.1 Previous Studies 75

4.2.2 Uncertainty Analysis 77

4.2.3 Probabilistic Model 79

4.3 Modeling Wave-Induced Bending Moment 81

4.3.1 Previous Studies 81

4.3.2 Uncertainty Analysis 83

4.3.3 Probabilistic Model 86

4.4 Load Combinations 88

4.5 Summary 93

CHAPTER 5 DEVELOPMENT OF A TIME-VARIANT PROBABILISTIC CORROSION MODEL – APPLICATION TO DECK LONGITUDINAL PANELS OF TANKERS 95

5.1 Introduction 95

5.2 Previous Research on Corrosion Models 95

5.2.1 Conventional (Linear/Steady-state) Models 96

5.2.2 Nonlinear Deterministic Models 97

5.2.3 Non-Linear Probabilistic Models 100

5.2.4 Phenomenological Model 104

5.3 Development of a New Probabilistic Corrosion Model 105

5.3.1 Modeling Description 107

5.3.2 Data Analysis 107

5.3.3 Prediction of Corrosion Wastage 115
5.3.4 Comparison Study 133
5.4 Summary 134
CHAPTER 6 APPLICATION AND RESULTS 136
6.1 Introduction 136
6.2 Reliability Assessment for Sample Tankers 136
6.2.1 Sample Tankers 136
6.2.2 Calculation of Failure Probability by Monte Carlo Simulation 137
6.2.3 Convergence of Simulation 140
6.2.4 Sensitivity Analysis 142
6.2.5 Analysis Results 148
6.3 Determination of the Target Reliability Levels 157
6.4 Determination of Inspection Intervals 159
6.5 Summary 160
CHAPTER 7 CONTRIBUTIONS AND FUTURE WORK 163
7.1 Contributions 163
7.2 Future Work 166
BIBLIOGRAPHY 169

LIST OF FIGURES

Figure 1.1 Total losses by causes for all vessel types greater than 500 GT (1994~2008) (IUMI 2008) 1

Figure 1.2 Total losses of tankers greater than 500 GT (1999~2008) (IUMI 2008) 2

Figure 1.3 "Erika" sank off the French coast on December 12, 1999 (Source: www.cedre.fr) 2

Figure 1.4 Typical thirty-year gauging survey plan for oil tankers 6

Figure 1.5 A typical tanker's structures and a longitudinally stiffened deck panel ... 12

Figure 2.1 A reliability-based procedure for scheduling thickness measurement of the deck panel over a vessel's lifetime 18

Figure 2.2 Projection of failure probability of deck panels 20

Figure 2.3 Unstiffened plate panel model for uniaxial compression 24

Figure 2.4 Stiffened panel model for uniaxial compression 26

Figure 2.5 Stiffener cross sections 26

Figure 2.6 Schematic time-dependent reliability problem 41

Figure 2.7 Schematic equivalent time-independent reliability problem 43

Figure 2.8 Schematic 1^{st} and 2^{nd} inspection intervals in terms of deck panel's ultimate strength failure 50

Figure 2.9 Schematic corrosion models for updating after inspection 52

Figure 3.1 Comparison of selected formulations with test data for predicting the critical buckling stress of the unstiffend plate panel..... 64

Figure 3.2 Comparison of selected formulations with test data for predicting the ultimate strength of the unstiffened plate panel..... 65

Figure 3.3 The modeling uncertainty of the adopted ultimate strength formulations for unstiffend plate panel and stiffened panel..... 66

Figure 4.1 Seaborne crude oil trade map 2006 (Source: Lloyd's MIU)..... 85

Figure 5.1 Conventional corrosion wastage models 97

Figure 5.2 Corrosion model proposed by Guedes Soares & Garbatov (1999) 98

Figure 5.3 Corrosion model proposed by Qin & Cui (2002) 99

Figure 5.4 Corrosion model proposed by Ivanov et al. (2003) 100

Figure 5.5 Corrosion model proposed by Sun & Bai (2001) 102

Figure 5.6 Corrosion model proposed by Paik et al. (2003) 103

Figure 5.7 Corrosion model proposed by Melchers (2003) 105

Figure 5.8 As-built thickness of deck plates (cargo oil tanks) 108

Figure 5.9 As-built thickness of deck plates (ballast tanks)..... 109

Figure 5.10 As built thickness of upper deck longitudinal stiffener web plates (cargo oil tanks)..... 109

Figure 5.11 As-built thickness of upper deck longitudinal stiffener web plates (ballast tanks)..... 110

Figure 5.12 As-built thickness of upper deck longitudinal stiffener flanges (cargo oil tanks)..... 110

Figure 5.13 As-built thickness of upper deck longitudinal stiffener flanges (ballast tanks)..... 111

Figure 5.14 Scatter plot of corrosion wastage of deck plates (cargo oil tanks) 112

Figure 5.15 Scatter plot of corrosion wastage of deck plates (ballast tanks) 112

Figure 5.16 Scatter plot of corrosion wastage of upper deck longitudinal stiffener web plates (cargo oil tanks) 113

Figure 5.17 Scatter plot of corrosion wastage of upper deck longitudinal stiffener web plates (ballast tanks) 113

Figure 5.18 Scatter plot of corrosion wastage of upper deck longitudinal stiffener flanges (cargo oil tanks) 114

Figure 5.19 Scatter plot of corrosion wastage of upper deck longitudinal stiffener flanges (ballast tanks) 114

Figure 5.20 Derived equations of mean value and standard deviation of corrosion wastage of deck plates (cargo oil tanks) 117

Figure 5.21 Derived equations of mean value and standard deviation of corrosion wastage of deck plates (ballast tanks) 117

Figure 5.22 Derived equations of mean value and standard deviation of corrosion wastage of upper deck longitudinal stiffener web plates (cargo oil tanks) ……...118

Figure 5.23 Derived equations of mean value and standard deviation of corrosion wastage of upper deck longitudinal stiffener web plates (ballast tanks) 118

Figure 5.24 Derived equations of mean value and standard deviation of corrosion wastage of upper deck longitudinal stiffener flanges (cargo oil tanks) .. 119

Figure 5.25 Derived equations of mean value and standard deviation of corrosion wastage of upper deck longitudinal stiffener flanges (ballast tanks) 119

Figure 5.26 Comparative analysis of corrosion rate of upper deck structures 120

Figure 5.27 Histograms of corrosion wastage of deck plates for 22-year-old tankers (cargo oil tanks) 121

Figure 5.28 Histograms of corrosion wastage of deck plates for 20-year-old tankers (ballast tanks) 122

Figure 5.29 Histograms of corrosion wastage of upper deck longitudinal stiffener web plates for 22-year-old tankers (cargo oil tanks) 122

Figure 5.30 Histograms of corrosion wastage of upper deck longitudinal stiffener web plates for 21-year-old tanker (ballast tanks) 123

Figure 5.31 Histograms of corrosion wastage of upper deck longitudinal stiffener flanges for 19-year-old tankers (cargo oil tanks) 123

Figure 5.32 Histograms of corrosion wastage of upper deck longitudinal stiffener flanges for 18-year-old tankers (ballast tanks) 124

Figure 5.33 Annual probability density function of corrosion wastage prediction of deck plates in way of ballast tanks 126

Figure 5.34 Changes of Weibull parameters with ship's age for corrosion wastage prediction of deck plates 127

Figure 5.35 Changes of Weibull parameters with ship's age for corrosion wastage prediction of upper deck longitudinal stiffener web plates 128

Figure 5.36 Changes of Weibull parameters with ship's age for corrosion wastage prediction of upper deck longitudinal stiffener flanges 129

Figure 5.37 Time-variant probability density function of corrosion wastage of deck plates 130

Figure 5.38 Time-variant probability density function of corrosion wastage of upper deck longitudinal stiffener web plates 131

Figure 5.39 Time-variant probability density function of corrosion wastage of upper deck longitudinal stiffener flanges 132

Figure 6.1 Test of MCS convergence (deck panel of the 20-year-old tanker 90B) . 142

Figure 6.2 Time-variant relative contribution of variables to the variance of failure probability for deck plate panel ultimate strength failure (using the tanker 90B as an example) 144

Figure 6.3 Time-variant relative contribution of variables to the failure probability of deck stiffened panel ultimate strength failure (using the tanker 90-B as an example) 148

Figure 6.4 Time-variant reliability indices of unstiffened deck plate panels for sample tankers (cargo oil tanks) 149

Figure 6.5 Time-variant reliability indices of unstiffened deck plate panels for sample tankers (ballast tanks) 150

Figure 6.6 Time-variant reliability indices of stiffened deck panels based on beam-column buckling failure mode for sample tankers (cargo oil tanks) 151

Figure 6.7 Time-variant reliability indices of stiffened deck panels based on beam-column buckling failure mode for sample tankers (ballast tanks) 152

Figure 6.8 Time-variant reliability indices of stiffened deck panels based on torsional buckling failure mode for sample tankers (cargo oil tanks) 153

Figure 6.9 Time-variant reliability indices of stiffened deck panels based on torsional buckling failure mode for sample tankers (ballast tanks) 154

Figure 6.10 Time-variant reliability indices of the deck panels for the sample tanker 90A (cargo oil tanks) 157

Figure 6.11 Calibration of target reliability levels for inspection planning of deck panels 158

LIST OF TABLES

Table 2.1 Reduction factor α_z of the ship structure at 20 years from selected publications (modified from Wang et al, 2008) 37

Table 2.2 Estimates of the reliability indices for tanker structures 46

Table 2.3 Target reliability indices 47

Table 2.4 Definition of the target failure probabilities (reliability indices) for ship structural inspection 49

Table 3.1 Selected ultimate strength models for simple supported unstiffened plate panels under uniaxial compression along short edge 56

Table 3.2 Selected critical buckling stress models for simple supported unstiffened plates under uniaxial compression along short edge 57

Table 3.3 Mean and COV of modeling uncertainty of the critical buckling stress/ultimate strength formulations for unstiffened plate panel under uniaxial compression along short edges (ABS 2005) 61

Table 3.4 Mean and COV of modeling uncertainty of the critical buckling stress for the stiffened panel under uniaxial compression along short edges (ABS 2005) 61

Table 3.5 Mean and COV of modeling uncertainty of selected critical buckling stress/ultimate strength prediction formulations for unstiffened plate panel ……63

Table 3.6 Mean and COV of modeling uncertainty of selected ultimate strength prediction formulations for stiffened panel 63

Table 3.7 Statistical information for Young's modulus E 68

Table 3.8 Statistical information for yield stress σ_y for shipbuilding steels 69

Table 3.9 Statistical analysis on the yield stress σ_y of shipbuilding steels provided by two major Asian steel makers in 2007 70

Table 3.10 Statistical information for as-built plate thickness t_{p_0} 71

Table 3.11 Statistical information for the stiffener spacing s 71

Table 3.12 Statistical information for the stiffener geometries (Hess & Ayyub 1996) ……72

Table 3.13 Recommended probabilistic characteristic of strength basic random variables for reliability analysis 73

Table 4.1 Typical uncertainty models of SWBM for tankers 77

Table 4.2 Uncertainty measure of wave loads (Modified from Moan et al 2006).... 87

Table 4.3 Random variables in loading for the reliability analysis 94

Table 5.1 Summary of corrosion measurement databases on oil tankers (Wang et al 2003) 106

Table 5.2 Equations for predicting the mean values and standard deviations of corrosion wastage..... 116

Table 5.3 Comparisons of corrosion wastage prediction for upper deck structures of 20-year-old tankers 133

Table 6.1 Principal particulars of the sample tankers 138

Table 6.2 Stochastic models of the random variables related to the reliability assessment..... 141

Table 6.3 Sensitivity factors of the unstiffened plate panels for the 20-year-old sample tanker 90B..... 143

Table 6.4 Sensitivity factors of the stiffened panels for the 20-year-old sample tanker 90B (beam-column buckling failure mode) 146

Table 6.5 Sensitivity factors of the stiffened panels for the 20-year-old sample tanker 90-B (torsional buckling failure mode)..... 147

Table 6.6 Failure probabilities of unstiffened deck plate panels for sample tankers at selected ages (cargo oil tanks) 149

Table 6.7 Failure probabilities of unstiffened deck plate panels for sample tankers at selected ages (ballast tanks)..... 150

Table 6.8 Failure probabilities of stiffened deck panels based on beam-column buckling failure mode for sample tankers at selected ages (cargo oil tanks) ……...152

Table 6.9 Failure probabilities of stiffened deck panels based on beam-column buckling failure mode for sample tankers at selected ages (ballast tanks) ……..153

Table 6.10 Failure probabilities of stiffened deck plate panels based on torsional buckling failure mode for sample tankers at selected ages (cargo oil tanks) ……...154

Table 6.11 Failure probabilities of stiffened deck panels based on torsional buckling failure mode for sample tankers at selected ages (ballast tanks) 155

Table 6.12 Governing failure mode of deck stiffened panels for sample tankers 155

Table 6.13 Rank of reliability level of the deck panels for sample tankers at the time of service..... 156

Table 6.14 Suggested target failure probabilities (reliability indices)..... 158

Table 6.15 Required first inspection interval (year) for sample tankers' deck panels ……...159

Table 6.16 Required second inspection interval (year) for sample tankers' deck panels ……...159

LIST OF ABBREVIATIONS

2D	Two-dimensional
3D	Three-dimensional
ABS	American Bureau of Shipping
AISC	American Institute of Steel Construction
API	American Petroleum Institute
CAS	Condition Assessment Scheme
COV	Coefficient of Variation
CSR	Common Structure Rules
DNV	Det Norske Veritas
ESP	Enhanced Survey Program
FEA	Finite Element Analysis
FORM	First Order Reliability Method
FPI	Floating Production Installation
FPSO	Floating Production Storage and Offloading
HGSM	Hull Girder Section Modulus
HWA	Heavy Weather Avoidance
IACS	International Association of Classification Societies
IMO	International Maritime Organization
ITOPF	International Tanker Owners Pollution Federation
IUMI	International Union of Marine Insurance

KR	Korea Register
LHS	Latin Hypercube Sampling
LR	Lloyd's Register
MARPOL	Marine Pollution
MCS	Monte Carlo Simulation Method
MPP	Most Probable Point
MVFOSM	Mean Value First Order Second Moment Method
NK	Nippon Kaiji Kyokai
RSM	Response Surface Method
SORM	Second Order Reliability Method
SSC	Ship Structures Committee
SWBM	Still-Water Bending Moment
TSCF	Tanker Structure Cooperative Forum
WBM	Wave-Induced Bending Moment
VLCC	Very Large Crude Carrier

LIST OF SYMBOLS

A_p	Area of the effective plating
A_s	Area of the stiffener
b_{eff}	Effective breadth of plating
b_f	Stiffener flange breadth
B	Breadth of the ship
C_b	Block coefficient of the ship
C_s	Imperfection reduction factor
C_T	Torsional buckling coefficient
C_W	Wave coefficient
C_x	Plate buckling reduction factor
d_w	Stiffener depth
D	Ship depth
E	Young's modulus
f	Probability density function
F	Cumulative distribution function
F_E	Elastic buckling force
g	Limit state function
I	Hull girder moment inertia
I_e	Moment of inertia of the stiffener with fully effective plating
I_P	Polar moment of inertia

I_T	St. Venant's moment of inertia
I_{ϖ}	Sectorial moment of inertia
k	Shape parameter of Weibull distribution
K	Buckling factor
l	Stiffener span
L	Ship rule length
M_0	Bending moment due to lateral deformation
M_{SW}	Still-water bending moment
M_T	Total bending moment
M_W	Wave-induced bending moment
P_f	Probability of failure
P_f^*	Target probability of failure
P_r	Proportional linear elastic limit of steel
P_z	Nominal lateral load
r	Radius of gyration of the stiffener with fully effective plating
$r_{cor(s)}$	Steady corrosion rate
s	Stiffener spacing
stdev	Standard deviation
t_{cor}	Corrosion wastage
t_f	Stiffener flange thickness
t_{f_o}	Original as-built stiffener flange thickness
$t_{f(cor)}$	Corrosion wastage of the stiffener flange
t_{insp}	Gauged date during thickness measurement
t_p	Plate thickness
t_{p_o}	Original as-built plate thickness

$t_{p(cor)}$	Corrosion wastage of the plate
t_w	Stiffener web thickness
t_{w_o}	Original as-built stiffener web thickness
$t_{w(cor)}$	Corrosion wastage of the stiffener web
T_c	Coating life
T_i	Time to inspection
T_R	Reference time period
u	Location parameter of Gumbel distribution
v	Scale parameter of Gumbel distribution
w	Later deformation of the stiffener
w_0	Initial imperfection
z_0	Distance of neutral from the base line of the plate
z_{deck}	Vertical distance of the deck to the baseline
z_{NA}	Vertical position of the horizontal neutral axis of the hull cross section
Z_d	HGSM to the deck
Z_{d_o}	As-built HGSM to the deck
Z_e	Section modulus of stiffener including effective plating
α	Aspect ratio of the plate
β	Slenderness ratio of the plate
β_R	Reliability index
β_R^*	Target reliability index
χ	Modeling uncertainty
ε	Degree of fixation
γ_Z	Reduction factor of HGSM
η_{allow}	Allowable utilization factor

λ	Reference degree of slenderness
λ_c	Critical degree of slenderness
λ_s	Slenderness ratio of the stiffener
λ_T	Reference degree of slenderness for torsional buckling
μ	Mean value
ν	Poisson's ratio of steel
θ	Scale parameter of Weibull distribution
σ_b	Bending stress
σ_{cr-bc}	Critical beam-column buckling stress of the plate panel
σ_{cr-p}	Critical buckling stress of the plate
σ_{cr-t}	Critical torsional buckling stress of the plate panel
σ_E	Elastic compressive stress
σ_{ET}	Reference torsional buckling stress
σ_{u-p}	Ultimate strength of the plate
$\sigma_{u(panel)}$	Ultimate strength of the stiffened panel
σ_x	Compressive stress of the deck panel
σ_{y-p}	Yield stress of the plate
$\sigma_{y(panel)}$	Yield stress of the stiffened panel
σ_{y-s}	Yield stress of the stiffener
ψ	Stress ratio
ψ_W	Load combination factor

ABSTRACT

Reliability-Based Inspection Planning with Application to Deck Structure Thickness Measurement of Corroded Aging Tankers

by

Jinting Guo

Chair: Anastassios N. Perakis

Structural inspection is a critical part of the ship structural integrity assessment. Corrosion, as a very pervasive type of structural degradation, can potentially lead to catastrophic failure or unanticipated out-of-service time. In order to mitigate the unfavorable consequences of age-related structural failure, a wisely planned inspection is needed. The current practice of calendar-based inspection of ship structures may cause either an unexpected stoppage during normal routine due to unpredicted structural failures or yield higher costs for unnecessary inspections. Therefore, a strategy to determine timely and effective inspection plans is highly desirable.

Probabilistic tools have been used in ship structure analysis for years. Recently, there is revived interest in the reliability-based inspection planning of ship structures.

This study is devoted to demonstrating a practical methodology and procedure that adopts a reliability-based approach in structural inspection planning of ship structures. Scheduling a gauging survey for deck panels of oil tankers is used to demonstrate the proposed procedure.

This approach includes the derivation of explicit limit state functions for the ultimate strength failure of deck panels based on the equations stated in the International Association of Classification Societies' Common Structure Rules for double hull oil tanker (2008), and quantifies the various types of uncertainties involved. A time-variant probabilistic corrosion model is derived based on the gauging data collected by the American Bureau of Shipping. Monte Carlo Simulation method with Latin Hypercube Sampling is used for calculating time-variant probability of ultimate strength failure is obtained. By comparing the calculated failure probabilities with the target reliability levels, the inspection intervals can then be determined.

The reliability formulations derived in this study are applied to a case study in which the reliability assessment of the deck panels and associated inspection planning of a total of six oil tanker ship designs are carried out. Sensitivity analyses are also performed to investigate the relative contribution of each basic variable. The limitation of the proposed procedure is also discussed along with potential future work.

CHAPTER 1

INTRODUCTION

1.1 Background

According to the International Tanker Owners Pollution Federation (ITOPF 2009), there were 709 incidents of tanker hull failure that took place between 1974 and 2008. As shown in a recent study by the International Union of Marine Insurance (IUMI 2008), structural damage is a major factor that contributes to marine incidents (see Figure 1.1) and statistical analyses of total losses of tankers revealed the increasing trend of vessel losses with the age of the vessel (see Figure 1.2).

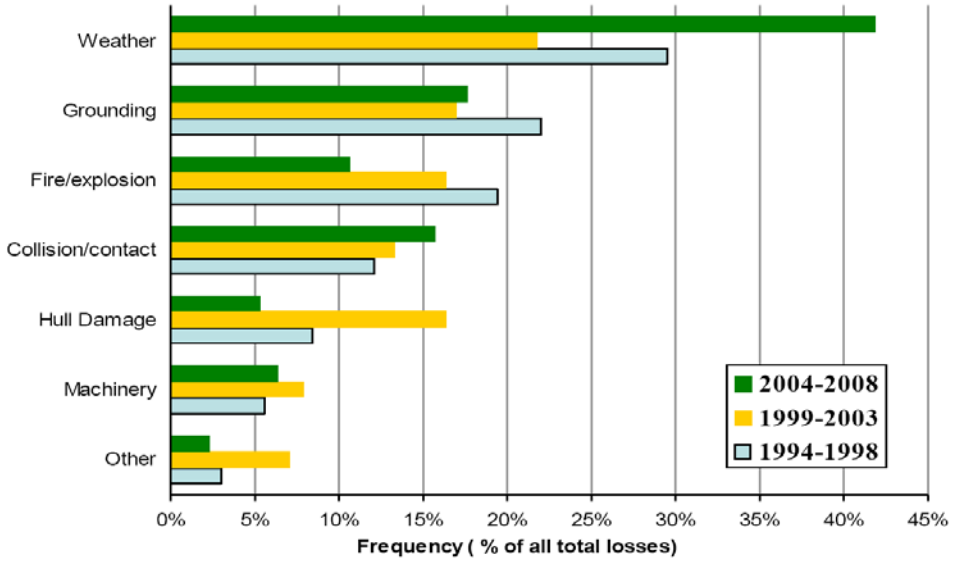

Figure 1.1 Total losses by causes for all vessel types greater than 500 GT (1994~2008) (IUMI 2008)

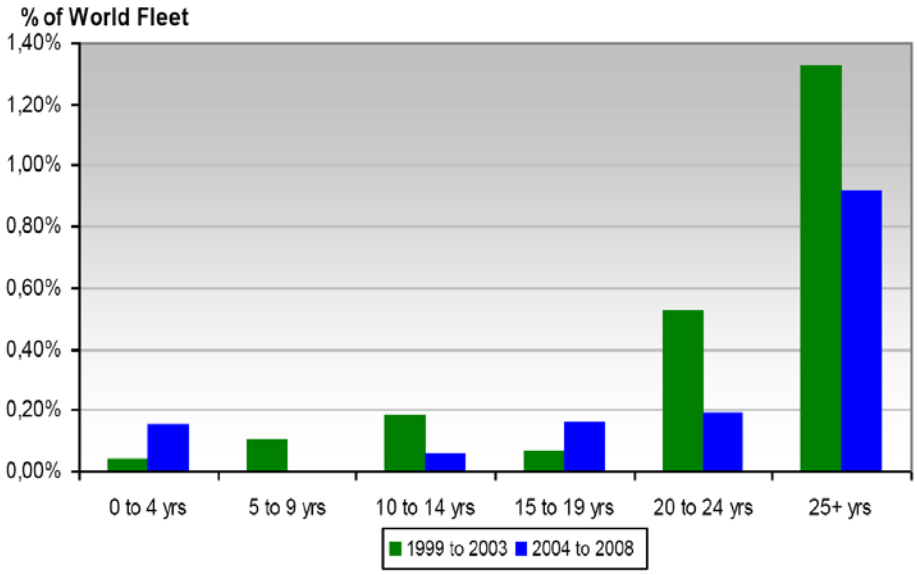

Figure 1.2 Total losses of tankers greater than 500 GT (1999~2008) (IUMI 2008)

Figure 1.3 shows a major structural failure of a Seawaymax oil tanker. This 25-year-old 37283 deadweight tonne single hull tanker "Erika" broke into two parts and sank off the French coast on December 12, 1999. According to the investigations, structural degradation caused by undetected corrosion, insufficient maintenance, and inadequate inspections were believed to cause the overall failure of this aging tanker.

Figure 1.3 "Erika" sank off the French coast on December 12, 1999 (Source: www.cedre.fr)

Corrosion wastage is a very pervasive type of structural degradation in ships and offshore structures. If neglected, such degradations can potentially lead to catastrophic failure, oil outflow, loss of cargo, or unanticipated out-of-service time. Hence, it is important to properly plan inspections in order to monitor corrosion.

1.1.1 Current Practice of Hull Inspections

In general, hull inspections include inspections during construction and in-service inspections. The primary function of construction inspections is to monitor and maintain that the ship structures are constructed in compliance with the appropriate drawings and standards which have been approved by classification societies. In-service inspections, as a critical part of the ship structural integrity assessment process, are to certify a ship's strength to some pre-defined levels of safety. The primary functions of in-service inspections include (Ma et al 1999):

- Give early warning of defects and damages
- Record and document such defects and damages
- Define alternatives to manage the defects and damages
- Choose and implement the best alternative
- Monitor the effects of defects and damages

Note: The term "inspections" discussed in this thesis refers to the "in-service inspections".

Throughout a ship's life, there will be mandatory inspections periodically required by classification societies, port and flag administration, and insurance company. Additionally, owners or operators may also carry out their own voluntary inspections.

Due to the different objectives between mandatory and voluntary inspections, the frequency and extent of details of the inspections may be different. The mandatory inspections can be classified into three types: annual surveys, intermediate surveys and special surveys. Each type of survey has its list of specific tasks to be performed, such as machinery survey, close-up examination, thickness measurement, tank testing, etc. The main goal of the voluntary inspections is to prolong the life of the fleet and help in repair planning.

In order to reduce the high cost associated with the inspections and optimize the extent of the inspections for large ships, a significant amount of studies on inspection planning have been undertaken and joint efforts of several organizations have been carried out since the 1980s. A series of guidance notes focusing on tanker inspection and maintenance were developed by the Tanker Structure Cooperative Forum (TSCF 1986, 1992, 1995). In the 1990s, the Ship Structure Committee (SSC) also had projects related to optimization of ship inspections (Holzman 1992, Ma & Bea 1992, Demsetz et al 1996). The United States Coast Guard (USCG) developed a critical area inspection program for Trans-Alaskan Pipeline Service (TAPS) tankers (Sipes 1990, 1991). To work towards providing the safety of tankers under a unified requirement, the International Association of Classification Societies (IACS) initiated and has continued updating an Enhanced Survey Program (ESP) since 1994 (IACS 1994). In addition to ESP requirements, classification societies also introduced Condition Assessment Scheme (CAS) as an optional response to the commercial needs of charterers for greater information regarding vessel condition over and above minimum classification requirements. After the Erika accident in 1999 and Prestige accident in 2002, the International Maritime Organization (IMO)

amended Regulation 13G of MARPOL Annex I to enforce CAS for single-hull tankers of 15 years or older (IMO 2003). Other reviews of current practices of ship inspections can be found in Ayyub et al (2002), Rizzo et al (2007), Paik & Melchers (2008), and Rizzo & Lo Nigro (2008).

Although advances have been made in the development of optimized inspection strategies, the current practices of hull inspections still mainly rely on experience. The inspection frequency is calendar-based and does not depend on a rigorous engineering analysis. Past successful experiences may be useful for predicting the future based on certain limits, such as the size of vessel, speed, construction quality, and exposed environmental and loading conditions. However, the limits of a vessel's size and speed have already been reached and the construction quality has been improved with the advancement of shipbuilding technology. The routes of trading vessels have been extended while the chance of facing harsher environments has increased with a wider and more frequent range of international trade. Therefore, blind use of previous experience to determine inspection frequency is not reliable. Such practice may explicitly take into account neither the likelihood of potential structural failures nor their consequences. As a result, the experience-based inspection planning may cause an unexpected stoppage during normal routine due to unpredicted structural failures or result in increased costs due to unnecessary inspections. Therefore, a strategy to determine timely and effective inspection plans is highly desirable.

The inspections for corrosion wastage are usually carried out by a gauging survey. Gauging survey (thickness measurement) is required as part of classification surveys during the service life of the ship. A typical thirty-year survey plan based on rule-required

thickness measurement for oil tankers is shown in Figure 1.4. The first thickness measurement will be conducted in the first special survey if extensive areas of wastage are found. For tankers older than 15 years, the gauging survey is required when intermediate and special surveys are carried out. The costs associated with the thickness measurement are generally high and paid by the owner or operators. In order to reduce the unnecessary costs without compromising structural safety, an effective thickness measurement plan is to be conducted.

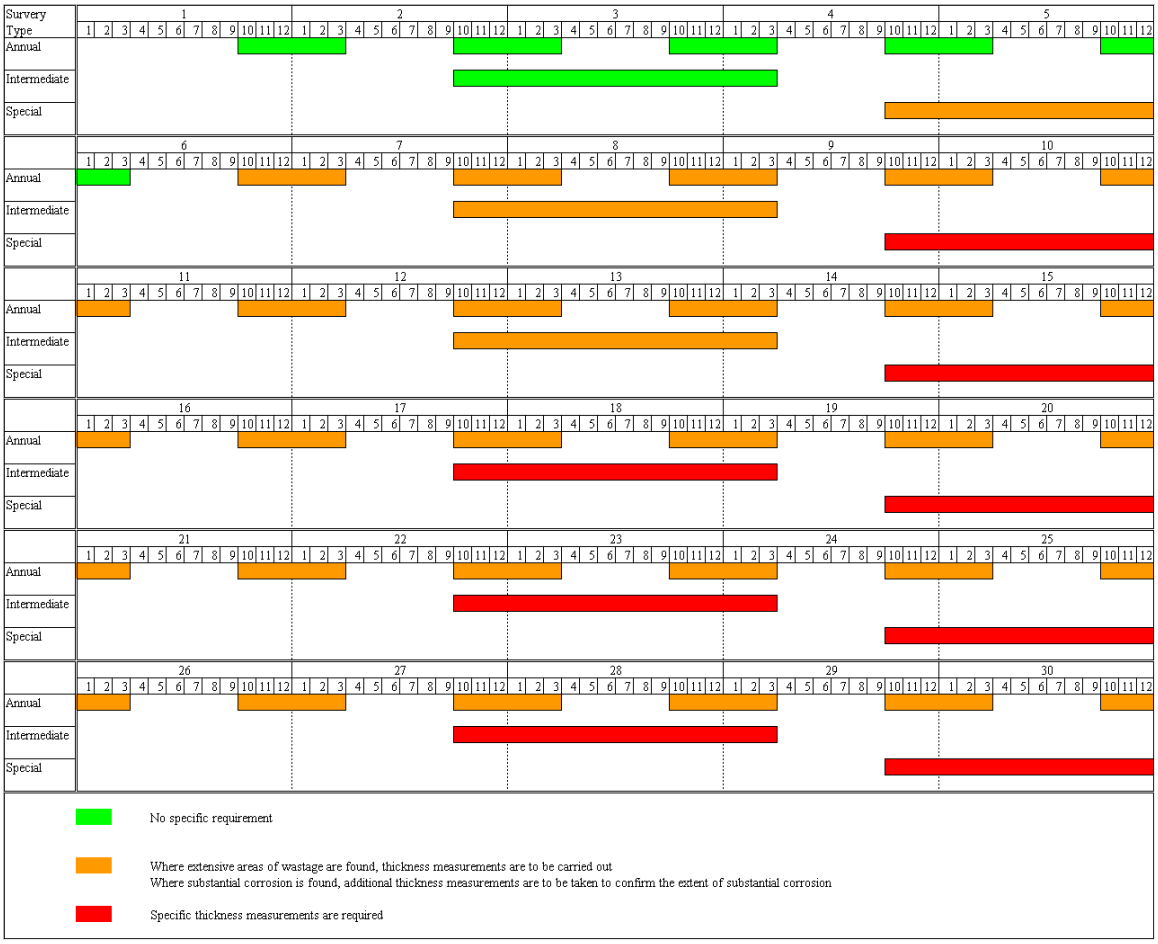

Figure 1.4 Typical thirty-year gauging survey plan for oil tankers

1.1.2 Reliability-Based Inspection Planning for Marine Structures

The traditional approach to inspection planning combines various inspection criteria in a qualitative manner to define the required inspection frequency and inspection scope. Such criteria may include proposed service lives, hazard and failure modes, target levels, past inspection data, and previous experiences (Onoufriou 1999). The reliability-based inspection planning techniques aim toward encompassing all these criteria in a quantitative manner based on reliability analysis.

Since the 1980s, structural reliability techniques have been widely applied to risk-based inspection planning for offshore structures (Skjong 1985; Bea 1993; Iwan et al 1993; Shetty et al 1997; Onoufriou 1999; and Lotsberg et al 2000). In recent years, there have been increased interest and significant developments in the area of reliability-based inspection planning for aging ships and Floating Production Storage and Offloading (FPSO) structures. Various models have been developed to quantify the effect of the degradation mechanisms such as corrosion wastage. By taking into account uncertainties in loading, response, and structural strength, the inspection plan can be proposed by performing the structural reliability analysis.

Fujimoto et al (1996) carried out a fatigue reliability analysis using Markov Chain Model for six structural members of bulk carrier. The essential information in the reliability analysis was collected from the professional experiences of naval engineers. The effect of repeated inspections and the inspection intervals for achieving certain target failure probabilities were investigated.

Garbatov & Guedes Soares (2001) studied the maintenance planning for a floating production unit, considering both the level of reliability and repair cost. Different ap-

proaches were proposed to quantify the repair costs resulting from different reliability-based maintenance strategies. It was recognized that for some strategies the dominating factors for the decision of inspection is the time interval between inspections.

Ku et al (2004) outlined the essential steps of a structural reliability calculation that is used later in determining a risk-based inspection plan for a Floating Production Installation (FPI). Using the deterministic finite element analysis (FEA) stress results, coupled with uncertain degradation mechanisms, the structural reliability analysis was carried out to determine the timing for inspection of structural components.

Sun & Guedes Soares (2006) proposed a reliability-based inspection plan for FPSO based on corrosion renewal criteria that account simultaneously for thickness reduction, hull girder ultimate strength, stiffened panel buckling strength, and plate ultimate strength. It was concluded that the necessity of inspection gradually become more demanding with the increase of failure consequences, lower limit of safety level, likelihood of failure, the vessel's age, and the probability of renewal.

Moan & Ayala-Uraga (2008) established a fatigue reliability-based formulation for assessment of deteriorating ship structures subjected to multiple climate conditions throughout their service life. The inspection's contribution was emphasized when the vessel is exposed to different climate conditions.

A few more papers (Kim et al 2000, Moan & Vårda 2001, Ku et al 2005, Moan 2005) have also discussed the reliability-based inspection and maintenance planning of the ship and offshore structures from different viewpoints.

1.1.3 Structural Reliability Analysis on Ship Structures

Structural reliability analysis is a key component in the reliability-based inspec-

tion process. Since Dunn (1964) first implemented reliability methods to ship structures, a significant amount of work has been published by various authors.

As one of the pioneers, Mansour et al (1984) discussed a comprehensive framework comprising all aspects of reliability methods and code development. Thayamballi et al. (1987) compared the assessment of the ship structural performance based on both conventional deterministic and reliability-based probabilistic approaches to interpret the experience-based ship design from a reliability standpoint. Calculation methods and experience related to hull girder ultimate strength, wave-induced loads as well as limit states were discussed.

In the 1990s, many efforts were devoted to the feasibility study of reliability-based analysis for ship structures. The focus was placed on the reliability-based calibration of classification rules. Mansour & Hovem (1994) demonstrated a reliability-based ship structural analysis and enumerated the benefits of using a reliability-based method in comparison to traditional methods. Mansour et al (1997) introduced a comprehensive approach for assessing the ship reliability levels associated with failures of hull girder, stiffened panels and unstiffened plate panels. A detailed procedure was described and recommendations were made for target reliability levels for different ship types and failure modes. In order to assist the development of ship longitudinal strength requirements, Casella & Guedes Soares (1998) carried out a reliability analysis on two oil tankers that had comparable dimensions but different designs. The results showed that a large scatter existed in the design safety levels of ships, even when the classification societies' unified requirements were satisfied.

Considering the degradation due to corrosion and fatigue, the reliability-based ap-

proach also provides a viable tool for evaluating the structural integrity of aging ships. Hart et al (1985) described the structural reliability analysis of stiffened panels of two large oil tankers considering two different levels of corrosion diminution. In that paper, the advance Level II structural reliability theory was applied and the uncertainties which influence structural performance were discussed. In the past ten to fifteen years, continuous research combining reliability-based procedures with ultimate strength of ship structures and effects of corrosion and fatigue have been carried out by several authors. Wirsching et al (1997) studied the relationship between hull girder ultimate strength and the hull girder section modulus, and adopted a linear corrosion wastage model to evaluate the reliability of corroded ship hulls. Paik et al (1997, 1998) developed a procedure for the assessment of ship hull girder ultimate strength reliability taking into account the degradation on primary members due to general corrosion. A closed form formulation for the prediction of hull girder ultimate strength and a new corrosion model based on gauging data were applied to assess the reliability of corroded tanker hulls. Guedes Soares & Garbatov (1999a, 1999b) used the proposed nonlinear mathematic corrosion model to calculate the reliability of a maintained ship hull subjected to general corrosion and fatigue under combined loads.

As a ship ages, the integrity of the structural capacity not only decreases due to the effects of degradation, but the uncertainties associated with it also increase over time. During the maintenance and operation of ship structures, it may no longer be adequate to consider the uncertainties determined at the design and construction stages. For this reason, the time-variant reliability formulations have been extensively applied to evaluate the reliability levels of ship structures over a vessel's lifetime considering the time-

dependent corrosion wastage and potential loading combinations. Shi (1992) proposed a time-variant method to estimate the long-term failure probability of corroded ship structures. The influences of general corrosion on ultimate strength were specifically emphasized and the sensitivity factors of the failure probability were provided. Guedes Soares & Teixeira (2000) calculated the time-variant failure probability of two bulk carriers using the long-term loading formulation and analytical hull girder ultimate strength formulation. Sensitivity study on the effects of the variables in different loading conditions was performed. Sun & Bai (2000) and Akpan et al. (2002, 2003) modeled corrosion as a time-dependent random function and used SORM to calculate the instantaneous reliability of the primary hull structure. The procedures to assess the time-variant reliability of tankers, bulk carriers and FPSO structures subjected to degradations due to corrosion and fatigue-induced cracking were presented by several authors (Paik et al 2003, Sun& Bai 2003, Hu et al 2004, Moan et al 2004, Hu & Cui 2005, Moatsos & Das 2005). Timelines presenting vessels relating the probability of hull girder failure to ship age were obtained. Different models for corrosion wastage were applied and the hull girder ultimate strength was estimated. The effects of various repair schemes on reliability were discussed. Another comprehensive review of the state of the art ship structural reliability approaches can be found in ISSC (2006).

1.1.4 Analyzed Deck Panels

In typical tanker structures, as shown in Figure 1.5, deck plate panels are reinforced by deck longitudinals in the longitudinal direction and transversely supported by widely spaced transverse structures (such as transverse bulkheads and deck girders). The deck longitudinals are T-beams, angles, bulbs or flat bars, while the deck transverses are

typically T-beam sections. These transverse members usually have significantly greater stiffness in the plane of the lateral load, while the longitudinals have greater stiffness in the aspects of bending and axial loading. The boundary conditions for the ends and along the sides of a deck panel can be considered simply supported.

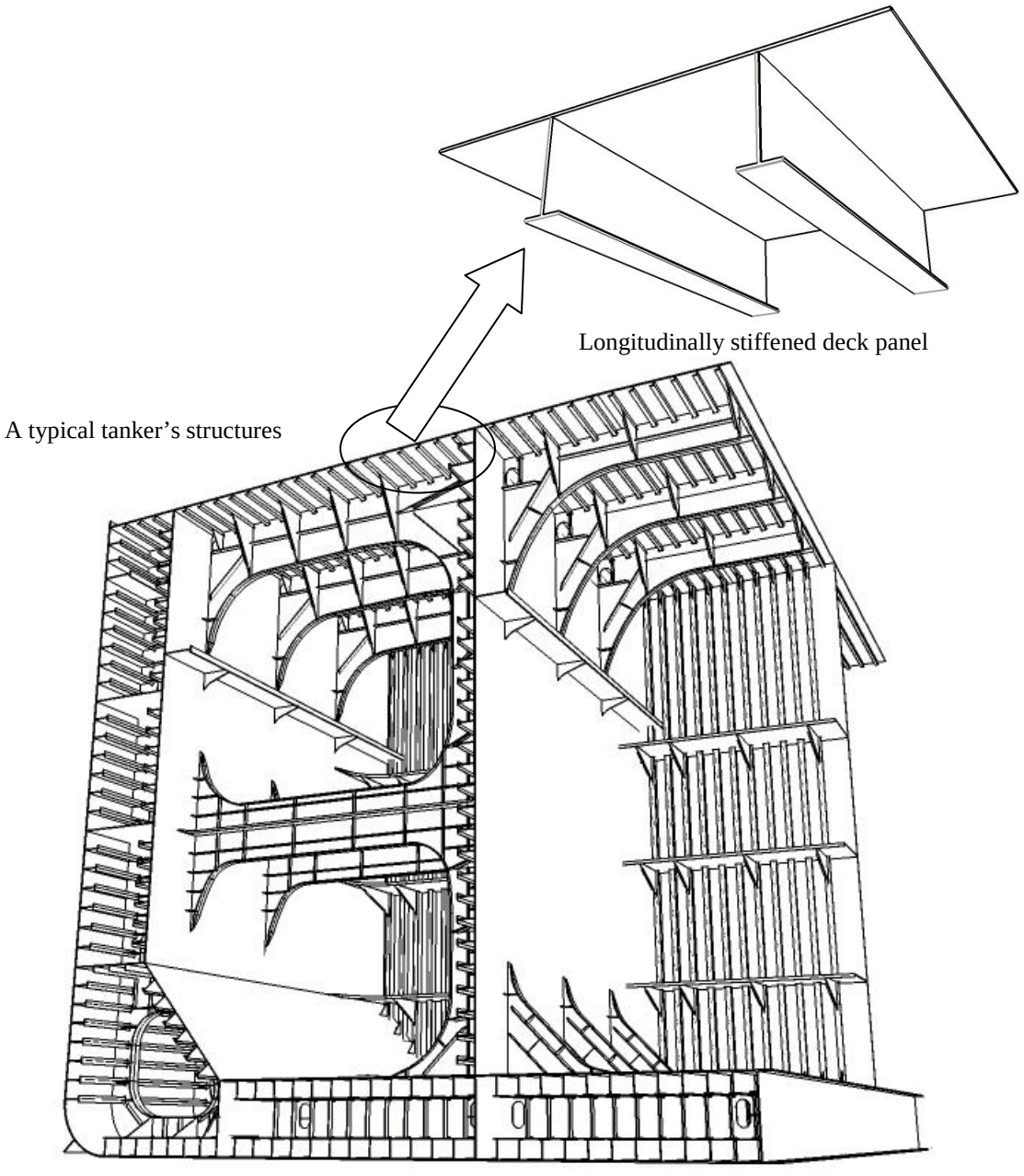

Figure 1.5 A typical tanker's structures and a longitudinally stiffened deck panel

Deck panels experience large in-plane compression or tension primarily in the ship's longitudinal direction caused by hull girder bending and small bending moment due to lateral pressures. For tankers, lateral pressure applied on the deck structure is negligible. Therefore, in the present study only the in-plane stress is considered.

The collapse of a deck panel involves the failure of both plate and stiffener. In most cases, local buckling of unstiffened deck plate between stiffeners takes place prior to failure of other structures. The transverse boundary of the deck panels is usually designed strong enough to provide sufficient flexural rigidity. Thus, the collapse of the deck panel is governed by the strength of the longitudinally stiffened panel.

Compared with hull girder failure, the local failures of ship structures are more likely to occur. As one of the fundamental building components in the construction of ships, the deck panel is often highly stressed. Although the failure of deck panels may not lead to the structural collapse of the vessel, it will affect the hull girder reliability. Therefore, the failure probability of the deck panels is a very important measure of a vessel's structural integrity. Only a few publications focus on the assessment of panel reliability (Hart et al 1985, Nikoladis et al 1993, Assakkaf & Ayyub 1995, Wang et al 1996, Mansour et al 1997, Guedes Soares & Garbatov 1999, Assakkaf et al 2002, Sun & Guedes Soares 2006, Guo et al 2008) in contrast to thousands devoted to hull girder reliability.

1.2 Objective

The principal objective of this dissertation study is to develop a reliability-based approach for inspection planning. Scheduling a gauging survey for deck panels of oil tankers is used to demonstrate the method considering ultimate strength failure of cor-

roded panels.

This approach accounts for and quantifies the various types of uncertainties involved, which include physical properties of materials, fabrication tolerance, measurement errors, corrosion wastage, loads, as well as the strength models that are employed. Furthermore, taking into account the structural degradation due to corrosion and applying the advanced time-variant probabilistic reliability analysis, this approach is capable of quantitatively assessing the failure probability of deck panels over a vessel's lifetime. Referring to the target reliability level, the intervals of thickness measurement can then be determined. This methodology could also provide a rational framework and basis for evaluating the failure probability of other ship structures.

The reliability procedures developed herein are believed to have substantial potential to provide the ship owners and operators with a tool for rationalizing the determination of the inspection interval in order to maximize the efficiency of inspections to minimize cost of inspection by avoiding unnecessary gauging surveys.

1.3 Organization

The dissertation is subdivided into seven chapters which are organized as follows:

- In **Chapter 1**, the background information, problem statement, objectives and dissertation structure are presented. In this chapter, the brief background information about aging tanker's failure due to structural degradation is presented. A literature review on the current inspection practice of ship structures, reliability-based inspection planning and the current development of ship structure reliability analysis is provided.

- In **Chapter 2**, a rational reliability-based framework for planning the gauging survey for ship structures is developed. The inspection planning of deck panels of aging tankers is analyzed to illustrate the proposed reliability-based procedure. The main phases of the procedure are discussed. It includes projecting the time-variant failure probability, evaluating the projection by target failure probability levels, and predicting the intervals of gauging surveys.
- In **Chapter 3**, the uncertainty modeling of strength capacity prediction for deck panels of the tankers is discussed. A variety of available analytical formulations for estimating the ultimate strength of unstiffened and stiffened panels are reviewed and compared. The various types of uncertainties involved in the reliability analysis are discussed and quantified.
- In **Chapter 4**, the uncertainty modeling of load effects experienced by deck panels of the tankers is discussed. Previous studies on probabilistic prediction of still-water bending moment (SWBM) and wave-induced bending moment (WBM) are reviewed. A notional uncertainty model is adopted to estimate the total bending moment applied on deck panels based on the practical way of establishing the link with the current industry practice.
- In **Chapter 5**, a new procedure to determine a time-variant probabilistic nonlinear corrosion model based on gauging data is developed. An extensive literature review on all the available corrosion models is provided. A comparative study between the newly developed corrosion model and previously available models are presented.
- In **Chapter 6**, an illustration of the proposed procedures using six sample

tankers is provided. The calculated results are presented including the time-variant failure probability and corresponding inspection plans. Sensitivity analysis is performed to determine the dominant variables.

- In **Chapter 7**, the contributions of this research work are presented with recommendations for future work.

CHAPTER 2

RELIABILITY-BASED INSPECTION PROCEDURE

2.1 Introduction

As described in Chapter 1, ship structures need to be inspected on a regular basis throughout a vessel's life. Ship structural inspection will be moving toward a more rational and probability-based procedure. Compared with the traditional experience-based method, such a procedure takes into account more information during the evaluation of structural integrity. This information includes uncertainties in the strength of structural elements, in loads experienced by the structures, effects of degradations, and modeling errors in analysis procedures. Therefore, reliability-based inspection planning is more flexible and rational than the traditional procedure.

Thickness measurement (gauging survey) is one of the mandatory procedures to monitor the condition of ship structures. In order to reduce unnecessary expenditures without sacrificing the safety control, a rational procedure is developed to optimize the intervals of the thickness measurement. The main phases in the proposed reliability-based procedure for planning the thickness measurement of deck panel are illustrated in Figure 2.1.

Before deciding when a gauging survey is required, the first step is to prepare all the necessary data including design parameters, operational and environmental conditions,

and previous inspection plan and maintenance records.

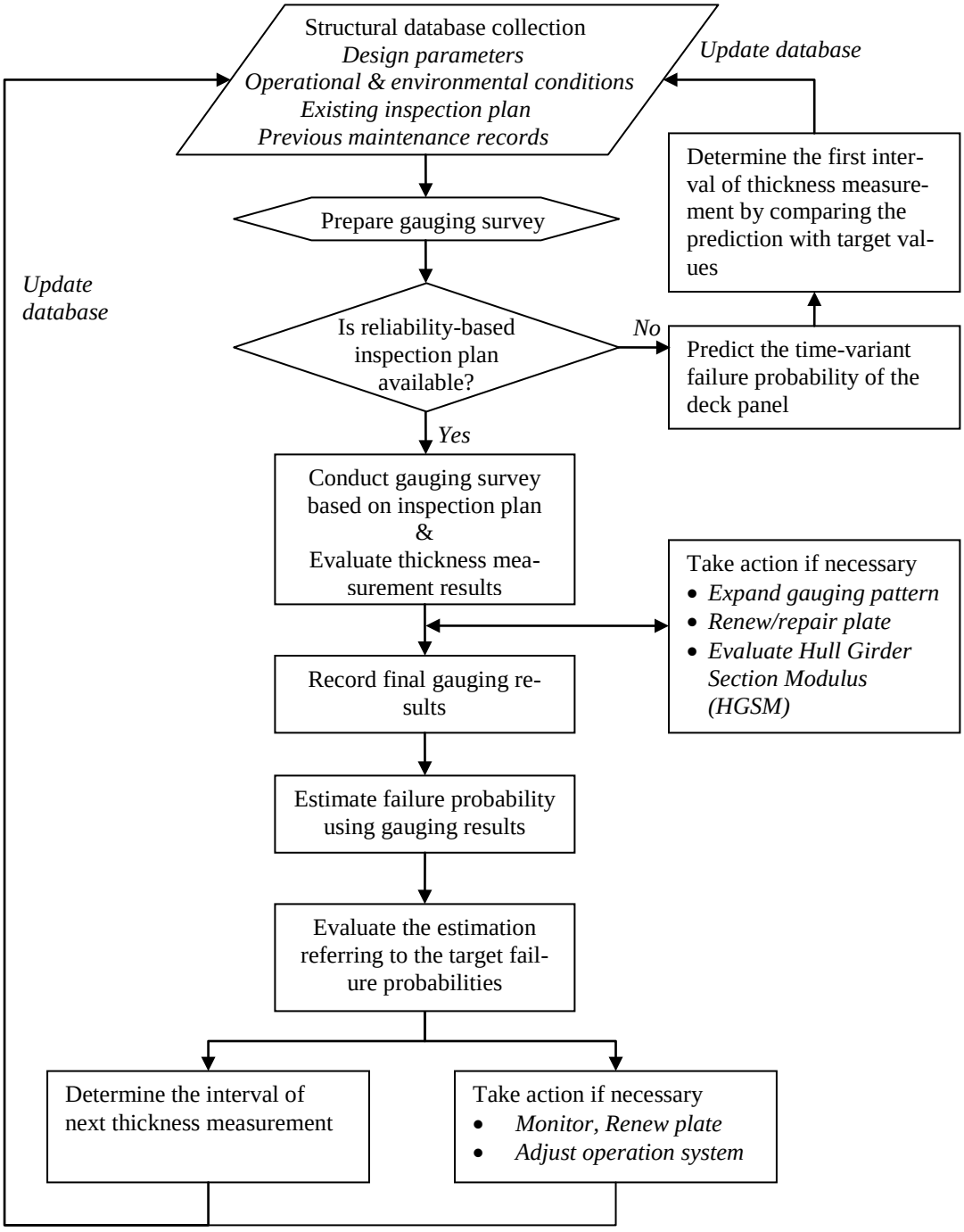

Figure 2.1 A reliability-based procedure for scheduling thickness measurement of the deck panel over a vessel's lifetime

If the first interval of the thickness measurement for the deck structures of a tanker is to be determined, the first step is to perform a time-variant reliability analysis to obtain the failure probability during the service life of the tanker. When the calculated time-variant failure probability reaches the target level, a gauging survey is recommended. The first interval of thickness measurement is then determined, and the existing inspection plan will be updated.

By conducting the first-time thickness measurement, knowledge is obtained about the degradation effect due to corrosion which enables us to update the previous predicted corrosion wastage. It is noted that there is a possible phase that is required before recording the final gauging results. When substantial corrosion is suspected, the gauging pattern on that particular plate is required to be expanded. If the gauged thickness exceeds the allowable corrosion wastage indicated in the classification rules, immediate action is required, i.e., plating repair or replacement. After the gauging results are finalized, the updating of the inspection plan can be performed. The detailed updating scheme is discussed in Section 2.4.

2.2 Evaluation of Time-Variant Reliability of a Tanker's Deck Panels

From Figure 2.1, it is clear that evaluation of the time-variant failure probability is the key to planning an effective and timely inspection. The failure probability is calculated using reliability analysis based on limit state functions. The process of time-variant reliability analysis of a typical tanker's deck panel is illustrated in Figure 2.2.

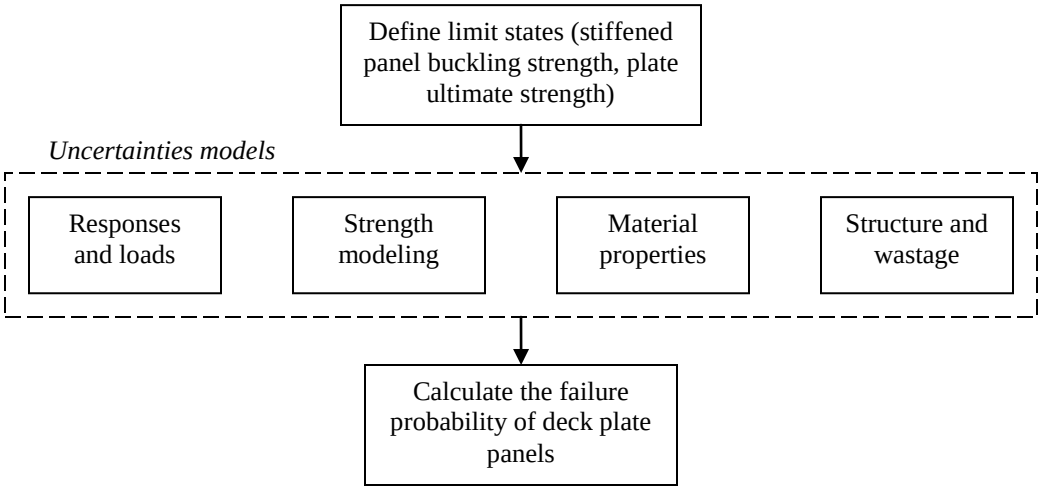

Figure 2.2 Projection of failure probability of deck panels

2.2.1 Limit State Function

The limit states when considering only deck panels can be classified as serviceability limit state and ultimate limit state. Serviceability limit state requires the structure to remain functional for its intended operational parameters and the structure must not cause any occupant discomfort under routine conditions. Ultimate limit state on the other hand requires the structure to not fail when subjected to extreme loading. In general, it is based on safety considerations or ultimate load-carrying capacity of a panel. The aim of inspection is to prevent structural failures and their resulting safety, environmental or economic concerns. Therefore, ultimate limit state is the basis for the reliability analysis in the present study.

As indicated in Chapter 1, deck panels of a tanker are assumed to only experience in-plane stress in the ship's longitudinal direction due to hull girder bending. The vertical sagging bending moment causes the deck panels to be in compression, while hogging bending moment puts the deck panels in tension. Since the ultimate strength capacity in

tension is higher than that in compression, the ultimate strength failure occurs when applied compressive stress exceeds the ultimate strength of the deck panels.

The failure modes of deck panels include local failure of unstiffened panels, collapse of the longitudinally stiffened panels, and overall collapse of the gross panels involving global failure of both longitudinal and transverse stiffeners. Since the deck structures are designed to prevent the overall mode of collapse, the failure of gross panels rarely occur in tankers. Therefore, in the present study, only failure modes of unstiffend and stiffened panels are discussed. The limit states of ultimate strength failure of deck panels are given by the following formulations depending on the failure mode (Mansour 1997):

Ultimate failure of stiffened panel (Secondary failure mode):

$$g(\cdot) = \sigma_{u(panel)} - \sigma_x \tag{2-1}$$

Ultimate failure of unstiffened plate (Tertiary failure mode):

$$g(\cdot) = \sigma_{u-p} - \sigma_x \tag{2-2}$$

where $\sigma_{u(panel)}$ and σ_{u-p} represent the ultimate load-carrying capacity of the stiffened deck panel and plate between stiffeners, respectively. σ_x is the compressive stress due to load applied on the deck. $g(\cdot)$ signifies the limit state.

2.2.2 Compressive Stress of Deck Panel

The compressive stress of ship's longitudinal plate panels are induced by the hull girder bending and the local bending of the secondary structures due to lateral load. The relative contribution of these two loads to the total stress experienced by a plate panel depends on the location of the plate panel and the type of bending of the hull girder. As

the longitudinal deck panel is located relatively far from the neutral axis of the hull girder, it experiences small lateral pressure and large in-plane compression primarily in the ship's longitudinal direction due to the bending moment in the vertical plane. Therefore, the stress component induced by the hull girder bending dominates. Because of the small effect of local lateral loads on the deck, for the prediction of the plate panel failure in respect to its ultimate strength, it can be considered that only the stress components induced by the hull girder vertical bending is relevant and shear lag effects may be neglected (Mansour & Hovem, 1994).

Neglecting the local bending of the secondary structures due to the action of the lateral load applied, it is considered that the nominal compressive stress σ_x of the deck panel is only induced by the hull girder vertical bending moment during sagging. Based on the beam theory, the compressive stress is calculated by the following equation:

$$\sigma_x = \frac{M_T}{Z_d} \tag{2-3}$$

where M_T represents the total bending moment, which is a combination of the still-water bending moment (SWBM) M_{SW} and wave-induced bending moment (WBM) M_W. Strictly speaking, M_{SW} and M_W influence each other and the two random variables are statistically dependent. However, in a practical sense, they are often treated as statistically independent variables (Mansour & Hovem 1994). There are several methods to combine the SWBM and WBM. The detailed review and discussion of these methods are included in Chapter 4.

The section modulus to the deck Z_d is defined as:

$$Z_d = \frac{I}{z_{deck} - z_{NA}} \tag{2-4}$$

where z_{deck} is the vertical distance of the deck panels to the baseline, z_{NA} is the vertical position of the horizontal neutral axis of the hull cross section, and I is the hull girder moment inertia relative to the horizontal neutral axis.

2.2.3 Ultimate Strength Prediction of the Deck Panels

The deck panels of the tankers considered in the present study are located in the cargo/ballast center tanks which are situated amidships. When considering only the effect of the membrane compressive stress induced by hull girder vertical bending during sagging, the deck panels are subject to uniaxial compression in the longitudinal direction. The design formulations introduced in the IACS Common Structure Rules (CSR) for buckling strength assessment are applied in the present study for predicting the ultimate strength of the deck panels (IACS 2008b).

As described in the previous section, the structural elements of the deck panels include unstiffened plate panel between longitudinal stiffeners and the stiffened panel. The ultimate strength of these two types of structural elements is predicted by the specific design formulations indicated in IACS CSR for double hull oil tankers (IACS 2008b).

Unstiffened plate panel:

Figure 2.3 schematically represents the specific case in which the unstiffened plate panel is subject to the uniaxial compression in the longitudinal direction. The ultimate strength of the plate panel is given by:

$$\sigma_{u-p} = C_x \sigma_{y-p} \tag{2-5}$$

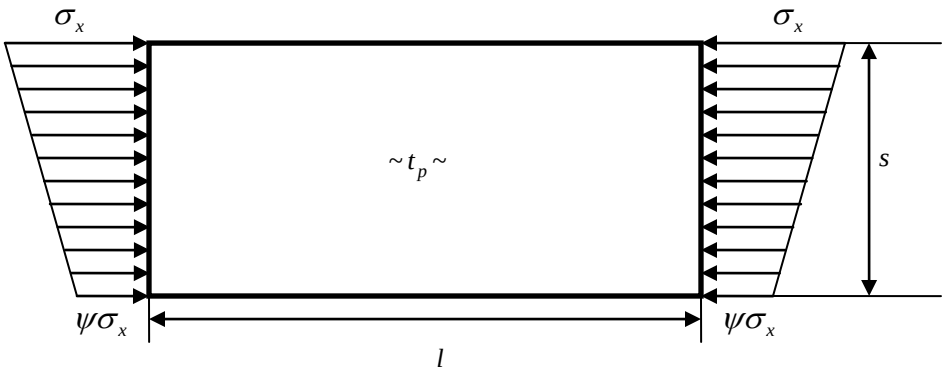

Figure 2.3 Unstiffened plate panel model for uniaxial compression

where σ_{y-p} is the material minimum yield stress of the plate and C_x is a reduction factor, which is defined as:

$$C_x = \begin{cases} 1 & \text{for } \lambda \le \lambda_c \\ c\left(\frac{1}{\lambda} - \frac{0.22}{\lambda^2}\right) & \text{for } \lambda > \lambda_c \end{cases} \tag{2-6}$$

where c is a parameter function of the stress ratio. λ and λ_c are the reference degree of slenderness and the critical degree of slenderness, respectively. The parameters c and λ_c are given by the following equations:

$$c = (1.25 - 0.12\psi) \le 1.25 \tag{2-7}$$

$$\lambda_c = \frac{c}{2}\left(1 + \sqrt{1 - \frac{0.88}{c}}\right) \tag{2-8}$$

The reference degree of slenderness is given by:

$$\lambda = \sqrt{\frac{\sigma_{y-p}}{K\sigma_E}} \tag{2-9}$$

with the buckling factor K , which is the function of the stress ratio ψ . For typical de-

sign cases of plate panels above or below the horizontal neutral axis of ship hull structure, the stress ratio is normally assumed to be in the interval $0 \le \psi \le 1$ (IACS 2006b). For this particular case, the buckling factor K is defined as:

$$K = \frac{8.4}{\psi + 1.1} \tag{2-10}$$

For horizontal plate panels, such as the deck and bottom structures, the compressive stress is uniformly distributed and the stress ratio ψ is assumed to equal 1. However, for vertical or inclined plate panels, the distribution is not uniform (IACS 2006b). Therefore, for deck panels, the buckling factor satisfies $K = 4$.

The reference stress σ_E is the ideal elastic compressive stress given by the following equation:

$$\sigma_E = 0.9E\left(\frac{t_p}{s}\right)^2 \tag{2-11}$$

where E is the modulus of elasticity of the material, t_p is the plate thickness and s is the spacing between longitudinal stiffeners. For the time-variant reliability evaluation, the plate thickness is to be defined as:

$$t_p(T) = t_{p_o} - t_{p(cor)}(T) \tag{2-12}$$

The plate thickness used for ultimate strength calculations should be equal to the original as-built thickness t_{p_o} deducted by predicted time-dependent corrosion wastage $t_{p(cor)}$, which will be discussed in Chapter 5.

Applying Eq. (2-6) ~ (2-11) into Eq. (2-5), the ultimate strength of the unstiffened plate panel subject to uniaxial compression in the longitudinal direction can be approximately expressed as a function of plate slenderness ratio β:

$$\sigma_{u-p} = \begin{cases} \sigma_{y-p} & \text{for } \beta \le 1.58 \\ \left(\dfrac{2.14}{\beta} - \dfrac{0.89}{\beta^2} \right) \sigma_{y-p} & \text{for } \beta > 1.58 \end{cases} \tag{2-13}$$

where the plate slenderness ratio β is given by:

$$\beta = \frac{s}{t_p} \sqrt{\frac{\sigma_{y-p}}{E}} \tag{2-14}$$

Stiffened panel:

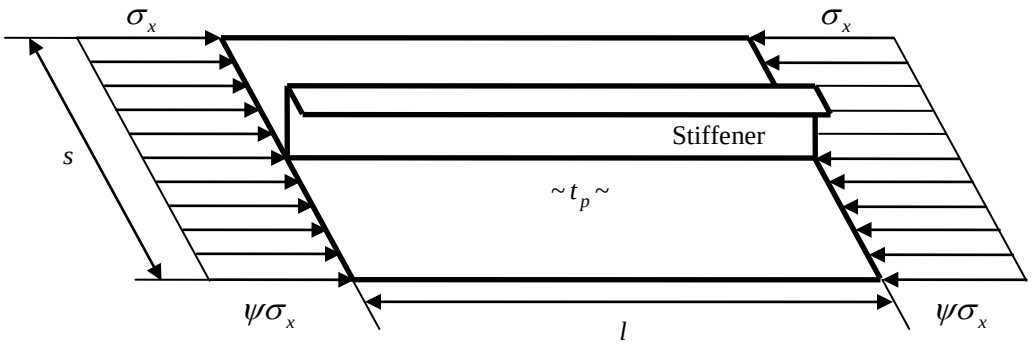

Figure 2.4 Stiffened panel model for uniaxial compression

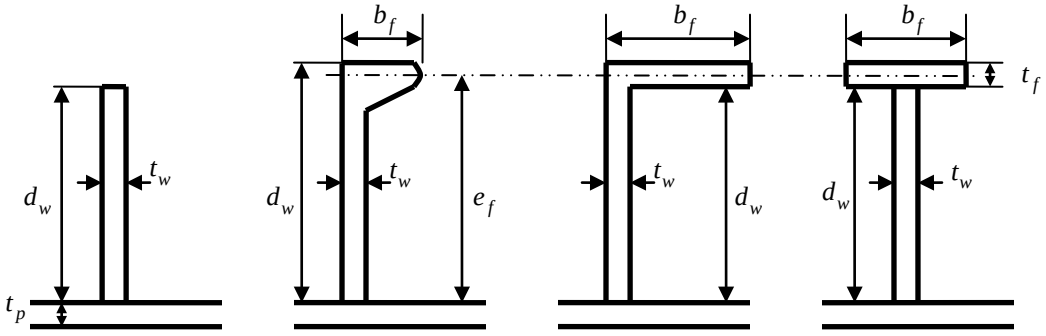

a) Flat bars b) Bulb flats c) Angles d) T bars

Figure 2.5 Stiffener cross sections

Figure 2.4 schematically illustrates the case of the stiffened panel subject to the uniaxial in-plane compressive loads in the longitudinal direction. The cross-sectional parameters for different types of stiffeners are shown in Figure 2.5. Typically, the failure models of such longitudinally stiffened panels include the overall failure of the stiffened panel and the local failure of its plate or stiffener.

The overall failure of the stiffened panel is highly undesirable since it reduces the hull girder capacity to resist the applied bending moments. A well-designed structure does not collapse when the local plate fails as long as the stiffeners can resist the extra load due to the plate failure. However, if the lateral rigidity of the stiffeners is not sufficiently high, they may buckle as columns due to the increased compressive load. This failure mode is called beam-column buckling. Another failure mode of stiffeners is torsional (tripping) buckling due to inadequate torsional rigidity. If stiffeners fail, the plate panels will lose almost all the lateral support to sustain in-plane compressive load and consequently induce the overall failure of the stiffened panel. Hence, the overall stability of longitudinally stiffened panels under longitudinal in-plane compressive loads is governed by the lateral and torsional rigidity of stiffeners.

There are different formulations for calculating the ultimate strength of the stiffened panel. According to IACS (2008b), the failure modes of beam-column buckling and stiffener torsional (tripping) buckling are considered to evaluate the ultimate strength of the stiffened panel.

Beam-column buckling of stiffeners:

Based on the maximum allowable buckling utilization factor, the critical beam-column buckling stress of the plate panel is calculated by the following equation:

$$\sigma_{cr-bc} = \eta_{allow}\sigma_{y-s} - \sigma_b \tag{2-15}$$

where the allowable buckling utilization factor η_{allow} is defined as a function of the vertical position of the stiffened panels in the hull girder cross section. For stiffened panels above $0.5D$, with D the ship depth, $\eta_{allow} = 1.0$ applies. For those below $0.5D$, the allowable utilization factor is $\eta_{allow} = 0.9$. Hence, $\eta_{allow} = 1.0$ is applied here for deck panels. σ_{y-s} is the material minimum yield stress of the stiffeners. For the stiffened panels without lateral pressure, the bending stress σ_b is equal to:

$$\sigma_b = \frac{M_0}{Z_e} \tag{2-16}$$

where Z_e is the section modulus of stiffener including effective breadth of plating b_{eff}, which is given by:

$$b_{eff} = \min\left(C_x s, C_s s\right) \tag{2-17}$$

with average reduction factor C_x for buckling of the two attached plate panels according to Eq. (2-6).

$$C_s = 0.0035\left(\frac{l}{s}\right)^3 - 0.0673\left(\frac{l}{s}\right)^2 + 0.4422\left(\frac{l}{s}\right) - 0.0056 \le 1 \tag{2-18}$$

where l is the effective span of stiffeners.

Due to the lateral deformation w of stiffener, bending moment M_0 is defined as:

$$M_0 = F_E\left(\frac{P_z w}{c_f - P_z}\right) \qquad \text{where } \left(c_f - P_z\right) > 0 \tag{2-19}$$

Because the lateral load is not considered, the lateral deformation w is equal to the assumed imperfection w_0, which is given by:

$$w_0 = \min\left(\frac{l}{250}, \frac{s}{250}, 10\right) \tag{2-20}$$

The ideal elastic buckling force F_E of the stiffener is given by:

$$F_E = \frac{\pi^2 E I_e}{l^2} \tag{2-21}$$

where the moment of inertia of the stiffener I_e, including effective width of attached plating b_{eff}, is to comply with the requirement $I_e \geq st_p^3/12$.

When applied membrane stress σ reaches the maximum critical beam-column buckling stress σ_{cr-bc}, the nominal lateral load P_z acting on the stiffener is defined as:

$$P_z = \frac{\pi^2 \sigma_{cr-bc} s t_p}{l^2}\left(1 + \frac{A_s}{st_p}\right) \tag{2-22}$$

where A_s is the sectional area of the stiffener without attached plating.

The parameter c_f is given by:

$$c_f = \frac{\pi^2 F_E}{l^2}\left(1 + c_p\right) \tag{2-23}$$

where

$$c_p = \frac{1}{1 + \frac{0.91}{c_a}\left(\frac{12 I_e}{st_p^3} - 1\right)} \tag{2-24}$$

with

$$c_a = \begin{cases} \left(\frac{l}{2s} + \frac{2s}{l}\right)^2 & \text{for } l \geq 2s \\ \left[1 + \left(\frac{l}{2s}\right)^2\right]^2 & \text{for } l < 2s \end{cases} \tag{2-25}$$

By combining Eq. (2-15), (2-16), (2-19) and (2-22), the critical beam-column buckling stress σ_{cr-bc} is obtained by solving the following equation:

$$\frac{QwF_E\sigma_{cr-bc}}{Z_e\left(c_f - Q\sigma_{cr-bc}\right)} + \sigma_{cr-bc} = \sigma_{y-s} \tag{2-26}$$

where

$$Q = \frac{\pi^2 st_p}{l^2}\left(1 + \frac{A_s}{st_p}\right) \tag{2-27}$$

Therefore, the critical beam-column buckling stress σ_{cr-bc} can be expressed as:

$$\sigma_{cr-bc} = \frac{H - \sqrt{H^2 - 4Z_e^2 Q\sigma_{y-s}c_f}}{2Z_e Q} \tag{2-28}$$

where

$$H = Z_e Q\sigma_{y-s} + Z_e c_f + wQF_E \tag{2-29}$$

Torsional (Tripping) buckling of stiffeners:

The tripping of stiffeners is more likely to take place when the torsional rigidity of the stiffener is small. Once tripping occurs, the stiffener twists sideways about the edge of the stiffener web attached to the plating and the failure of a stiffened panel will occur. The buckled or collapsed plating is left with little stiffening and overall collapse may follow (Paik & Thayamballi, 2003).

The critical torsional buckling stress is given by:

$$\sigma_{cr-t} = \eta_{allow} C_T \sigma_{y-s} \tag{2-30}$$

where the torsional buckling coefficient C_T is defined as:

$$C_T = \begin{cases} 1.0 & \text{for } \lambda_T \le 0.2 \\ \dfrac{1}{\phi + \sqrt{\phi^2 - \lambda_T^2}} & \text{for } \lambda_T > 0.2 \end{cases} \tag{2-31}$$

$$\phi = 0.5\left(1 + 0.21\left(\lambda_T - 0.2\right) + \lambda_T^2\right) \tag{2-32}$$

The reference degree of slenderness for torsional buckling is given by:

$$\lambda_T = \sqrt{\frac{\sigma_{y-s}}{\sigma_{ET}}} \tag{2-33}$$

with the reference stress for torsional buckling defined as:

$$\sigma_{ET} = \frac{E}{I_P}\left(\frac{\varepsilon \pi^2 I_\varpi}{l^2} + 0.385 I_T\right) \tag{2-34}$$

where the degree of fixation ε is given by:

$$\varepsilon = 1 + \sqrt{\frac{l^4}{100 I_\varpi \left(\dfrac{s}{t_p^3} + \dfrac{4\left(e_f - 0.5 t_f\right)}{3 t_w^3}\right)}} \tag{2-35}$$

The polar moment of inertia of the stiffener I_P, the St. Venant's moment of inertia of the stiffener I_T, and the sectorial moment of inertia of stiffener I_ϖ are defined in the equations below depending on the type of stiffener considered.

$$I_P = \begin{cases} \dfrac{d_w^3 t_w}{3} & \text{Flat bars} \\ \dfrac{A_w\left(e_f - 0.5 t_f\right)^2}{3} + A_f e_f^2 & \text{Bulb flats, angles and T bars} \end{cases} \tag{2-36}$$

$$I_T = \begin{cases} \dfrac{d_w t_w^3}{3}\left(1-0.63\dfrac{t_w}{d_w}\right) & \text{Flat bars} \\ \dfrac{\left(e_f-0.5t_f\right)t_w^3}{3}\left(1-0.63\dfrac{t_w}{e_f-0.5t_f}\right) & \\ \quad +\dfrac{b_f t_f^3}{3}\left(1-0.63\dfrac{t_f}{b_f}\right) & \text{Bulb flats, angles and T bars} \end{cases} \tag{2-37}$$

$$I_{\varpi} = \begin{cases} \dfrac{d_w^3 t_{w}^3}{36} & \text{Flat bars} \\ \dfrac{A_f e_f^2 b_f^2}{12}\left(\dfrac{A_f+2.6A_w}{A_f+A_w}\right) & \text{Bulb flats, angles} \\ \dfrac{b_f^3 t_f e_f^2}{12} & \text{T bars} \end{cases} \tag{2-38}$$

where A_w and A_f are the areas of the stiffener web and flange. The web thickness t_w and the flange thickness t_f are to be defined as:

$$t_w(T) = t_{w_o} - t_{w(cor)}(T) \tag{2-39}$$

$$t_f(T) = t_{f_o} - t_{f(cor)}(T) \tag{2-40}$$

The depth of web thickness d_w, flange breadth b_f, and the distance from plate to center of flange e_f for different types of stiffeners are illustrated in Figure 2.5.

The ultimate strength of the stiffened panels is to be the minimum of the beam-column and torsional critical buckling stress, given by:

$$\sigma_{u(panel)} = \min\left(\sigma_{cr-bc}, \sigma_{cr-t}\right) \tag{2-41}$$

2.2.4 Uncertainties and Their Measures

In reliability analysis, all the variables are regarded as random variables with a certain level of uncertainty. One of the keys to a reliability analysis is the quantitative

measure of the uncertainties involved.

The uncertainties of the deck panel's ultimate capacity prediction include the following four groups:

- Variation in physical properties of materials including yielding stress and Young's modulus;
- Variation in thickness and geometry of the structures due to the fabrication tolerance and measurement errors;
- Uncertainty of the corrosion wastage prediction due to limited information on the variables;
- Modeling uncertainties due to assumptions made in analytical and prediction models, simplified methods, and idealized representations of real performances.

To develop the probabilistic model of loads, an understanding of the following is required:

- Vessel's reference cargo loading condition to analyze the uncertainties of the SWBM;
- Environmental condition and wave data, operational status and analytical computation model to analyze the uncertainties of the WBM.

The inherent uncertainties, such as variations in material properties and waves, arise from the natural variability in the random variable. These can not be reduced through better information. Some other uncertainties are due to simplified assumptions, uncertain definitions, and human errors related to the particular random variable. These types of uncertainties can potentially be reduced through better information (Paik &

Frieze, 2001).

When considering the uncertainties, the limit state associated with deck panel ultimate failure can be written as follows:

$$g(\cdot) = \chi_u \sigma_u - \sigma_x \tag{2-42}$$

where χ_u, the random variable representing the modeling uncertainties associated with the ultimate strength prediction of deck panel, is defined as:

$$\chi_u = \frac{\sigma_u \text{(experimental result)}}{\sigma_u \text{(prediction by calibrated formula)}} \tag{2-43}$$

The limit state function for deck panel ultimate failure, Eq. (2-42), contains three variables. However, it is recalled that the variable σ_u involves parameters related to geometric and material properties of various structural members in a functional form:

Unstiffened plate panel:

$$\sigma_{u-p} = \sigma_{u-p}\left(t_p, s, \sigma_{y-p}, E\right) \tag{2-44}$$

Stiffened panel:

$$\sigma_{u(panel)} = \sigma_{u(panel)}\left(t_p, t_w, t_f, d_w, b_f, s, l, \sigma_{y-s}, E\right) \tag{2-45}$$

Also the compressive stress σ_x is the function of SWBM, WBM and the section modulus:

$$\sigma_x = \sigma_x\left(M_{SW}, M_W, Z_d\right) \tag{2-46}$$

Therefore, the number of random variables considered in the limit state function is normally significantly more than in Eq. (2-42).

By regression analyses based on statistical observations, the probabilistic characteristics of the random variables for strength prediction and loads modeling can be ob-

tained. In addition to the mean value and standard deviation of the random variables, the type of the probability distribution has a crucial impact in reliability analysis. In the present study, these probabilistic characteristics of deck panel's strength prediction and applied compressive stress are compared and analyzed in a rational way. The details are included in Chapters 3 and 4.

2.2.5 Time-Variant Evaluation

Due to the corrosion, fracture, fatigue cracking, and thermal effect, the structural resistance, which is the ultimate strength of deck panel in this study, will be a function of time. Only the corrosion effects are considered in this study. The impact of cracking on structural safety is generally considered in a fatigue analysis. Thermal effect is important for the reliability study of FPSO structures.

Because of corrosion, the plate thickness of the deck panels (including deck plate and longitudinal stiffener) as well as the hull girder section modulus (HGSM) decrease with ship aging.

For the unstiffened plate panels, Eq. (2-13) can be presented with time-variant variables as follows:

$$\sigma_{u-p}(T)=\begin{cases}\sigma_{y-p} & \text{for } \beta(T)\le 1.58\\ \left(\dfrac{2.14}{\beta(T)}-\dfrac{0.89}{\beta(T)^2}\right)\sigma_{y-p} & \text{for } \beta(T)>1.58\end{cases} \tag{2-47}$$

where the time-dependent slenderness ratio of the plate is

$$\beta(T)=\frac{s}{t_p(T)}\sqrt{\frac{\sigma_{yp}}{E}} \tag{2-48}$$

Similarly, the ultimate strength of the stiffened panel can be expressed by:

$$\sigma_{u(panel)}(T) = \min[\sigma_{cr-bc}(T), \sigma_{cr-t}(T)] \tag{2-49}$$

Due to the time-variant corrosion effects, the thickness of each member of the panel varies with time. Thus, the beam-column critical buckling stress and torsional critical buckling stress are also functions of time according to the derived equations in Section 2.2.3.

The time-dependent HGSM to the deck $Z_d(T)$ is determined by taking into account the corrosion wastage information known in every location of the hull structure. By introducing the reduction factor of HGSM $\gamma_Z(T)$, it can be defined as:

$$Z_d(T) = [1 - \gamma_Z(T)] Z_{d_o} \tag{2-50}$$

where Z_{d_o} is the as-built HGSM to the deck. The as-built HGSM is a function of the sectional dimensions and the as-built scantlings of longitudinal components. As the corrosion takes place on the longitudinal members, HGSM decreases over time, as a result, stresses applied to a deck panel increase.

The time-variant reduction factor is considered as a very effective tool to measure the loss of HGSM during the vessel's entire life. During the last two decades, some analytical studies on HGSM of corroded aging ship hulls were carried out by assuming corrosion wastage of individual structural members (Hart et al 1985, Ivanov 1987, Guedes Soares & Garbatov 1996, Wirsching et al 1997, Ayyub et al 2000, Paik et al 2003).

Based on a dataset of as-gauged hull structures, a statistical study for the loss of HGSM was performed by Wang et al (2008). The dataset demonstrated a high variation of HGSM over time, and Weibull distribution is assumed to represent the time-variant reduction factor. It was also found that most of the publications overestimated the loss of HGSM. The comparisons for 20-year old vessels are listed in Table 2.1. However, it is

not easy to conclude what is the best way to calculate the reduction factor with the many uncertainties involved. In the present study, the calibrated formulas are applied to predict the loss of HGSM. The mean and standard deviation of $\gamma_Z(T)$ are given by (Wang et al 2008):

$$\begin{cases} \mu\left(\gamma_Z(T)\right) = 0.0062(T-6.5)^{2/3} \\ \text{stdev}\left(\gamma_Z(T)\right) = 0.008(T-6.5)^{3/4} - 0.0062(T-6.5)^{2/3} \end{cases} \tag{2-51}$$

Table 2.1 Reduction factor α_z of the ship structure at 20 years from selected publications (modified from Wang et al, 2008)

Reference	Mean	COV	Comments
Hart et al (1985)	3.19%	-	Calculated for a large tanker with corrosion control based on assumed corrosion rate
	13.38%	-	Calculated for a large tanker without corrosion control based on assumed corrosion rate
Ivanov (1987)	4.2%	-	Calculated for a bulk carrier based on assumed corrosion wastage
Guedes Soares & Garbatov (1996)	20%	0.3	Calculated for a single hull very large crude carrier (VLCC) based on assumed corrosion wastage
Wirsching et al (1997)	8%	0.25	Calculated for single hull tankers based on assumed corrosion wastage
Ayyub et al (2000)	7%	-	Calculated for a single hull tanker based on assumed corrosion wastage
Paik et al (2003)	12%	-	Calculated for a double hull tanker based on average corrosion wastage
	7.5%	-	Calculated for a conversion single hull FPSO based on assumed corrosion wastage
Wang et al (2008)	3.2%	0.593	Statistical result of hundreds single hull tankers
	3.6%	0.694	Calibrated result for hundreds single hull tankers based on statistical results

Also, structural loads have fluctuations and uncertain natures through the structural life. These characteristics are transferred directly to the load effects which is compressive stress σ_x in this study. The time-dependent nominal compressive stress of the deck panel can be written as:

$$\sigma_x(T) = \frac{M_T(T)}{[1-\gamma_Z(T)]Z_{d_o}} \tag{2-52}$$

Combining Eq. (2-40), (2-42), (2-44) and (2-47), the time-variant limit state function of the deck panel's ultimate strength failure can be presented as follows:

Unstiffend plate panel:

$$g(T) = \begin{cases} \chi_u \sigma_y - \dfrac{M_T(T)}{[1-\gamma_Z(T)]Z_{d_o}} & \text{for } \beta(T) \le 1.58 \\ \chi_u \left(\dfrac{2.14}{\beta(T)} - \dfrac{0.89}{\beta(T)^2} \right) - \dfrac{M_T(T)}{[1-\gamma_Z(T)]Z_{d_o}} & \text{for } \beta(T) > 1.58 \end{cases} \tag{2-53}$$

Stiffened panel:

$$g(T) = \chi_u[\min(\sigma_{cr-bc}(T), \sigma_{cr-t}(T)] - \frac{M_T(T)}{[1-\gamma_Z(T)]Z_{d_o}} \tag{2-54}$$

2.2.6 Prediction of Time-Variant Failure Probability

In general, the time independent failure probability of the deck panel can be computed from:

$$P_f = P(g \le 0) = P(\sigma_u \le \sigma_x) = \iint\limits_{g \le 0} f_{\sigma_u, \sigma_x}(\sigma_u, \sigma_x) d\sigma_u d\sigma_x \tag{2-55}$$

where $f_{\sigma_u, \sigma_x}(\sigma_u, \sigma_x)$ is the joint probability density function of ultimate strength σ_u and nominal compressive stress σ_x, and the domain of integration is over all values of σ_u and σ_x where g is not positive.

As indicated in the previous section, σ_u is a function of material properties and structural dimensions, while σ_x is a function of different variables that govern the applied loads M_T and HGSM Z_d, each of which may be uncertain. Therefore, the limit

state functions Eq. (2-1) and (2-2) can be generalized simply as $g(X)$, where X is the vector of all relevant basic variables. The generalization of Eq. (2-55) becomes:

$$P_f = P[g(X) \le 0] = \int \dots \int_{g(X) \le 0} f_X(X) dX \tag{2-56}$$

where $f_X(X)$ is the joint probability density function of the n-dimensional vector X of basic variables. The region of integration $g(X) \le 0$ denotes the space of limit state violation.

Furthermore, σ_u and σ_x are not independent. Dependence between basic variables usually adds complexity to a reliability analysis. However, the dependence structure between variables is not well known and the correlation matrix is not available. For practical consideration, in this study, the basic variables are assumed to be independent. Then, $f_X(X)$ is simplified as:

$$f_X(X) = \prod_{i=1} f_{x_i}(x_i) = f_{x_1}(x_1) \cdot f_{x_2}(x_2) \cdot f_{x_3}(x_3) \cdot f_{x_4}(x_4) \dots \tag{2-57}$$

with $f_{x_i}(x_i)$ the marginal probability density function for the basic variable x_i

Only in special cases, such as linear limit state function with all normally distributed random variables, can the integration of Eq. (2-56) over the failure domain be performed analytically (Stevenson & Moss 1970, Ang & Tang 1975, Melchers 1999). In general, limit state functions usually are not linear and the basic variables are unlikely to be all normally distributed. In addition, when the number of variables n exceeds a certain level ($n > 5$), the numerical integration cannot be considered feasible due to the growth of round-off errors and excessive computation times (Davis & Rabinovitz, 1975).

Therefore, simplification and numerical approximation need to be applied to pre-

dict the probability of structural failure (Mansour 1990). The following categories of probability approaches are widely used in marine-related reliability analysis:

- First Order Reliability Method (FORM)
- Second Order Reliability Method (SORM)
- Mean Value First Order Second Moment Method (MVFOSM)
- Response Surface Method (RSM)
- Monte Carlo Simulation Method (MCS)

The theory of each reliability method above is well established and can be found in Ayyub and McCuen (1997). FORM and SORM give approximate results on the limit state functions around the most probable points (MPPs). MVFOSM and RSM make approximations on the limit state functions around the mean point. Although MVFOSM and RSM are usually more effective, they can only provide a rough prediction of failure probability. FORM and SORM are asymptotically correct with respect to the reliability index while MCS provides "exact" failure probability because of the true limit state functions used. One drawback of using MCS is it is a time consuming approach. However, as computer capabilities have increased, MCS for structural reliability analysis has gained new respectability.

When the probabilistic characteristics of variables involved in the strength and stress calculation are available, a time-independent approach can represent the reliability at the initial phase of life, at some intermediate point in life or at the end of the structure's life. However, as a ship ages, the load-carrying capability of its structural components decreases and the uncertainties associated with its strength grows. In order to monitor ship structures during their lifetime, time-variant failures of probability need to be ob-

tained.

In time-variant reliability, the basic variables X will be substituted by stochastic processes $X(T)$. The failure probability of the deck panel at time t becomes:

$$P_f(T) = P[g(T) \le 0 \ \ddagger P[\sigma_u(T) \le \sigma_x(T)] = P[\sigma_u(T) \le \frac{M_T(T)}{Z_d(T)}] = \iint_{g[X(T)] \le 0} f_{X(T)}[X(T)] d\ X(T) \quad (2\text{-}58)$$

Figure 2.6 schematically shows the time-dependent reliability problem of the deck panels. The changes in instantaneous probability density functions $f_{\sigma_u}(T)$ and $f_{\sigma_x}(T)$ are also depicted in Figure 2.6.

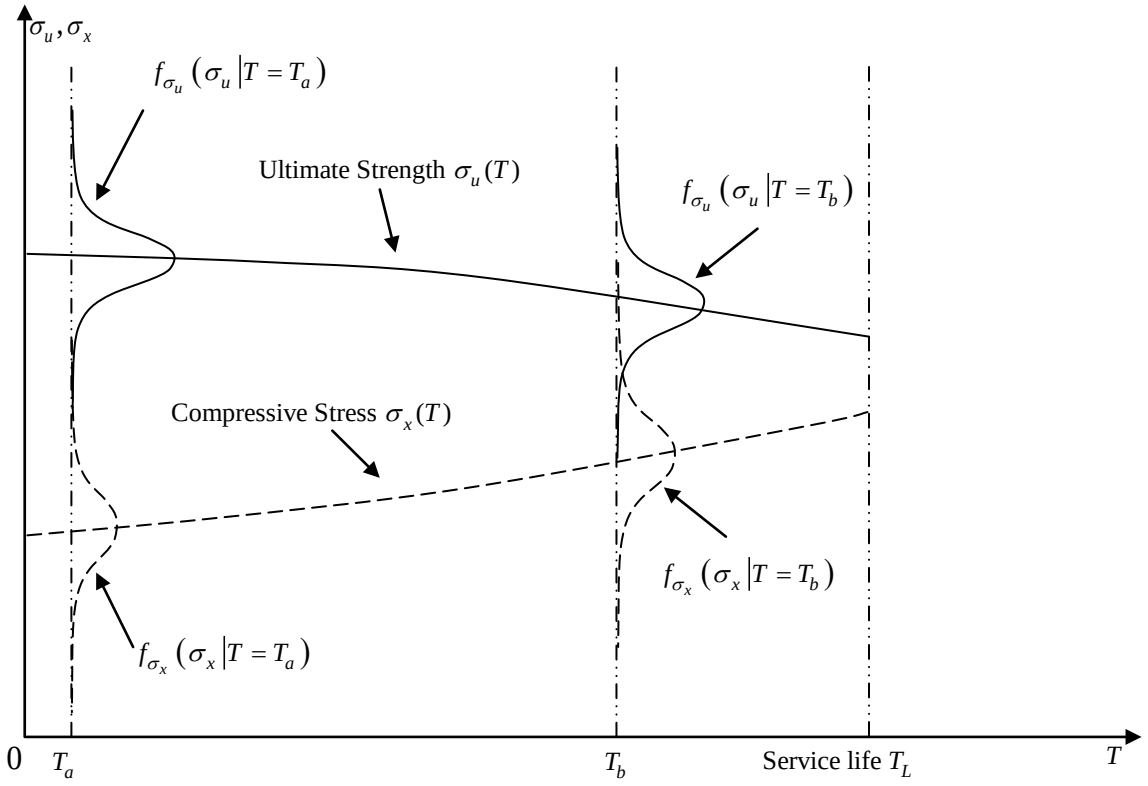

Figure 2.6 Schematic time-dependent reliability problem

With aging, the ultimate strength of the deck panel σ_u has a tendency to decrease

due to the corrosion wastage of individual structure members, while the applied compressive stress σ_x increases because of the decrease of the HGSM. Also, the uncertainties in both quantities usually increase with time. As shown in the figure, $f_{\sigma_u}(T)$ and $f_{\sigma_x}(T)$ become wider and flatter with time and the mean values of σ_u and σ_x also change with time.

The typical way to deal with the time-dependent reliability problem is to transform it to an equivalent time-independent reliability problem which can be solved using the previously mentioned reliability approaches (Guedes Soares & Ivanov 1989). In general, the variations of ultimate strength and compressive stress due to corrosion effects develop relatively slowly during the service lifetime. This allows a continuous reduction of structural capacity and an increase of compressive stress applied on the structure to be substituted by a series of discrete periods during which the strength and the load effects are modeled as constants, but discontinuities are allowed at the separation between time periods.

As shown in Figure 2.7, the stochastic process representation of the ultimate strength and compressive stress are substituted by piecewise discrete series of random variables.

The time-variant problem becomes a series of time-independent problems. In each period $\Delta T = T_L / N$, the stochastic load $M_T(\Delta T)$ is substituted by a random variable describing the largest load in that period of time. With this assumption, Eq. (2-58) becomes:

$$P_f(\Delta T) = P[\sigma_u(\Delta T) \le \frac{M_{T(\max)}(\Delta T)}{Z_d(\Delta T)}] \tag{2-59}$$

where $M_{T(\max)}(\Delta T)$ denotes the maximum total bending moment in the period ΔT. Giv-

en that during each period of time the ultimate strength of the deck panel $\sigma_u(\Delta T)$ and HGSM $Z_d(\Delta T)$ are constants, time-independent approaches such as Monte Carlo Simulation can be used to calculate the failure probability of the deck panel for each period. This is the justification to substitute the time-variant reliability problem by the time-independent reliability analysis.

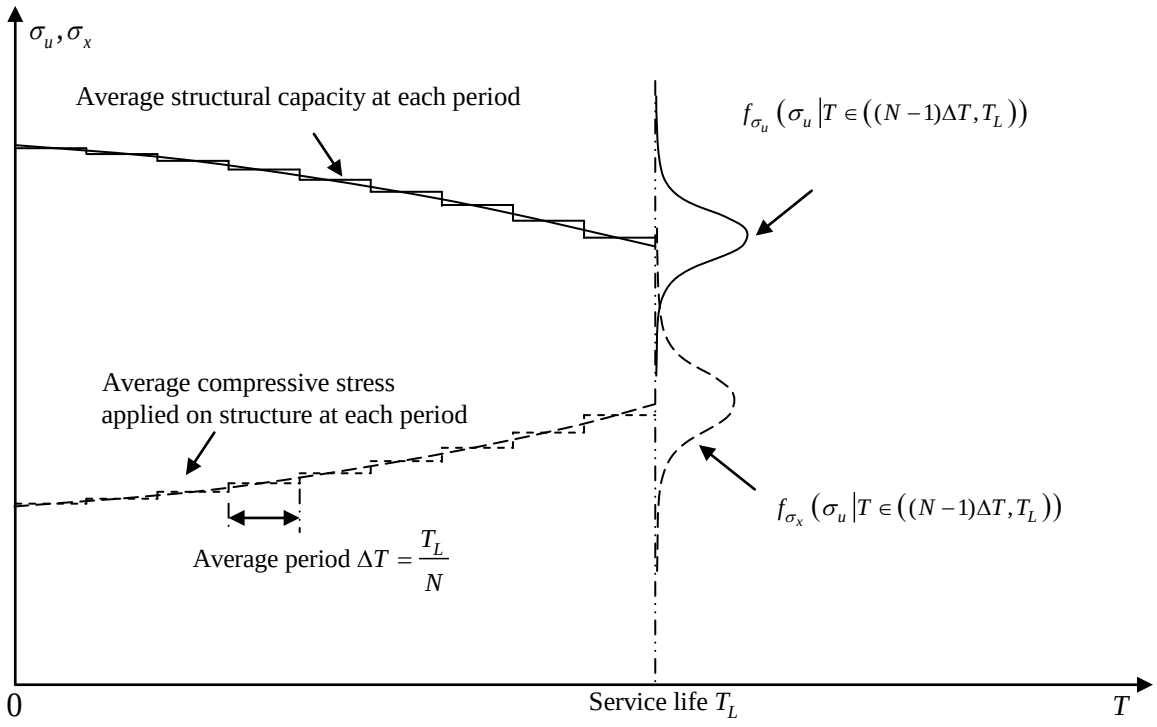

Figure 2.7 Schematic equivalent time-independent reliability problem

2.3 Target Levels of Failure Probability

In the marine industry, in-service inspections are required to ensure the safety and operability of the marine structures and prevent sudden failure due to degradation of the ultimate strength. According to Figure 2.1, selecting a target failure probability level P_f^*

(or equivalent reliability index β_R^*) is required in order to determine reliability-based inspection intervals for ship structures such as the deck panel. The relation between P_f and β_R may be estimated from the following equation:

$$P_f = \Phi(-\beta_R) \tag{2-60}$$

where Φ is the standard cumulative normal distribution function.

The selection of target failure probability levels is very difficult because the target values usually depend on type of structures, the reliability formulation, the consequences of failure, type of uncertainties, and the inspection and maintenance plan. In general, the target failure probability is selected based on the following methods (Paik & Frieze 2001, Ayyub et al 2002):

- *Expert Recommendations*: Based on prior experience, reasonable values may be recommended by a regulatory body or professionals for novel structures without a statistical database on failures.
- *Calibration*: The target values are calibrated from existing structures having a history of successful service.
- *Economic Considerations*: The target values are selected to minimize total expected costs over the service life of the structure.

The second approach is more commonly used since it is based on previously successful cases. Ideally, the successful design based on classification rules can be used to determine the implied reliability and to set the target level in a consistent manner, which can guide the future design and inspection plan. However, even for a particular type of structure, it is difficult to reach a consensus on commonly accepted target level due to the continuous development of rules, uncertainties of structures, and the various methods of

calculation, social concerns and political issues.

In the past thirty years, different target reliability levels have been developed for calibrating new and existing ship and offshore structures. The reliability indices for tanker structures are summarized in Table 2.2 based on available reliability analyses previously performed by different investigators. From the table, it is seen that the "first yield of hull girder" failure criterion yields high β_R since the criterion ignores loss of plate effectiveness. Therefore, it overestimates the reliability of the hull girder. For "hull girder ultimate strength" failure criterion, the calculated β_R values vary in a wide range. For the same vessels, the difference in reliability indices between stiffened deck panel and hull girder is about 0.5.

According to Paik and Frieze (2001), the regression equations of reliability indices over the period of 1991 to 2000 were obtained based on the review of previously related analyses. Although ship structures have become more efficient over time, the decreasing trend does not necessarily mean that the vessels themselves are becoming less reliable. It is because we increase our knowledge to reduce the scope of uncertainty by considering more sophisticated failure modes and more conservative assumption of loading effects.

However, it is very difficult to have an absolute way to determine the target reliability based on the widespread values summarized in Table 2.2. Due to the different calculation methods and the probabilistic models adopted for the variables, these values obtained from previous reliability analyses can be only considered as guidance for the relative effect of failure and consequence type. The target reliability indices for tanker structures suggested in the related papers are summarized in Table 2.3.

Table 2.2 Estimates of the reliability indices for tanker structures

Reference	Limit state	Analysis method	Reference time (years)	Reliability index	Comments
Mansour (1974)	First yield of hull girder	MVFOSM	20	4.9 ~ 6.4	12 sample tankers
Hart et al (1985)	Deck buckling	FORM+	1	2.2	Corrosion rate of 0.01 mm/year
			1	0.9	Corrosion rate of 0.15 mm/year
Thayamballi et al (1987)	Compressive failure of stiffened deck panel	MVFOSM	20	1.7 ~ 2.4	11 sample tankers
Shi (1992)	Hull girder ultimate strength	FORM	1	4.0	No corrosion considered
			20	3.26	
		FORM+	20	0.6	-
			1	1.2	
Chen et al (1993)	First yield of hull girder	MVFOSM+	20	3.4	Nominal corrosion margins in ABS (1993) are considered
	Hull girder ultimate strength			2.0	
Mansour & Hovem (1994)	Hull girder buckling collapse	FORM	20	1.49	-
	Buckling of longitudinals		20	0.57	
Mansour & Wirsching (1995)	Deck buckling	FORM	20	2.81	-
Kim & Kim (1995)	Compressive failure of stiffened deck panel	-	-	3.71 ~ 4.19	34 Sample ships
	Hull girder ultimate strength	-	-	2.88 ~ 5.41	
Casella et al (1997)	Hull girder ultimate strength	FORM	1	2.74	A double hull tanker
				3.39	A single hull tanker
Leheta & Mansour (1997)	Failure of stiffened deck panels	FORM	20	2.24	-
Wirsching et al (1997)	Hull girder ultimate strength	FORM+	20	1.88	Corrosion rate of 0.2mm/year
				2.35	Corrosion rate of 0.1mm/year
Mansour et al (1997)	First yield of hull girder	FORM	20	3.31	-
	Hull girder ultimate strength			0.81	
Casella & Rizzuto (1998)	Hull girder ultimate strength	FORM	1	3.4~3.77	Five different load combinations are considered
Paik et al (1998)	Hull girder ultimate strength	SORM+	1	2.2	-
			20	1.1/1.5	
Guedes Soares & Teixeira (2000)	Hull girder ultimate strength	FORM	1	2.34	-
Teixeira et al (2005)	Hull girder ultimate strength	FORM	1	4.07	-
			20	3.38	
Moan et al, (2006)	Hull girder ultimate strength	-	1	3.18/3.16	Based on the SWB calculation in IACS (2006)
				3.73/3.67	Consideration of heavy weather avoidance (HWA)
Parunov et al (2007)	Hull girder ultimate strength	FORM+	1	2.25	20-year corrosion from ship rules
			20	1.65	
ABS (2008)	First yield of hull girder	MVFOSM+	20	4.65 ~ 4.99	-
	Hull girder ultimate strength			2.34 ~ 3.63	

Table 2.3 Target reliability indices

Reference	Failure Mode	Target Reliability Indices	Comments
Lotsberg (1991)	Type I	3.09/3.71/4.26	Annual reliability indices are suggested considering these failure consequences: Not serious/Serious/Very serious
	Type II	3.71/4.26/4.75	
	Type III	4.26/4.75/5.20	
Guedes Soares et al (1996)	Primary^{+}	3.7/3.0	Annual reliability indices were adopted for the intact/corroded condition of ships. A linear relationship was assumed when the ships are in the state between these two values.
Mansour et al (1996)	Primary^{++}	4.5	Target safety indices relative to service life of tanker
	Primary^{+}	4.0	
	Secondary	3.5	
	Tertiary	3.0	
Mansour (1997)	Primary^{++}	5.0/6.0	Target reliability indices for the commercial ships/naval ships
	Primary^{+}	3.5/4.0	
	Secondary	2.5/3.0	
	Tertiary	2.0/2.5	
Assakkaf et al (2002)	Unstiffend / Stiffened Panel	3.0~4.0	Target reliability indices were recommended to derive partial safety factors for the reliability-based design.
	Grillages	2.0~3.0	
Sun & Guedes Soares (2003)	Primary^{++}	5.0/4.5	Annual target reliability indices are suggested for the intact/corroded condition of FPSO structures.
	Primary^{+}	3.7/3.0	
	Secondary	3.0/2.4	
	Tertiary	2.5/2.1	
Ku et al (2004)	Consequence I	4.5	Target reliability indices are established for Floating Production Installations based on the risk diagram developed by Whitman (1984). Economy impact is also considered.
	Consequence I^{+}	4.0	
	Consequence II	3.2	
	Consequence III	2.5	
	Consequence IV	1.5	
Moan et al (2006)	Primary^{+}	3.0/3.5	Annual target reliability indices are suggested considering the effects of HWA/No HWA.
Horte et al (2007)	Primary^{+}	3.09	Based on calculation of CSR benchmark tankers
ABS (2008)	Primary^{++}	4.8/4.0	Annual target reliability indices are suggested for the intact/time for repair condition of tankers and FPSOs.
	Primary^{+}	3.5/2.8	

Type I: ductile failure with reserve strength capacity resulting from strain hardening
Type II: ductile failure without reserve capacity
Type III: brittle fracture and instability
Primary^{+}: Hull girder ultimate failure
Primary^{++}: Hull girder initial yield failure
Secondary: Stiffened panel failure mode
Tertiary: Unstiffened panel failure mode
Consequence I: Total loss of vessel due to initial yield failure plus the loss of production for a time period of approximately two years
Consequence I^{+}: Total loss of vessel due to ultimate failure plus the loss of production for a time period of approximately two years
Consequence II/III/IV: One/two/three order of magnitude less than Consequence I in terms of financial loss

In common reliability-based structural design, the following inequality is to be satisfied (Mansour et al 1997).

$$\beta_{R-\text{primary}} > \beta_{R-\text{secondary}} > \beta_{R-\text{teritary}} \tag{2-61}$$

The primary failure modes include fully plastic moment mode, initial yield moment mode, and the ultimate collapse mode. The last one is always the governing mode of failure and is normally used in current design practice. The secondary mode of failure relates to failure of a stiffened panel of the hull while the tertiary mode of failure is associated with failure of an unstiffened plate between stiffeners.

Most of the target reliability levels were developed for the purpose of determining the implicit reliability level in an acceptable structural design and calibrating the structural design codes. Hull girder failure would have very serious consequences and reliability of hull girder is one of the most important parameters in the design stage. Therefore, it is not surprising that most of the structural reliability analysis publications focus only on the failure mode of hull girder collapse. The study on target failure probability of panel structures is rare. It is noteworthy that a large number of ultimate failures of panel structures will have catastrophic consequences on the structural integrity of hull girder. Thus, quantifying the implicit or target level of panel structures' reliability will gradually be valued.

Another point to note is that the target failure probability (reliability index) refers to a given time period, typically a year or the service life. Annual and service life values of failure probability can be related for ultimate failure events (relating to extreme loads for a certain period). In general, if the emphasis is cost-effectiveness of the ship, service life values are more relevant. Periodic inspection intervals of ship structures are usually calculated in years. Thus, annual failure probabilities are favored for inspection-related

studies.

In order to monitor the condition of the deck panels and plan follow-up actions accordingly, three levels of target failure probability (reliability index) are considered based on professional judgment applied to the available data (Table 2.4). From the review of historical data such as the ABS corrosion wastage database, it can be observed that substantial corrosion on deck panel in the first 10 years is limited. Therefore, it would be reasonable to target year 10 as the first time after construction to take the thickness measurement of the deck structures. This is the basis of the "Level 1" index. Normally, Special Surveys are conducted every five years. The "Level 1" reliability index would also trigger inspections at 5-years interval. According to industry practice, as shown in Figure 1.4, gauging surveys are to be conducted in the interval of a maximum 2.5 years for tankers reaching 15 years of age. The "Level 2" index is meant to reflect this enhanced inspection practice. According to ABS (2007a), plate components with corrosion wastage of 15% relative to the as-built thickness are to be replaced. This renewal criterion is used to obtain the "Level 3" index.

Table 2.4 Definition of the target failure probabilities (reliability indices) for ship structural inspection

Level of target failure probabilities (reliability indices)	Trigger
$P_{f1}^{*}(\beta_{R1}^{*})$	5-years interval
$P_{f2}^{*}(\beta_{R2}^{*})$	2.5-years interval
$P_{f3}^{*}(\beta_{R3}^{*})$	Renewal/Repair

2.4 Scheduling Thickness Measurements

As shown in Figure 2.1, the proposed procedure for inspection planning includes two stages:

- Predicting the time for the first thickness measurement;
- Updating the following inspection intervals according to available gauging data.

The inspection intervals are schematically depicted in Figure 2.8.

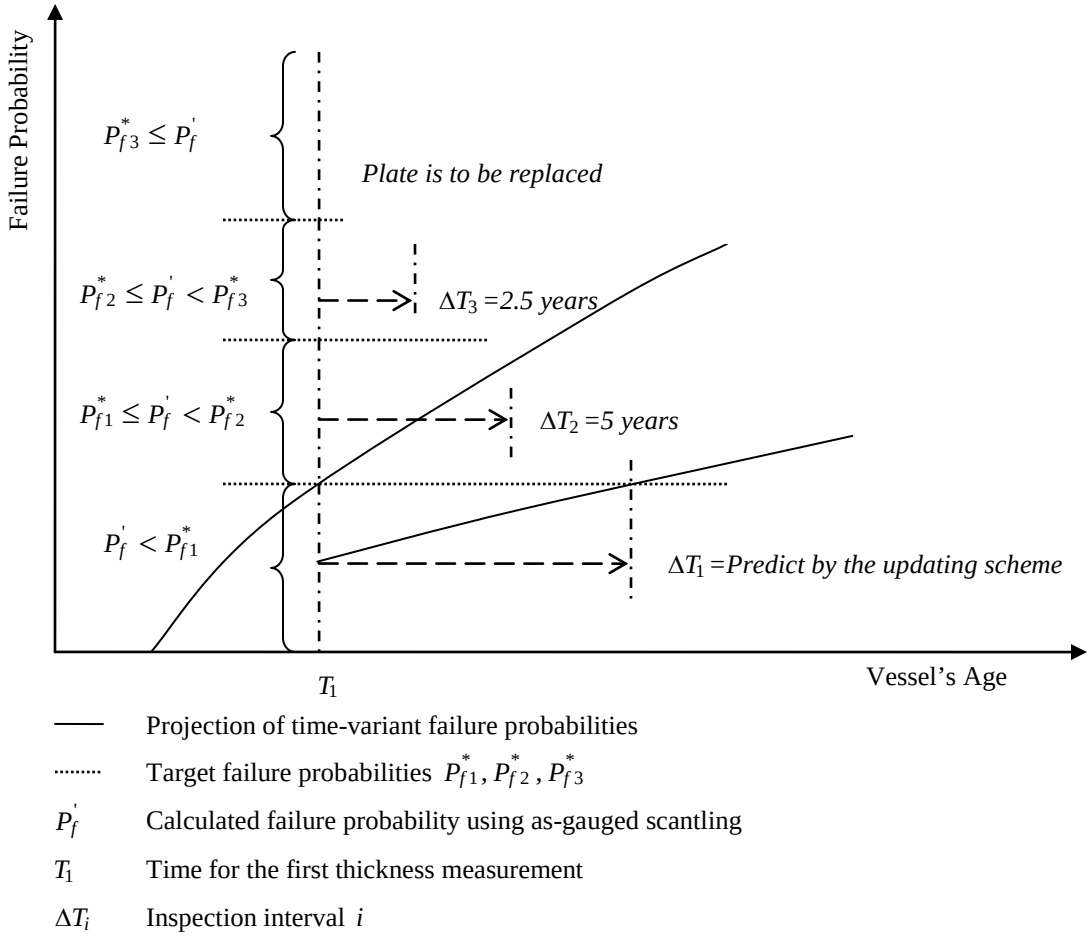

Figure 2.8 Schematic 1st and 2nd inspection intervals in terms of deck panel's ultimate strength failure

The first thickness measurement is to be conducted when projected time-variant failure probability (reliability index) of the deck panel P_f (β_R) becomes equal to or greater than the "Level 1" target value P_{f1}^{*} (β_{R1}^{*}). At the scheduled time, thickness mea-

surements of deck panels will be taken and the failure probability will be re-evaluated based on the as-gauged scantlings.

The second inspection interval can be determined by the following:

- If $P_f^{'}$ ($\beta_R^{'}$) is equal to or greater than P_{f3}^{*} (β_{R3}^{*}), the deck plate panel is considered not to have adequate reliability and the plate should be renewed to bring the failure probability back to a lower level.
- If $P_f^{'}$ ($\beta_R^{'}$) is equal to or greater than P_{f2}^{*} (β_{R2}^{*}), but lower than the "Level 3" target value P_{f3}^{*} (β_{R3}^{*}), the next inspection will be conducted in 2.5 years.
- If $P_f^{'}$ ($\beta_R^{'}$) is equal to or greater than P_{f1}^{*} (β_{R1}^{*}), but lower than the "Level 2" target value P_{f2}^{*} (β_{R2}^{*}), the next inspection will be conducted in 5 years.
- If the calculated failure probability (reliability index) $P_f^{'}$ ($\beta_R^{'}$) using the as-gauged scantling is lower than P_{f1}^{*} (β_{R1}^{*}), the next inspection can be predicted using the updating scheme.

Following the same procedure, all the inspection intervals for the deck plate panels over the lifetime of the vessel can be obtained.

The updating scheme includes three steps: 1) updating the corrosion model, 2) evaluating the failure probabilities of deck panels in the consequent years, and 3) determining the interval by comparing the projected failure probability with the target value P_{f1}^{*}.

Generally, the quantitative corrosion models applied in the marine industry represent the worst scenarios. After the first gauging survey, the corrosion models can be updated based on the application of Bayes' rule using the gauging data. After updating,

the corrosion model should predict corrosion wastage as close as possible to the actual degradation process rather than the worst scenario along the service life.

The corrosion updating process is schematically illustrated in Figure 2.9. It is assumed that the coating life T_c of the original corrosion model and the updated model remains the same. The measured corrosion wastage at inspection time T_i is considered as a random variable due to some measurement error.

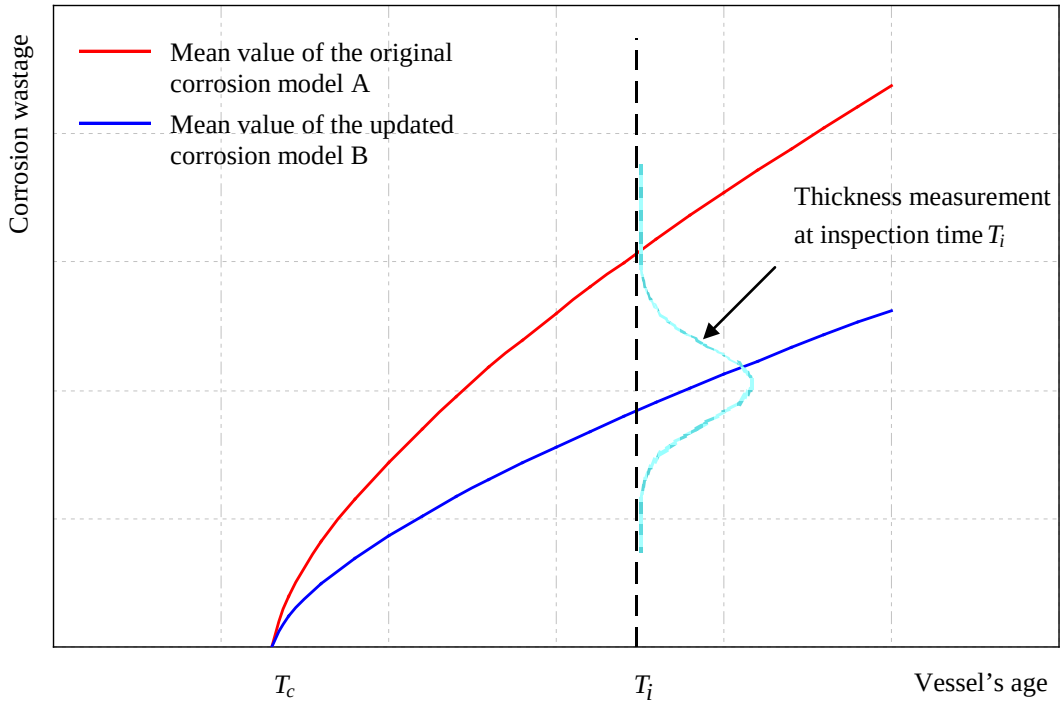

Figure 2.9 Schematic corrosion models for updating after inspection

Using Bayes' formulations, this method is summarized below:

$$f_{t_{cor}}\left(t_{cor}\middle|t_{insp}\right)=\text{CON}\cdot f_{t_{cor}}\left(t_{cor}\right)L_{insp}\left(t_{insp}\middle|t_{cor}\right) \tag{2-62}$$

where the marginal probability density function $f_{t_{cor}}\left(t_{cor}\right)$ is the prior probability density function of corrosion wastage. $f_{t_{cor}}\left(t_{cor}\middle|t_{insp}\right)$ is the posterior probability density function of corrosion wastage given measured wastage t_{insp} at inspection time T_i. L_{insp} is the like-

lihood function of corrosion wastage given t_{insp}. CON is a normalizing constant so chosen as to make the integral of the function equal to 1, so that it is indeed a probability density function.

2.5 Summary

This chapter develops the procedure employed for reliability-based inspection of ship structures. Scheduling a gauging survey for deck panels of oil tankers is used to demonstrate the procedure considering different failure modes of deck panels, which include ultimate strength failure of unstiffend plate panel, beam-column buckling and torsional buckling of stiffeners. The main phases of the procedure, which include prediction of time-variant failure probability, evaluation of the prediction based on target value, and determination of the interval of gauging survey, are discussed. Various types of uncertainty involved in the reliability assessment are taken into account. The detailed quantitative uncertainty models will be discussed in the following chapters.

CHAPTER 3

PROBABILISTIC CAPACITY PREDICTION FOR DECK PANELS OF TANKERS

3.1 Introduction

Failure of deck, bottom or side shell stiffened panels can lead to progressive collapse and ultimate hull girder failure (Paik & Frieze 2001). In order to evaluate the reliability level of the ship structures, determinations of the ultimate state, not only of the hull girder, but also of the entire group of local structural panels are required.

As indicated in Chapter 2, the ultimate failure of deck panels of a tanker occurs when experienced in-plane compression in the ship's longitudinal direction exceeds the ultimate strength of the deck panels. The ultimate strength of deck panels is formulated as a function of parameters related to geometric and material properties including plate thickness, yield stress and Young's modulus. In a reliability-based analysis, these parameters are treated as random variables. Their uncertainties must be quantified.

3.2 Previous Studies on Strength Model

The behavior strength of stiffened and unstiffened plate panels have been extensively investigated since the last century. Several advanced theoretical and numerical buckling and ultimate strength models have been developed in the 1990s and 2000s. Re-

views on pre-1975 available strength formulations for unstiffened and stiffened panels were carried out by Fanlkner (1975) and Guedes Soares & Soreide (1983). Recent studies on the ultimate strength of plate structures are reviewed in ISSC (2006c).

The maritime industry traditionally uses the critical (elastic–plastic) buckling strength, which is based on a plasticity correction to the elastic buckling strength of steel plates. The Johnson–Ostenfeld formulation is often applied for this approximation scheme. The estimated critical buckling strength is believed to be smaller than the plate ultimate strength (Paik & Thayamballi 2003).

3.2.1 Unstiffened Plate Panel

Since the first ultimate strength model for an unstiffened plate (Faulkner 1975) was introduced, studies on this topic have continued over several decades and significant progress has been achieved. However, due to the assumptions made and applicability, different formulations were developed. A review of the strength models with regard to both critical buckling and ultimate strength of a rectangular plate under uniaxial uniform compression is presented herein.

Table 3.1 and Table 3.2 list the commonly applied formulations in predicting the ultimate strength and critical buckling stress of an unstiffened plate. For comparison purposes, all the formulations are re-casted as functions of the slenderness ratio of the plate, which is defined as

$$\beta = \frac{s}{t_p}\sqrt{\frac{\sigma_{y-p}}{E}} \tag{3-1}$$

where σ_{y-p} is the yield stress of the material, s is the spacing between longitudinal stif-

feners, t_p is the thickness of the plate, and E is the modulus of elasticity. The proportional linear elastic limit P_r and Poisson's ratio ν of steel are assumed to be 0.6 and 0.3, respectively.

Table 3.1 Selected ultimate strength models for simple supported unstiffened plate panels under uniaxial compression along short edge

Reference	Description
ABS (2004), API (2004)	$\sigma_{u-p} = \begin{cases} \sigma_{y-p} & \text{for } \beta < 1 \\ \left(\frac{2}{\beta} - \frac{1}{\beta^2}\right)\sigma_{y-p} & \text{for } \beta \geq 1 \end{cases}$
ABS (2008a), Frankland (1940)	$\sigma_{u-p} = \begin{cases} \sigma_{y-p} & \text{for } \beta < 1.25 \\ \left(\frac{2.25}{\beta} - \frac{1.25}{\beta^2}\right)\sigma_{y-p} & \text{for } \beta \geq 1.25 \end{cases}$
DNV (1995)	$\sigma_{u-p} = \begin{cases} \frac{\sigma_{y-p}}{\sqrt{1+0.077\beta^4}} & \text{for } \beta \leq 1.90 \\ \frac{\sigma_{y-p}}{0.74\beta} & \text{for } 1.90 < \beta \leq 9.51 \end{cases}$
IACS (2008)	$\sigma_{u-p} = \begin{cases} \sigma_{y-p} & \text{for } \beta \leq 1.58 \\ \left(\frac{2.14}{\beta} - \frac{0.89}{\beta^2}\right)\sigma_{y-p} & \text{for } \beta > 1.58 \end{cases}$
Faulkner (1975)	$\sigma_{u-p} = \left(\frac{2}{\beta} - \frac{1}{\beta^2}\right)\sigma_{y-p}$ for $\beta \geq 1$
Mansour (1986)	$\sigma_{u-p} = \begin{cases} \frac{\pi}{\beta\sqrt{2.73}}\sigma_{y-p} & \text{for } \beta \geq 3.5 \\ \left(\frac{2.25}{\beta} - \frac{1.25}{\beta^2}\right)\sigma_{y-p} & \text{for } 1.0 \leq \beta < 3.5 \\ \sigma_{y-p} & \text{for } \beta < 1.0 \end{cases}$
Guedes Soares (1988)	$\sigma_{u-p} = \begin{cases} \left(\frac{1.6}{\beta} - \frac{0.8}{\beta^2}\right)\sigma_{y-p} & \text{for merchant ships} \\ \left(\frac{1.5}{\beta} - \frac{0.75}{\beta^2}\right)\sigma_{y-p} & \text{for naval ships} \end{cases}$

Table 3.2 Selected critical buckling stress models for simple supported unstiffened plates under uniaxial compression along short edge

Reference	Description
ABS (2004, 2008a)	$\sigma_{cr-p} = \begin{cases} \left(1-0.06\beta^2\right)\sigma_{y-p} & \text{for } \beta < 2.57 \\ \dfrac{3.98}{\beta^2}\sigma_{y-p} & \text{for } \beta \geq 2.57 \end{cases}$
IACS (2006), ABS (2008b)	$\sigma_{cr-p} = \begin{cases} \left(1-\dfrac{\beta^2}{14.4}\right)\sigma_{y-p} & \text{for } \beta < 2.68 \\ \dfrac{3.6}{\beta^2}\sigma_{y-p} & \text{for } \beta \geq 2.68 \end{cases}$
API (2004)	$\sigma_{cr-p} = \begin{cases} \dfrac{1}{1+0.019\beta^4}\sigma_{y-p} & \text{for } \beta < 2.69 \\ \dfrac{3.62}{\beta^2}\sigma_{y-p} & \text{for } \beta \geq 2.69 \end{cases}$
DNV (1995)	$\sigma_{cr-p} = \dfrac{\sigma_{y-p}}{\sqrt{1+0.077\beta^4}}$
DNV (2002)	$\sigma_{cr-p} = \begin{cases} \dfrac{\sigma_{y-p}}{1.15} & \text{for } \beta \leq 1.28 \\ \left(\dfrac{1.66}{\beta}-\dfrac{0.69}{\beta^2}\right)\sigma_{y-p} & \text{for } \beta > 1.28 \end{cases}$

3.2.2 Stiffened Panel

Similar to the studies on unstiffened plate panels, the first research on stiffened panels also dates back to the last century. Since the 1980s, highly appreciated works on developing both analytical and empirical strength models of plate structures subject to different loading and boundary conditions have been carried out (Carlsen 1980, Nishihara 1983, Smith et al. 1987, Herzog 1987, Hughes 1988, Bonello et al. 1992, Gordo & Guedes Soares 1993, Pu & Das 1994, Paik & Pedersen 1995, 1996, Paik & Lee 1998, Paik et al. 2000, 2001, Yanagihara et al. 2003, Harada et al. 2004, Steen et al. 2004, Byklum et al. 2004, Fujikubi 2005).

Based on re-evaluations of experimental data and empirical formulations by vari-

ous researchers, Herzog (1987) developed a simple ultimate strength model for the stiffened panels under uniaxial compression.

The ultimate strength $\sigma_{u(panel)}$ of a longitudinally stiffened panel is given by

$$\sigma_{u(panel)} = \begin{cases} m\sigma_{y(panel)}\left[0.5+0.5\left(1-\frac{\lambda_s}{2}\right)^2\right] & \text{for } \frac{s}{t_p} \le 45 \\ m\sigma_{y(panel)}\left[0.5+0.5\left(1-\frac{\lambda_s}{2}\right)^2\right] \cdot \left[1-0.007\left(\frac{s}{t_p}-45\right)\right] & \text{for } \frac{s}{t_p} > 45 \end{cases} \tag{3-2}$$

where the yield strength of the whole panel $\sigma_{y(panel)}$ is given by

$$\sigma_{y(panel)} = \frac{A_p\sigma_{yp} + A_s\sigma_{ys}}{A_s + A_p} \tag{3-3}$$

The area of the effective plating A_p and stiffener A_s are given by

$$A_p = st_p \tag{3-4}$$

$$A_s = d_w t_w + b_f t_f \tag{3-5}$$

The stiffener slenderness ratio λ_s is given by

$$\lambda_s = \frac{l}{\pi r}\sqrt{\frac{\sigma_{y(panel)}}{E}} \tag{3-6}$$

where l is the length of the stiffener, E is the modulus of elasticity, r is the radius of gyration of the stiffener with fully effective plating and is given by

$$r = \sqrt{\frac{I_e}{A_p + A_s}} \tag{3-7}$$

The moment of inertia of the stiffener with fully effective plating I_e is given by

$$I_e = \frac{st^3}{12} + st\left(z_0 - \frac{t}{2}\right)^2 + \frac{d_w^3 t_w}{12} + d_w t_w \left(z_0 - t - \frac{d_w}{2}\right)^2 + \frac{b_f t_f^3}{12} + b_f t_f \left(z_0 - t - d_w - \frac{t_f}{2}\right)^2 \quad (3\text{-}8)$$

The distance of neutral axis from the base line of the plate z_0 is given by

$$z_0 = \frac{st\left(\frac{t}{2}\right) + d_w t_w \left(t + \frac{d_w}{2}\right) + b_f t_f \left(t + d_w + \frac{t_f}{2}\right)}{A_p + A_s} \quad (3\text{-}9)$$

The corrective factor m, which accounts for initial deformation and residual stress, is defined as follows:

$$m = \begin{cases} 1.2 & \text{no or average imperfection and no residual stress} \\ 1.0 & \text{average imperfection and average residual stress} \\ 0.8 & \text{average or large imperfection and high residual stress} \end{cases} \quad (3\text{-}10)$$

According to Hughes (1988), three modes of collapse were considered while determining the ultimate strength of longitudinally stiffened panels due to compression. These modes include:

- Compression failure of the stiffener (Mode I Collapse)
- Compression failure of the plating (Mode II Collapse)
- Combined failure of stiffener and plating (Mode III Collapse)

The ultimate axial strength $\sigma_{u(panel)}$ for a longitudinally stiffened panel is defined as the minimum of the ultimate values of above three failure modes, namely:

$$\sigma_{u(panel)} = \min\left(\sigma_{uI}, \sigma_{uII}, \sigma_{uIII}\right) \quad (3\text{-}11)$$

The following equation (3-12) is an empirical formulation proposed by Paik and Lee (1996) for predicting the ultimate strength of longitudinal stiffened panels based on 130 collapse test data.

$$\sigma_{u(panel)} = \sigma_{y(panel)} \left[0.95 + 0.936\lambda_s^{\,2} + 0.170\beta^2 + 0.188\lambda_s^{\,2}\beta^2 - 0.067\lambda_s^{\,4} \right]^{-0.5} \quad \text{(3-12)}$$

where the plate slenderness ratio β is given by

$$\beta = \frac{s}{t_p}\sqrt{\frac{\sigma_{y(panel)}}{E}} \quad \text{(3-13)}$$

The stiffener slenderness ratio λ is given by Eq. (3-6). The comparison between the ultimate strength prediction by this formulation and the experimental data and numerical results validate the rationality of the formulation.

Some models have been adopted by industry organizations and classification societies, such as American Institute of Steel Construction (AISC), American Petroleum Institute (API), American Bureau of Shipping (ABS), Det Norske Veritas (DNV) and International Association of Classification Societies (IACS). The detailed mathematical expressions of these models can be found in the relative documents (AISC 2006, API 2000, ABS 2004, 2007a, 2007b, DNV 1995, 2002, IACS 2006b). The state of the art in ultimate strength of unstiffened and stiffened panel can be found in Ioannis & Das (2006).

3.3 Uncertainties of Ultimate Strength Prediction

3.3.1 General

Different classification rules and organizations' guides adopted different formulations for predicting the buckling stress and ultimate strength of plate structures. All the predictions are made by using theories based on the principles of mechanics. However, different assumptions of loading types and boundary conditions, and the approximations taken during computations will result in the differences between these formulations. The

uncertainties associated with the strength models usually cannot be eliminated. One method of study revealing this type of uncertainty is comparing their predictions with more accurate and reliable experimental results. The modeling uncertainty factor χ_u can be obtained by determining the ratio of the test results to the predicted results (Hoadley & Yura 1985). According to this definition, the strength prediction is on the conservative side if modeling uncertainty χ_u is greater than 1.0.

In this section, analyses of uncertainty present in buckling stress/ultimate strength prediction of plate structures are carried out based on the formulations widely applied by classification societies and organizations' guides.

ABS (2005) analyzed a total of 580 test data, which includes 221 tests for unstiffened plates and 359 tests for stiffened panels, to compare the predictions of several existing strength formulations for plate structures. Table 3.3 and Table 3.4 present the statistical characteristics, including mean and coefficient of variation (COV) of the modeling uncertainty for critical buckling stress and ultimate strength of the long plate panels under uniaxial compression along short edges.

Table 3.3 Mean and COV of modeling uncertainty of the critical buckling stress/ultimate strength formulations for unstiffened plate panel under uniaxial compression along short edges (ABS 2005)

	Critical Buckling Stress			Ultimate Strength	
	ABS (2004)	DNV (1995)	API (2000)	API (2000) & ABS (2004)	DNV (1995)
Mean	1.1149	1.1731	1.0747	0.9559	1.0744
COV	0.2845	0.2723	0.3050	0.1481	0.1495

Table 3.4 Mean and COV of modeling uncertainty of the critical buckling stress for the stiffened panel under uniaxial compression along short edges (ABS 2005)

	ABS (2004)	DNV (1995)	API (2000)
Mean	0.9914	1.3616	1.0350
COV	0.1799	0.3042	0.1915

3.3.2 Uncertainty Analysis

In order to determine the modeling uncertainty of the strength models that predict the buckling and ultimate strength of the deck panels, the datasets collected by Frieze (2002) are analyzed herein. The modeling uncertainty for each case is obtained by dividing the test results by the value obtained from the strength formulations. Then, the mean of all of these modeling uncertainty values is calculated along with the standard deviation so that the COV can be determined.

Since the datasets were collected from numerous publications and all the tests were performed for different research purposes, the geometries, boundary conditions and the material properties of the testing plate panels vary in a wide range. In order to assess the accuracy in terms of modeling uncertainty in the evaluation of the buckling stress and ultimate strength of the deck panels, some test data have been discarded through the following screening:

- The aspect ratio α and slenderness ratio β of the deck plates typically vary in a range of $2 \le \alpha \le 9$ and $1.2 \le \beta \le 3.5$, respectively. Therefore, only tested plate panels which satisfy the requirements of aspect and slenderness ratio are analyzed.
- Based on the assumption that the deck panels only experience in-plane compression in the ship's longitudinal direction caused by hull girder bending moment, only the datasets for panels under uniaxial compression along short edges are included.
- The assumption is that the deck plates are simply supported all around and are subjected to the uniaxial compression along short edges. Therefore, the

clamped supported test plates are excluded from the analysis.

Table 3.5 and Table 3.6 show the results of the modeling uncertainty χ of the selected strength prediction formulations.

Table 3.5 Mean and COV of modeling uncertainty of selected critical buckling stress/ultimate strength prediction formulations for unstiffened plate panel

Reference	Critical Buckling Stress		Ultimate Strength	
	Mean	COV	Mean	COV
IACS (2006)	1.07	12.62%	-	-
IACS (2007)	-	-	0.87	9.82%
ABS (2007b)	1.07	12.62%	0.90	9.95%
API (2000)	1.03	13.91%	0.98	9.41%
ABS (2004)	1.00*/1.05**	12.02%*/13.08%**	0.98	9.41%
ABS (2007a)	1.00*/1.05**	12.02%*/13.08%**	-	-
DNV (2002)	1.11	9.06%	-	-
DNV (1995)	1.14	13.11%	1.10	9.56%
Frankland (1940)	-	-	0.90	9.95%
Faulkner (1975)	-	-	0.98	9.41%
Mansour (1986)	-	-	0.90	9.95%
Guedes Soares (1988)	-	-	1.21	9.41%

Note: * For plate panels between angles or tee stiffeners

** For plate panels between flat bars or bulb plates

Table 3.6 Mean and COV of modeling uncertainty of selected ultimate strength prediction formulations for stiffened panel

Reference	Mean	COV
Paik & Lee (1996)	1.07	16.62%
Herzog (1987)	0.79	18.00%
ABS (2004)	0.96	20.76%
DNV (2002)	0.93	23.85 %
DNV (1995)	1.01	24.23%
API (2000)	1.13	22.89%
IACS (2007)	0.88	22.06%

Figure 3.1 and Figure 3.2 show the relationship between critical buckling stress/ultimate strength and slenderness ratio of the deck plate.

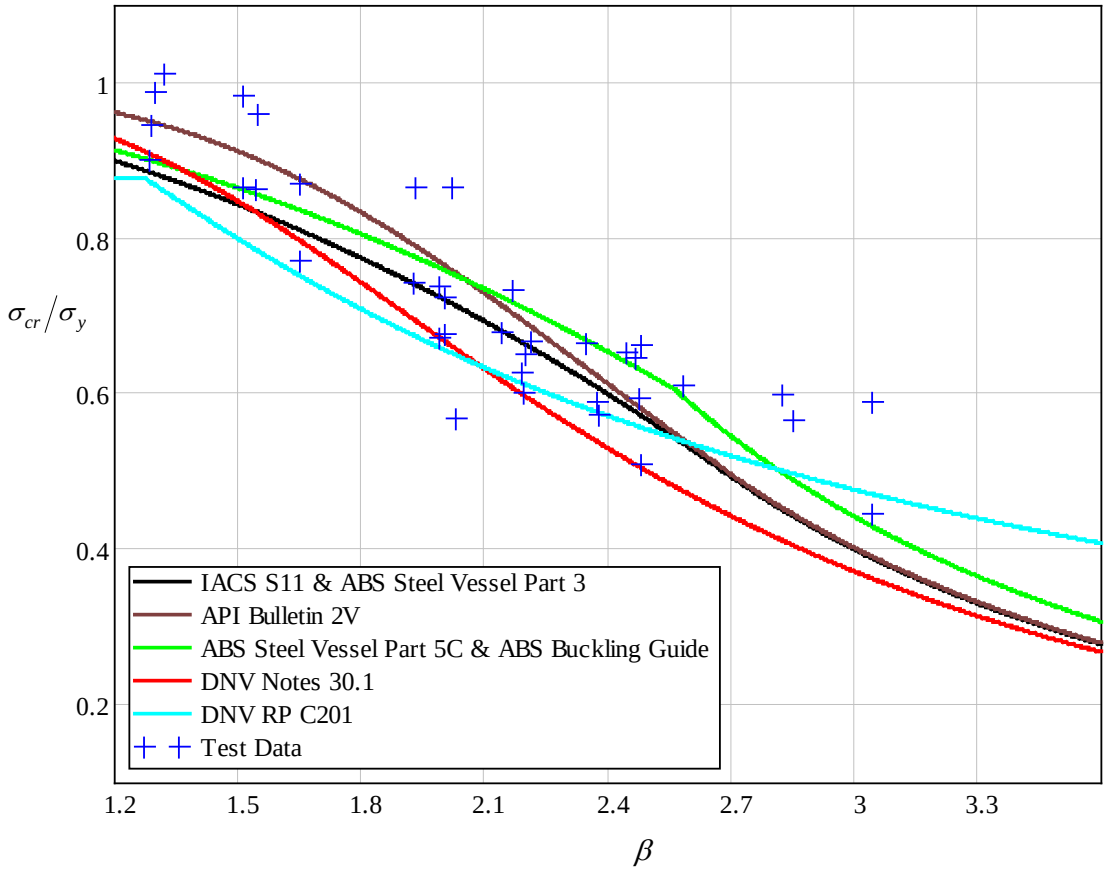

Figure 3.1 Comparison of selected formulations with test data for predicting the critical buckling stress of the unstiffend plate panel

From the results, the following conclusions may be drawn:

Unstiffened plate panel:

All the mean values of the modeling uncertainty for predicting the critical buckling stress are equal or greater than 1, while most of the mean values of the modeling uncertainty in the ultimate strength prediction formulations are less than 1. The corresponding COV for critical buckling stress formulations and ultimate strength is around 9~13%.

Stiffened panel:

The predictions of the ultimate strength vary in a wider range compared with unstiffened plate panel. The COVs are around 15% ~ 25%. The relatively large COV is not

surprising because there are still a lot of arguments about the methods for deriving the strength formulations of stiffened panel. In the present study, only uniaxial compression load is considered. When considering all possible loading combinations applied on the panels, even larger COVs of the strength formulations are expected.

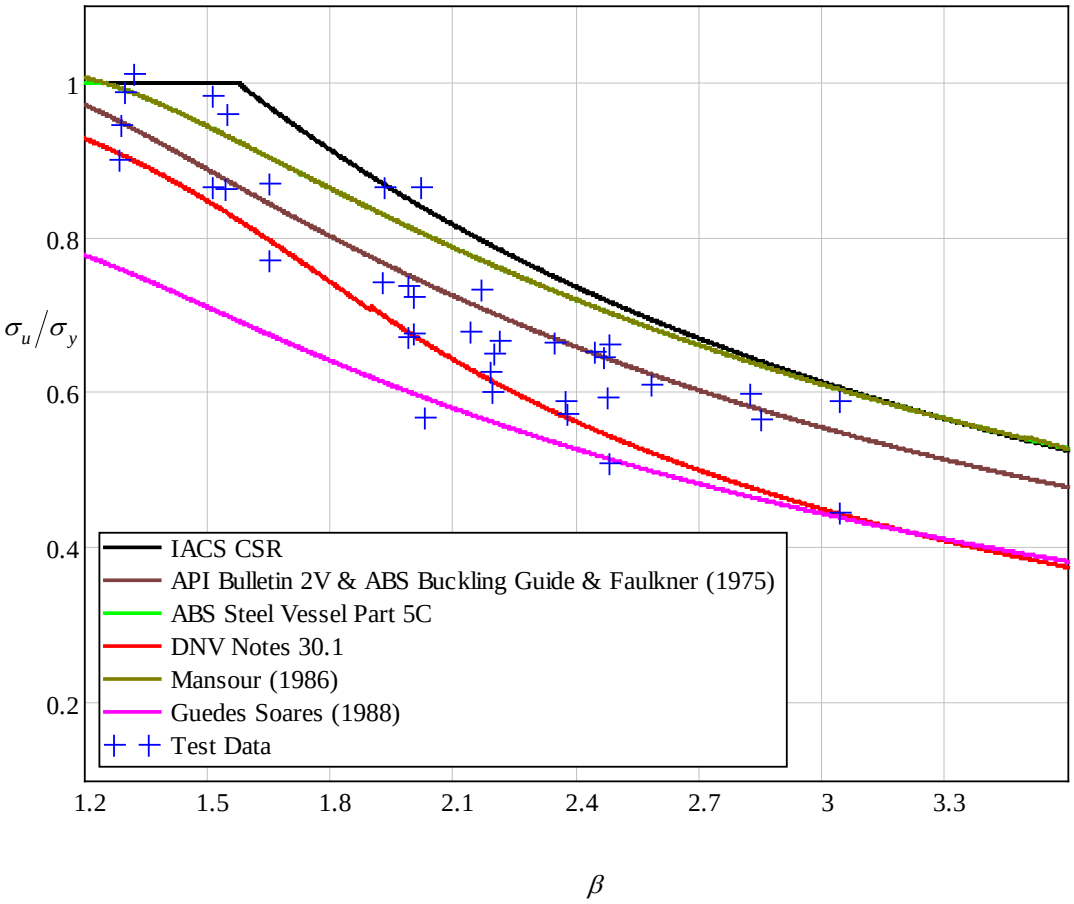

Figure 3.2 Comparison of selected formulations with test data for predicting the ultimate strength of the unstiffened plate panel

3.3.3 Results

It is revealed that the modeling uncertainty of ultimate strength prediction is significant. This study does not provide evidence about which formula has the smallest modeling uncertainties. Although the modeling uncertainty χ_u for some formulations is

greater than 1, those formulations are not necessarily conservative approaches because additional conditions, such as deductible corrosion and type of stiffeners, need to be included to evaluate the strength capacity. For example, certain corrosion wastage values are deducted before applying the equations in accordance to the classification rules. Therefore, the projected results will be close to actual values if the model uncertainty is taken into account. This conclusion will make the argument about the formulation application less important.

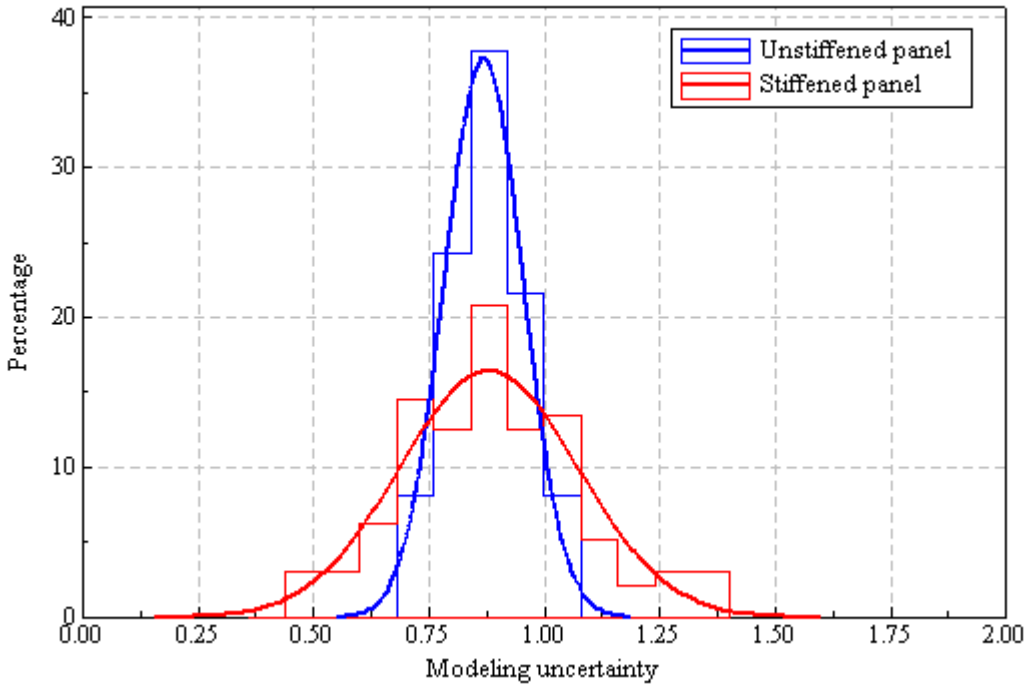

Figure 3.3 The modeling uncertainty of the adopted ultimate strength formulations for unstiffend plate panel and stiffened panel

In this study, the formulation adopted by IACS (2008b) is applied to predict the ultimate strength of the deck panels. As illustrated in Figure 3.3, the modeling uncertainty of the formulations predicting the ultimate strength of the deck panel is well fit by normal distribution.

Although the test is trying to capture close-to-actual results, the statistical results obtained here are different compared with the realistic value due to uncertainties involved in the test. The residual stress and imperfection of the plate were not considered in the test for plate capacity prediction. This will certainly reduces the uncertainties involved in the test. On the other hand, in the case of the test for stiffened panel capacity prediction, the uncertainties involved in the test increase due to the welding quality and the purpose of the test. In addition, more detailed and strict conditions may be applied to screen out the test data to yield a more proper estimation. In the present study, hence, mean value of 0.9 and COV of 15% are selected to present the modeling uncertainty for predicting the ultimate strength of the unstiffened plate panel and stiffened panel.

3.4 Uncertainties in the Material Properties of Steels for Shipbuilding

3.4.1 Uncertainties in Young's Modulus

According to Galambos & Ravindra (1978) and Mansour (1984), the uncertainties of Young's modulus (modulus of elasticity) E are due to different steel types, heat, mills, etc. The quality of the steel depends on the manufacturing process and source of material. In order to predict the influence of these factors on the uncertainties, some interesting works have been carried out by several researchers based on experimental data. The statistical characteristics from selected papers are summarized in Table 3.7.

It is difficult to accurately estimate the probabilistic characteristics of E based on a small sample size of data. To study the effect of the largest possible variation of the random variables, the calculated average mean and COV of E in Atua et al (1996) to-

gether with the assumption of normal distribution are applied in this study.

Table 3.7 Statistical information for Young's modulus E

Reference	Mean / Rule Value *	COV of E	Comments
Johnson & Opila (1941)	0.992	-	-
Caldwell (1972)	1	0.026	Normal distribution is assumed
Galambos & Ravindra (1978)	0.967	0.06	For both tension and compression behaviors
Mansour et al (1984)	1.002	0.031	Weighted average mean is calculated
Guedes Soares (1988)	-	0.04	Samples are from one steel mill
	-	0.06	Samples are from different steel mills
Atua et al (1996)	0.963	0.105	Normal distribution is fitted
Hess et al (2002)	0.990	0.0179	Lognormal or normal distribution are assumed

Notes: * Rule Value of $E = 2.06 \times 10^7$ N/cm^2 $= 2.1 \times 10^6$ kgf/cm^2 $= 30 \times 10^6$ lbf/in^2

3.4.2 Uncertainties in Yield Stress

Galambos & Ravindra (1978) suggested that numerical or statistical analysis on yield stress of steels is probably worthless due to the different measurement methods. Nevertheless, a significant amount of statistical studies have been conducted.

Table 3.8 provides a survey of a large amount of statistical information for yield stress for shipbuilding steels available in the public literature and ABS internal databases. The yield stress ratio is introduced presenting the ratio of tested results to the nominal values in the classification rules. It appears that the yield stresses of steels vary, and that these uncertainties can be traced down to steel grades, steel makers, steel production process, and so on. Based on the data collected by Kaufman and Prager (1990), Atua et al (1996) studied the effect of various independent variables to the yield stress ratio, which include steel type, plate thickness, temperature, production year, and direction of applied load. It was concluded that the yield stress ratio is mainly controlled by the steel type and

plate thickness.

In the present study, the statistical analysis of data from two major steel makers in Asia is performed. The data are collected from the coupon tests carried out in recent years. As shown in Table 3.9, most of the mean values of steel's yield stress are about 15~25% higher than nominal values specified in classification rules, and the COVs are smaller than 8%. Also from the table, the yield stress ratio of mild steels is usually higher than that of high tensile steel. By comparing the COVs in Table 3.9 with those summarized in Table 3.8, the smaller COVs may be attributed to the better quality control in the steel makers or the improvement of steel making technologies.

Table 3.8 Statistical information for yield stress σ_y for shipbuilding steels

Reference	Steel Type	Mean / Rule Value*	COV	Comments
Caldwell (1972)	-	-	0.066	Normal distribution was assumed.
Galambos & Ravindra (1978)	-	1.05	0.1	For flanges
		1.10	0.11	For webs
Russian shipyard (1979)	OS	1.298	0.079	-
	HT 36	1.155	0.05	-
Mansour et al (1984)	-	-	0.089	More than 60,000 samples with weighted COV, lognormal distribution was suggested.
Guedes Soares (1988)	-	-	0.10	Samples were from different steel mills.
	-	-	0.08	Samples were from one steel mill
Hess et al (2002)	OS	1.097	0.068	Based on the data from Galambos & Ravindra (1978), Mansour et al (1984) and Guedes Soares (1988). The lognormal distribution is assumed.
	HT 32	1.078	0.089	

Notes: * Rule value of yield stress:

235 Mpa (24 kgf/mm^2, 34×10^3 lbf/in^2) for ordinary steel (OS)

315 Mpa (32 kgf/mm^2, 46×10^3 lbf/in^2) for high tensile (HT) 32 steel

355 Mpa (36 kgf/mm^2, 51×10^3 lbf/in^2) for high tensile (HT) 36 steel

390 Mpa (40 kgf/mm^2, 57×10^3 lbf/in^2) for high tensile (HT) 40 steel

Table 3.9 Statistical analysis on the yield stress σ_y of shipbuilding steels provided by two major Asian steel makers in 2007

Reference	Steel Type	Mean / Rule Value *	COV	Number of Samples
Steel maker I	AH 32	1.222	0.058	325
	AH 36	1.148	0.082	165
	DH 32	1.223	0.061	72
	DH 36	1.196	0.075	178
	EH 32	1.434	0.044	188
	EH 36	1.300	0.058	220
Steel maker II	A	1.230	0.044	8365
	AH 32	1.206	0.042	7038
	AH 36	1.189	0.038	3041
	AH 40	1.197	0.042	367

The goodness-of-fit tests suggest that both the normal and lognormal distributions are applicable choices for describing the yield strength of steel. Since the focus of the present study is on aging ships, it is decided to assume that the mean value of steel's yield stress is 1.1 and 1.08 times the classification-defined nominal value for mild steel and high tensile steel, respectively, and the corresponding COV is 10%. The assumptions are considered conservative when compared with the data in Table 3.9. Further data analysis of other steel makers around the world can be helpful in building a more precise uncertainty model of yield stress of the shipbuilding steels.

3.4.3 Uncertainties Due to Manufacturing Tolerance in Shipbuilding

Efforts were made by many researchers to quantify the variations in the geometries of the plates and stiffeners since the 1970s. Several statistical analysis reports are available in public literature (Wierzchowski 1971, Caldwell 1972, Barsa & Stanley 1978, Daidola & Barsa 1980, Guedes Soares 1988, Hess & Ayyub 1996, Ayyub 1998, Assakkaf 1998, Hess et al 2002). Based on statistical information from selected sources, the

calculated average mean values and the COVs of the plate thickness t_p and stiffener spacing s are summarized in Table 3.10 and Table 3.11.

Not much literature is available for the statistical data on the length of plate (span of the stiffener) l. According to the Japanese shipbuilding quality standards, the following equation could be used to estimate the coefficient of variation for the span of stiffener (Basar & Stanley 1978, Daidola & Basar 1980):

$$\mathrm{COV}(l) = \frac{\delta_l}{\mu_l} = \frac{0.106}{l - 0.037} \tag{3-14}$$

where the standard deviation δ_l is 0.106 inch, the mean value μ_l is 0.037 inch smaller than the nominal span of stiffener l.

Table 3.10 Statistical information for as-built plate thickness t_{p_0}

Reference	Average mean	Average COV	Comments
Wierzchowski (1971)	-	0.04	-
Caldwell (1972)	$0.9652t_{p_0}$	$0.2301/t_{p_0}$	-
Hess et al (2002) (Calculation based on data from Daidola & Barsa 1980 and Ayyub 1998)	t_{p_0}	$0.6299/t_{p_0}$	Only including the measurement taken after construction
	t_{p_0}	$0.3531/t_{p_0}$	Only including the measurement taken before cut
	t_{p_0}	$0.4369/t_{p_0}$	Including all the measurements

Note: t_p = nominal plate thickness (mm)

Table 3.11 Statistical information for the stiffener spacing s

Reference	Average mean	Average COV	Comments
Wierzchowski (1971)	-	0.01	-
Caldwell (1972)	-	0.0019	-
Barsa & Stanley (1978), Daidola & Barsa (1980)	$s - 0.013$	$0.093/(s-0.013)$	Normal distribution was assumed.
Hess et al (2002)	$s - 0.2514$	-	Calculation based on data from Daidola & Barsa 1980 Sample size of 261

Note: s = nominal stiffener spacing (inch)

Hess & Ayyub (1996) studied the variability of the stiffener depth d_w, the stiffener web thickness t_w, the stiffener flange thickness t_f and the stiffener flange breadth b_f and drew the following conclusions:

- The measurements of the stiffener depth d_w may be affected by localized distortion in the plating, tilting of the stiffener web and flange, and variations in the surface coating.
- The factors influencing the measurement of the stiffener web thickness t_w and the stiffener flange thickness t_f include the measurement equipment, such as an ultrasound device or a micrometer, the amount of paint covering on the structures, and the degree of taper of the flange.
- Since using a ruler with the accuracy of 0.03125 inch, the measurement of the stiffener flange breadth b_f generally is not as good as other measurements with respect to the level of precision.

Table 3.12 summarizes the statistical results of stiffener geometries analyzed by Hess & Ayyub (1996).

Table 3.12 Statistical information for the stiffener geometries (Hess & Ayyub 1996)

	Mean / Nominal Value	COV	Distribution
Stiffener depth d_w	0.99545	0.0187	Normal
Stiffener web thickness t_w	1.25504	0.0904	Lognormal
Stiffener flange thickness t_f	1.13208	0.0917	Lognormal
Stiffener flange breath b_f	1.01444	0.0161	Lognormal

3.5 Summary

Summarizing the statistical information and re-evaluating the data based on literature review on strength variables, this chapter quantifies the probabilistic characteristics of these variables that are needed for reliability assessment of deck panels. These characteristics include the mean value, the coefficient of variation, and the underlying probability distribution type for each random variable. Table 3.13 gives a summary of these variables based on the analysis in Sections 3.3 and 3.4.

The values in Table 3.13 are recommended herein to be applied in the reliability assessment of the ship structural elements. Some of these values are selected based on engineering judgment, and these values can be updated when new data become available on the subject.

Table 3.13 Recommended probabilistic characteristic of strength basic random variables for reliability analysis

Variable		Mean / Nominal Value*	COV	Distribution
Young's modulus E (MPa)		0.963	10.5%	Normal
Yield stress σ_y (MPa)	Mild	1.1	10%	Lognormal
	High Tensile	1.08	10%	Lognormal
Plate thickness t_p (mm)		1.0	$0.4369/t_p$	Normal
Stiffener spacing s (mm)		$(s-0.3302)/s$	$2.362/(s-0.3302)$	Normal
Stiffener span l (mm)		$(l-0.9398)/l$	$2.692/(l-0.9398)$	Normal
Stiffener depth d_w (mm)		1.0	1.87%	Normal
Stiffener web thickness t_w (mm)		1.26	9.04%	Lognormal
Stiffener flange thickness t_f (mm)		1.13	9.17%	Lognormal
Stiffener flange breath b_f (mm)		1.0	1.61%	Lognormal
Modeling uncertainty χ_u		0.9	15%	Normal

Notes:* Nominal value refers to the classification defined value or reference value.

CHAPTER 4

PROBABILISTIC MODELING OF LOADS ON DECK PANELS

4.1 Introduction

Prediction of load effects experienced by ship structures over their lifetime is important. As indicated in Chapter 1, deck structures are mainly subjected to compression or tension in the ship's longitudinal direction due to bending of the hull girder. The hull girder total bending moment is normally considered as the sum of still-water and wave-induced bending moments.

Still-water bending moment (SWBM) arises primarily from the ship's self-weight, cargo or deadweight distribution, and buoyancy. It is different in each loading condition. Wave-induced loads include vertical and horizontal bending moments, torsional moment, shear force, hydrodynamic pressure, springing and slamming loads. They mainly depend on the ship's principal characteristics, the environmental conditions, and the operational conditions. Unlike containerships with wide cargo hatches, oil tankers have closed sections. Thus, the torsional stresses are smaller. The horizontal bending moment and shear force are excited by low frequency waves, and they usually do not result in significant stresses on ship structures. For deck structures, hydrodynamic pressure, springing and

slamming effects are negligible. Therefore, the most important wave load parameter considered in the present study for structure reliability analysis of tanker's deck panels isthe wave-induced vertical bending moment (WBM).

4.2 Modeling Still-Water Bending Moment

SWBM can be either taken from the rule-required value or calculated through analysis of the relevant load cases during operation. Development of theoretical models for SWBM was unsuccessful due to the lack of detailed data about the cargo loading process. Hence, the probabilistic method was considered to be a practical way to model the variability of SWBM based on statistical analysis of still-water loads collected from voyage data of the actual ships.

4.2.1 Previous Studies

Since the first attempt to present the still-water loads for ships in probabilistic terms by Trafalski (1967), a significant amount of work has been published. During the 1970s, several papers presented the results of probabilistic still-water loads by analyzing the real cargo plans of different ship types (Abrahamsen et al. 1970, Truhin 1970, Lewis 1973, Maximadji 1973, Król 1974, Ivanov & Madjarov 1975, Mano et al. 1977, Sőding 1979, Dalzell et al. 1979). Between the 1980s and 2000s, more data became available to researchers to refine the models and observe more details (Akita 1982, Guedes Soares & Moan 1982 1988, Kaplan et al. 1984, Guedes Soares 1984 1990a 1990b, Moan & Jiao 1988, Guedes Soares & Dias 1996, Guedes Soares & Dogliani 2000). Recently, statistical analyses were performed based on the loading conditions in the loading manuals (Horte

et al. 2007, Ivanov & Wang 2008) and loading instrument records (Rizzuto 2009). Summarizing the above mentioned research, together with reviews from ISSC (2006) and Moan (2006), the following conclusions can be drawn:

- The variations of SWBM appear to be random and are subjected to the extreme values governed by the operators.
- The probabilistic models of SWBM are ship type dependent. On a particular ship, different probabilistic models may be applicable depending on the operating routes.
- Normal distribution is one of the most common probability density functions to describe the probabilistic character of the SWBM during ships' operation.
- The containerships and general cargo ships generally have small variations in each cargo loading condition. Tankers and ore carriers, however, have very different loading conditions during operation. Different probabilistic models are proposed to present the results corresponding to each possible loading condition, such as ballast, partial loaded and fully loaded.
- Due to the gradual consumption of fuel and redistribution of fuel during the voyages, the difference in still-water condition between ship's departure and arrival may need to be taken into account.
- The still-water loads need to be modeled separately for the sagging and hogging conditions because of the different limit states applied.
- Due to the on-board control of still-water loads, ships normally operate with a lower level of SWBM when compared with the maximum allowed value. The

probability density function of SWBM may be truncated and the truncation limitation may be introduced as a random variable.

Some uncertainty models of SWBM suggested for tankers in selected publications are listed in Table 4.1. The big difference between the tabulated models reveals that there is a lack of consensus on defining the uncertainties of tankers' SWBM.

Table 4.1 Typical uncertainty models of SWBM for tankers

Reference	Uncertainty Model	Comments
Moan et al. 1977	Mean value is 0.514 (ballast) and 0.74 (loaded) times the reference value. COV is 1.444 (ballast) and 0.299 (loaded). Normal distribution was suggested.	Log-book data of 28 ballast conditions and 42 loaded conditions from 13 tankers Reference value was the minimum design value
Akita 1982, Kaplan et al 1984	COV is 0.989 (ballast) and 0.522 (loaded).	Data from log-books of 8 tankers.
Guedes Soares & Moan 1988	Mean value is 0.33 (ballast) and 0.263 (loaded) times the reference value. COV is 0.667 (ballast) and 1.21 (loaded). Normal distribution was suggested.	Voyage data of 225 ballast conditions and 738 loaded conditions from 39 single hull tankers Reference value was the maximum allowed value from classification.
Horte et al. 2007	Average mean value is 0.63 times the reference value. Average COV is 0.365. Normal distribution was suggested (mean is 0.7 times the reference value, COV is 0.286).	Loading conditions in the loading manuals of 8 double hull tankers Ballast conditions were ignored. Reference value was the maximum value in the loading manual.
Ivanov & Wang 2008	Mean value is 0.756 (ballast) and 0.593 (loaded) times the reference value. COV is 0.229 (ballast) and 0.772 (loaded). Normal, Weibull, Log-Normal and Rayleigh distributions appear to fit for the different considerations.	Hundreds of loading conditions in the loading manuals of 22 double hull and 12 single hull tankers Reference value was the permissible value approved by the classification society's rules.
Garre & Rizzuto 2009	Mean value is about 0.98 times the maximum value. COV is less than 0.04 times the maximum value.	Loading instrument records of 70 voyages of 2 double hull tankers

4.2.2 Uncertainty Analysis

It is desired to obtain a rational method for the estimation of a SWBM model to

perform a reliability analysis. It is important that the proposed method reflects actual cargo loading and ballasting operations of the tankers. However, it is very difficult to develop a general probabilistic model of SWBM for tankers. The main challenges to model the uncertainties in SWBM include:

- *Selection of methods for determining the probabilistic distribution of SWBM:* statistical analysis of real cargo plans for ships, statistical analysis of the loading manuals, or qualitative approach based on experience and engineering intuition.
- *Determination of the reference value of SWBM:* rule-permissible values, the largest SWBM in the vessel's loading manual, or the largest SWBM that is observed in the vessel operation.

Most of the statistical analyses were carried out by using the data of vessels built around the 1970s and 1980s. The result or observation from the analyses is outdated due to the adoption of double hull designs, which result in changes in tankers' compartmentation, widespread use of devices to monitor and control hull stress, and the increase in market demand. Therefore, there is a lack of persuasive evidence to consider adopting any of the models listed in Table 4.1 as a general uncertainty model of SWBM.

Over the years, more cargo loading conditions have been proposed and included in the tanker's loading manual. This has been taken into account by developing different uncertainty models to present the results for each loading condition. It is noted that some cargo loading distributions may or may not be regularly adopted throughout the entire service life of the tankers. However, most authors assumed that all the listed cargo loading conditions are equally likely to be applied on a regular basis. The assumption is,

however, not valid.

With the introduction of loading instruments, SWBM is closely monitored and controlled by the crew. Whether human interference needs to be considered in the uncertainty modeling remains in further discussions. The randomness of SWBM does not disappear but has changed. The impact of this change has not been investigated and discussed.

4.2.3 Probabilistic Model

In order to establish a notional probabilistic SWBM model reflecting generally-accepted practice, we adopt the following assumptions:

- A tanker operated alternately between the full (homogeneous) load condition, which results in sagging, and the ballast condition, which causes the hogging condition.
- The class-permissible SWBM is taken as the reference value $M_{SW\text{-Ref}}$.

  As one of the most important parameters for hull structural design, the class-permissible value of SWBM is always indicated in the loading manuals of all tankers to avoid the load exceedance. It is also programmed in the loading computers to serve as a limit during normal operations. The value could reflect the extreme value of SWBM during the vessel's lifetime, and the extreme value is applied herein for the reliability analysis.
- The value of SWBM is assumed to vary in a narrow range.

  Because the SWBM of a tanker is carefully monitored and controlled by crew with the assistance of onboard loading computers, the class-permissible

SWBM is unlikely to be exceeded by a large margin in normal operations. The uncertainties in this case are mainly due to the variation of tank filling level, consumption of fuel oil during sailing, and the accuracy of the loading computer. Studies have shown that the influences of filling levels are limited (Garre & Rizzuto 2009) and the difference in SWBM between departure and arrival conditions (due to fuel consumption) is often less than 5%. According to classification requirements, the accuracy of the loading computer is normally controlled to be within a range of 3%.

Therefore, the mean value and COV of the SWBM are defined by the following:

$$\mu\left(M_{SW}\right) = M_{SW\text{-Ref}} \tag{4-1}$$

$$\mathrm{COV}\left(M_{SW}\right) = 0.05 \tag{4-2}$$

The SWBM variable is assumed to follow the Type I extreme-value distribution, generally called Gumbel distribution. The probability density function is given by:

$$f\left(M_{SW}\right) = \frac{1}{v_{sw}}\left\{\exp\left[\frac{1}{v_{sw}}\left(u_{sw} - M_{SW}\right) - \exp\left(\frac{1}{v_{sw}}\left(u_{sw} - M_{SW}\right)\right)\right]\right\} \tag{4-3}$$

where u_{sw} and v_{sw} are the location and scale parameters, which is given by:

$$u_{sw} = \mu\left(M_{SW}\right) - \frac{0.5772\sqrt{6}}{\pi}\mathrm{Stdev}\left(M_{SW}\right) \tag{4-4}$$

$$v_{sw} = \frac{\sqrt{6}}{\pi}\mathrm{Stdev}\left(M_{SW}\right) \tag{4-5}$$

The assumption that the class-permissible SWBM equals the maximum SWBM for all intended cargo loading conditions may not be true in some cases. However, this value is a very important limit for a tanker operation. It represents a legitimate agreement

among all parties of the shipping industry – owner, shipyard, classification society, and flag state.

4.3 Modeling Wave-Induced Bending Moment

The WBM is a stochastic process due to the randomness of the ocean condition. An exact mathematical representation as function of time is very difficult to achieve. It can be represented by either short-term or long-term analysis. The short-term WBM corresponds to a random sea state which is considered as stationary with a duration of several hours. The long-term load effects may be obtained by combining short-term distributions for all sea states, wave headings and forward speeds. In assessing the reliability of ship structures, extreme values and long-term (annual or lifetime) prediction of WBM and their statistics are more beneficial.

4.3.1 Previous Studies

The prediction of wave-induced bending moment acting on an ocean-going vessel has been a focus in the marine industry. Since the 1940s, a number of published studies introduced calculations of WBM using approaches ranging from a simplified ship rule formulas-based method to a three-dimensional (3-D) nonlinear time domain approach. These methods were summarized and classified in ISSC (2006b).

Ever since the work of St. Denis and Pierson (1953) showing that the superposition technique can be applied to probabilistic predictions of ship motions and wave loads, there was a clear trend of using direct calculations to predict WBM. The common way to establish the design loads for direct calculations is by the long-term response analysis.

In principle, the long-term extreme value is obtained by combining the response of all the sea states. For the linear system, the long-term response can be effectively obtained. In the case of nonlinear response, time domain simulations are in general required and this is time consuming. Simplified methods and procedures have been developed in order to improve the efficiency of the direct calculation of the nonlinear long-term extreme value, such as Jensen et al (1990, 1996), Adegeest et al (2000), Baarholm and Moan (2000) and Pastor (2001). However, such direct calculation procedures are not very useful at the design state unless all the detailed sea states and route data of ships are known.

Application of probabilistic approaches is playing an increasing role in the marine industry, especially for the reliability analysis of ship structures. As pioneers, Ochi (1981) and Mansour (1981) indicated the principles of extreme value statistics and applied them in reliability-based designs for ships. Then, simplified methods were developed in the application of a direct long-term analysis for non-Gaussian response, such as Farnes (1990), Farnes & Moan (1994), Videiro & Moan (1999) and Jensen & Mansour (2002).

Comprehensive reviews of wave-induced load calculation methodology can be found in ISSC (2000, 2003, and 2006). The main focus here is the simplified closed form approaches. These approaches can be easily used to provide a reasonable estimate of probabilistic characteristics for reliability-based structural analysis. It is noted that these need to be compared with other comprehensive methods and validated against experimental and full-scale measurement data.

Kamenov-Toshkov et al. (2006) developed an approximate method for the calculation of the design WBM. With this method, the strength of aging vessels with any re-

maining life can be assessed. Based on the assumption that the probabilistic distribution of the WBM is identical at different time periods, this model was used to estimate the extreme loading condition.

Kawabe and Moan (2007) developed a method showing that the maximum wave-induced load with a probability exceedance around 10^{-8} in the long-term distribution is decided mostly by the most severe short-term wave conditions. However, Kurata et al (2008) pointed out the inaccuracy of the approach, which breaks down the long-term distribution into several environmental factors including significant wave height, average wave period and heading angle.

Derbanne et al (2008) carried out long-term predictions of nonlinear WBM through calculations of statistical parameters for every short-term sea state. By assuming the short–term characteristics are well described by the Weibull distribution, Weibull parameters of responses over the entire scatter diagram can be determined by calculating a limited number of short-term sea states.

4.3.2 Uncertainty Analysis

The predictions of WBM are influenced by many factors. The uncertainties are categorized by the following groups:

- **Uncertainties of ocean environment and wave data**

These uncertainties particularly vary between geographical regions, depending on the nature of wave conditions and the reported measurements and forecasts of wave. Notable research by Guedes Soares & Moan (1991) and Guedes Soares & Schellin (1996) found a significant difference between the vertical wave bending moment of tankers and

container vessels based on the North Atlantic data provided by BMT (1986) and the older data given by Walden (1964), Hogben & Lumb (1967). It was concluded that the predictions of wave loads should always refer to the latest available wave data. However, it was argued that the scatter diagrams issued by IACS (2000) would imply non-conservative predictions of severe sea states because the diagrams were developed based on observations on board and the influence of heavy weather avoidance (HWA) was not taken into account. Shu & Moan (2006) compared the IACS scatter diagrams with the recent wave data validated by wave buoy measurements, and showed that the new set of data implies larger response compared with IACS data. Since data relating to extreme sea states are more unpredictable than those for frequent sea states, extreme responses of large ships will be more uncertain than those of smaller ships.

- **Uncertainties of vessel's operation**

The uncertainties associated with a vessel's operation depend on the vessel's trading route, routing service and control of speed. The speed of the vessel has an impact on the WBM experienced by the vessel. Speed reduction reduces the loads. Sagli (2000) found that the average model uncertainty of a linear/nonlinear strip theory was about 0.9 in sagging, and 1.0 and 1.15 for hogging with speed of 0 and 0.14 knots, respectively. The COV was between 6%~9%. Moe et al (2005) carried out full-scale measurements of an ore carrier trading in the North Atlantic. They showed that the speed reduction is important during ballast condition in head sea but less important when the vessel is in cargo conditions in following sea.

The design wave loads should reflect the tanker's actual operation, which is dependent on the intended trading routes and services. The basis of tankers' design is the

assumption that tankers will be operating in the North Atlantic Ocean for a period of 20 to 25 years. However, as illustrated by Figure 4.1, only a small portion of crude oil is transported in the North Atlantic. This will have a huge impact on the reliability analysis when using the classification-developed WBM based on the notional assumption of routing plan.

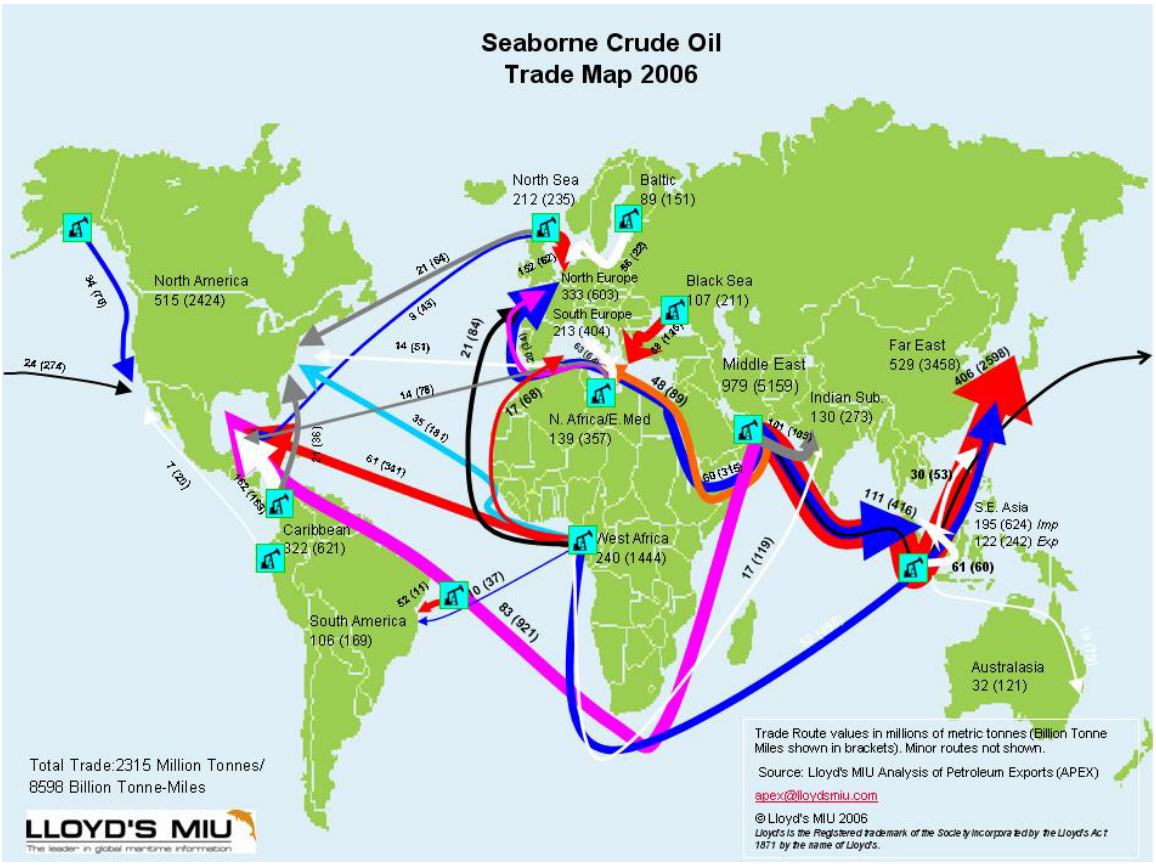

Figure 4.1 Seaborne crude oil trade map 2006 (Source: Lloyd's MIU)

- **Uncertainties of hydrodynamic analysis methods**

WBM is calculated using a two-dimensional (2D) strip theory or three-dimensional (3D) hydrodynamics model. Guedes Soares & Moan (1985) proposed model uncertainties for linear analysis by using different strip theories applied and nonlinear

correction factors. Using direct calculations of long-crested wave, Frieze et al (1991) suggested that a model uncertainty of the linear bending moments in an FPSO is a mean value of 0.9 and coefficient of variation (COV) of 0.1. Moan & Shu (2006) assessed the relative model uncertainty of 3D and 2D linear hydrodynamic analysis methods by comparing the most probable 20-year WBM estimated through long-term analyses. It is suggested that there is a 15%-25% difference between a linear 3D and 2D model and this should be reflected in the model uncertainty.

4.3.3 Probabilistic Model

To establish the link with the current practice, the IACS design value, which is based on a vessel operating in the North Atlantic environment with a design life of 20 years, is taken as the reference value of WBM. This technical basis is widely accepted by the industry. At the midship section area ($0.4L$ to $0.65L$ from the perpendicular at the aft end), the reference value is given by:

$$M_{W\text{-Ref}} = \begin{cases} -0.11 C_W L^2 B \left(C_b + 0.7 \right) & \text{kN-m} \quad \text{for sagging} \\ 0.19 C_W L^2 B C_b & \text{kN-m} \quad \text{for hogging} \end{cases} \tag{4-6}$$

where the wave coefficient C_W is to be taken as:

$$C_W = \begin{cases} 10.75 - \left(\dfrac{300 - L}{100} \right)^{\frac{3}{2}} & \text{for } 150 \le L \le 300 \\ 10.75 & \text{for } 300 < L \le 350 \\ 10.75 - \left(\dfrac{L - 350}{150} \right)^{\frac{3}{2}} & \text{for } 350 < L \le 500 \end{cases} \tag{4-7}$$

where L, B and C_b are the rule length, the breadth and the block coefficient of the vessel, respectively.

The mean value and COV of the WBM are assumed as follows:

$$\mu(M_W) = qM_{W\text{-Ref}} \tag{4-8}$$

$$\text{COV}(M_W) = 0.10 \tag{4-9}$$

where q is a constant. This factor depends upon whether or not annual loads instead of long-term (20 years) loads are considered in the reliability analysis. It can be determined by obtaining the ratio between the most probable largest WBM for 1 year and 20 year reference period. Moan et al (2006) carried out a series of long-term predictions of WBM at amidships at zero speed considering full scatter diagrams as well as those with truncation of waves (significant wave height is greater than 10m). They concluded that the ratio between the most probable largest value at exceedance probability of $10^{-6.7}$ and 10^{-8} varies between 0.80 to 0.85. The value of 0.80 can therefore be selected to scale the IACS design wave loads to the annual wave load used.

Based on a comprehensive study of WBM uncertainties, Moan et al (2006) compared the predicted WBM with the IACS value. Details of the study related to tanker structures are shown in Table 4.2. From the results, the combined effects result in a bias of about 1.10. Therefore, COV of the extreme WBM is assumed as 0.10.

Table 4.2 Uncertainty measure of wave loads (Modified from Moan et al 2006)

Uncertainty factor	Bias (predicted value compared with IACS value)	Comments
Wave scatter diagram	1.00~1.10	Wave buoy measurement vs. IACS scatter diagrams
Direction of waves	1.10	Unidirectional vs. uniformly distributed heading
Wave crest	1.10	Long-crested vs. short-crested
Heavy weather avoidance	0.80~0.90	Avoid significant wave height over 10m vs. no HWA
Speed	1.05~1.10	Full speed vs. zero speed
Hydrodynamic analysis	0.80~1.00	Linear 3D theory vs. linear 2D strip theory

The rational design of ships requires the consideration of the extreme value of the wave loading occur during the ship's service life. It has been shown that the extreme WBM can be described by a Type I extreme-value (Gumbel) distribution (Hart et al 1985, Mansour 1990, Guedes Soares 1996). The probability density function is given by:

$$f\left(M_W\right)=\frac{1}{v_w}\left\{\exp\left[\frac{1}{v_w}\left(u_w-M_W\right)-\exp\left(\frac{1}{v_w}\left(u_w-M_W\right)\right)\right]\right\} \tag{4-10}$$

where u_w and v_w are the location and scale parameters given by:

$$u_w=\mu\left(M_W\right)-\frac{0.5772\sqrt{6}}{\pi}\mathrm{Stdev}\left(M_W\right) \tag{4-11}$$

$$v_w=\frac{\sqrt{6}}{\pi}\mathrm{Stdev}\left(M_W\right) \tag{4-12}$$

4.4 Load Combinations

The respective extreme values of SWBM and WBM do not occur simultaneously due to their different random natures. To determine the extremes of the combined loads for reliability analysis, a rational load combination theory needs to be employed.

In general, there are two methods for combining the SWBM and WBM. The stochastic methods, such as the up-crossing method (Rice 1954), load coincidence method (Wen 1977), and Ferry Borges method (Ferry Borges & Castanheta 1971), combine the two stochastic processes directly, while the deterministic methods, such as the peak coincidence method and Turskra's rule (Turskra 1970), combine the characteristic values of the stochastic processes.

- **Peak coincidence method**

In the existing classification rules, such as ABS (2007b), IACS Requirements S11 (2006a), and IACS CSR (2008a), the combination of the SWBM and WBM follows the peak coincidence method. It assumes the extreme values of these two loads occur at the same instance. Hence, the maximum value of total bending moment at a reference time period of T_R is given by:

$$M_T\big|_{\max,T_R} = \max_{T_R}\left(M_{SW}(T)\right) + \max_{T_R}\left(M_W(T)\right) \tag{4-13}$$

This method is believed to be conservative. The corresponding value should be considered as an upper bound for the total loading process. However, the maxima of all load effects will not occur simultaneously. Thus, the maximum of the combined process is smaller than the sum of the maxima of the individual loads.

- **Turskra's rule**

Turkstra's rule only considers the points when one of the other processes is at its maximum value. According to this rule, the extreme value of one load is combined by the companion values of the other loads. Thus, the total extreme moment can be defined as the maximum of two formulations:

$$M_T\big|_{\max,T_R} = \max\left(\max_{T_R}\left(M_{SW}(T)\right) + M_W^+, \max_{T_R}\left(M_W(T)\right) + M_{SW}^+\right) \tag{4-14}$$

where $\max_{T_R}\left(M_{SW}(T)\right)$ and $\max_{T_R}\left(M_W(T)\right)$ are the extreme value of the SWB and WBM in a reference time period of T_R, M_W^+ and M_{SW}^+ are their corresponding companion load values. Typically, they are taken as the mean value of $M_W(T)$ and $M_{SW}(T)$.

Turkstra's rule provides a good approximation for linear combination of independent processes. However, it is indicated in Wen (1977) that this rule is not conservative

for the estimation of failure probability. Also, this method is unsatisfactory when SWBM and WBM have the same magnitude (Casella & Rizzuto, 1998).

- **Up-crossing method**

If SWBM and WBM are considered as mutually independent continuous processes, the probability distribution of the total bending moment at a time interval $[0,T]$, can be obtained using the assumption that the up-crossing follows a Poisson distribution:

$$F_{M_T} = \exp\left(-\int_0^{T_R} o(m,T)dT\right) \tag{4-15}$$

where $o(m,T)$ is the up-crossing rate of the threshold level $M_T = m$ at time T.

The expected up-crossing rate may be determined by using Rice's formula (Rice 1946), and the up-crossing formula can be represented by a simple upper bound (Melchers 1987):

$$o(m) \le \int_{-\infty}^{\infty} o_{M_{SW}}(i) f_{M_W}(m-i)di + \int_{-\infty}^{\infty} o_{M_W}(i) f_{M_{SW}}(m-i)di \tag{4-16}$$

where $o_{M_{SW}}(i)$ and $o_{M_W}(i)$ are the up-crossing rate for the process $M_{SW}(T)$ and $M_W(T)$. According to Larrabee (1978), the Eq. (4-16) is exact since SWBM and WBM satisfy the following conditions:

$$P\left[M_{SW}(T) > 0 \cap M_W(T) < 0\right] = 0 \tag{4-17}$$

$$P\left[M_{SW}(T) < 0 \cap M_W(T) > 0\right] = 0 \tag{4-18}$$

- **Load coincidence method**

Wen (1977) presented this method to calculate the up-crossing rate by considering up-crossings of each process acting alone as well as both processes overlapping. Taking

into account the load occurrence rate, intensity variation, random duration of each occurrence, and simultaneous occurrence of WBM and SWBM, the probability distribution of the maximum combined load effect over a given time interval can be obtained. According to Wen (1990), this method is good regardless of the number of the processes considered, and is always on the conservative side.

- **Ferry Borges Method**

Ferry Borges and Castanheta (1971) proposed a simple model assuming that the loads change intensity after each time interval, during which they remain constant. The intensity of loads in each time interval is an outcome of identically distributed and mutually independent random variables. This model requires all intervals to be of equal duration and gradually establishes better approximation with the increase of the corresponding period. The assumption of independence between successive cycles of response is not exact but is considered reasonable (Waston 1954).

Considering still-water and wave-induced load processes $M_{SW}(T)$ and $M_W(T)$ with durations T_1 and T_2, such that $T_1 > T_2$, the probability distribution of the maximum of the combined processes during time T_R can be determined by:

$$f_{M_T}(x) = \left\{ \int_{-\infty}^{x} f_{M_{SW}}(z) \left[F_{M_W}(x-z) \right]^{T_2/T_1} dz \right\}^{T_R/T_1} \tag{4-19}$$

When T_1/T_2 is an integer, which is satisfied for most cases when $T_1 \gg T_2$. Within the duration of T_1, the maximum value of a linear combination of M_{SW} and M_W can be expressed as (Mano & Kawabe 1978):

$$M_T\big|_{\max,T_R} = \max_{T_R}\left(M_{SW} + M_W\right) = M_{SW} + \max_{T_1/T_2}\left(M_W\right) \tag{4-20}$$

It has been verified that the combined value from the Ferry-Borges and Castanheta method is very close to the one obtained by using the up-crossing method. Hence, the Ferry-Borges and Castanheta method is believed to be accurate and efficient (Guedes Soares 1992, Wang & Moan 1996).

- **Load combination factor method**

For practical design and reliability analysis consideration, the load combination factors for SWBM ψ_{SW} and WBM ψ_W are introduced to estimate the total bending moment M_T:

$$M_T = \psi_{SW} M_{SW} + M_W = M_{SW} + \psi_W M_W \tag{4-21}$$

These load combination factors are used to account for the correlation between loads and the probability of simultaneous occurrence of their maximum values.

The load combination factors are usually calculated using the Ferry-Borges method based on an assumed operating scenario (Guedes Soares & Moan 1985, Mansour 1997). Through case studies for a FPSO, Wang & Moan (1995) compared the commonly applicable load combination methods and concluded that the stochastic methods all lead to identical predictions, the peak coincidence method is very conservative and Turkstra's rule underestimates the combined value.

When the extreme distributions are considered at a 0.5 exceedance level, the combination factor ψ_W can be determined by solving the following relationship (Guedes Soares 1992, Dogliani 1995):

$$F_{M_T} = F_{M_{SW}}(T) + \psi_W F_{M_W}(T) \tag{4-22}$$

Then ψ_W is given by:

$$\psi_W = \frac{F_{M_T}^{-1}(0.5) - F_{M_{SW}}^{-1}(0.5)}{F_{M_W}^{-1}(0.5)} \tag{4-23}$$

The exceedance level of 0.5 was chosen based on engineering judgment. It is not too different from the probability of exceedance of the most probable largest value of wave-induced load effects derived from a long-term distribution. The value of ψ_W does not change significantly over a wide range of the exceedance probability (Casella et al, 1996) and can be between 0.50 and 0.90 (Guedes Soares 1992).

The load combination factors are dependent on the probabilistic characters of the SWBM and WBM, as well as the reference period. Indicated in IACS CSR (2008a), the load combinations factors are determined as a function of loading conditions, location of structures and stress components.

Associated with the selected values of SWBM, WBM and the annual reduction factor in previous sections, the load combination factor ψ_W presented in this study is considered to be 0.9375. The total bending moment representing annual load is expressed as:

$$M_T = M_{SW} + 0.9375 M_W \tag{4-24}$$

This value is an approximation based on server sea state (stationary condition) and the assumption that this severe sea state is the most important sea condition as far as the load combination factor is concerned.

4.5 Summary

Based on literature review and rational uncertainty analysis, the probabilistic models of SWBM and WBM are proposed in this chapter. Combining these two random

processes using combination factors, the total loads experienced on the deck panels can be obtained.

Table 4.3 summarizes the probabilistic characteristics of the load variables recommended herein for assessment of the ship structures. Some of these values are based on engineering judgment. They might not be applicable in every case, but they establish a direct link between reliability analysis and current industry practice.

Table 4.3 Random variables in loading for the reliability analysis

Variable	Mean	COV	Distribution Type
M_{SW}	$M_{SW-\mathrm{Ref}}$	0.05	Type I Extreme
M_W	$qM_{W-\mathrm{Ref}}$	0.10	Type I Extreme
q	0.80	-	Deterministic
ψ_W	0.9375	-	Deterministic

Notes: $M_{SW-\mathrm{Ref}}$ is taken as the classification permissible SWBM

$M_{W-\mathrm{Ref}}$ is taken as the classification maximum design value, which is given by Eq. (4-6)

q is considered as a reduction factor for annual loads.

CHAPTER 5

DEVELOPMENT OF A TIME-VARIANT PROBABILISTIC CORROSION MODEL – APPLICATION TO DECK LONGITUDINAL PANELS OF TANKERS

5.1 Introduction

Corrosion is one of the most primary age-related deteriorations encountered by ship structures. In order to avoid any potential casualties due to this type of deterioration, the effect of corrosion was studied for analyzing the structural degradation of ships.

According to the mechanics, corrosion is categorized as general (uniform), pitting, grooving and weld metal corrosion. In general, the localized corrosion can cause oil or gas leaks, while the general corrosion is more likely to affect structural strength. Although both localized and general corrosion must be included in corrosion management and control, it is validated using nonlinear finite element analysis that the pitting loss of material is assumed to be equivalent to the uniform corrosion loss by averaging the readings from thickness measurement (Paik et al. 2003). Therefore, only general corrosion wastage is considered in this study.

5.2 Previous Research on Corrosion Models

In general, common causes of corrosion in ship hull structure include galvanic

corrosion, direct chemical attack and anaerobic corrosion. Starting with a linear corrosion model proposed by Southwell et al. (1979) based on experimental evidence, many corrosion wastage models have been proposed and widely accepted for the prediction of corrosion wastage in the marine industry. This section reviews the mathematical models for predicting time-variant corrosion wastage.

5.2.1 Conventional (Linear/Steady-state) Models

In the beginning, the conventional corrosion models were developed with a constant corrosion rate to present a linear relationship between the material lost and time. After several further studies, a nonlinear model was proven to be more appropriate. Southwell et al. (1979) proposed a linear, Eq. (5-1), and a bilinear equation, Eq. (5-2), respectively, to estimate the corrosion wastage thickness.

$$t_{cor}(T) = 0.076 + 0.038T \tag{5-1}$$

$$t_{cor}(T) = \begin{cases} 0.090T & 0 \le T < 1.46 \\ 0.076 + 0.038T & 1.46 \le T < 16 \end{cases} \tag{5-2}$$

Melchers (1998) suggested a trilinear, Eq. (5-3), and power approximation, Eq. (5-4), for corrosion wastage thickness.

$$t_{cor}(T) = \begin{cases} 0.170T & 0 \le T < 1 \\ 0.152 + 0.0186T & 1 \le T < 8 \\ -0.346 + 0.083T & 8 \le T < 16 \end{cases} \tag{5-3}$$

$$t_{cor}(T) = 0.1207T^{0.6257} \tag{5-4}$$

The conventional corrosion models are illustrated in Figure 5.1. The models are conservative in the early stages since the effect of coating is not considered.

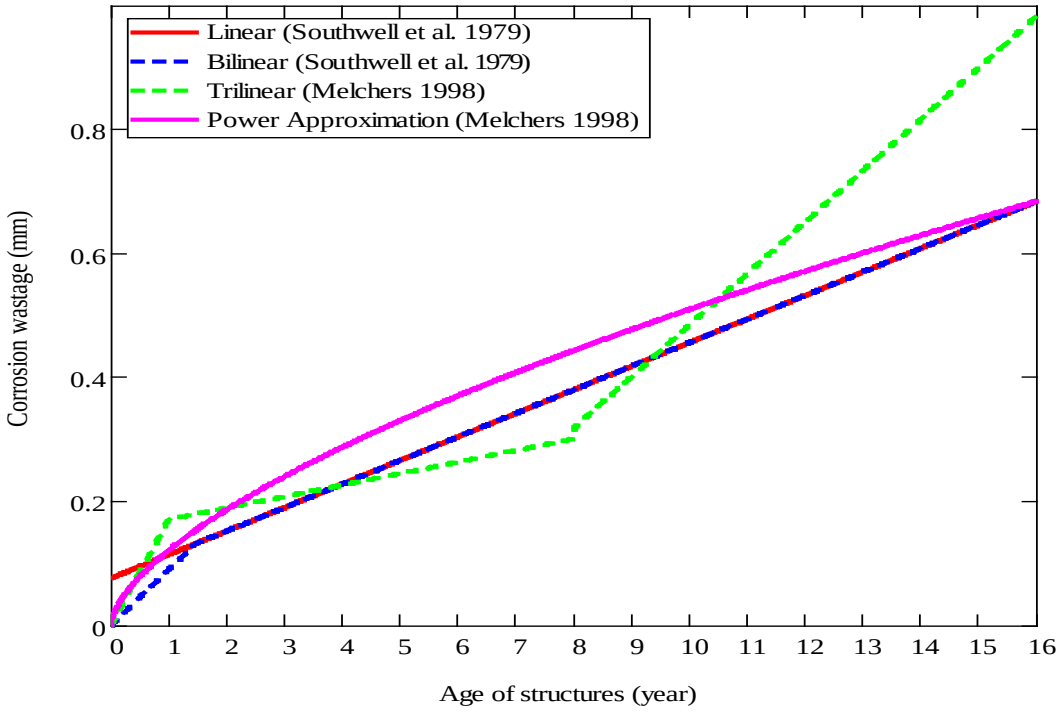

Figure 5.1 Conventional corrosion wastage models

5.2.2 Nonlinear Deterministic Models

Figure 5.2 shows a corrosion wastage model which was introduced by Guedes Soares and Garbatov (1999). In their study, the time-variant corrosion rate was divided into three different phases. During the first phase ($T \in [0, T_c]$), it is assumed that there is no corrosion due to the corrosion protection system. This phase varies in the range of 1.5~5.5 years according to Emi et al. (1993). With the damage to the corrosion protection, the second phase ($T \in [T_c, T_c + T_t]$) is initiated. For typical ship plating, Maximadj et al. (1982) suggested a period of around 4-5 years for this phase. The third phase ($T > T_c + T_t$) is where the corrosion process progress stops as the corroded material forms on the plate surface protecting it from contact with the corrosive environment. The corrosion wastage is expressed by Eq. (5-5):

$$t_{cor}(T) = \begin{cases} 0 & T \le T_c \\ t_{cor(\infty)}\left(1 - e^{-(T-T_c)/T_t}\right) & T > T_c \end{cases} \tag{5-5}$$

where T_c is the coating life, which is equal to the time interval between the painting of the surface and the time when its effectiveness is lost, and T_t is the transition time.

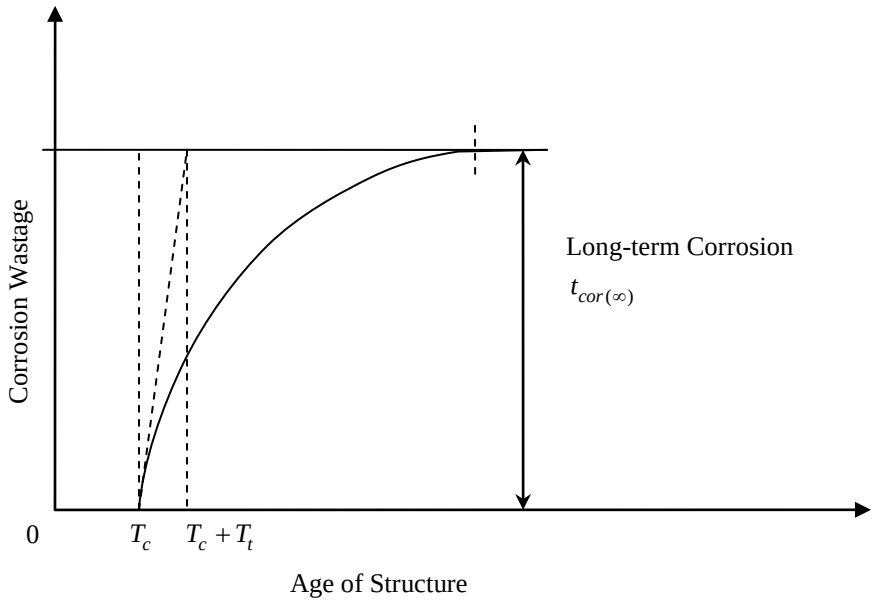

Figure 5.2 Corrosion model proposed by Guedes Soares & Garbatov (1999)

Another three-phase corrosion model (Figure 5.3) was introduced by Qin and Cui (2002). First, no corrosion takes place when the corrosion protection system is fully effective. Second, corrosion accelerates when the pitting corrosion occurs and progresses due to decrease of effectiveness of the protection system. Third, the corrosion decelerates and the long-term corrosion rate is assumed to be zero. The corrosion wastage was described as follows:

$$t_{cor}(T)=\begin{cases}0 & T\le T_c\\ t_{cor(\infty)}\left\{1-\exp\left[-\left(\dfrac{T-T_c}{a}\right)^b\right]\right\} & T>T_c\end{cases} \tag{5-6}$$

where $t_{cor(\infty)}$, a, b and T_c are four model parameters to be determined by analyzing available corrosion wastage data. This model is flexible and can describe other corrosion models using the same principle.

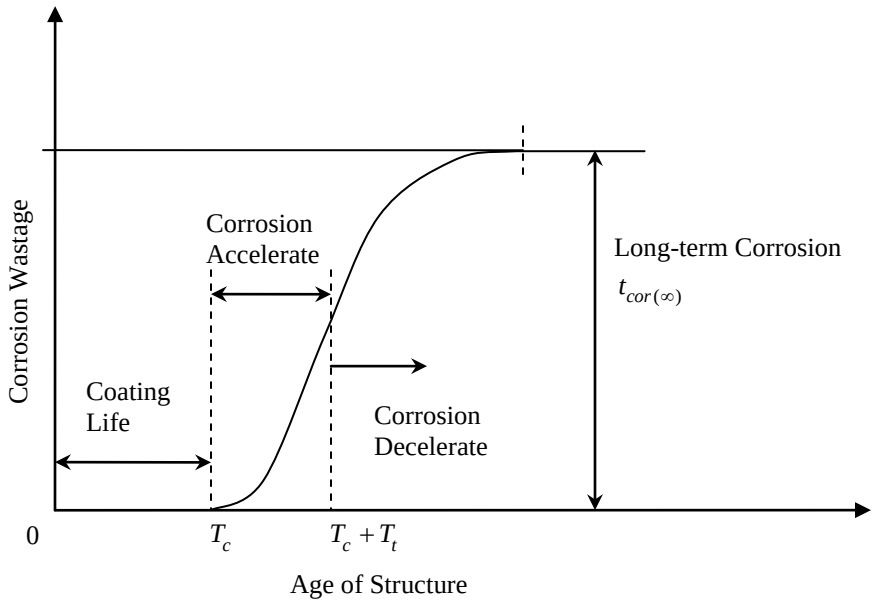

Figure 5.3 Corrosion model proposed by Qin & Cui (2002)

As shown in Figure 5.4, three phases of the corrosion wear were assumed by Ivanov et al. (2003). When the protective coating is intact, there is no corrosion wastage of the structure in the first phase ($T\in[0,T_c)$). A linear corrosion rate is assumed in the second phase ($T\in[T_c,T_c+T_t)$) for simulating a gradual acceleration of corrosion after the coating breaks down. When the coating completely fails, the corrosion reaches the final phase ($T>T_c+T_t$) with a steady corrosion rate.

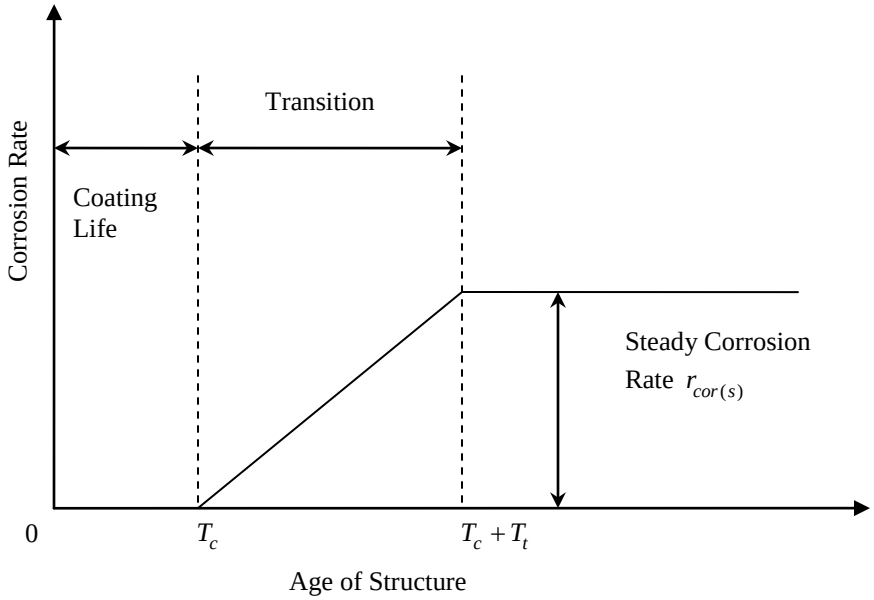

Figure 5.4 Corrosion model proposed by Ivanov et al. (2003)

5.2.3 Non-Linear Probabilistic Models

The corrosion characteristics of ship hull are influenced by many factors including the corrosion protection system (e.g., cathodic protection, coating), the operational parameters (e.g., type of cargo, the loading/unloading cycle of cargo) and the environmental conditions (e.g., humidity, temperature, oxygen and water velocity). Due to the uncertainties involved, a probabilistic model is more appropriate to describe the expected corrosion. Based on the linear (Eq. 5-1) and bilinear (Eq. 5-2) models, Melchers (1995) introduced the probabilistic corrosion models through statistical analysis. The extended models are:

$$\begin{cases} \mu\left(t_{cor}(T)\right) = 0.076 + 0.038T \\ \text{stdev}\left(t_{cor}(T)\right) = 0.051 + 0.025T \end{cases} \tag{5-7}$$

$$\begin{cases} \mu\left(t_{cor}(T)\right) = \begin{cases} 0.090T & 0 \le T < 1.46 \\ 0.076 + 0.038T & 1.46 \le T < 16 \end{cases} \\ \text{stdev}\left(t_{cor}(T)\right) = \begin{cases} 0.062T & 0 \le T < 1.46 \\ 0.035 + 0.017T & 1.46 \le T < 16 \end{cases} \end{cases} \tag{5-8}$$

A nonlinear model was also proposed to fit the data:

$$\begin{cases} \mu\left(t_{cor}(T)\right) = 0.084T^{0.823} \\ \text{stdev}\left(t_{cor}(T)\right) = 0.056T^{0.823} \end{cases} \tag{5-9}$$

Yamamoto and Ikegami (1996) proposed a corrosion model for transverse bulkheads of bulk carriers by analyzing a thickness measurement database of 50 bulk carriers. In this model, corrosion is assumed to be caused by an extremely large number of pits that were growing progressively and individually. Corrosion does not occur in the first period of the corrosion wastage process due to the effective anti-corrosive paint coating. The life of coatings T_c was assumed to follow the log-normal distribution. According to the empirical observations of coating deterioration (Emi et al. 1993), the COV of coating life is assumed to be 0.4. The second period starts from the active pitting point to the progressive pitting point. The transit time T_t is assumed to follow the exponential distribution (Matoba et al. 1994). In the last period, corrosion progress is assumed to stop and the corrosion rate becomes zero. The progressive pitting corrosion follows the following equation:

$$t_{cor}(T) = a\left(T - T_c\right)^b \tag{5-10}$$

where a is a random variable following the lognormal distribution and the value of b varies from 1/3 to 1 according to the material, environmental conditions, etc. (Komai et al. 1987, Kondo 1987, Masuda et al. 1986).

Sun and Bai (2001) introduced a time-variant corrosion rate model. As shown in

Figure 5.5, the corrosion process was divided into three phases which is same as the model of Guedes Soares and Garbatov (1999). The corrosion wastage was expressed as follows:

$$t_{cor}(T)=\begin{cases}0 & T \le T_c \\ r_{cor(s)}\left[T-\left(T_c+T_t\right)+T_t e^{-(T-T_c)/T_t}\right] & T > T_c\end{cases} \tag{5-11}$$

where T_t is the transition time. The coating life T_c and the steady corrosion rate $r_{cor(s)}$ are assumed to be fitted by a Weibull distribution and a normal distribution, respectively.

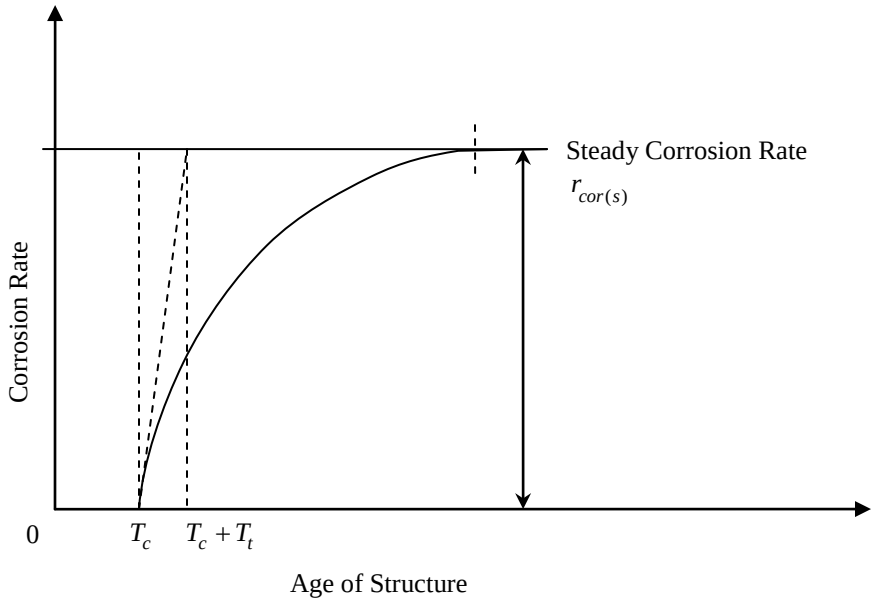

Figure 5.5 Corrosion model proposed by Sun & Bai (2001)

Based on measurements taken from a total of 7503 corrosion data for 44 existing bulk carriers, Paik et al. (1998) proposed a two-phase probabilistic corrosion model for 16 primary members of bulk carriers. The coating life was assumed to follow the normal distribution. The mean and COV of coating life was assumed between 5-10 years (Løseth et al. 1994) and 0.4 (Emi et al. 1993) respectively. After corrosion starts, Eq. (5-10) was applied to describe the corrosion wastage. As the indicative annual corrosion rate, the

coefficient a was assumed to follow a Weibull distribution.

Paik et al. (2003) developed a time-variant corrosion model for 34 different members of tankers and FPSOs based on measurements gathered from hundreds of tankers and FPSOs. As illustrated in Figure 5.6, the corrosion behavior is categorized into three phases: 1) durability of coating which follows the lognormal distribution (Yamamoto and Ikegami, 1996); 2) transition to visibly obvious corrosion that follows exponential distribution (Yamamoto and Ikegami, 1996); 3) Either the linear, convex or concave curve, which is based on the operational factors affecting the corrosion progress, is used to describe the trend of corrosion progress in the third phase. The convex curve reflects the phenomenon of gradual buildup of protective rust layers so that the corrosion rate decreases with the progress of corrosion. The linear curve is applicable where the rust layers are continually removed. The concave curve represents the accelerating corrosion.

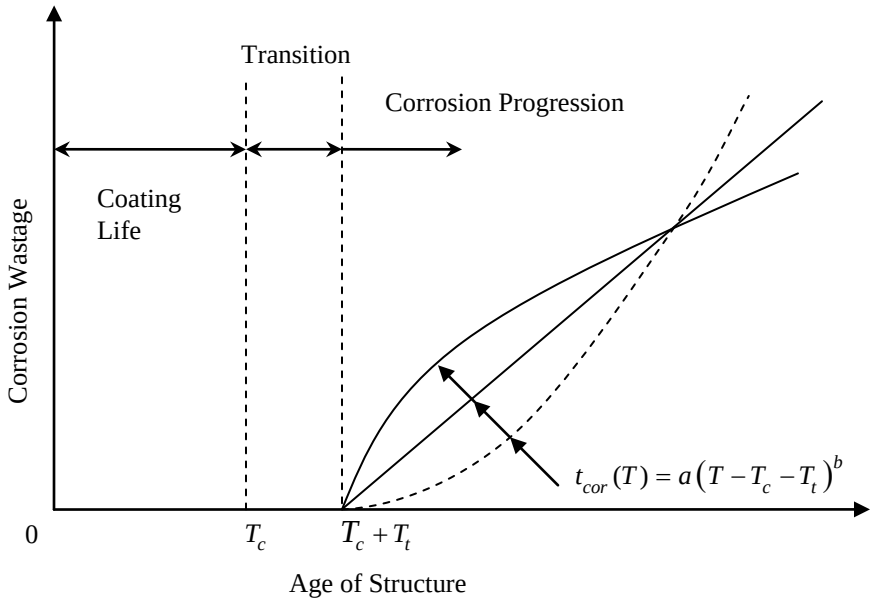

Figure 5.6 Corrosion model proposed by Paik et al. (2003)

The corrosion wastage was expressed as follows:

$$t_{cor}(T) = a\left(T - T_c - T_t\right)^b \tag{5-12}$$

where the coating life T_c was treated as a constant parameter instead of random variable. Transition time T_t was conservatively taken as zero indicating the corrosion starts immediately after the breakdown of coating. The value of b, which typically varies from 0.3-1.5, determines the shape of the curve. The statistical characteristics of the coefficient a is considered as a Weibull function.

5.2.4 Phenomenological Model

The above-mentioned corrosion models are essentially empirical. Based on corrosion mechanisms, Melchers (2003) proposed a probabilistic phenomenological corrosion model (see Figure 5.7) considering the effect of environmental and other factors. For unprotected steel structure, the corrosion process was divided into four stages in the model: initial corrosion, oxygen diffusion control, limitation on food supply for aerobic activity and anaerobic activity.

In order to account for the uncertainties caused by modeling approximations, variability in environmental conditions and variations in material, the probabilistic model was presented as follows:

$$w_{cor}(T, \mathrm{E}_{cor}) = b_{cor}\left(T, \mathrm{E}\right)\mu\left(T, \mathrm{E}_{cor}\right) + \varepsilon_{cor}\left(T, \mathrm{E}_{cor}\right) \tag{5-13}$$

where $w_{cor}(T, \mathrm{E}_{cor})$ is the weight loss of material, $\mu(T, \mathrm{E}_{cor})$ is a mean value function, $b_{cor}(T, \mathrm{E}_{cor})$ is a bias function, $\varepsilon_{cor}(t, \mathrm{E}_{cor})$ is a zero mean error function, E_{cor} is a vector of the environmental parameters.

The model clearly relies on input of environmental variables. Although main environmental parameters E_{cor} in some stages have been recognized and quantified, determining the remaining part of $\mu(T, E_{cor})$ and analyzing the data to estimate $\varepsilon_{cor}(t, E_{cor})$ are still required.

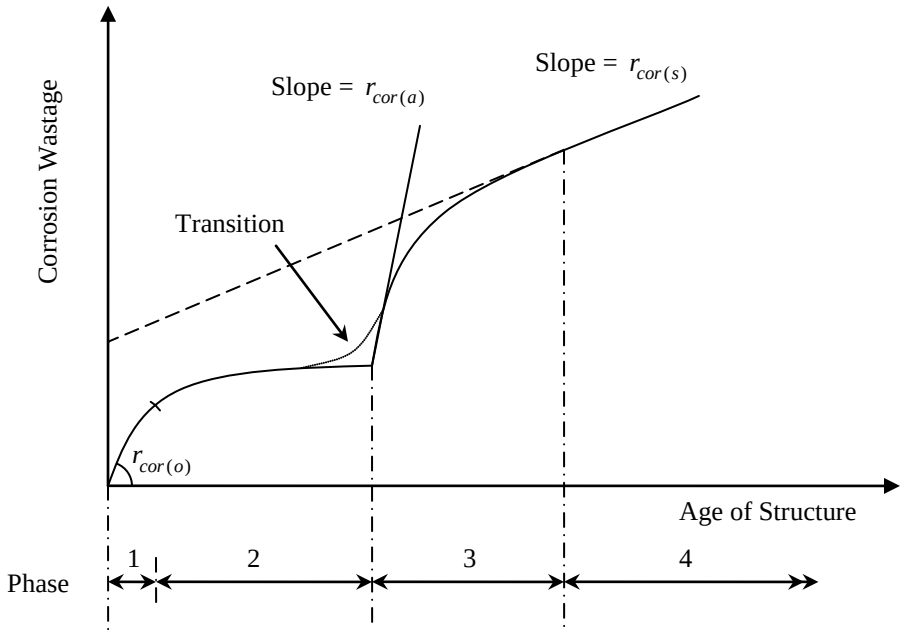

Figure 5.7 Corrosion model proposed by Melchers (2003)

5.3 Development of a New Probabilistic Corrosion Model

Corrosion has been recognized as a very complex phenomenon and it is influenced by many factors. Because of the wide uncertainties of the steel composition and environmental influences, it is very difficult to apply the fundamental model to quantitate the corrosion wastage. There is a need to develop models based on corrosion mechanisms and to calibrate them with the corrosion wastage databases to improve prediction of corrosion in marine structures. Melchers's phenomenological model is a very valuable at-

tempt but not so practical due to the difficulty of simulating the real seawater condition in the laboratory. Therefore, in the current stage, a statistically-derived corrosion model based on the reliable corrosion data is considered practical and reasonable.

At the present time, there are several databases of corrosion wastage in the public domain. The Tanker Structure Co-operative Forum (TSCF) (1992) published a set of corrosion data from 52 oil tankers. Yamamoto and Ikegami (1998) introduced a database of 50 bulk carriers. Paik et al. developed a probabilistic corrosion rate estimation model based on the measurements of 44 bulk carriers (1998) and more than 100 oil tankers (2003). Harada et al. (2001) collected data from 197 oil tankers. Wang et al. (2003) introduced a database of 140 oil tankers developed by ABS. Table 5.1 presents the main details of corrosion databases on oil tankers in the literature summarized by Wang et al. (2003).

Table 5.1 Summary of corrosion measurement databases on oil tankers (Wang et al 2003)

Reference	Wang et al. (2003)	TSCF (1992)	Harada et al. (2001)	Paik et al. (2003)
Ship type	Single hull tankers	Single hull tankers	Single hull tankers	Single hull tankers
Data sources	SafeHull condition assessment program	Owner, class societies	Gauging records	Gauging reports
Number of vessels	140	52	197	>100
Number of reports	157	N.A.	346	N.A.
Number of measurements	110,082	N.A.	> 250,000	33,820
Ship length	168 ~ 401 meters	N.A.	100 ~ 400 meters	N.A
Service years at the time of gauging	12 ~ 26, 32 years	~ 25 years	~ 23 years	12 ~ 26 years
Ship class	ABS, LR, NK, DNV, KR	ABS, DNV, LR, NK	NK	KR, ABS
Build years	Mostly 1970's, some 1980's	1960s ~ 1980s	N.A.	N.A.
Year of measurement	1992 – 2000	N.A.	N.A.	N.A.

N.A. – Not Available

5.3.1 Modeling Description

One of the objectives in this study is to develop a time-variant probabilistic model to predict the corrosion wastage that will be used in reliability-based inspection planning of individual tankers. The procedure is described as follows:

1) Derive equations to present the mean and standard deviation of corrosion wastage by formulating the trends of the current data set, which was collected from a sizable fleet of single hull tankers that are still in service, or were in service in recent years (Wang et al. 2003).
2) Choose a probabilistic distribution to present corrosion wastage in each year.
3) Determine the parameters of probabilistic density function using mean and standard deviation derived in step (1).

5.3.2 Data Analysis

Six sets of corrosion data, deck plates and associated stiffener webs and flanges of ballast and cargo tanks of tankers provided by ABS are analyzed here. The first set of data (see Figure 5.8) includes 4,465 measurements of deck plate from cargo tanks with as-built thickness varying from 12.7 to 35 mm. The second set of data (see Figure 5.9) includes 1,168 measurements of deck plates from ballast tanks with as-built thickness varying from 13.5 to 35mm. The third set of data (see Figure 5.10) includes 10,761 measurements of web plates of upper deck longitudinals from cargo tanks with as-built thickness varying from 8.5 to 38 mm. The fourth set of data (see Figure 5.11) includes 1,974 measurements of web plates of upper deck longitudinals from ballast tanks with as-built thickness varying from 10.16 to 38 mm. The fifth set of data (see Figure 5.12) includes

765 measurements of flanges of upper deck longitudinals from cargo tanks with as-built thickness varying from 12.5 to 30 mm. The sixth set of data (see Figure 5.13) includes 166 measurements of flanges of upper deck longitudinals from ballast tanks with as-built thickness varying from 16 to 30 mm.

The data contains some groups of identical measurements. In order to treat all the data as independent measurements, these groups of data have to be reduced to one measurement in each group to refit the data. The measured thickness that is less than 0.01 mm than as-built thickness or greater than as-built thickness might be considered as renewed plate after the ship's delivery. These data were screened out from the database so that the influence of the renewed plates in the database is minimized. Although there are some renewed plates in the remaining database, their contribution to the statistical analysis is negligible.

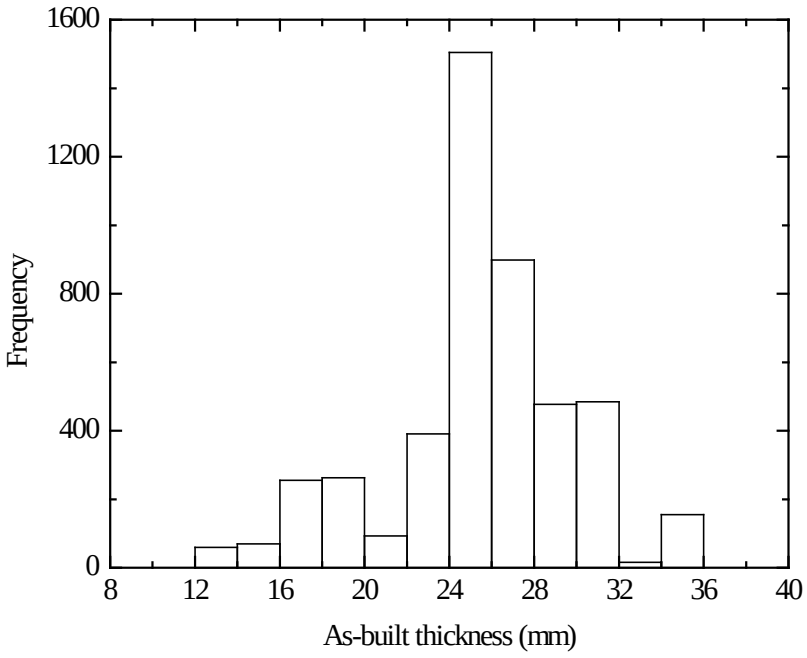

Figure 5.8 As-built thickness of deck plates (cargo oil tanks)

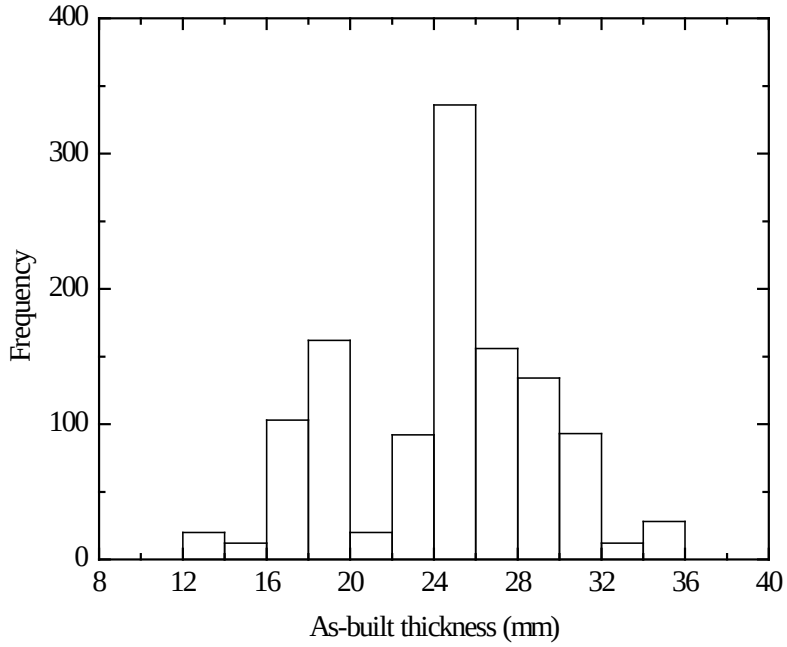

Figure 5.9 As-built thickness of deck plates (ballast tanks)

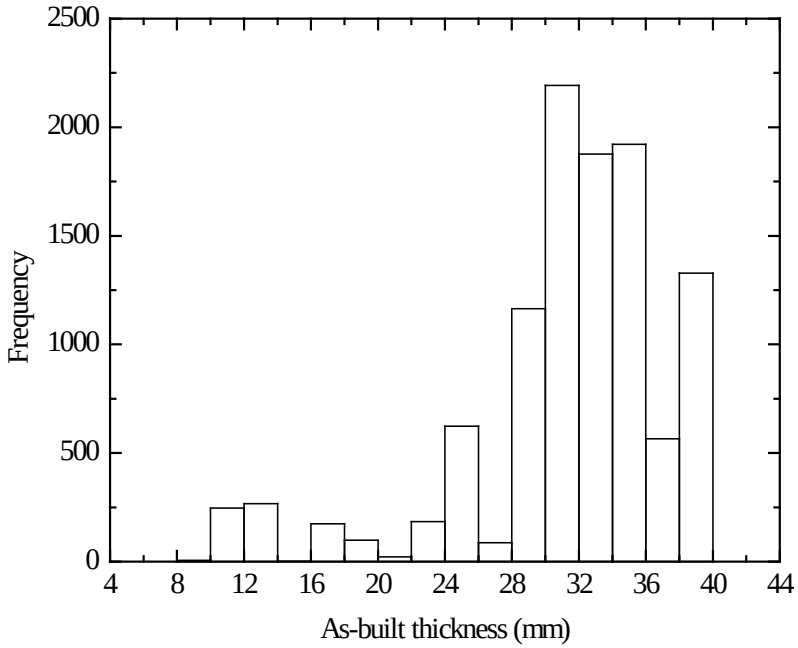

Figure 5.10 As built thickness of upper deck longitudinal stiffener web plates (cargo oil tanks)

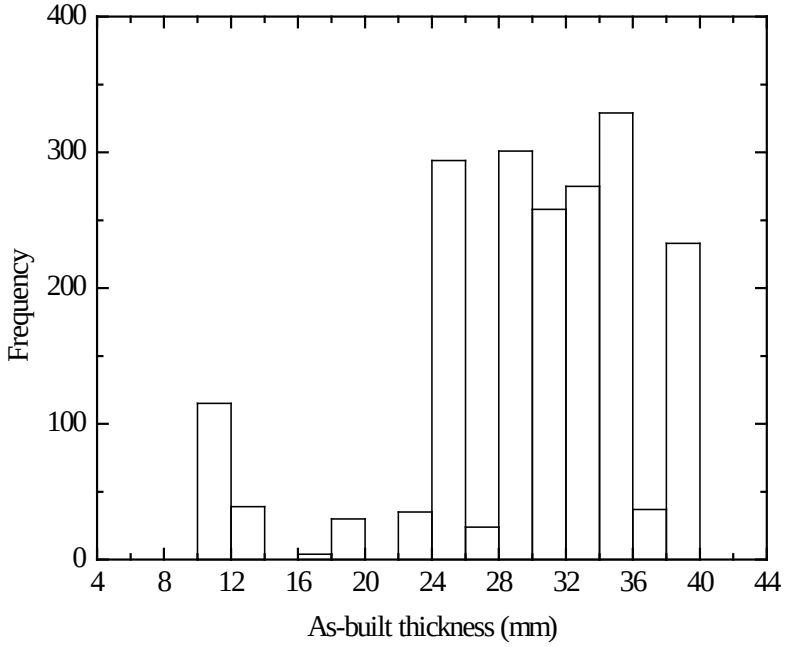

Figure 5.11 As-built thickness of upper deck longitudinal stiffener web plates (ballast tanks)

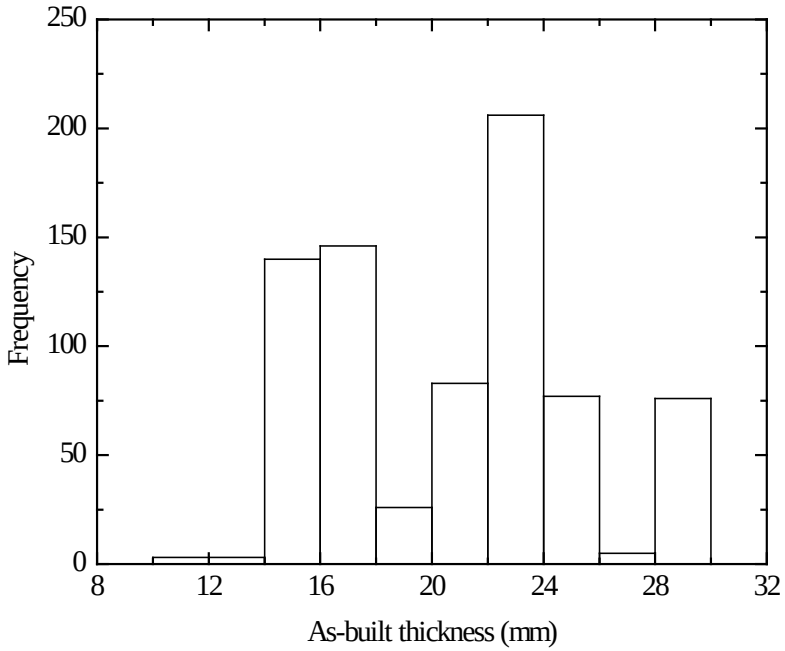

Figure 5.12 As-built thickness of upper deck longitudinal stiffener flanges (cargo oil tanks)

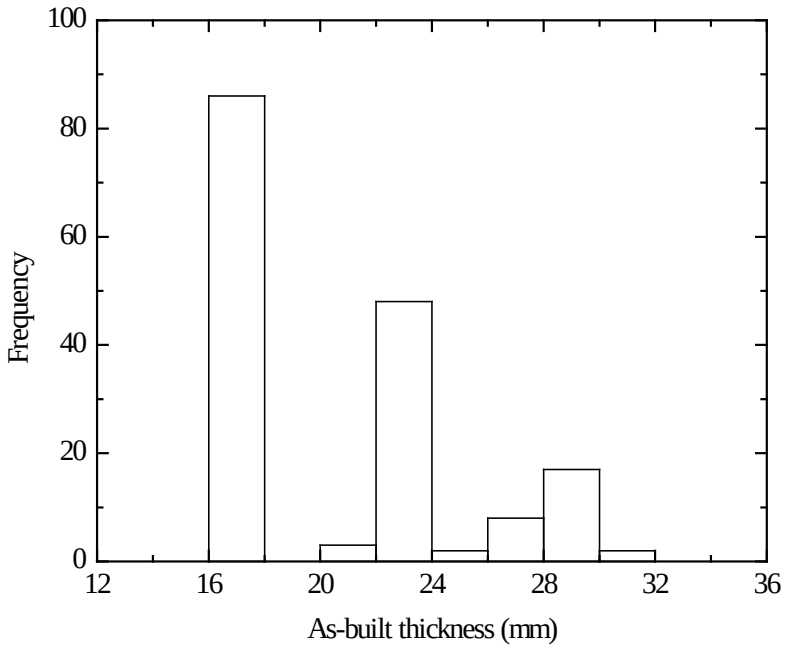

Figure 5.13 As-built thickness of upper deck longitudinal stiffener flanges (ballast tanks)

The frequency scatter plots of corrosion wastage for the above-mentioned six sets of data are shown in Figure 5.14 ~ Figure 5.19. It appears that the datasets show a very high level of scatter. The following conclusions may be drawn:

- With aging, the corrosion wastage of tankers will increase in severity.
- Corrosion wastage measurements spread over a wide range. Hence, the mean value and standard deviation fluctuate with ships age.
- The maximum corrosion wastage is much higher than the average.
- The maximum corrosion wastage of deck plate seems to be higher in cargo tanks than in ballast tanks.
- In cargo tanks, corrosion wastage of the longitudinal web plate and deck plate seem to be similar.

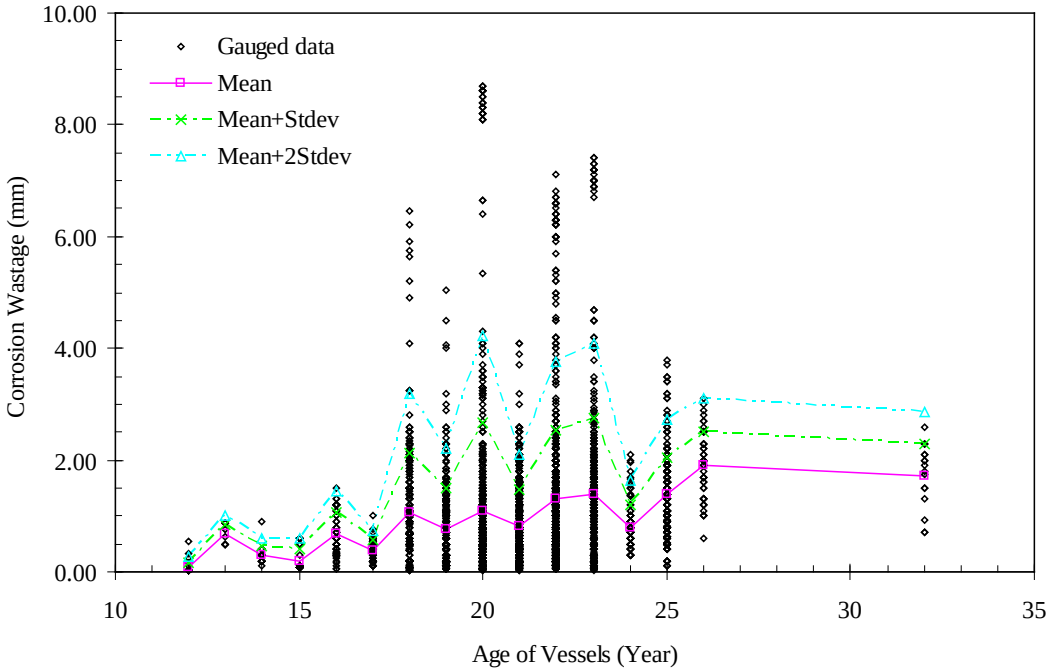

Figure 5.14 Scatter plot of corrosion wastage of deck plates (cargo oil tanks)

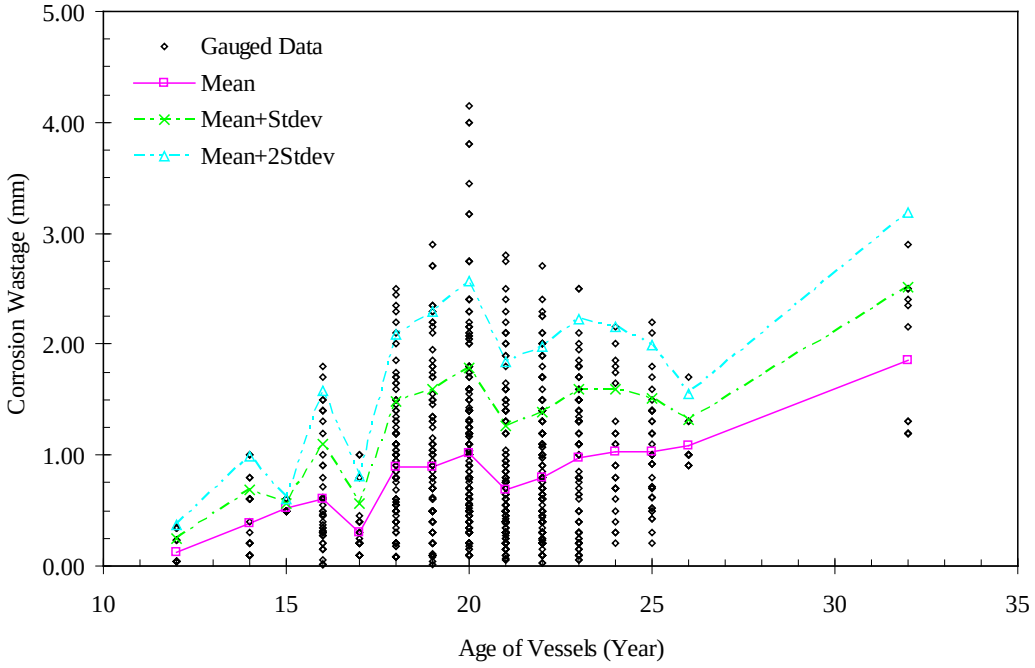

Figure 5.15 Scatter plot of corrosion wastage of deck plates (ballast tanks)

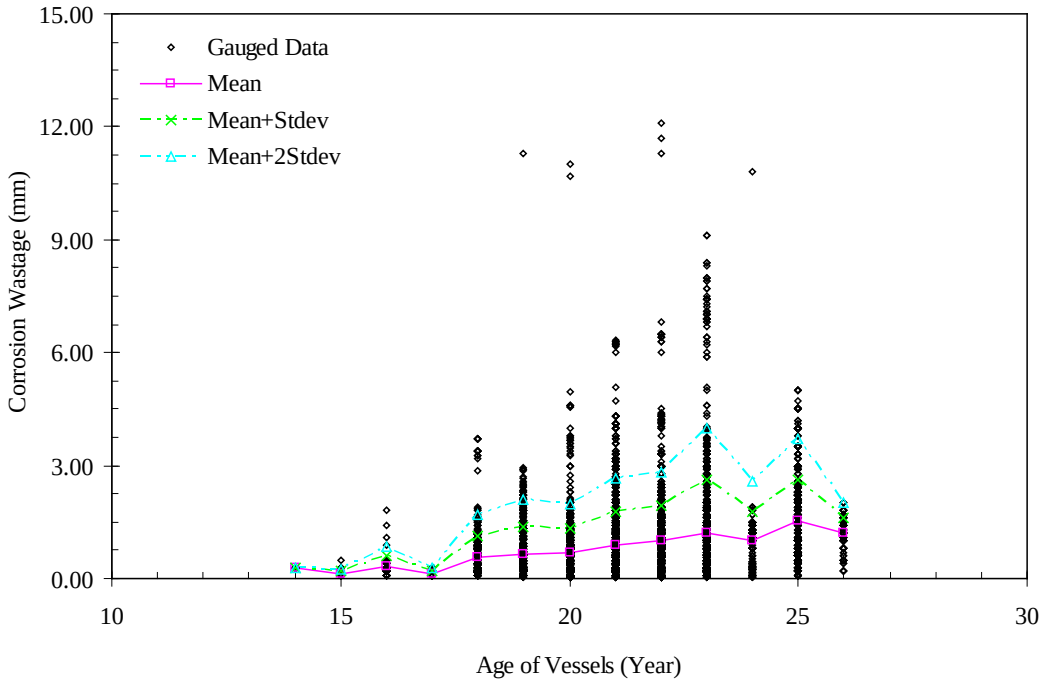

Figure 5.16 Scatter plot of corrosion wastage of upper deck longitudinal stiffener web plates (cargo oil tanks)

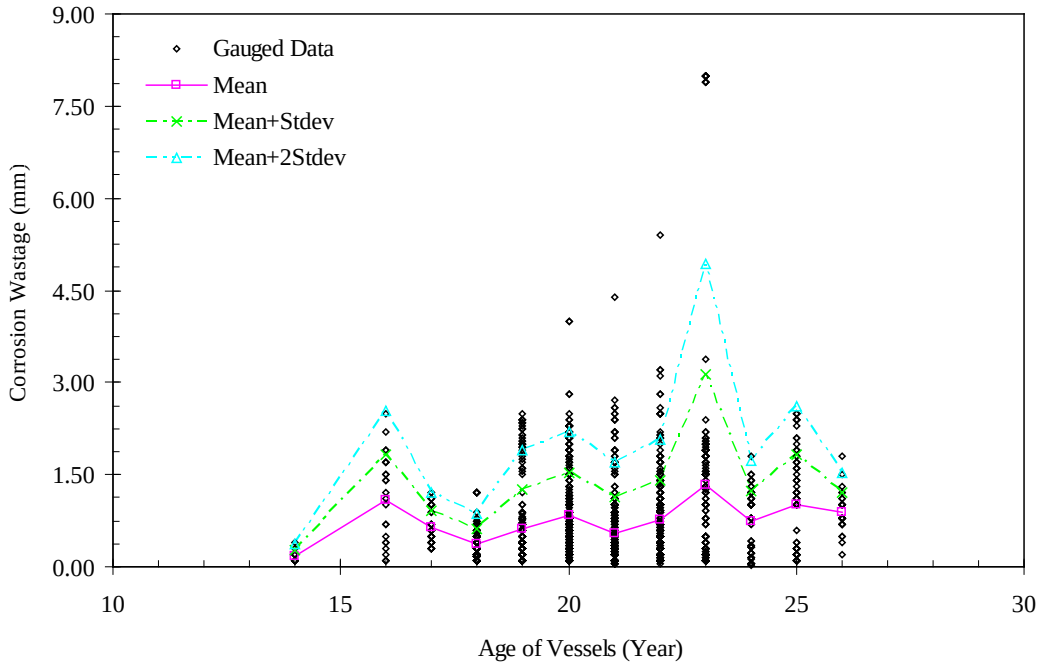

Figure 5.17 Scatter plot of corrosion wastage of upper deck longitudinal stiffener web plates (ballast tanks)

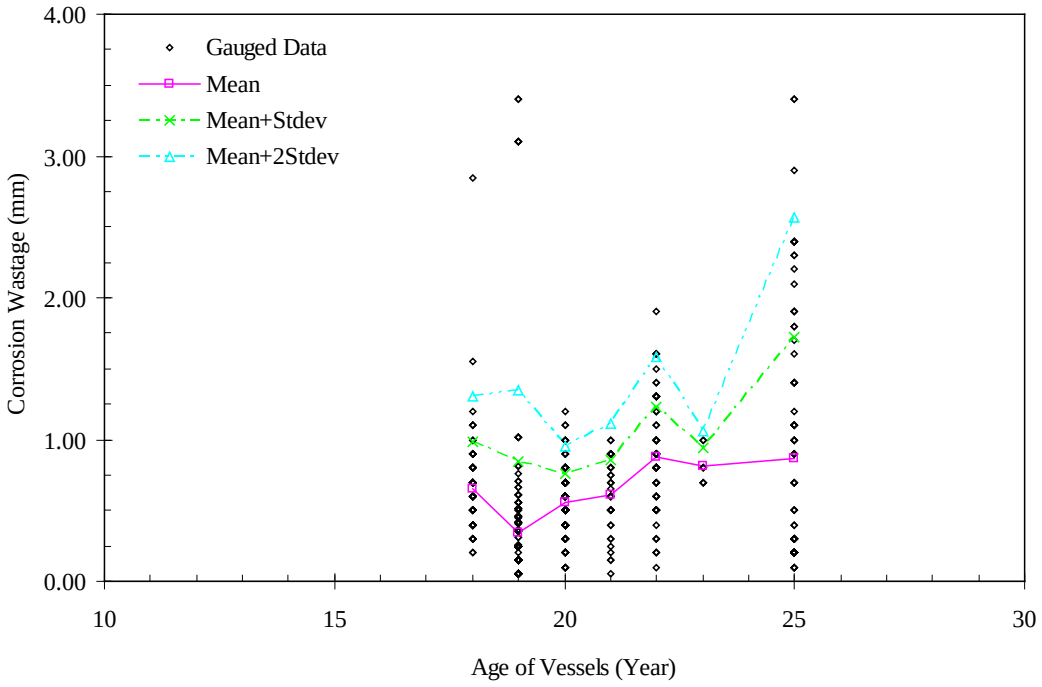

Figure 5.18 Scatter plot of corrosion wastage of upper deck longitudinal stiffener flanges (cargo oil tanks)

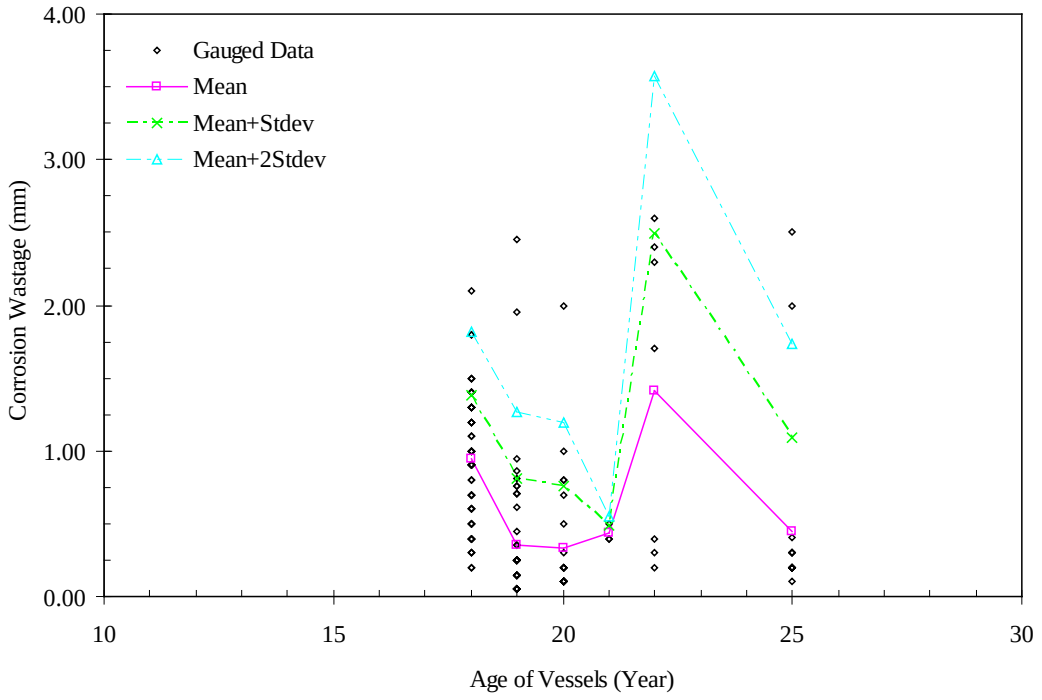

Figure 5.19 Scatter plot of corrosion wastage of upper deck longitudinal stiffener flanges (ballast tanks)

5.3.3 Prediction of Corrosion Wastage

The following equation is assumed for the corrosion wastage at T years old. This assumption is commonly applied (Yamamoto & Ikegami 1998, Paik et al. 1998, 2003, Harada et al. 2001, Gardiner & Melchers 2001, Wang et al. 2003, Sun & Guedes Soares 2006).

$$t_{cor}(T) = a\left(T - T_c\right)^b \tag{5-14}$$

where $t_{cor}(T)$ is the corrosion wastage at age T, T_c is the year when the plates or stiffeners start to deviate from the as-built condition; a and b are constants that can be determined from the measurement data.

The age when the corrosion starts, T_c, is itself a random variable. It may follow some of the following distributions, such as the Lognormal distribution (Yamamoto & Ikegami 1998, Paik et al. 2003), the Normal distribution (Paik et al. 1998), and the Weibull distribution (Sun & Bai 2002). It can also vary over a wide range. It is generally acknowledged that coating breakdown starts to take place in certain locations when a ship is between 2 to 10 years old. Therefore, it can be expected that T_c varies from 2 to 10 years.

It does not seem very meaningful to attempt to have a curve fitting all data points. The number of data points varies from year to year, i.e., there are more data points in some years than in others. The following were considered in deriving formulae for the mean values and standard deviations by best fitting of the data set:

- The mean value of corrosion wastage increases with ship's age.
- The standard deviation of corrosion wastage also increases with ship's age.
- The trends are better revealed or presented by ship with more data points.

- The coating life T_c is assumed to be a constant value.
- The estimated equations cover the most severe investigated data due to the conservative consideration.

Table 5.2 lists a set of equations thus derived. T_c is assumed to be 6.5 years when calculating $\mu(t_{cor})$ and 5 years when calculating $\mu(t_{cor})+\text{stdev}(t_{cor})$ which was proposed by Wang et al. (2008). Figure 5.20 through Figure 5.25 show the derived equations in comparison to the measurement data.

Table 5.2 Equations for predicting the mean values and standard deviations of corrosion wastage

Members	Tank Type	Mean	Standard Deviation
Deck plates	Cargo	$\mu\left(t_{p(cor)}(T)\right)=0.215\left(T-6.5\right)^{2/3}$	$\text{stdev}\left(t_{p(cor)}(T)\right)=0.349\left(T-5\right)^{3/4}-0.215\left(T-6.5\right)^{2/3}$
	Ballast	$\mu\left(t_{p(cor)}(T)\right)=0.18\left(T-6.5\right)^{2/3}$	$\text{stdev}\left(t_{p(cor)}(T)\right)=0.235\left(T-5\right)^{3/4}-0.18\left(T-6.5\right)^{2/3}$
Upper deck longitudinals (web plates)	Cargo	$\mu\left(t_{w(cor)}(T)\right)=0.217\left(T-6.5\right)^{2/3}$	$\text{stdev}\left(t_{w(cor)}(T)\right)=0.298\left(T-5\right)^{3/4}-0.217\left(T-6.5\right)^{2/3}$
	Ballast	$\mu\left(t_{w(cor)}(T)\right)=0.244\left(T-6.5\right)^{2/3}$	$\text{stdev}\left(t_{w(cor)}(T)\right)=0.359\left(T-5\right)^{3/4}-0.244\left(T-6.5\right)^{2/3}$
Upper deck longitudinals (flanges)	Cargo	$\mu\left(t_{f(cor)}(T)\right)=0.141\left(T-6.5\right)^{2/3}$	$\text{stdev}\left(t_{f(cor)}(T)\right)=0.182\left(T-5\right)^{3/4}-0.141\left(T-6.5\right)^{2/3}$
	Ballast	$\mu\left(t_{f(cor)}(T)\right)=0.228\left(T-6.5\right)^{2/3}$	$\text{stdev}\left(t_{f(cor)}(T)\right)=0.298\left(T-5\right)^{3/4}-0.228\left(T-6.5\right)^{2/3}$

Note: It is assumed that the corrosion starts when $T \geq 6.5$ year.

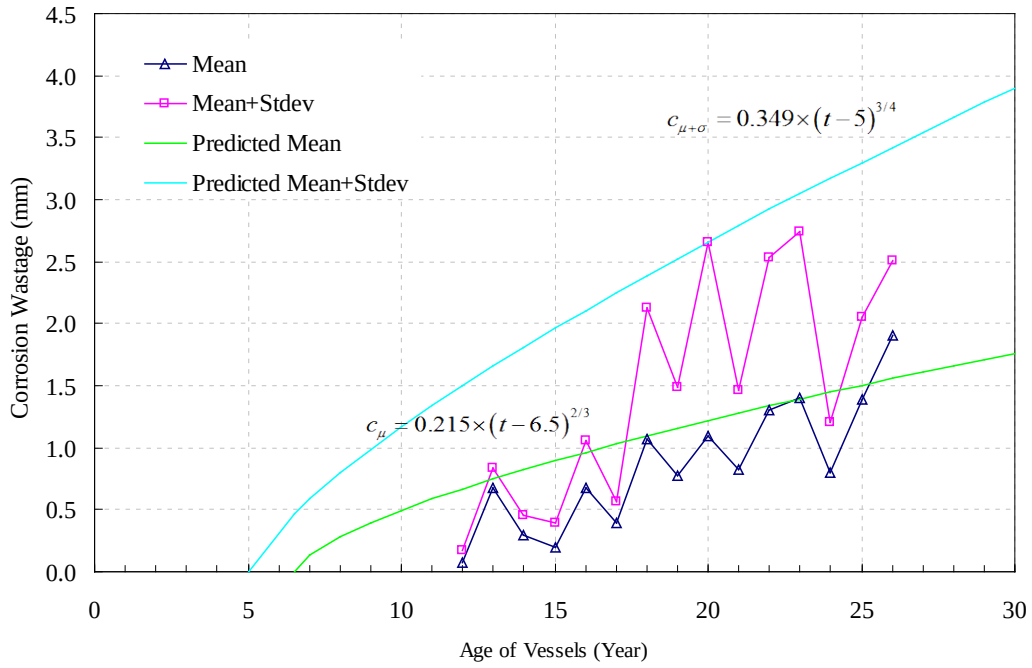

Figure 5.20 Derived equations of mean value and standard deviation of corrosion wastage of deck plates (cargo oil tanks)

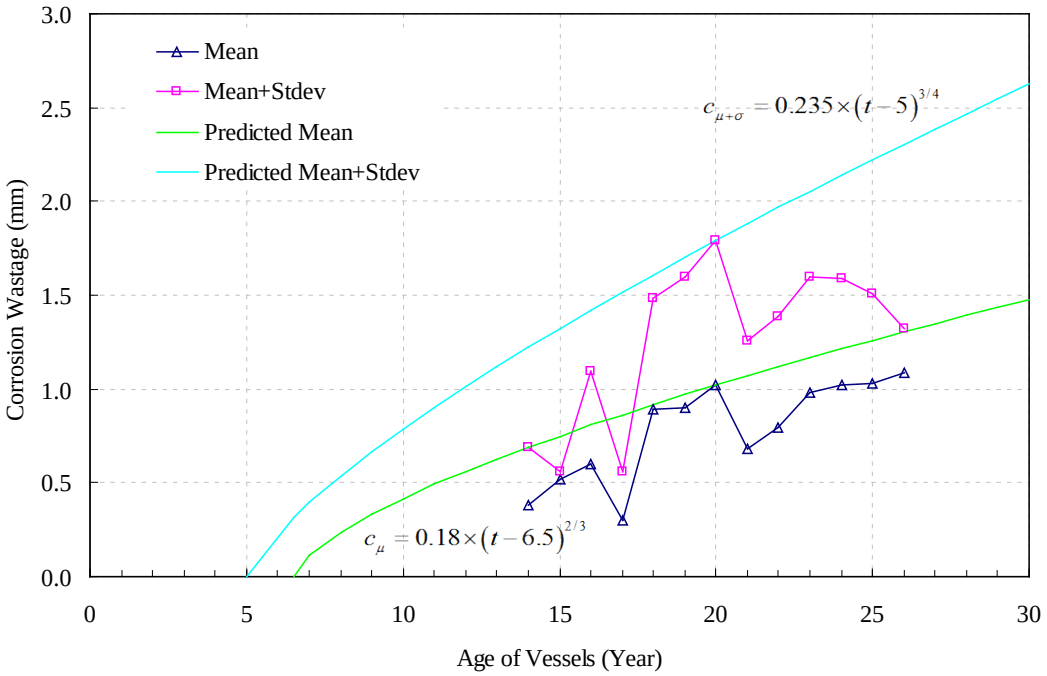

Figure 5.21 Derived equations of mean value and standard deviation of corrosion wastage of deck plates (ballast tanks)

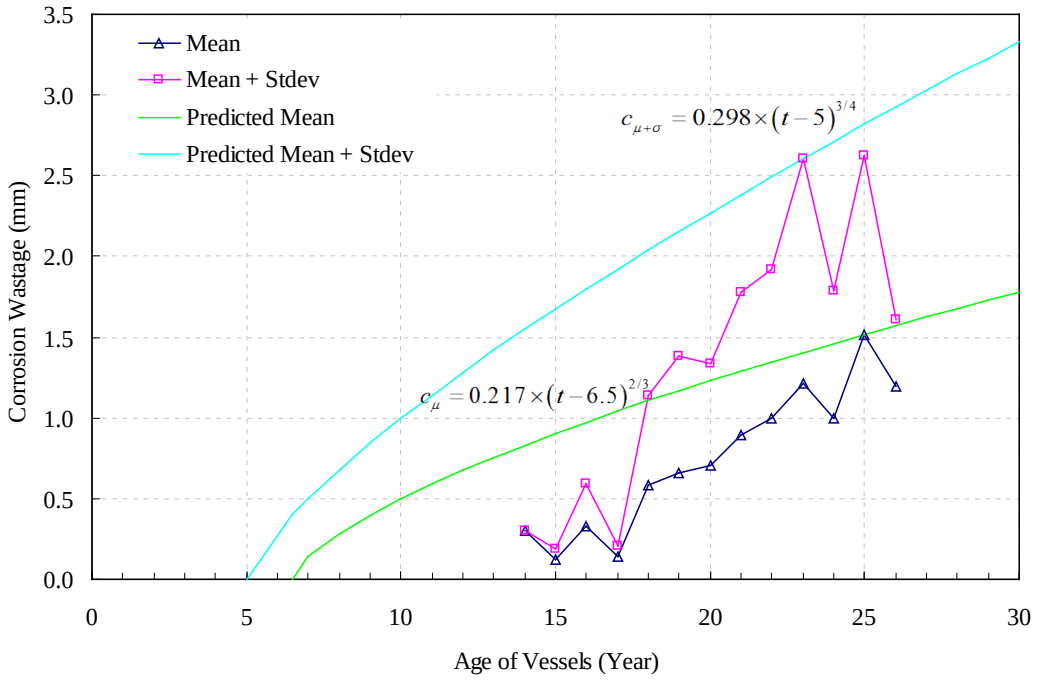

Figure 5.22 Derived equations of mean value and standard deviation of corrosion wastage of upper deck longitudinal stiffener web plates (cargo oil tanks)

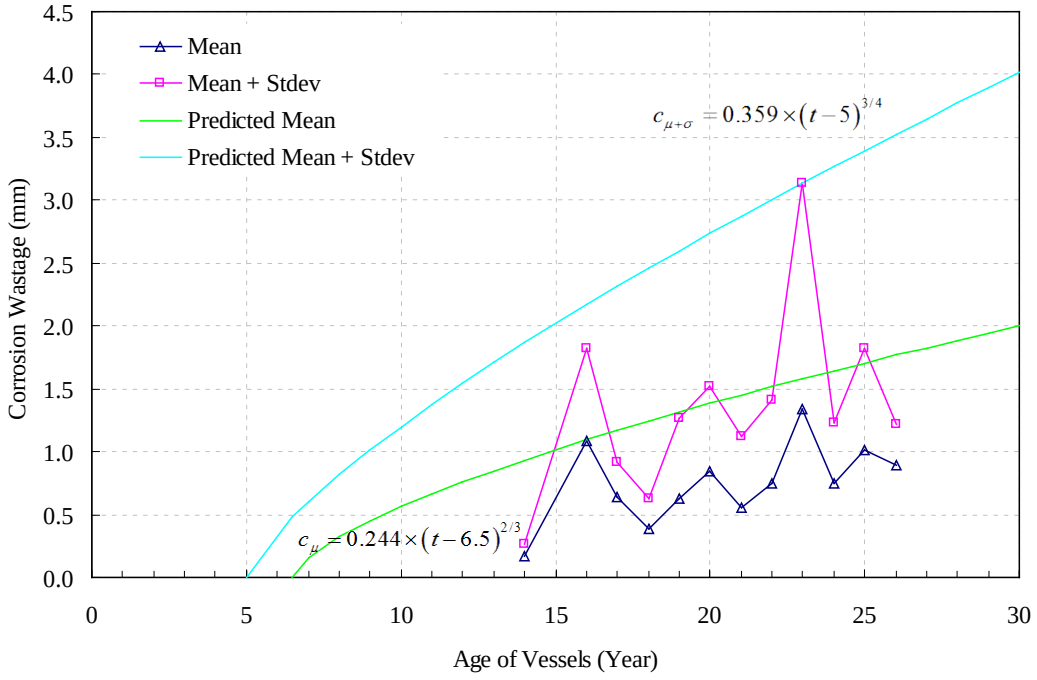

Figure 5.23 Derived equations of mean value and standard deviation of corrosion wastage of upper deck longitudinal stiffener web plates (ballast tanks)

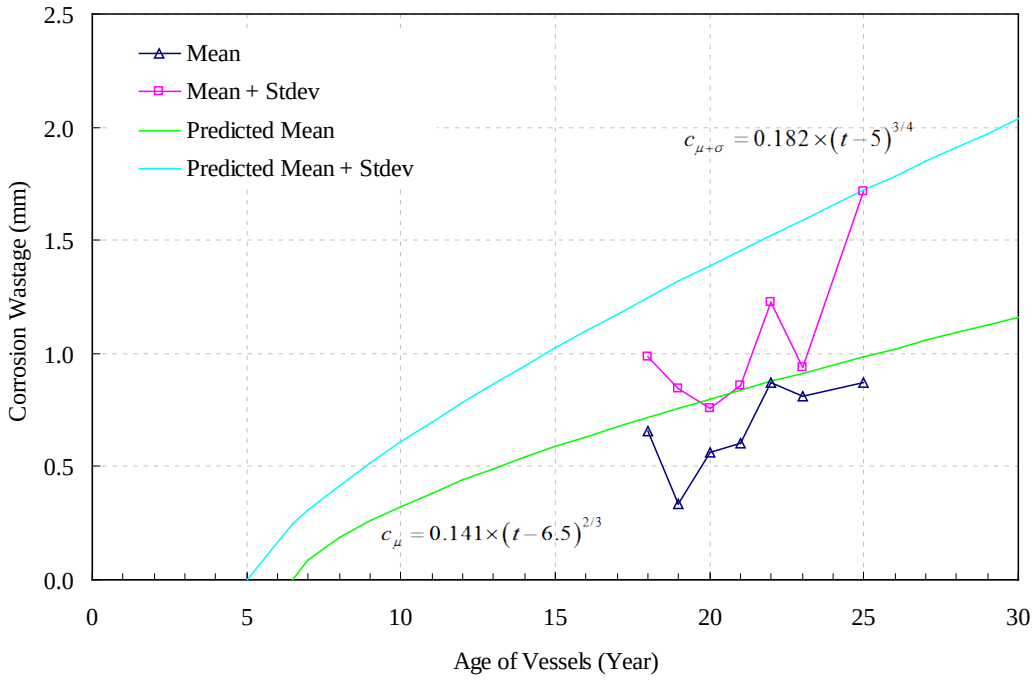

Figure 5.24 Derived equations of mean value and standard deviation of corrosion wastage of upper deck longitudinal stiffener flanges (cargo oil tanks)

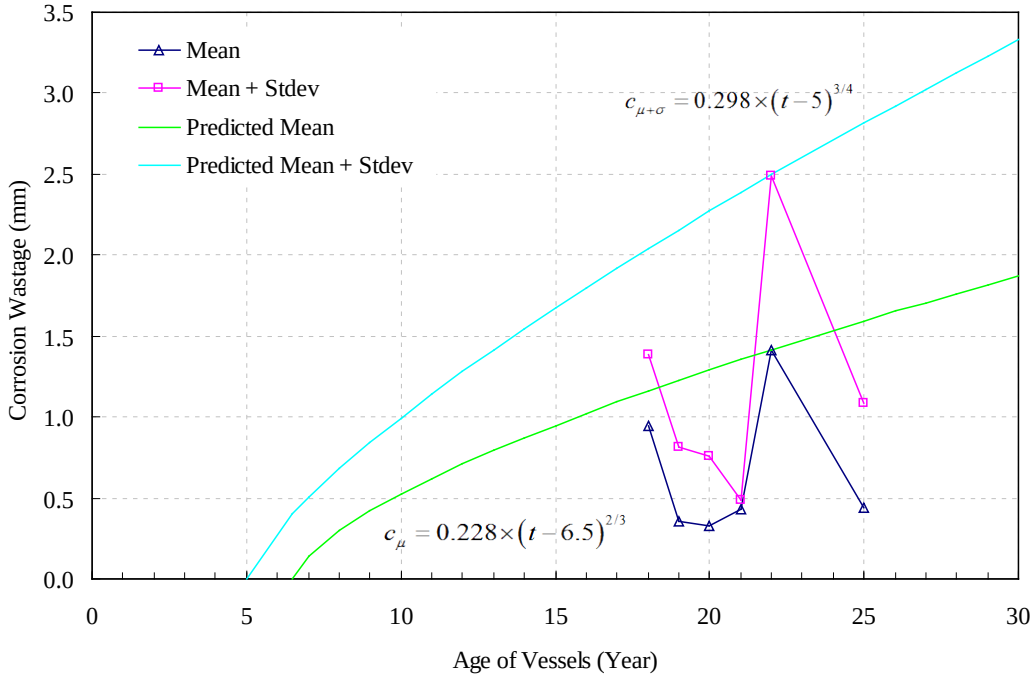

Figure 5.25 Derived equations of mean value and standard deviation of corrosion wastage of upper deck longitudinal stiffener flanges (ballast tanks)

The corrosion rate defined as the first derivative of the corrosion wastage is also analyzed and presented in Figure 5.26. It is observed that the corrosion rate of upper deck longitudinal stiffener web plates in ballast tanks is highest. It is also apparent from the figure that the rate of decrease of the corrosion rate is almost the same for each member.

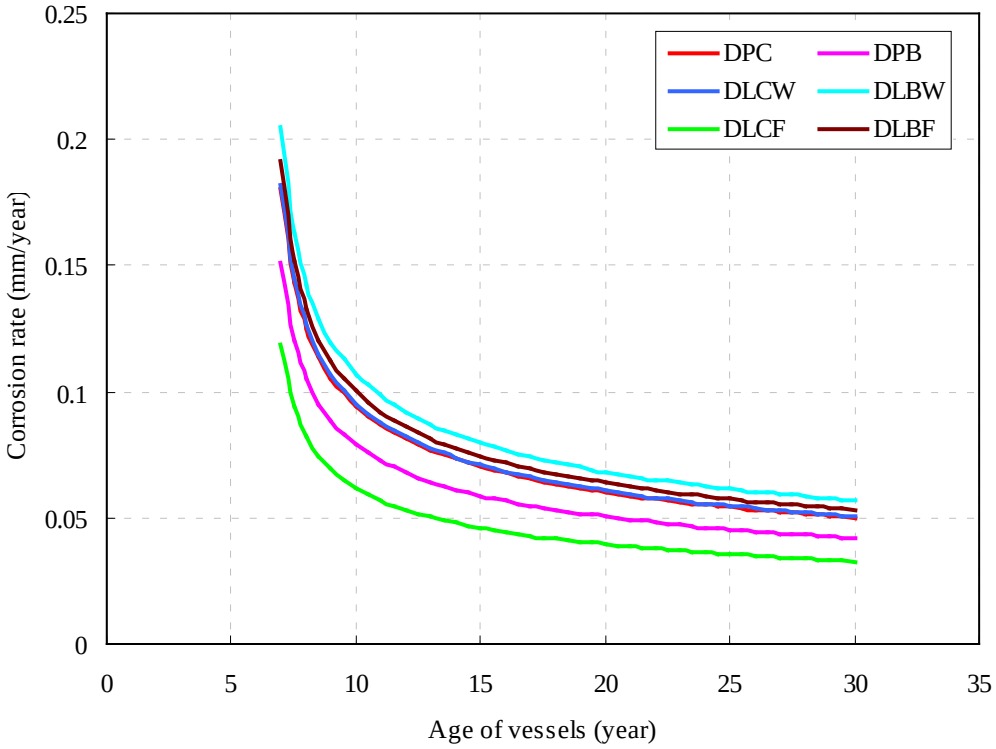

Notes:
DPB: Deck Platting in Ballast Tank
DPC: Deck Platting in Cargo Tank
DLBW: Deck Longitudinals in Ballast Tank (Web)
DLCW: Deck Longitudinals in Cargo Oil Tank (Web)
DLBF: Deck Longitudinals in Ballast Tank (Flange)
DLCF: Deck Longitudinals in Cargo Oil Tank (Flange)

Figure 5.26 Comparative analysis of corrosion rate of upper deck structures

In order to provide a detailed description of the variability of the data, it has been grouped by year and some histograms of the measurement in selected year are presented in Figure 5.27 ~ Figure 5.32. These figures also demonstrate the high variation of corro-

sion wastage.

To define the probability density function of the corrosion wastage, the frequencies observed in the data were compared to the expected frequencies of the theoretical distribution. For this purpose, the Kolmogorov-Smirnov goodness-of-fit test is applied. Under certain conditions, some "exotic" probabilistic distributions may appear to be the best fit following the criterion. It was decided to ignore these atypical or "exotic" functions. Clearly, there does not exist a consistent probability distribution function that can fit equally well with all ship ages for different structure types.

Several distributions were evaluated and it was concluded that Weibull and log-normal distributions appear to be better candidates for representing the corrosion wastage over ships' life, and the Weibull distribution seems to be slightly better.

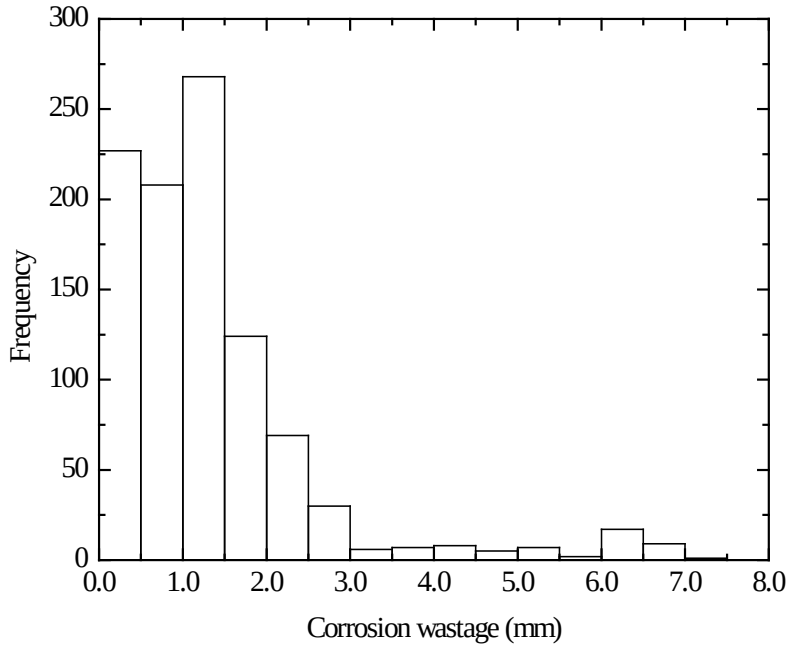

Figure 5.27 Histograms of corrosion wastage of deck plates for 22-year-old tankers (cargo oil tanks)

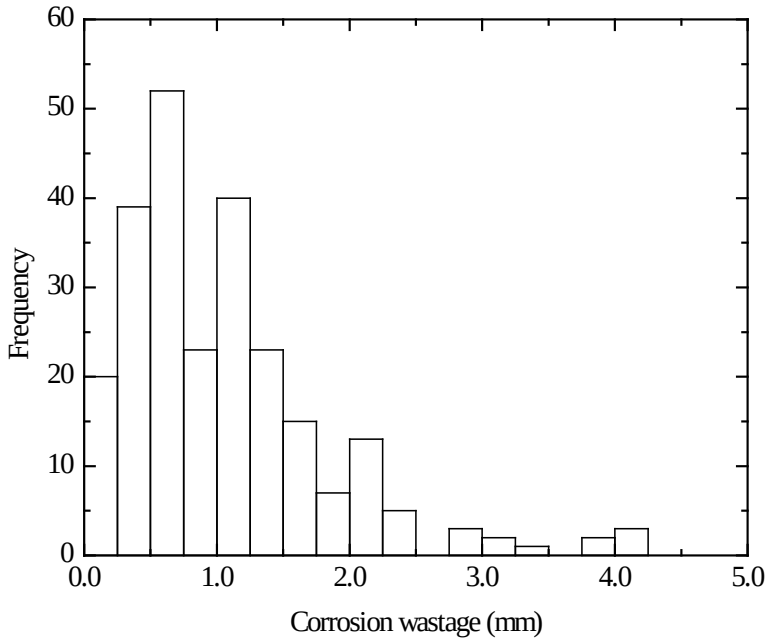

Figure 5.28 Histograms of corrosion wastage of deck plates for 20-year-old tankers (ballast tanks)

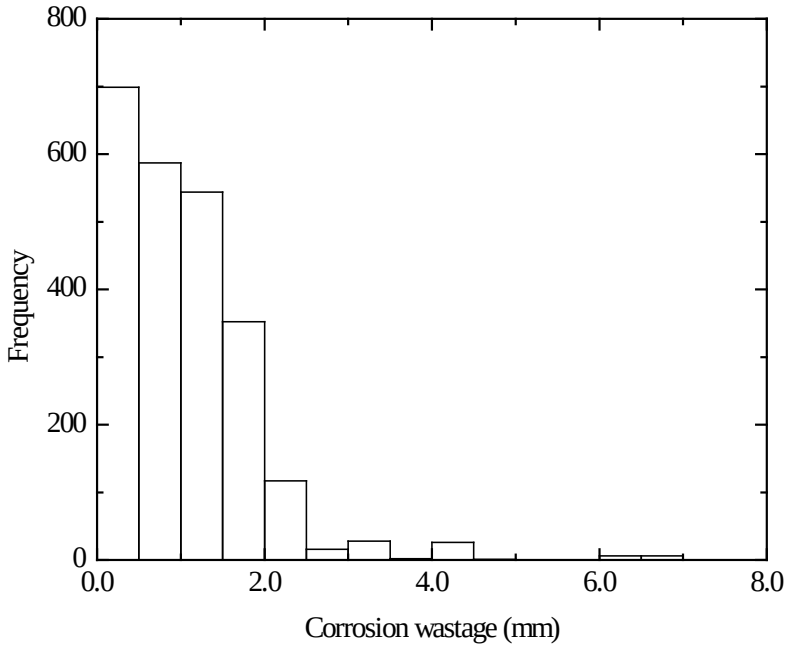

Figure 5.29 Histograms of corrosion wastage of upper deck longitudinal stiffener web plates for 22-year-old tankers (cargo oil tanks)

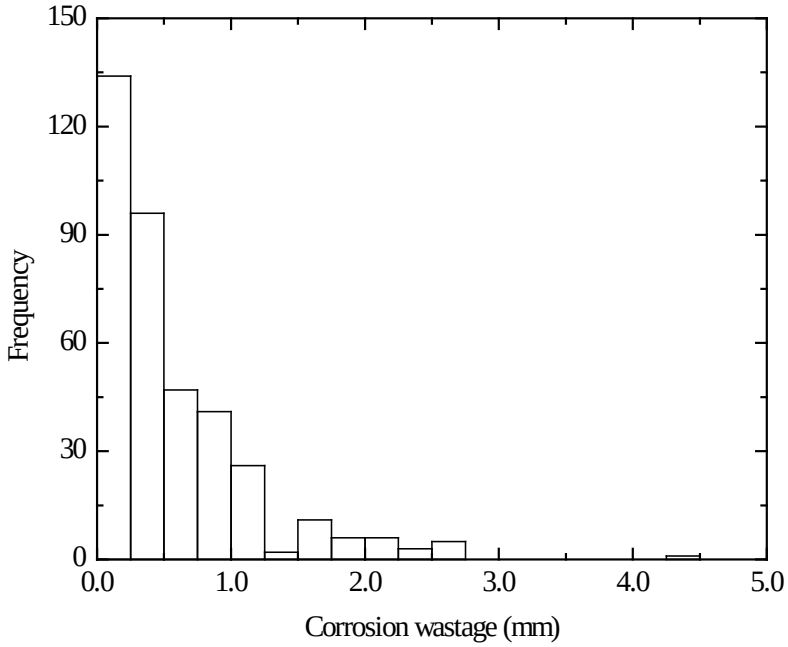

Figure 5.30 Histograms of corrosion wastage of upper deck longitudinal stiffener web plates for 21-year-old tanker (ballast tanks)

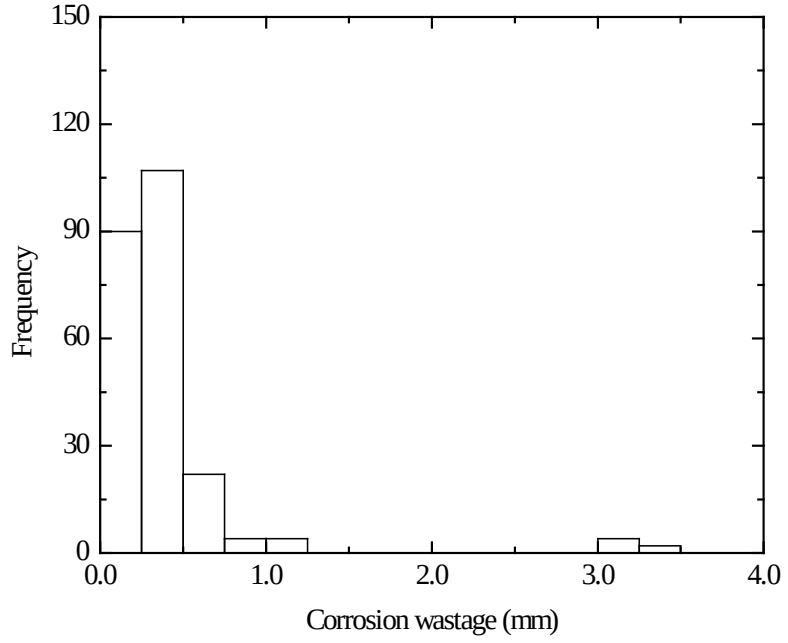

Figure 5.31 Histograms of corrosion wastage of upper deck longitudinal stiffener flanges for 19-year-old tankers (cargo oil tanks)

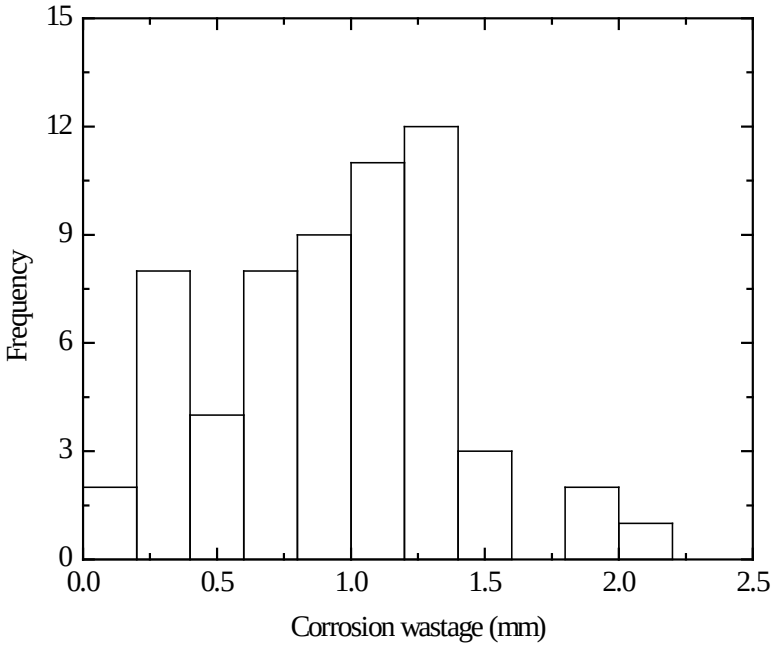

Figure 5.32 Histograms of corrosion wastage of upper deck longitudinal stiffener flanges for 18-year-old tankers (ballast tanks)

For the sake of convenience, it is assumed that corrosion wastage at year T follows a Weibull distribution or probability density function:

$$f_{t_{cor}}\left(t_{cor}\right)=\frac{k}{\theta}\left(\frac{t_{cor}}{\theta}\right)^{k-1}\exp\left(-\left(\frac{t_{cor}}{\theta}\right)^{k}\right) \tag{5-15}$$

where t_{cor} stands for the corrosion wastage, k is the shape parameter, and θ is the scale parameter. When these parameters are known, the mean value and variance of t_{cor} can be calculated by the formulations:

$$\mu\left(t_{cor}\right)=\theta\,\Gamma\left(1+\frac{1}{k}\right) \tag{5-16}$$

$$\text{stdev}\left(t_{cor}\right)=\sqrt{\theta^{2}\left\{\Gamma\left(1+\frac{2}{k}\right)-\left[\Gamma\left(1+\frac{1}{k}\right)\right]^{2}\right\}} \tag{5-17}$$

The analytical solutions of k and θ are not available from Eq. (5-16) and Eq. (5-17). Several methods, such as the graphic method (Mann et al 1974), the maximum likelihood method (Clifford 1965, Harter & Moore 1965) and the moment method (Justus et al 1978), have been commonly used to estimate Weibull parameters. Graphic methods are not very accurate but they are relatively fast. The maximum likelihood method and the moment method are considered more accurate and reliable compared to the graphical method. Ivanov & Wang (2008) proposed a method to estimate the Weibull parameters. An approximate analytical formula was obtained and it was proved accurate by comparing the results obtained by this method with the results of previous studies in literature. In the present study, this particular method is selected.

The following equations for the shape parameter k and scale parameter θ are recommended:

$$k = 0.0068 + 1.0189 \frac{\mu\left(t_{cor}\right)}{\text{stdev}\left(t_{cor}\right)} \tag{5-18}$$

$$\theta = \frac{\text{stdev}\left(t_{cor}\right)}{\Gamma\left(1+\frac{1}{k}\right)} \tag{5-19}$$

Knowing these parameters, the probability density function for the corrosion wastage at any given year can be obtained. One example for the corrosion wastage of deck plates in way of ballast tanks is shown in Figure 5.33. The graphs in this figure could be labeled as the annual probability distribution, which refers to ships of a specific age.

Given the values of the mean and standard deviation in Table 5.2, the time-variant equations can be derived to present the parameters of Weibull distribution function. The graphical illustration of the trend of the calculated shape and scale parameters vs. ship's

age are as shown in Figure 5.34 ~ Figure 5.36.

According to these derived Weibull parameters, the envelopes of the annual probability distribution of corrosion wastage for upper deck structure members in cargo tanks and ballast tanks are illustrated in Figure 5.37 ~ Figure 5.39. These figures can be used for the fleet manager to obtain the probability distribution of the corrosion wastage for all vessels in the fleet over the entire intended service lifetimes of the ships.

From the above results in respect to ships' age, the probability density functions of corrosion wastage become flatter and wider. This shows that as the ship becomes older, the net thickness of deck plates, web plates and flanges of the upper deck longitudianls vary in an even wider range and uncertainties associated with corrosion increase.

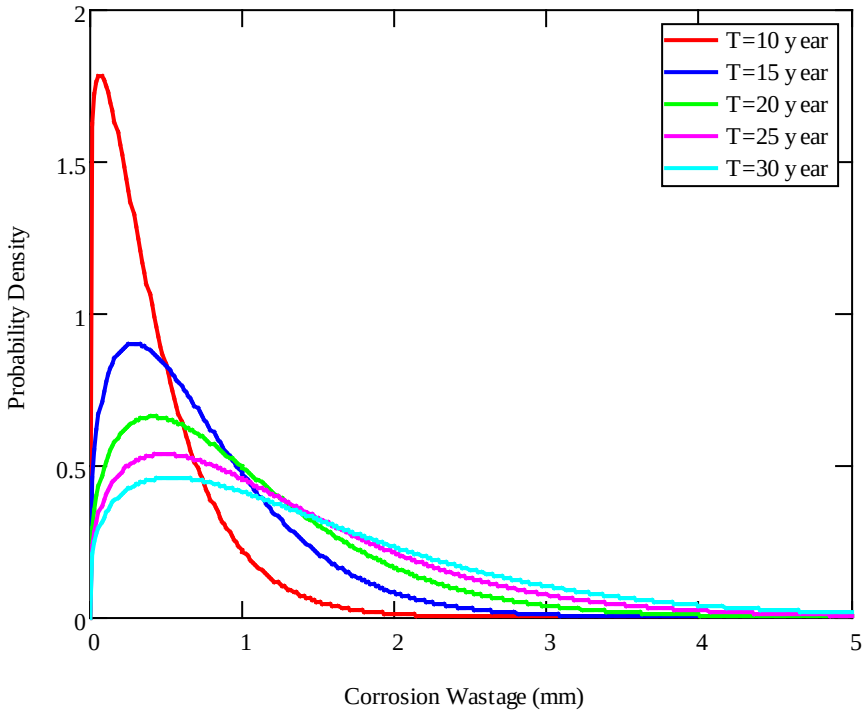

Figure 5.33 Annual probability density function of corrosion wastage prediction of deck plates in way of ballast tanks

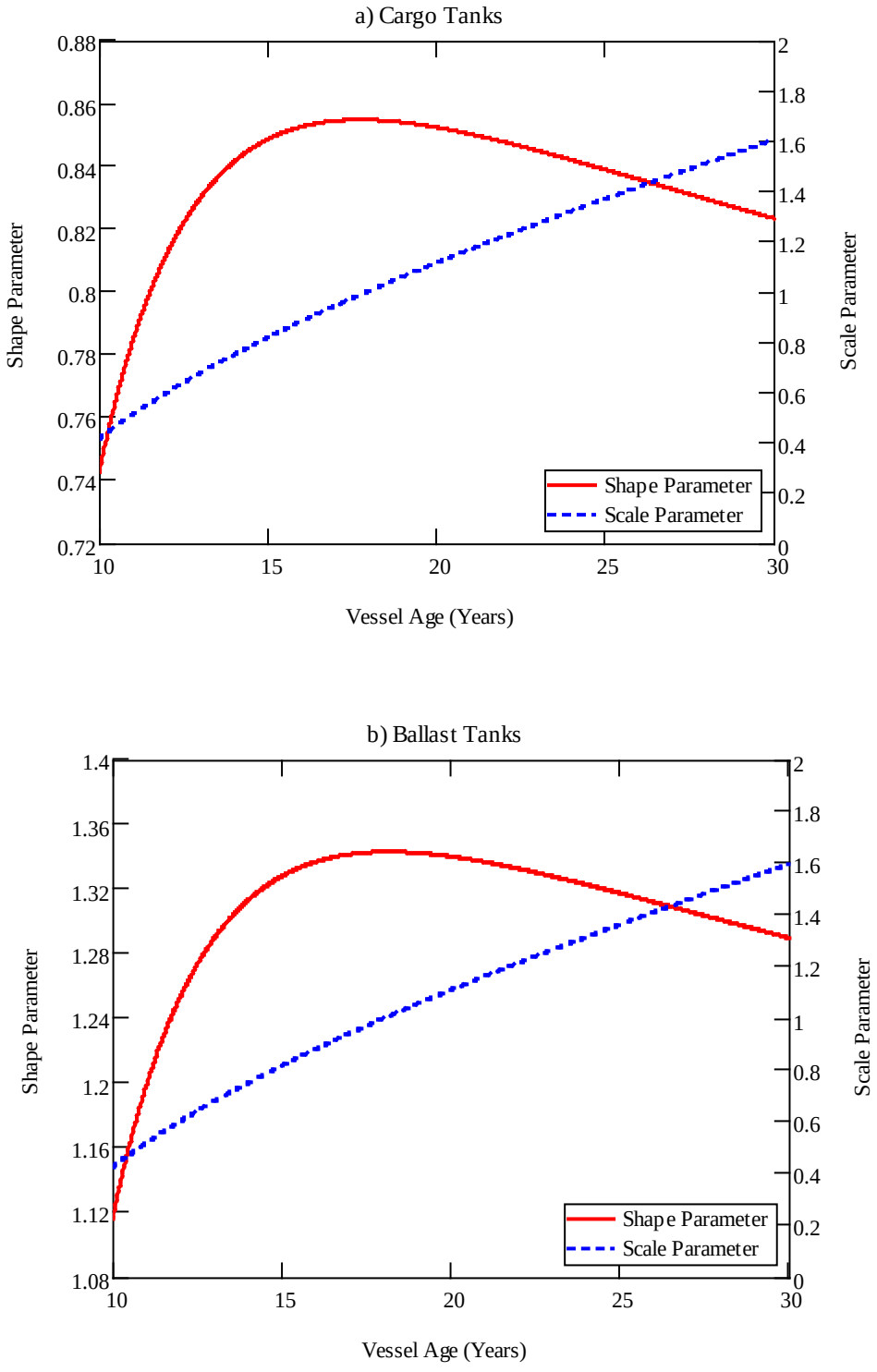

Figure 5.34 Changes of Weibull parameters with ship's age for corrosion wastage prediction of deck plates

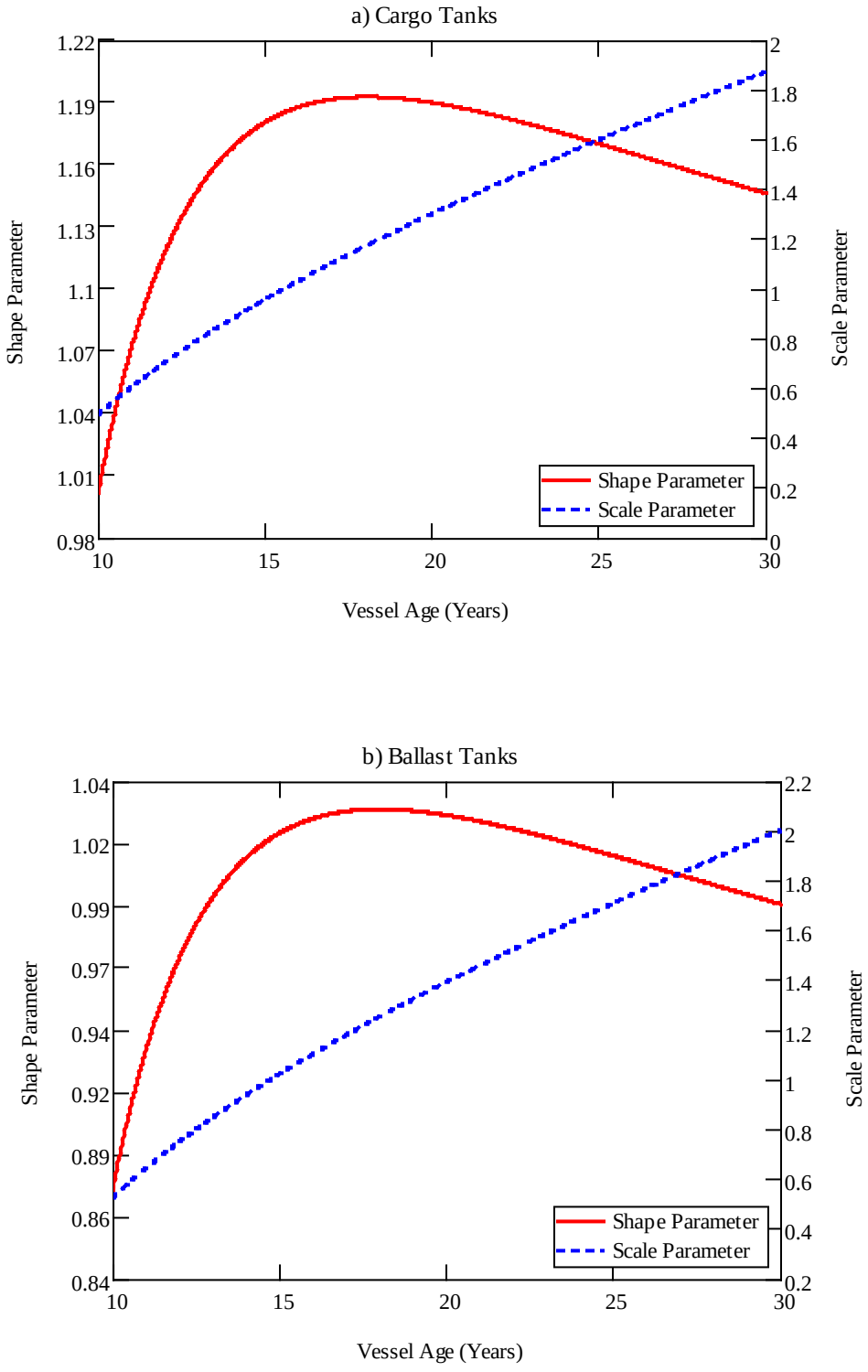

Figure 5.35 Changes of Weibull parameters with ship's age for corrosion wastage prediction of upper deck longitudinal stiffener web plates

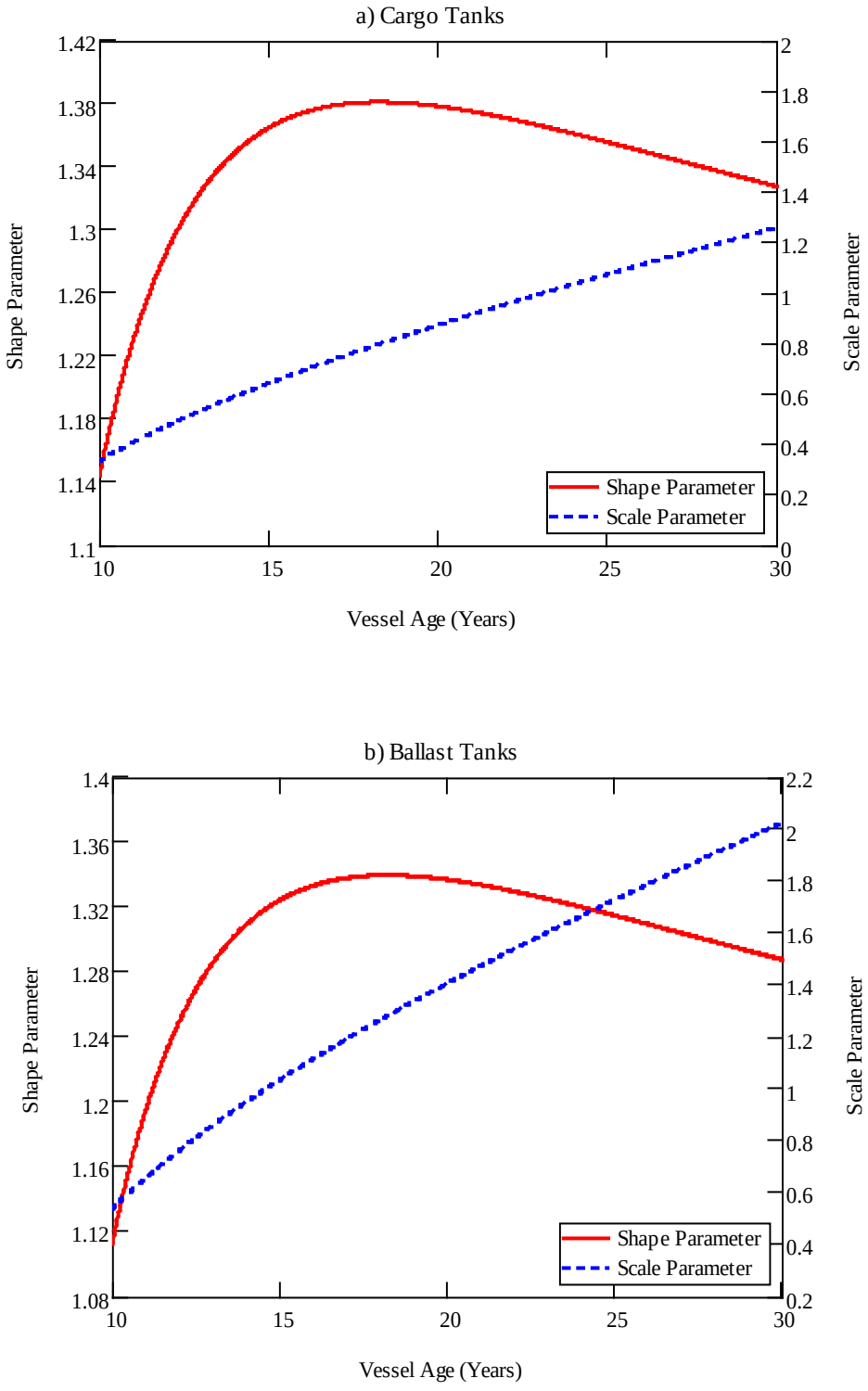

Figure 5.36 Changes of Weibull parameters with ship's age for corrosion wastage prediction of upper deck longitudinal stiffener flanges

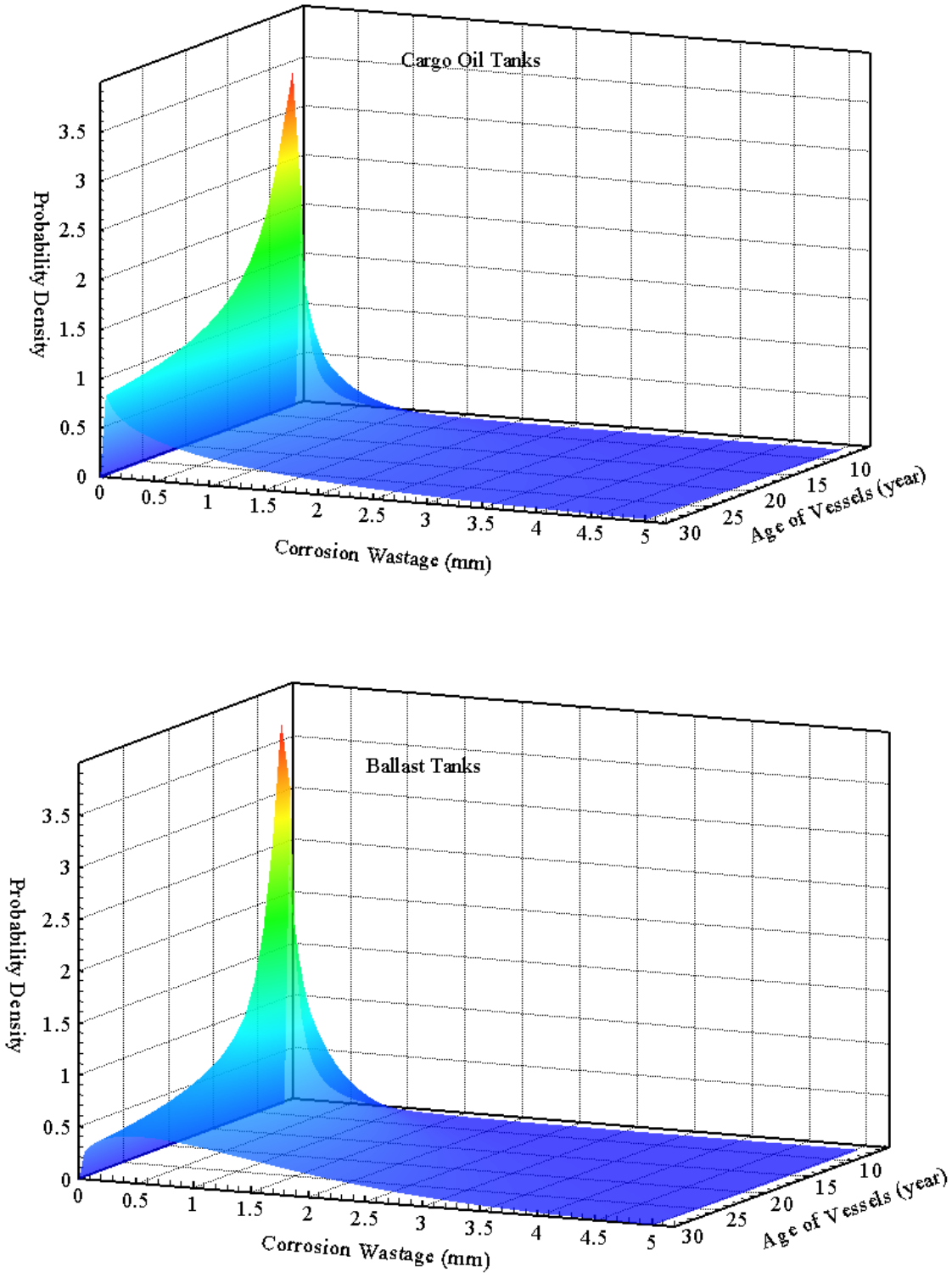

Figure 5.37 Time-variant probability density function of corrosion wastage of deck plates

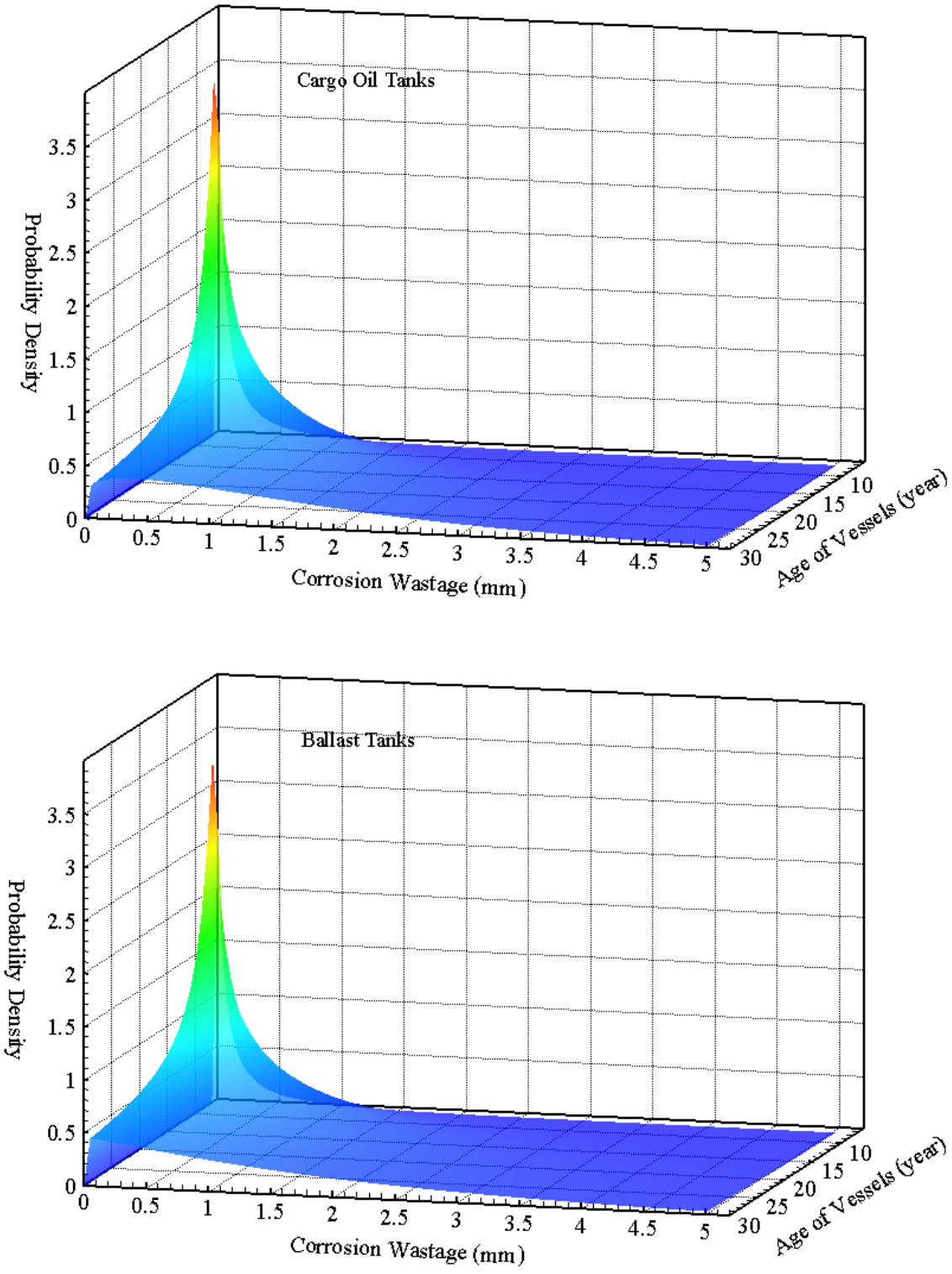

Figure 5.38 Time-variant probability density function of corrosion wastage of upper deck longitudinal stiffener web plates

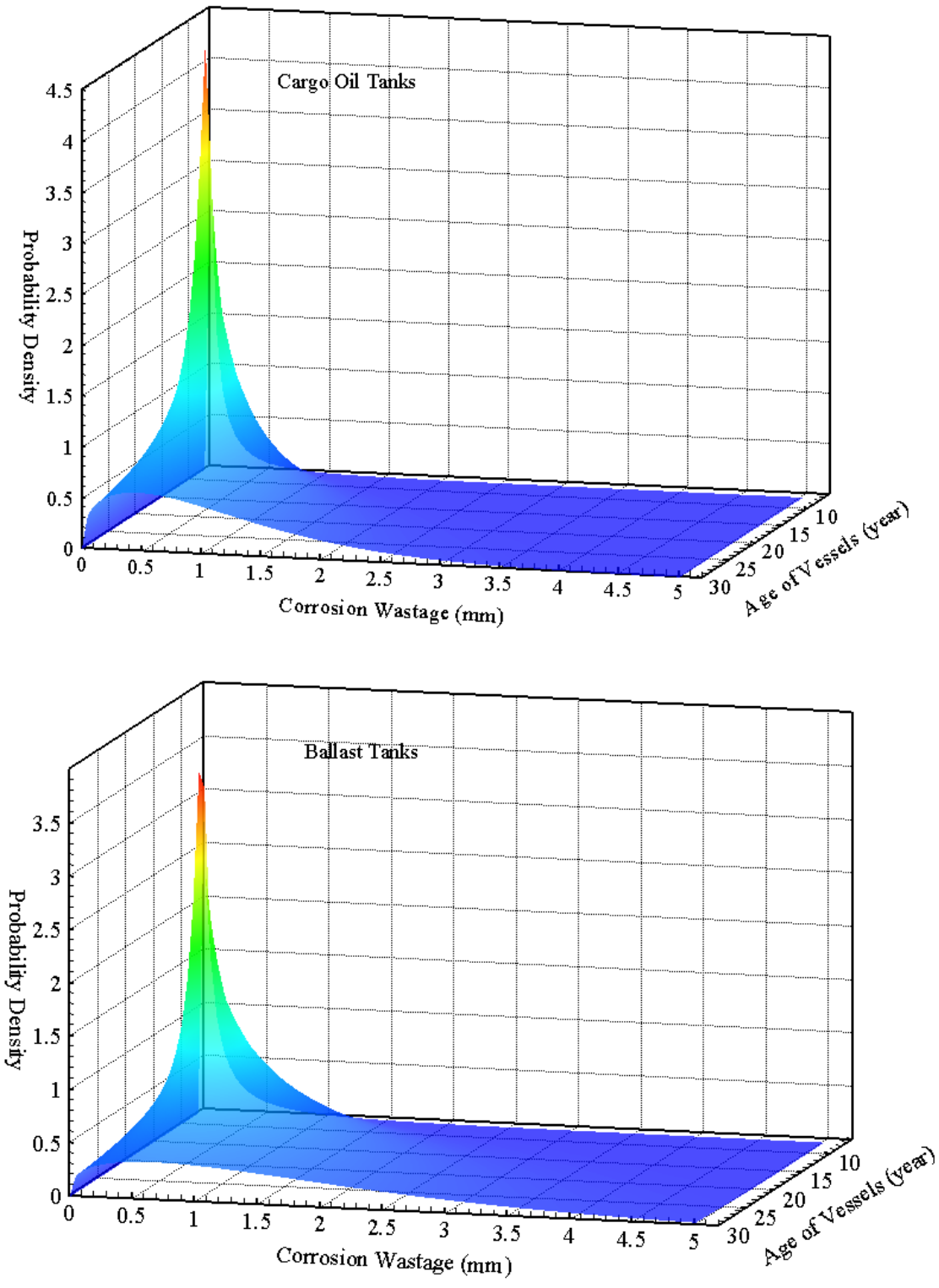

Figure 5.39 Time-variant probability density function of corrosion wastage of upper deck longitudinal stiffener flanges

5.3.4 Comparison Study

Table 5.3 tabulated results from three previous studies and the current study in the corrosion prediction of the deck structures of aging tankers. Representative results were selected and corrosion wastage for 20-year old tankers was compared. The prediction of the corrosion wastage differs from one to the other. This could be due to the fact that the available corrosion data is different and so are the assumptions made. The same corrosion data were applied by Garbatov et al. (2005) and the current study, but the latter predicted more severe corrosion. For conservative consideration, the newly derived corrosion model is used to predict the corrosion wastage of the deck structures and Weibull distribution is applied for presenting the corrosion wastage over a ship's life.

Table 5.3 Comparisons of corrosion wastage prediction for upper deck structures of 20-year-old tankers

Reference	Member group	Mean (mm)	COV	Coating life assumed (year)	Probabilistic term
Paik et al (2003)	DPB	1.2360	1.1172	5	Weibull distribution was used for presenting the corrosion rate.
		1.3550	1.1088	7.5	
		1.2080	1.0778	10	
	DPC	0.7335	0.6183	5	
		0.7262	0.6000	7.5	
		0.6820	0.5620	10	
	DLBW	3.1215	3.1277	5	
		3.0038	2.7529	7.5	
		2.8360	2.8754	10	
	DLCW	0.9300	0.7034	5	
		0.8950	0.7967	7.5	
		0.8450	0.6982	10	
	DLCF	0.7635	0.7630	5	
		0.7350	0.7374	7.5	
		0.6940	0.7086	10	
Garbatov et al (2005)	DPB	0.7712	0.4404	10.54	Lognormal distribution was used for presenting the corrosion wastage.
	DPC	1.0145	0.6513	11.494	
Present study (Guo et al, 2008)	DPB	1.0196	0.7686	6.5	Weibull distribution is used for presenting the corrosion wastage.
	DPC	1.2124	1.1778	6.5	
	DLBW	1.3794	1.3439	6.5	
	DLCW	1.2287	1.0366	6.5	
	DLBF	1.2924	0.9764	6.5	
	DLCF	0.7991	0.5867	6.5	

5.4 Summary

In this chapter, time-variant corrosion wastage prediction models for upper deck structures (deck plating, longitudinal web and flange) of oil tankers have been developed by the statistical analysis of a corrosion wastage measurement database. Due to the lack of data dealing with basic physical influencing parameters, the prediction of corrosion wastage based on purely phenomenological models may not be as accurate as statistical models. A statistics-based models are the most commonly used. Based on the derived corrosion model, the following conclusions can be drawn:

- It is found that Weibull distribution is one of the most proper approximations fitting the statistical distribution of the corrosion wastage at any time along the service life of a vessel.
- The corrosion model is different for the different upper deck members.
- The corrosion of the deck plate in cargo oil tank is more severe than that in ballast tank, while the corrosion of longitudinal web and flange is of greater severity for the ballast tank.
- Probabilistic characters of the corrosion wastage defined in the present study will be useful for structural reliability analysis of aging tanker structures.

The following should be noted when the current corrosion model is applied to reliability-based inspection planning:

- The derived equations are useful in a generic sense. They provide a good basis for the initial estimate of corrosion wastage over a vessel's lifetime.
- The current data set reflects the overall trends of a tanker fleet. It may contribute to more efficient management of the fleet because it reveals the risk of

not meeting certain criteria, such as IMO or Classifications Renewal Criteria requirements for the structures.

- An individual tanker may show a different trend in corrosion wastage. This model is dependent on trading route, cargo carried, operation, maintenance and other effects. When vessel-specific data such as gauging results become available, the corrosion wastage model needs to be updated to reflect a more accurate/reliable trend.

CHAPTER 6

APPLICATION AND RESULTS

6.1 Introduction

The reliability-based inspection plan of tankers' deck panels was predicted using the procedure developed in this study. First, the reliability assessment of deck panels was carried out using the reliability formulation for ultimate strength derived in Chapter 2. The target reliability level is determined according to the procedure proposed in Section 2.3 based on a selected benchmark tanker. The inspection interval was then determined by comparing the calculated time-variant probability of failure and the target reliability levels defined in Chapter 2. Sensitivity analysis is performed in this chapter to study the relative contribution of each design basic variable to the safety level achieved. The reliability-based inspection plan is compared with the current calendar-based inspection plan.

6.2 Reliability Assessment for Sample Tankers

6.2.1 Sample Tankers

From a pool of hundreds of tankers, six tankers were selected as sample tankers for demonstrating the application of the procedure based on the reliability-based methodology described in previous chapters of this dissertation. This selection consists of one

tanker built in the 1970s, one in the 1980s, three in the 1990s and one in the 2000s. In accordance with the flexible market scale of tanker capacity, this selection covers Product tanker, Panamax, Aframax, Suezmax and VLCC. These tankers were built to comply with the classification rules at the time of design and construction. As rules have gradually changed over the decades since these tankers were built, some of the tankers may not comply with the current design rules. The principal particulars of the vessels are summarized in Table 6.1.

6.2.2 Calculation of Failure Probability by Monte Carlo Simulation

The failure probability of deck panels was predicted using the reliability formulation for ultimate strength presented in Chapter 2. The analytical solution of Eq. (2-49) is difficult to obtain because it involves multi-dimensional probability integration. The Monte Carlo Simulation (MCS) method was used for this calculation. This method applies an iterative scheme for a deterministic model using sets of random numbers as inputs. It can be used for the complex, nonlinear or implicit function. The drawback, however, is that the calculation is time-consuming.

In the case of the time-variant failure probability calculation, the MCS technique samples each random variable randomly to give sampling values $\hat{\sigma}_u(T), \hat{\sigma}(T)$. Then, the limit state function, g, will be evaluated. After N trials, the probability of failure is approximated by:

$$P_f(T) \approx \frac{\tilde{N}\left(g\left(\hat{\sigma}_u(T), \sigma(T)\right) \le 0\right)}{N} \tag{6-63}$$

where $\tilde{N}\left(g\left(\hat{\sigma}_u(T), \sigma(T)\right)\right)$ denotes the number of trials for which $g\left(\hat{\sigma}_u(T), \sigma(T)\right) \le 0$. Obviously, the number N is influenced by the desired degree of accuracy of $P_f(T)$.

Table 6.1 Principal particulars of the sample tankers

Ship ID	70B	80B	90A	90B	90C	00A
Year built	1970s	1980s	1990s	1990s	1990s	2000s
Ship type	VLCC	Suezmax	VLCC	Aframax	Product	Panamax
Hull type	Single	Single	Double	Double	Double	Double
Length between perpendiculars, L_{BP} (m)	320	277	320	233	180	218.6
Rule length, L (m)	317.853	273.286	315.83	230.375	177.7	216.3
Breadth, B (m)	54.5	48	58	42	32.2	32.26
Depth, D (m)	27	23.5	31	21.3	19.15	20.2
Deadweight, DWT (Tonnage)	273859	149237	298324	104800	40000	72365
Block coefficient, C_b	0.8106	0.8316	0.823	0.832	0.8059	0.86
Section modulus at deck, Z_d (m^3)	82.06	45.7728	81.2604	29.9422	19.9308	21.2219
Transverse frame spacing, l (mm)	5300	4650	5120	4120	3510	3400
Longitudinal spacing, s (mm)	940	850	910	820	800	757
Deck plate thickness, t_p (mm)	27.5	19	20	16	14.5	14.5
Deck longitudinal type	Flat Bar	Flat Bar	T Bar	Angle	Flat Bar	Flat Bar
Web depth, d_w (mm)	450	370	350	250	230	230
Web thickness, t_w (mm)	35	30	12.5	12	19	20
Flange breadth, b_f (mm)	-	-	150	90	-	-
Flange thickness, t_f (mm)	-	-	15	16	-	-
Minimum yield stress, σ_y (N/mm^2)	315	315	315	315	235	315
Design SWBM (Sagging), M_{SW} (KN-m)	5979568.0	3784201.4	6168528.0	2275920.0	1471500.0	1527721.1
Design WBM (Sagging), M_W (KN-m)	9835575.2	6409266.2	10419234.4	3819893.9	1582820.0	2585890.0

Generation of random number

A key part of MCS is generating random numbers. Most MCS methods use pseudorandom numbers which are obtained on the basis of a formula. A commercial software named Crystal Ball® was applied to perform the simulation. It uses a Multiplicative Congruential Generator to generate the random number, where the iteration formula is given by:

$$x \leftarrow (62089911 \cdot x) \bmod \left(2^{31} - 1\right) \tag{6-64}$$

The generator has a period of length which equals $2^{31} - 2$, or 2,147,483,646. This means that the generated numbers will not repeat after 2×10^{10} trials. This would be adequate for many marine-related problems where the failure probability often falls in the range of 10^{-2} to 10^{-8}.

Latin Hypercube Sampling

The probability of failure is estimated as the ratio of the number of failures to the total number of simulation trials. If failure probability is small, such as 10^{-4}, Monte Carlo direct sampling would require a large number of trials to estimate the probability of failure within an acceptable level of statistical error. In addition, direct simulation requires binary definition of failure according to the limit state equation. Due to these drawbacks, MCS with direct sampling becomes unfeasible.

Latin Hypercube Sampling (LHS), a variant of MCS, was applied for the simulation because it ensures that the ensemble of random numbers is representative of the real variability. Traditional direct sampling is just an ensemble of random numbers without any guarantees. LHS was first developed by McKay et al (1979) to generate a distribution of plausible collections of parameter values from a multidimensional distribution. It was

further elaborated upon by Iman et al (1981a, 1981b). Differences of Latin hypercube sampling and other techniques were reviewed and discussed by Iman & Helton (1985).

With Latin hypercube sampling, each parameter's probability distribution is divided into several non-overlapping segments on the basis of equal probability, and a value for the parameter would be generated randomly from each segment. LHS is generally more precise when determining simulation statistics compared with conventional Monte Carlo direct sampling because the entire range of the distribution is sampled more evenly and consistently. With Latin hypercube sampling, the required number of trials to achieve the same level of statistical accuracy as with Monte Carlo sampling is remarkably reduced.

Random variables

Table 6.2 summarizes random variables related to this reliability assessment. Determination of these variables is based on previous studies presented in Chapters 3, 4 and 5.

6.2.3 Convergence of Simulation

MCS relies on a sampling of random variables. The calculation accuracy depends on the sampling number and is not affected by the distribution type and the number of basic variables.

In general, as more trials are calculated, the statistical error decreases and the results become more accurate. Figure 6.1 shows an example of the convergence. It is clear that in the instance where the number of simulations reaches 6×10^5, the calculated failure probabilities (reliability indices) were converged. Therefore, a million trials of MCS were applied to calculate the failure probability of the deck panels to achieve conver-

gence of the simulation.

Table 6.2 Stochastic models of the random variables related to the reliability assessment

Variable		Mean	COV	Distribution
Strength prediction				
Young's modulus E (MPa)		198378	0.105	Normal
Yield stress σ_y (MPa)	Mild steel	258.5	0.1	Lognormal
	HT32 steel	340.2	0.1	Lognormal
	HT36 steel	390.5	0.1	Lognormal
As-built plate thickness, t_{p_0} (mm)		t_{p_0}	$0.4369/t_{p_0}$	Normal
Stiffener spacing, s (mm)		$s-0.3302$	$2.362/(s-0.3302)$	Normal
Stiffener span, l (mm)		$l-0.9398$	$2.692/(l-0.9398)$	Normal
Web depth, d_w (mm)		d_w	0.0187	Normal
As-built web thickness, t_{w_0} (mm)		$1.26\,t_{w_0}$	0.0904	Lognormal
Flange breadth, b_f (mm)		$1.13\,b_f$	0.0917	Lognormal
As-built flange thickness, t_{f_0} (mm)		t_{f_0}	0.0161	Lognormal
Modeling uncertainty χ_u		0.9	0.15	Normal
Load effects				
SWBM M_{SW} (KN-m)		$M_{SW-\mathrm{Ref}}$	0.05	Type I Extreme
WBM M_W (KN-m)		$M_{W-\mathrm{Ref}}$	0.10	Type I Extreme
Combination factor ψ_W		0.75	-	Deterministic
Time-variant corrosion effect				
Plate wastage, $t_{p(cor)}(T)$ (mm)		Refer Table 5-2		Weibull
Web wastage, $t_{w(cor)}(T)$ (mm)				Weibull
Flange wastage, $t_{f(cor)}(T)$ (mm)				Weibull
Reduction factor of HGSM, $\gamma_z(T)$		Refer Eq. (2-46)		Weibull

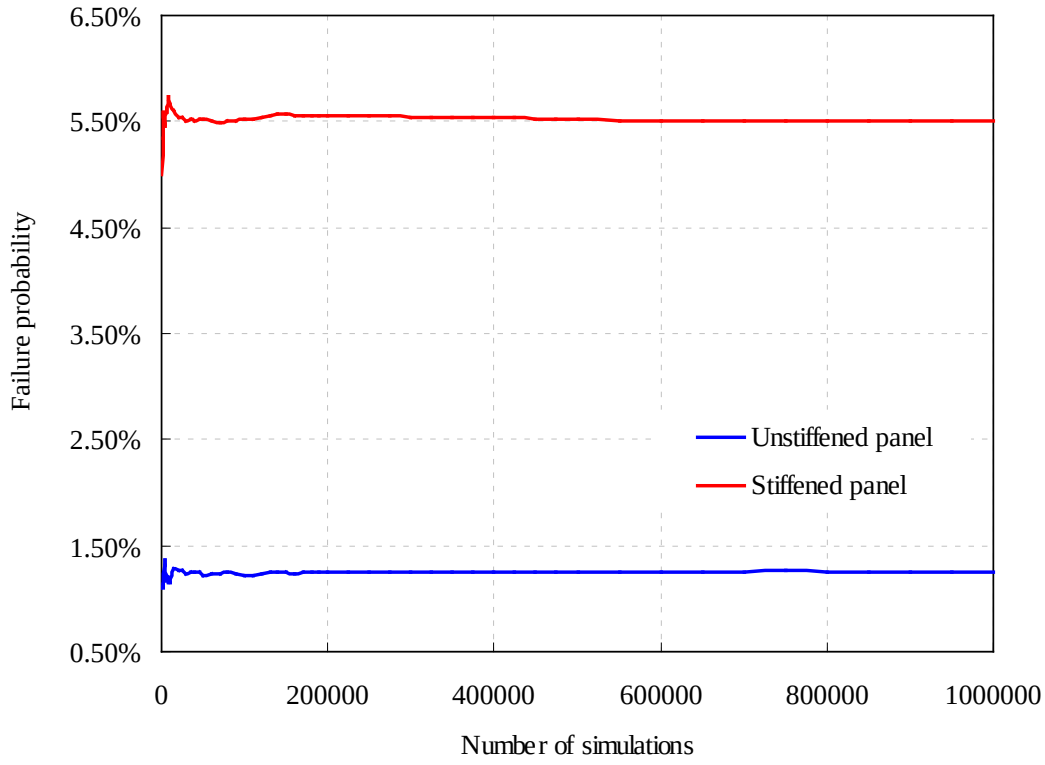

Figure 6.1 Test of MCS convergence (deck panel of the 20-year-old tanker 90B)

6.2.4 Sensitivity Analysis

As shown in Eq. (2-48) and (2-49), the limit states functions for ultimate strength failure of deck panels involve a large number of variables, which are represented by stochastic models indicated in Table 6.2. The computational demands rapidly increase as the number of dimensions increase. In order to reduce the number of random variables without compromising the accuracy of the calculated failure probability, sensitivity analyses were performed to study the relative contribution of each basic random variable to the failure probability.

The results are presented as factors α_i, with $i = 1, \ldots, n$, and n is the number of

basic variables associated with the reliability assessment. The results obtained for the 20-year-old sample tanker 90B are presented in Table 6.3 ~ Table 6.4 and Figure 6.2 ~ Figure 6.3. The goal was to identify the importance of the uncertainty associated with each random variable.

Unstiffened panel:

For the variance of failure probability of plate panels' ultimate strength failure, the uncertainties of the basic random variables that contributed most are the modeling uncertainty factor χ_u and the corrosion wastage of the plate $t_{p(cor)}$, as can be concluded from Table 6.3. Besides these two dominant basic variables, the contribution of the material yield stress σ_y and the WBM M_W are also important. The contribution of the reduction factor of HGSM γ_Z, as-built plate thickness t_{p_0}, and the SWBM M_{SW} are small. The Young's modulus E and stiffener spacing s have negligible contributions. Therefore, it is possible to treat the last two variables as deterministic variables without significantly affecting the failure probability of the deck plate. The sensitivity analyses for cargo oil tanks and ballast tanks yield similar results.

Table 6.3 Sensitivity factors of the unstiffened plate panels for the 20-year-old sample tanker 90B

Random viable	Cargo oil tanks	Ballast tanks
Modeling uncertainty, χ_u	49.72 % (-)	49.43% (-)
As-built plate thickness, t_{p_0}	1.37% (-)	1.37% (-)
Stiffener spacing, s	0.01% (+)	0.01% (+)
Corrosion wastage, $t_{p(cor)}(20)$	30.52% (+)	30.92% (+)
Young's modulus, E	0.04% (-)	0.04% (-)
Yielding strength, σ_y	8.17% (-)	8.12% (-)
SWBM, M_{SW}	0.96% (+)	0.95% (+)
WBM, M_W	7.46% (+)	7.40% (+)
Reduction factor of HGSM, $\gamma_Z(20)$	1.75% (+)	1.76% (+)

The corrosion wastage contributes positively, as higher values of this variable will decrease the ultimate strength σ_{u-p} of the unstiffened plate panels and consequently increase the failure probability due to ultimate strength failure. WBM and SWBM also have positive contribution since higher values of these variables will increase the compressive stress σ_x applied on the plate panels, and consequently its failure probability.

Because the corrosion wastage is a time-dependent variable, the relative contribution of each basic variable's uncertainty to the failure probability varies with the vessel's age. The trends of the plate panel failure probability for sample tanker 90B are indicated in Figure 6.2.

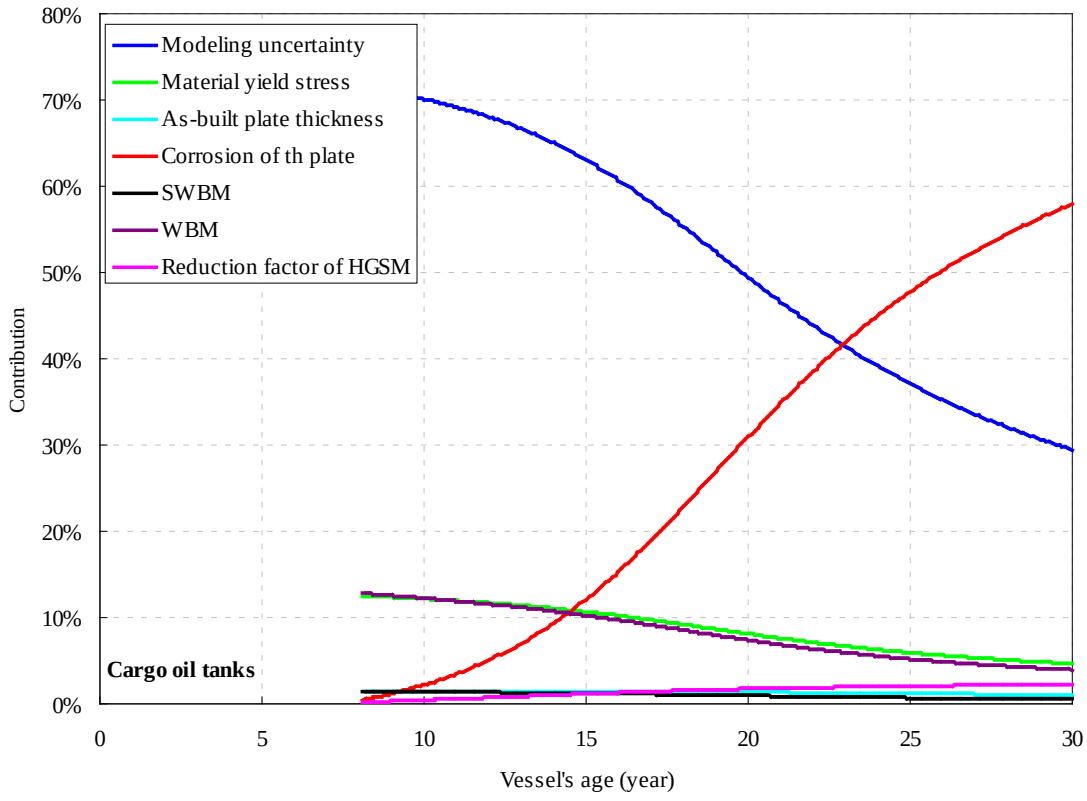

Figure 6.2 Time-variant relative contribution of variables to the variance of failure probability for deck plate panel ultimate strength failure (using the tanker 90B as an example)

Only the variables with important contributions to the variance of failure probability are included. As illustrated in the trends, the contribution of both corrosion wastage of deck plate $t_{p(cor)}$ and reduction factor of HGSM γ_Z increase with the tanker's age, while others decrease. The contribution of corrosion wastage on deck plate increases dramatically with age. Hence, corrosion wastage becomes the dominant governing variable. This proves the importance of the research on the corrosion effect of aging tankers. It can also be concluded that the local effect of corrosion $t_{p(cor)}$ has a greater contribution than the global effect of corrosion γ_Z when assessing the reliability of the unstiffened plate panel.

Stiffened panel:

For failure probability calculation of the stiffened panel's ultimate strength failure, sixteen random variables and two different failure modes are considered. As listed in Table 6.4 and Table 6.5, the sensitivity factors of each random variable for beam-column buckling failure mode and torsional buckling failure mode are similar.

The basic random variables that contributed most to the variance of the failure probability are the modeling uncertainty factor χ_u and the material yield stress σ_y. Besides these two dominant basic variables, the contribution of the WBM M_W, the SWBM M_{SW} and the reduction factor of HGSM γ_Z are also important. The as-built thickness of plate, web and flange, the Young's modulus E, stiffener spacing s and stiffener span l have negligible influence.

WBM and SWBM have positive contributions, since higher values of these variables will increase the compressive stress σ_x applied on the plate panels, and consequently its failure probability. The contribution of corrosion wastage varies slightly for

different failure modes. Although the uncertainties of the local corrosion wastage may have a small contribution towards the variance of the failure probability, the importance of these variables is undeniable for the calculation of the time-variant failure probability.

Table 6.4 Sensitivity factors of the stiffened panels for the 20-year-old sample tanker 90B (beam-column buckling failure mode)

Random viable	Cargo oil tanks	Ballast tanks
Modeling uncertainty, χ_u	60.68% (-)	60.72% (-)
Stiffener spacing, s	< 0.01% (+)	< 0.01% (+)
Stiffener span, l	< 0.01% (+)	< 0.00% (+)
As-built plate thickness, t_{p_0}	0.01% (+)	0.01% (+)
Web depth, d_w	0.04% (-)	0.04% (-)
As-built web thickness, t_{w_0}	0.01% (-)	0.01% (-)
Flange breadth, b_f	0.11% (-)	0.11% (-)
As-built flange thickness, t_{f_0}	< 0.01% (-)	< 0.01% (-)
Corrosion wastage, $t_{p(cor)}(20)$	0.04% (-)	0.02% (-)
Web wastage, $t_{w(cor)}(20)$	< 0.01% (+)	0.01% (+)
Flange wastage, $t_{f(cor)}(20)$	0.02% (+)	0.05% (+)
Young's modulus, E	< 0.01% (-)	< 0.01% (-)
Yielding strength, σ_y	24.49% (-)	24.44% (-)
SWBM, M_{SW}	1.20% (+)	1.20% (+)
WBM, M_W	10.97% (+)	10.96% (+)
Reduction factor of HGSM, $\gamma_Z(20)$	2.44% (+)	2.44% (+)

Due to the time-dependent corrosion wastage of the local deck structures as well as the hull girder, the relative contribution of each basic variable's uncertainty to the failure probability is a function of time. The trends for sample tanker 90B in terms of the

stiffened panel failure probability are indicated in Figure 6.3. According to the trends, the contribution of the reduction factor of HGSM γ_Z increases with the tanker's age, while others decrease. Compared to the trends for plate panel, the trends for stiffened panel reveal that the increase/decrease rates of the contribution for most variables to the variance of the failure probability are smaller. It is also concluded that the local effect of corrosion wastage has a smaller contribution than the global effect of corrosion γ_Z when assessing the reliability of the stiffened plate panel.

Table 6.5 Sensitivity factors of the stiffened panels for the 20-year-old sample tanker 90-B (torsional buckling failure mode)

Random viable	Cargo oil tanks	Ballast tanks
Modeling uncertainty, χ_u	61.74% (-)	61.77% (-)
Stiffener spacing, s	< 0.01% (+)	< 0.01% (+)
Stiffener span, l	< 0.01% (+)	< 0.00% (+)
As-built plate thickness, t_{p_0}	0.01% (-)	0.01% (-)
Web depth, d_w	0.02% (+)	0.02% (+)
As-built web thickness, t_{w_0}	0.02% (-)	0.02% (-)
Flange breadth, b_f	0.16% (-)	0.16% (-)
As-built flange thickness, t_{f_0}	< 0.01% (+)	< 0.01% (+)
Corrosion wastage, $t_{p(cor)}(20)$	0.07% (-)	0.03% (-)
Web wastage, $t_{w(cor)}(20)$	0.02% (+)	0.02% (+)
Flange wastage, $t_{f(cor)}(20)$	< 0.01% (-)	< 0.01% (-)
Young's modulus, E	< 0.01% (-)	< 0.01% (-)
Yielding strength, σ_y	22.54% (-)	22.52% (-)
SWBM, M_{SW}	1.22% (+)	1.22% (+)
WBM, M_W	11.67% (+)	11.67% (+)
Reduction factor of HGSM, $\gamma_Z(20)$	2.52% (+)	2.52% (+)

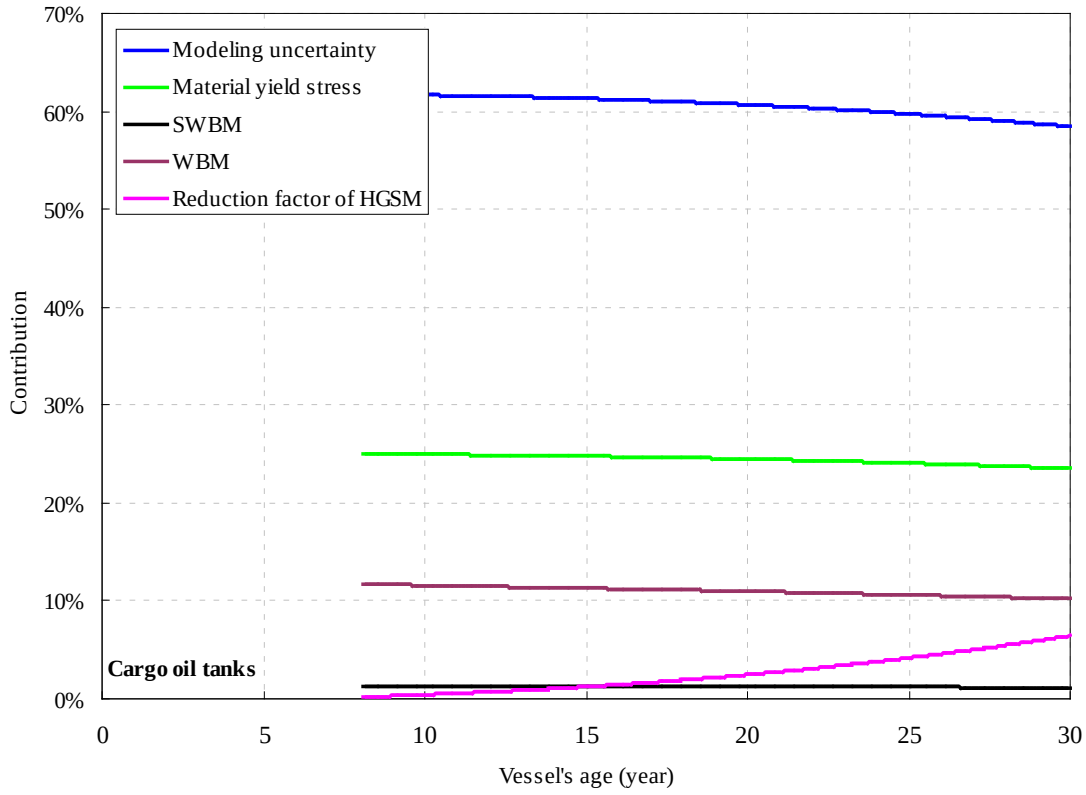

Figure 6.3 Time-variant relative contribution of variables to the failure probability of deck stiffened panel ultimate strength failure (using the tanker 90-B as an example)

6.2.5 Analysis Results

The time-variant probability density function of corrosion wastage and HGSM lost, together with random variables indicated in Table 6.2, are applied to Eq. (2-55) to perform the time-variant reliability assessments of the corroded aging tanker's deck panels. The detailed results using reliability index β_R and failure probability P_f for the six sample oil tankers are presented. The results include both unstiffened plate panel and stiffened panel.

Unstiffened deck plate:

The time-variant reliability indices obtained for the deck plate panels are presented in Figure 6.4 and Figure 6.5. Detailed results are listed in Table 6.6 and Table 6.7.

It is obvious that the reliability indices decrease as the tankers age. The possibilities of failure in cargo oil tanks are slightly higher than those in ballast tanks due to the slightly heavier corrosion wastage of the deck plate in cargo oil tanks.

Table 6.6 Failure probabilities of unstiffened deck plate panels for sample tankers at selected ages (cargo oil tanks)

Sample Tanker	Vessels' age (year)				
	10	15	20	25	30
70B	5.97×10^{-4}	7.53×10^{-4}	9.18×10^{-4}	1.11×10^{-3}	1.36×10^{-3}
80B	2.04×10^{-2}	2.94×10^{-2}	4.00×10^{-2}	5.34×10^{-2}	6.96×10^{-2}
90A	6.77×10^{-3}	1.04×10^{-2}	1.58×10^{-2}	2.44×10^{-2}	3.61×10^{-2}
90B	2.44×10^{-2}	3.77×10^{-2}	5.51×10^{-2}	7.66×10^{-2}	9.99×10^{-2}
90C	1.98×10^{-2}	3.32×10^{-2}	5.28×10^{-2}	7.70×10^{-2}	1.02×10^{-1}
00A	1.56×10^{-2}	2.75×10^{-2}	4.62×10^{-2}	6.96×10^{-2}	9.42×10^{-2}

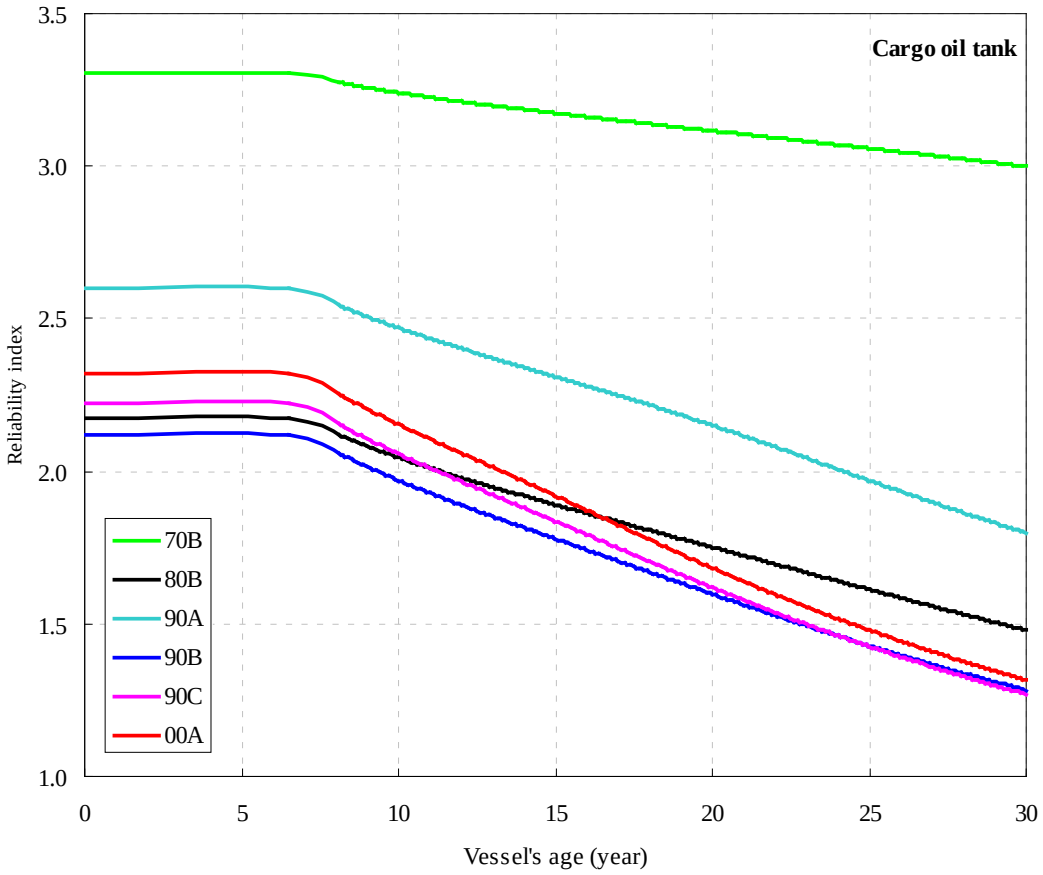

Figure 6.4 Time-variant reliability indices of unstiffened deck plate panels for sample tankers (cargo oil tanks)

Table 6.7 Failure probabilities of unstiffened deck plate panels for sample tankers at selected ages (ballast tanks)

Sample Tanker	Vessels' age (year)				
	10	15	20	25	30
70B	5.97×10^{-4}	7.53×10^{-4}	9.18×10^{-4}	1.11×10^{-3}	1.36×10^{-3}
80B	2.09×10^{-2}	2.93×10^{-2}	3.81×10^{-2}	4.81×10^{-2}	5.93×10^{-2}
90A	6.91×10^{-3}	1.02×10^{-2}	1.40×10^{-2}	1.86×10^{-2}	2.42×10^{-2}
90B	2.49×10^{-2}	3.66×10^{-2}	4.93×10^{-2}	6.38×10^{-2}	8.03×10^{-2}
90C	2.02×10^{-2}	3.10×10^{-2}	4.34×10^{-2}	5.83×10^{-2}	7.56×10^{-2}
00A	1.59×10^{-2}	2.49×10^{-2}	3.57×10^{-2}	4.89×10^{-2}	6.47×10^{-2}

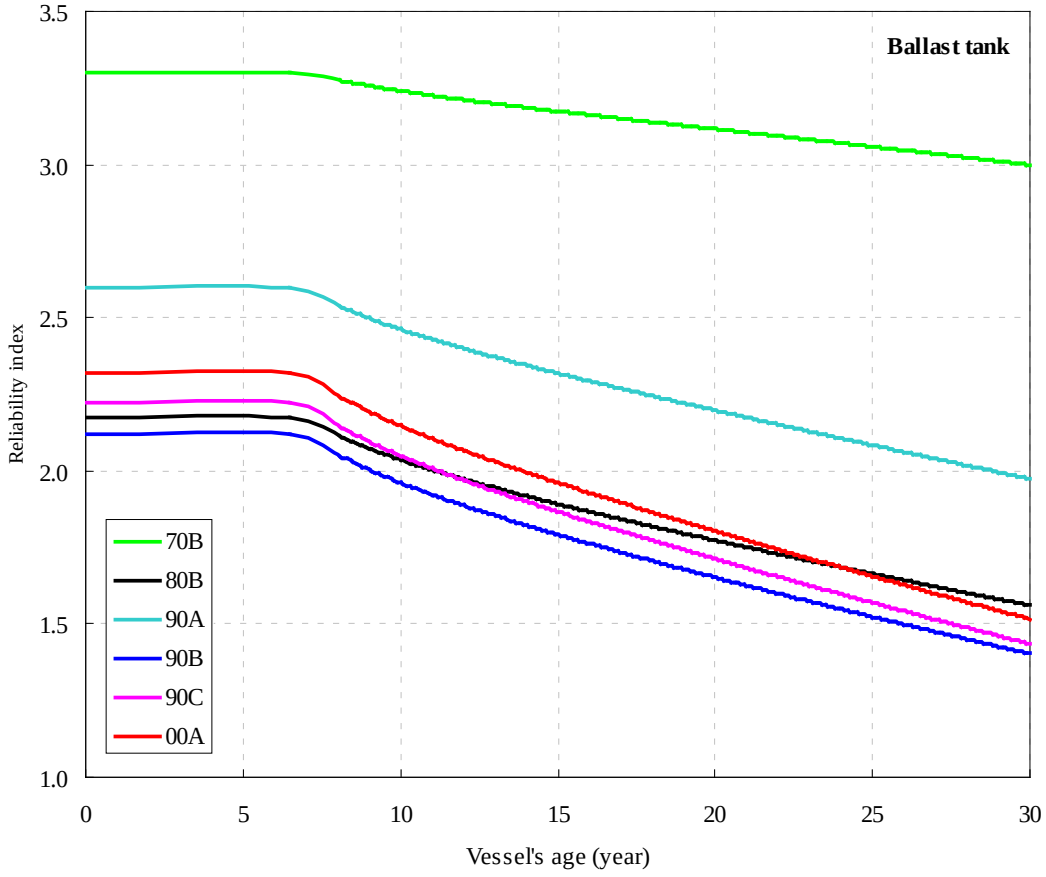

Figure 6.5 Time-variant reliability indices of unstiffened deck plate panels for sample tankers (ballast tanks)

Deck stiffened panels:

The time-variant reliability indices obtained for the deck plate panels are presented in Figure 6.6 ~ Figure 6.9, with the detailed results in Table 6.8 ~ Table 6.10. Two different failure modes are considered, beam-column buckling failure and torsional (tripping) buckling failure. As shown in the figures and tables, the reliability indices decrease as tankers age and the possibilities of failure in cargo oil tank are similar to those in ballast tank. By comparing Figure 6.6 with Figure 6.4, it can be concluded that the decrease of reliability indices of deck stiffened panels over the vessel's life is not as apparent as the tendency for unstiffened deck panels.

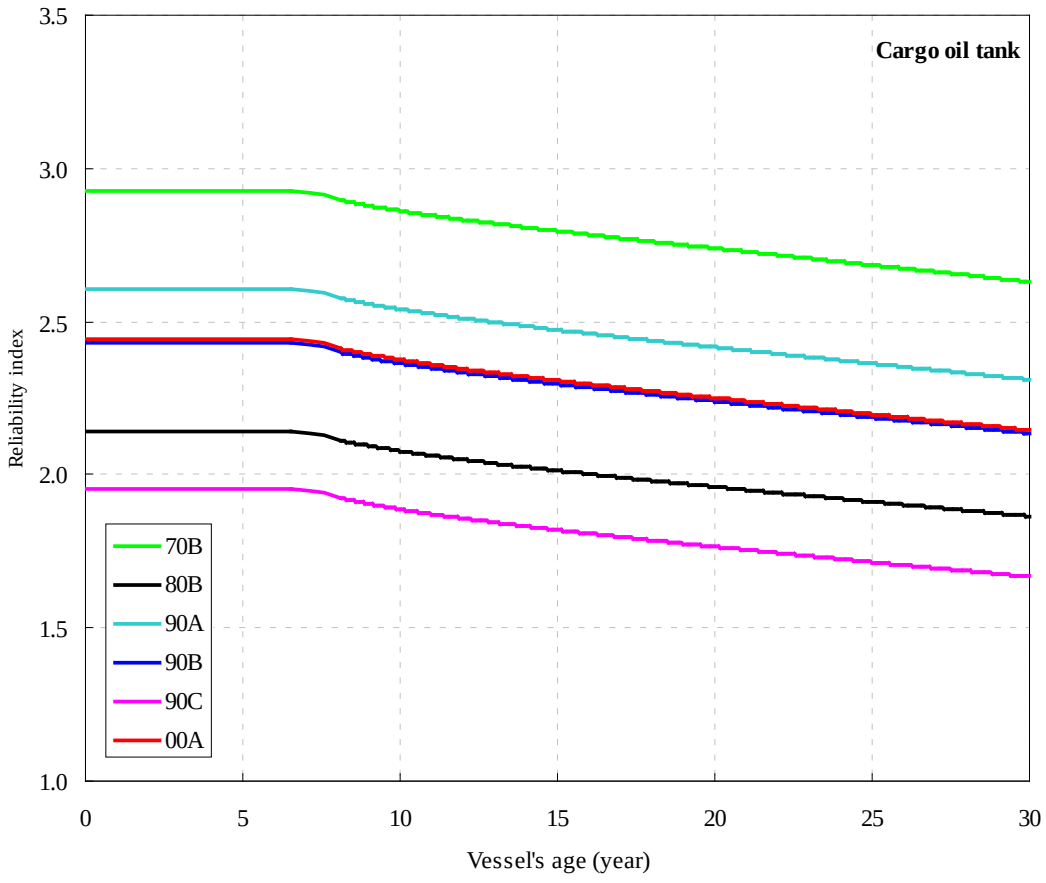

Figure 6.6 Time-variant reliability indices of stiffened deck panels based on beam-column buckling failure mode for sample tankers (cargo oil tanks)

Table 6.8 Failure probabilities of stiffened deck panels based on beam-column buckling failure mode for sample tankers at selected ages (cargo oil tanks)

Sample Tanker	Vessels' age (year)				
	10	15	20	25	30
70B	2.11×10^{-3}	2.59×10^{-3}	3.08×10^{-3}	3.63×10^{-3}	4.28×10^{-3}
80B	1.89×10^{-2}	2.20×10^{-2}	2.50×10^{-2}	2.79×10^{-2}	3.11×10^{-2}
90A	5.54×10^{-3}	6.70×10^{-3}	7.84×10^{-3}	9.06×10^{-3}	1.04×10^{-2}
90B	9.05×10^{-3}	1.08×10^{-2}	1.25×10^{-2}	1.44×10^{-2}	1.64×10^{-2}
90C	2.95×10^{-2}	3.44×10^{-2}	3.87×10^{-2}	4.31×10^{-2}	4.77×10^{-2}
00A	8.75×10^{-3}	1.05×10^{-2}	1.22×10^{-2}	1.40×10^{-2}	1.59×10^{-2}

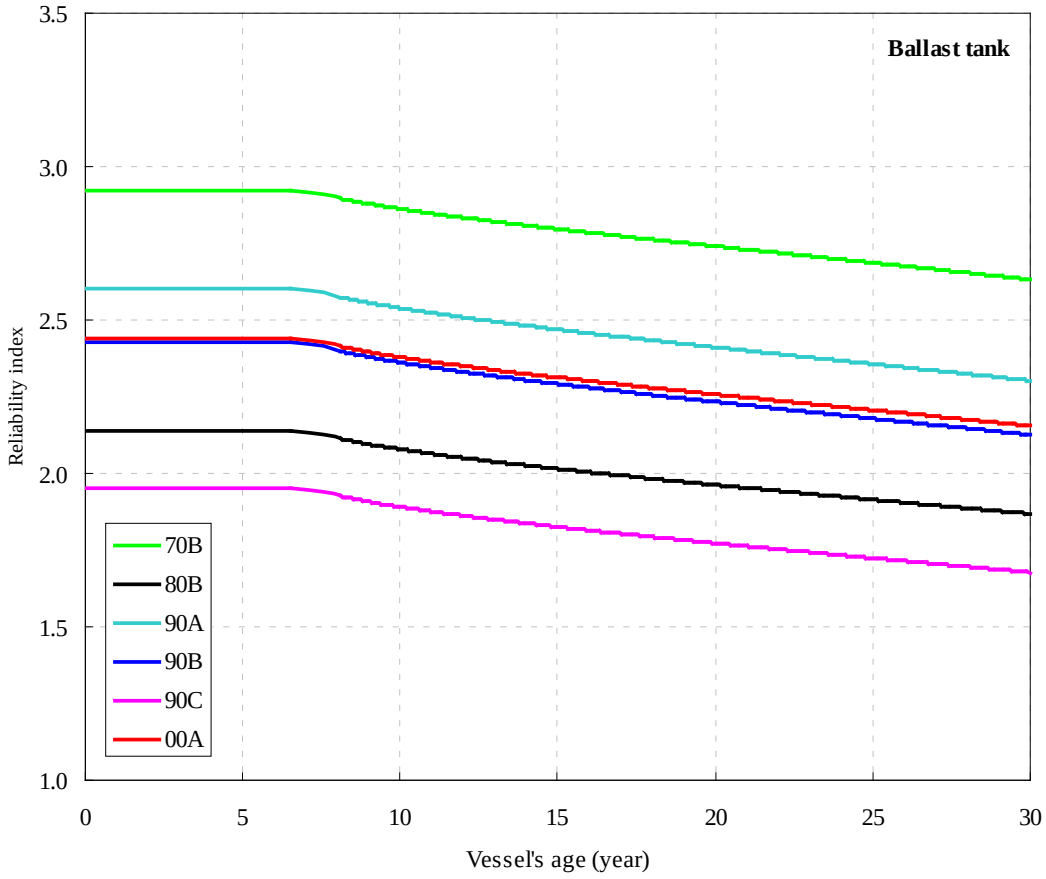

Figure 6.7 Time-variant reliability indices of stiffened deck panels based on beam-column buckling failure mode for sample tankers (ballast tanks)

Table 6.9 Failure probabilities of stiffened deck panels based on beam-column buckling failure mode for sample tankers at selected ages (ballast tanks)

Sample Tanker	Vessels' age (year)				
	10	15	20	25	30
70B	2.10×10^{-3}	2.58×10^{-3}	3.07×10^{-3}	3.61×10^{-3}	4.25×10^{-3}
80B	1.88×10^{-2}	2.20×10^{-2}	2.49×10^{-2}	2.78×10^{-2}	3.09×10^{-2}
90A	5.57×10^{-3}	6.77×10^{-3}	7.95×10^{-3}	9.22×10^{-3}	1.07×10^{-2}
90B	9.10×10^{-3}	1.10×10^{-2}	1.28×10^{-2}	1.47×10^{-2}	1.68×10^{-2}
90C	2.93×10^{-2}	3.40×10^{-2}	3.82×10^{-2}	4.23×10^{-2}	4.67×10^{-2}
00A	8.69×10^{-3}	1.04×10^{-2}	1.20×10^{-2}	1.37×10^{-2}	1.56×10^{-2}

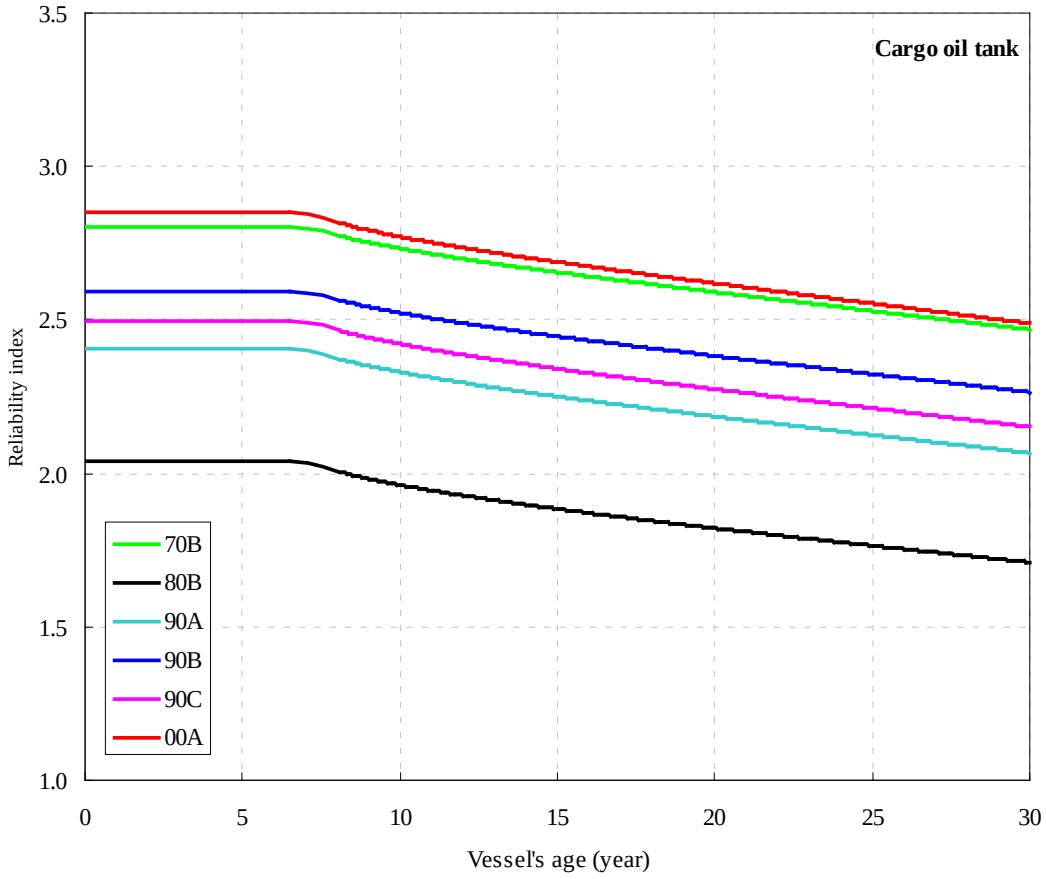

Figure 6.8 Time-variant reliability indices of stiffened deck panels based on torsional buckling failure mode for sample tankers (cargo oil tanks)

Table 6.10 Failure probabilities of stiffened deck plate panels based on torsional buckling failure mode for sample tankers at selected ages (cargo oil tanks)

Sample Tanker	Vessels' age (year)				
	10	15	20	25	30
70B	3.14×10^{-3}	3.96×10^{-3}	4.79×10^{-3}	5.71×10^{-3}	6.78×10^{-3}
80B	2.49×10^{-2}	2.98×10^{-2}	3.43×10^{-2}	3.88×10^{-2}	4.36×10^{-2}
90A	9.90×10^{-3}	1.22×10^{-2}	1.44×10^{-2}	1.68×10^{-2}	1.94×10^{-2}
90B	5.82×10^{-3}	7.22×10^{-3}	8.59×10^{-3}	1.01×10^{-2}	1.18×10^{-2}
90C	7.72×10^{-3}	9.62×10^{-3}	1.15×10^{-2}	1.35×10^{-2}	1.57×10^{-2}
00A	2.79×10^{-3}	3.59×10^{-3}	4.41×10^{-3}	5.33×10^{-3}	6.42×10^{-3}

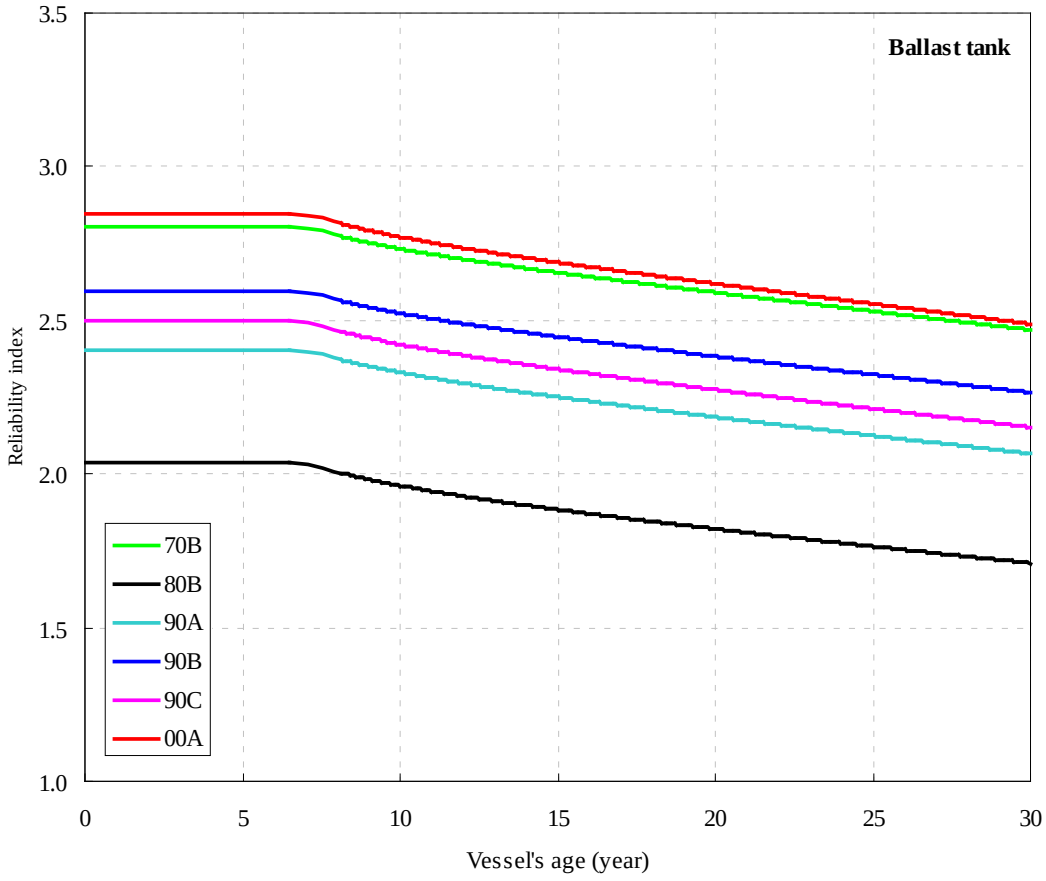

Figure 6.9 Time-variant reliability indices of stiffened deck panels based on torsional buckling failure mode for sample tankers (ballast tanks)

Table 6.11 Failure probabilities of stiffened deck panels based on torsional buckling failure mode for sample tankers at selected ages (ballast tanks)

Sample Tanker	Vessels' age (year)				
	10	15	20	25	30
70B	3.15×10^{-3}	3.98×10^{-3}	4.81×10^{-3}	5.75×10^{-3}	6.83×10^{-3}
80B	2.49×10^{-2}	2.99×10^{-2}	3.45×10^{-2}	3.91×10^{-2}	4.39×10^{-2}
90A	9.93×10^{-3}	1.23×10^{-2}	1.45×10^{-2}	1.70×10^{-2}	1.96×10^{-2}
90B	5.84×10^{-3}	7.25×10^{-3}	8.64×10^{-3}	1.02×10^{-2}	1.19×10^{-2}
90C	7.74×10^{-3}	9.66×10^{-3}	1.15×10^{-2}	1.36×10^{-2}	1.58×10^{-2}
00A	2.80×10^{-3}	3.61×10^{-3}	4.44×10^{-3}	5.39×10^{-3}	6.51×10^{-3}

According to Eq. (2-41), the ultimate strength of the stiffened panels is the minimum of the beam-column and torsional critical buckling stress. The reliability of the stiffened panels should be governed by either beam-column buckling or torsional buckling failure mode, whichever gives the lower reliability level. The governing failure model of stiffened deck panels for each sample tanker is indicated in Table 6.12. It can be concluded that the governing failure mode is not consistent between sample ships. However, while considering one specific vessel, the governing failure mode for cargo oil tank and ballast tank is consistent.

Table 6.12 Governing failure mode of deck stiffened panels for sample tankers

Sample tanker	70B	80B	90A	90B	90C	00A
Cargo oil tank	T	T	T	BC	BC	BC
Ballast tank	T	T	T	BC	BC	BC

Notes: BC: Beam-Column Buckling Failure Mode; T: Torsional Buckling Failure Mode

Without corrosion effect, the failure probabilities (reliability indices) calculated at the beginning of the service life for each sample tanker can be considered as the implicit reliability level of the deck panel structures for the sample tankers. The comparison of the implicit reliability levels of the unstiffened plate panel and stiffened panel leads to recog-

nition the critical design parameters for tankers at time of design. Table 6.13 shows the comparison results performed for each sample tanker.

Table 6.13 Rank of reliability level of the deck panels for sample tankers at the time of service

Sample Tanker	Reliability level rank		Reliability indices	
	Unstiffened plate	Stiffened panel	Unstiffened plate	Stiffened panel
70B	1	2	3.30	2.81
80B	1	2	2.17	2.04
90A	1	2	2.60	2.41
90B	2	1	2.12	2.43
90C	1	2	2.22	1.95
00A	2	1	2.32	2.44

Recalling the Eq. (2-61), the reliability level of stiffened panel (secondary failure mode) is to be higher than the level of unstiffened plate (tertiary failure mode) in common reliability-based structural design. However, the results indicated in Table 6.13 show some counterexamples. The main reason is that the designs of those tankers are not reliability-based. Tankers built in the 1970s usually have a much thicker deck plate than those built after the 1980s. This design causes the possibility of stiffened panel failure to be greater than plate failure. With the improvement of the ship structural analysis, the classification rules have been substantially updated since the 1970s. The importance of the stiffened panel has been highlighted. The results in Table 6.13 show that the reliability level of unstiffened plate panel significantly drops from the 1970s design to the current design, while the reliability level of stiffened panel maintains at a certain range.

With corrosion effects over a vessel's service life, the reliability of unstiffened plate panel may start higher but ends lower than the reliability of stiffened panel, and vice versa. Figure 6.10 shows an example in which the reliability of unstiffened plate panel is higher than that of stiffened panel for the first 18.5 years, but after that point the contrary

is true.

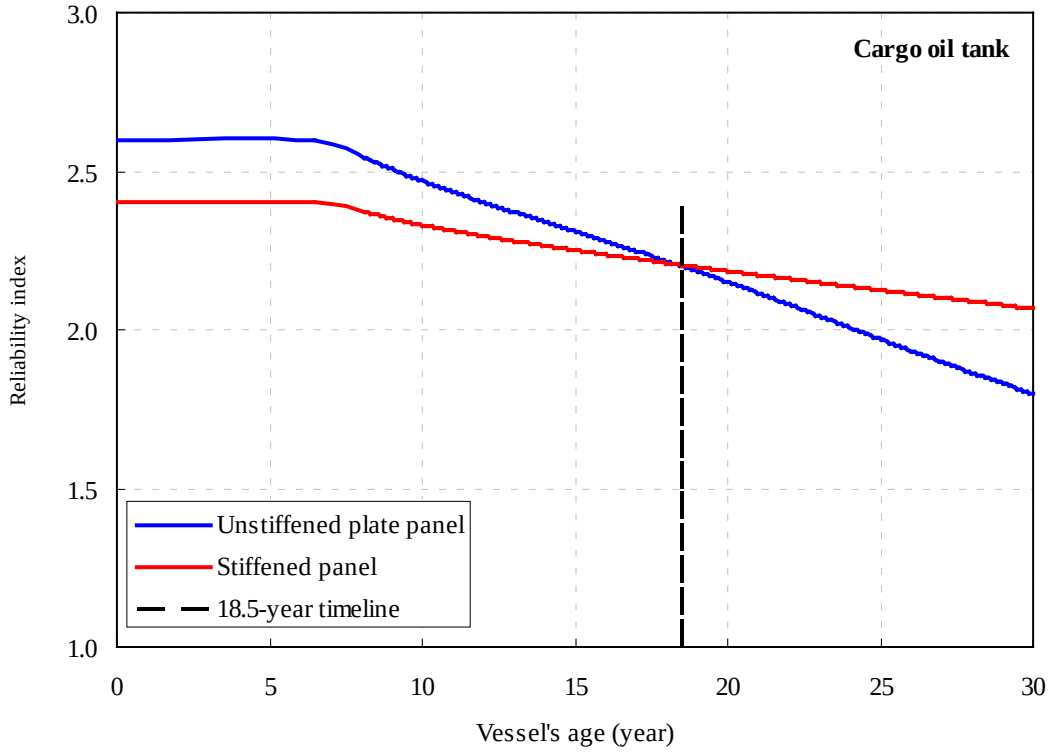

Figure 6.10 Time-variant reliability indices of the deck panels for the sample tanker 90A (cargo oil tanks)

6.3 Determination of the Target Reliability Levels

According to the review of the design parameters and original design analysis reports for hundreds of tankers, Tanker 90B was selected as the benchmark tanker to determine the target reliability levels. Her design is reflective of the current IACS panel strength requirements.

As indicated in Section 2.3, three levels of target reliability are considered. The calibrations of these values against benchmark Tanker 90B are illustrated in Figure 6.11.

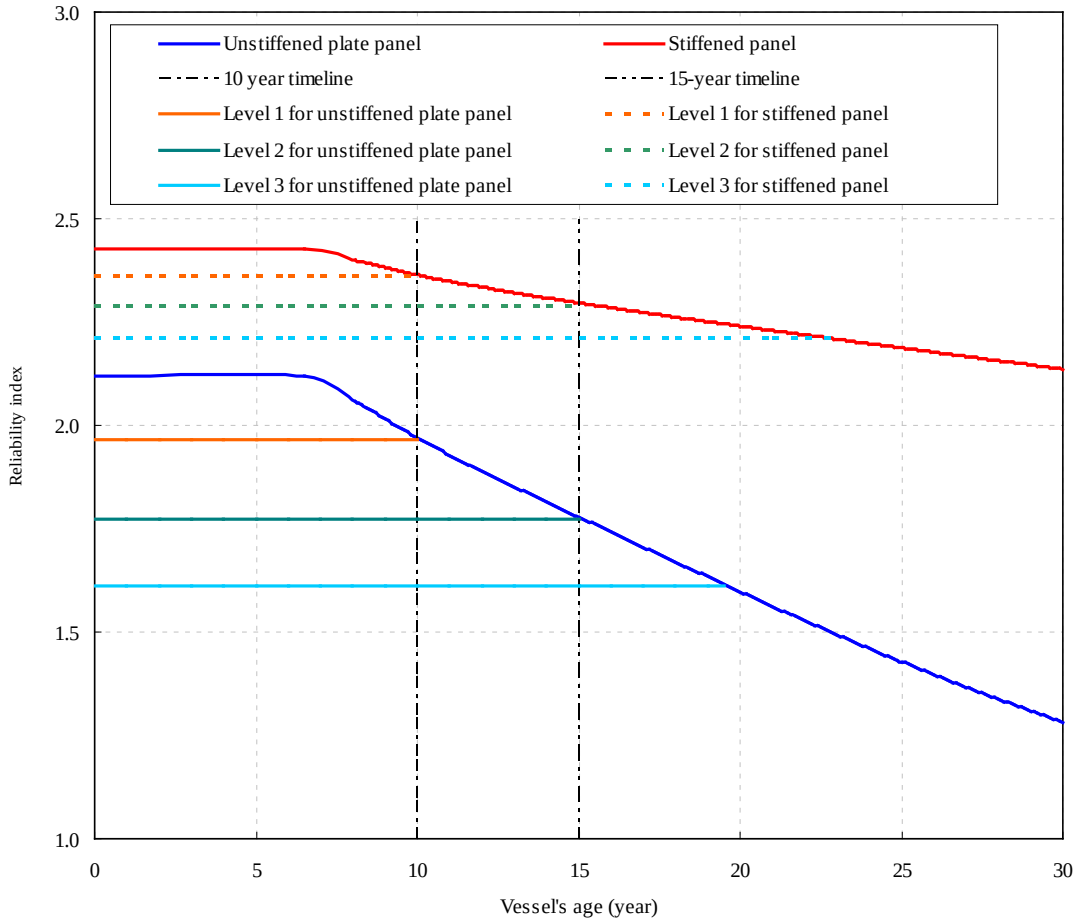

Figure 6.11 Calibration of target reliability levels for inspection planning of deck panels

The suggested values of the target failure probability (reliability index) are listed in Table 6.14. It is noted that the calibrated target values are not genuine but nominal. As discussed in Section 2.3, the target values are method-dependent.

Table 6.14 Suggested target failure probabilities (reliability indices)

Levels of target failure probability (reliability index)	Trigger	Failure mode	
		Unstiffened plate panel	Stiffened panel
$P_{f1}^{*}(\beta_{R1}^{*})$	5-years interval	2.44×10^{-2} (1.97)	9.14×10^{-3} (2.36)
$P_{f2}^{*}(\beta_{R2}^{*})$	2.5-years interval	3.84×10^{-2} (1.77)	1.10×10^{-2} (2.29)
$P_{f3}^{*}(\beta_{R2}^{*})$	Renewal/Repair	5.37×10^{-2} (1.61)	1.35×10^{-2} (2.21)

6.4 Determination of Inspection Intervals

The first required inspection intervals for the sample tankers are listed in Table 6.15 based on the calculated failure probabilities in Section 6.2.6 and suggested levels of target failure probability indicated in Table 6.14. Furthermore, it is assumed that the predicted mean value of corrosion wastage indicated in Table 5.2 was recorded at the first inspection, the second required inspection intervals can be obtained using the updating scheme specified in Section 2.4. The results are listed in Table 6.16.

Table 6.15 Required first inspection interval (year) for sample tankers' deck panels

	Tank type	70B	80B	90A	90B	90C	00A
Unstiffened plate	COT	>30	12.2	25	10	12.2	14
	BT	>30	12.3	30	10.2	12.1	14.7
Stiffened panel	COT	>30	6.5*	8.6	10	6.5*	10.8
	BT	>30	6.5*	9	9.8	6.5*	11.2

Notes: COT – Cargo oil tank BT – Ballast tank

* The inspection interval is determined by assumed corrosion starting point.

Table 6.16 Required second inspection interval (year) for sample tankers' deck panels

	Tank type	70B	80B	90A	90B	90C	00A
Unstiffened plate	COT	5	5	5	5	5	5
	BT	5	5	5	5	5	5
Stiffened panel	COT	5	2.5	2.5	2.5	2.5	2.5
	BT	5	2.5	2.5	2.5	2.5	2.5

As shown in Table 6.15, the inspection intervals for stiffened panel are always shorter than those for unstiffened plate. The difference between cargo oil tank and ballast tank is not apparent. It is noted that the initial design reliability levels of stiffened deck panels for Tanker 80B and 90C are lower than the suggested target level. This does not mean that the strength of deck panels for these two tankers is inadequate because the tra-

ditional scantling design is not reliability-based. Therefore, the reliability-based inspection planning demands a shorter inspection interval for these tankers.

For Tanker 70B, the reliability-based analysis shows that no thickness measurements of deck panels are necessary for nearly the entire life of the vessel. After the International Conventions for the Prevention of Marine Pollution from Ships (MARPOL) requirements became mandatory in 1983, with the change in length to depth proportions, ship builders tried to achieve optimum arrangements for ballast and cargo in order to comply with the Convention's requirements. As a result, due to the increase in ship depths, the scantlings of tankers built after 1980 dropped dramatically compared with those built in the 1970s. See also Table 6.1 for the scantlings of the sample tankers. Based on the same predicted corrosion wastage over the vessels' life and the same target failure probability, the required inspections are expected to be more frequent. The results in Table 6.15 reflect this finding.

6.5 Summary

In this chapter, six sample tankers were selected to illustrate the proposed procedure for reliability-based inspection planning. First, the failure probability was calculated by Monte Carlo Simulation with Latin Hypercube Sampling. The uncertainties of each random variable and time-dependent probabilistic corrosion models were adopted from previous chapters. A benchmark tanker was then selected by engineering judgment to calibrate the target reliability levels for inspection planning. Finally, the inspection intervals were predicted referring to the calibrated target values. The following are the main conclusions from the analysis:

- Due to the effect of corrosion wastage, the failure probability of deck panel increases with the vessel's age and varies in a wide range. The increment for unstiffened plate panel is higher than that for stiffened panel.
- For unstiffened plate panel, the decrease of reliability appears to be more significant for shorter ships such as the Product or Panamax oil tankers due to the smaller classification rule-required thickness compared with longer ships such as the Aframax, Suezmax or VLCC oil tankers.
- The local corrosion effects are much more significant compared with the global corrosion effects when assessing the reliability of unstiffened plate panel. However, the global corrosion effect plays a more important role than local corrosion effects when assessing the reliability of stiffened panel.
- The results of the sensitivity analysis have shown that the uncertainties of the following random variables need to be included in structural reliability analysis: loads, modeling uncertainty, corrosion wastage and the yield stress of the material.
- The implicit reliability levels estimated for the deck panel present significant variability between the six sample tankers. Within each tanker, the variability for unstiffened plate panel is greater than stiffened panel. This confirms that the stiffened panel buckling requirements are the governing design parameter with the development of classification rules.
- Latin Hypercube Sampling is a practical method for structural reliability analysis. It is more efficient than the traditional Monte Carlo Simulation, especially when dealing with marine-related problems.

- The required time to carry out the first gauging survey on deck structures for tankers built in the 1970s is much longer than those built after the 1980s.
- Compared with the current practices, the proposed reliability-based method provides a more accurate inspection plan. For different ships, the inspection intervals are different. However, additional inspections may be needed for verification beyond inspections planned using the proposed procedure.

The common practice of ship design is not reliability based. For this reason, the integrity of each vessel differs over time. Hence, reliability-based inspection planning is believed to be a more rational approach in monitoring the condition of a vessel.

CHAPTER 7

CONTRIBUTIONS AND FUTURE WORK

7.1 Contributions

The major objective of this dissertation is to develop a reliability-based approach for ship inspection planning. Aging tankers, which may potentially experience catastrophic failure due to structural degradation effects caused by corrosion, are frequently inspected to monitor the condition of structures. Thickness measurement (gauging survey), the best inspection procedure to monitor the corrosion condition on ship structures, is mandatory over a vessel's service life according to Classification requirements.

Current calendar-based inspection practices may cause an unexpected halt during a vessel's normal service routine due to unforeseen structural failures, or result in increased costs due to unnecessary inspections. Hence, as the most influential factor in planning an effective structural inspection of ships, inspection intervals need to be first determined by a rational approach. Deck panel, which is one of the most critical structural components of the ship hull structure, are highly stressed with the presence of vertical bending moment and may be severely corroded during the operation of the vessel. Therefore, a reliability-based approach was proposed to assist the scheduling of a gauging survey for deck panels of oil tankers, taking into account the ultimate strength failure

of corroded panels.

The major contributions of this research are summarized as follows:

- **Developed a time-variant probabilistic nonlinear corrosion model**

  Based on a corrosion database, a new procedure was developed to determine time-variant probabilistic nonlinear corrosion models for upper deck structures (deck plating, longitudinal web and flange) of oil tankers. The model derived in this dissertation is based on statistical analysis on a large amount of thickness measurement data. Due to the substantial uncertainties involved in the corrosion process on the ship structures, this statistics-based corrosion model may provide better prediction of corrosion wastage compared with purely phenomenological models based on laboratory data. This procedure is generic and can be applied to predict the corrosion wastage of any ship structural members at any selected vessels' age.

- **Developed a reliability-based method determining the inspection intervals**

  A rational reliability-based framework for planning the gauging survey for ship structures was presented in Chapter 2. The main phases of this framework include collection of data, assessment of reliability, evaluation of the calculated reliability against target levels, and determination of the inspection intervals. The reliability techniques presented here provide the ship owner or operator a tool for rationalizing the selection of interval for inspection.

- **Demonstrated important aspects of a procedure for assessing the time-variant ultimate strength reliability level of panel structures**

  Time-variant limit state functions for unstiffened deck plate and stiffened deck

panel were derived using ultimate strength formulations indicated by IACS CSR. Modeling uncertainties for each formula were analyzed based on the comparison study with the available test data. Probabilistic strength and load models were developed by extensive review of previous studies.

The reliability assessments of six sample tankers were carried out by Monte Carlo Simulation method with Latin Hypercube Sampling. The notional values of calculated reliability are only suitable for comparative assessments of structural performance. The results of the sensitivity study determined the important parameters for reliability analysis of panel structure. The reliability results of sample tankers revealed the inherent level of safety in the classification society's requirements for design, construction and service.

- **Calibrated the target levels of reliability index (failure probability) for inspection planning**

  A benchmark tanker was used to calibrate the target reliability levels for inspection planning. Three different levels with corresponding follow-up actions were suggested based on the link between the current inspection practice and the reliability analysis. Since many assumptions and approximations have been made, the suggested target levels must not be regarded as absolute and can only be used in a relative sense.

- **Proposed a method for updating corrosion model**

  An updating scheme for corrosion model using gauged data collected at each inspection was proposed. Based on the application of Bayes' rule, the corrosion model was updated to predict corrosion wastage as close as possible to

reflect the actual degradation process rather than the worst scenario.

7.2 Future Work

Although substantial progress has been made on the reliability-based inspection planning, research opportunities as well as challenges still exist in each frontier of this rapidly evolving field. As the extension of the work presented in this dissertation, some further consideration in reliability-based inspection planning of ship structures are as follows:

- It is not conservative to ignore the interaction between crack growth and corrosion thinning in the evaluation of the failure probability of aging tankers. Hence, evaluation of the dependence between corrosion wastage effect and corrosion fatigue effect should improve the accuracy of the results.
- The corrosion model derived in this study does not explicitly take into account the effect of pitting. An overall wastage of the members approach can limit the modeling of the actual corrosion process encounter. Therefore, the analysis of pitting effect may also improve the current procedure.
- The development of corrosion reliability updating analysis is highly desired. Although Bayes' updating formulation has been applied for updating the corrosion model in this study, the detailed updating scheme is not mature compared with the fatigue reliability updating. With further development of this technique, the optimal decision can be carried out by pre-posterior analysis.
- Since the modeling uncertainties are the most influential factor for the reliability assessment, an accurate uncertainty model will be highly desirable. There-

fore, ultimate strength models of unstiffened plate or stiffened panel require benchmarking against realistic mechanical collapse test data and nonlinear finite element results so that the probabilistic model of modeling uncertainties can be more accurate.

- Following the reliability-based procedure developed in this study, inspection intervals can be estimated for side shell, bottom, transverse frames, etc. By putting together the inspection plans for all the local members, a comprehensive optimized lifetime inspection plan for a vessel can be achieved.
- The current study has benefited from a well-maintained corrosion database. However, proper interpretation of collected data is still a major challenge. As shown in Chapter 5, the trends and predictions of the future vary in a wide range. Consensus among research groups is lacking on what method or approach should be used for the best interpretation of data. Comparative studies on existing predictions are advocated.
- Based on the reliability-based procedure with consideration of the failure consequences, the risk-based inspection planning can be developed. The results of risk analysis for inspection planning can provide the owner with additional justification for the choice of inspection intervals.
- Except for inspection interval, the scope (including areas and extent) of inspection is also essential for optimizing inspection. The method is to be developed to rank quantitatively the priorities of structural details to determine the critical areas to be inspected. The results from the limited inspection ex-

tent are used to infer the state of the structure as a whole. Therefore, the validity of this inference is to be investigated.

BIBLIOGRAPHY

[1] Abrahamsen E, Nordenstrom N and Røren EMQ (1970). Design and reliability of ship structures. *Proceedings Spring Meeting*, Society of Naval Architects and Marine Engineers.

[2] ABS (1993). *Guide for the dynamic based design and evaluation of tanker structures*, American Bureau of Shipping, Houston, TX, USA.

[3] ABS (2004). *Guide for buckling and ultimate strength assessment for offshore structures*, American Bureau of Shipping, Houston, TX, USA.

[4] ABS (2005). *Commentary on the guide for buckling and ultimate strength assessment for offshore structures*, American Bureau of Shipping, Houston, TX, USA.

[5] ABS (2007a). Part 5C, *Rules for building and classing steel vessels*, American Bureau of Shipping, Houston, TX, USA.

[6] ABS (2007b). Part 3, *Rules for building and classing steel vessels*, American Bureau of Shipping, Houston, TX, USA.

[7] ABS (2008). *Guidance notes for assessment of time-variant hull girder reliability of tanker and ship-shaped FPSO*, American Bureau of Shipping, Houston, TX, USA.

[8] Adamchak JC (1979). *Design equations for tripping of stiffeners under inplane and lateral loads.* David W. Taylor Naval Ship Research and Development Center Report 79/064, Bethesda, MD, USA.

[9] Adeegest L, Braathen A, Vada T (1998). Evaluation of methods for estimation of extreme nonlinear ship responses based on numerical simulations and model tests. *Proceedings of the 22nd Symposium on Naval Hydrodynamics*, 1: 70-84, Washington DC, USA.

[10] AISC (2006). *ASD/LRFD steel Construction Manual 13th edition*. American Institute of Steel Construction, Chicago, IL, USA.

[11] Akita Y (1982). Lessons learned from failure and damage of ships. Joint Sessions

1, *8th International Ship Structures Congress*, Gdansk, Poland.

[12] Akpan UO, Koko TS, Ayyub B and Dunbar TE (2002). Risk Assessment of Aging Ship Hull Structures in the Presence of Corrosion and Fatigue, *Marine Structures*, 15: 211-231.

[13] Akpan UO, Koko TS, Ayyub B and Dunbar TE (2003). Reliability assessment of corroding ship hull structure. *Naval Engineers Journal*, 37-48.

[14] Ang AHS and Tang WH (1975). Vol. I, Basic Principles. *Probability Concepts in Engineering Planning and Design*, John Wiley.

[15] API (2000). *Design of flat plate structures,* API Bulletin 2V, American Petroleum Institute, Washington DC, USA.

[16] Assakkaf IA and Ayyub BM (1995). Reliability-based design of unstiffened panels for ship structures. *Proceedings of the Joint ISUMA-NAFIPS*, April 1995, College Park, VA, USA,

[17] Assakkaf IA and Ayyub BM (2004), Comparative and uncertainty assessment of design criteria for stiffened panels, *Journal of Ship Research*, 48(3): 231-247.

[18] Assakkaf IA and Cárdenas-García JF (2003). Reliability-based design of doubler plates for ship structures. *Proceedings of the fourth international symposium on uncertainty modeling and analysis (ISUMA)*, 20-24 September 2003, College Park, VA, USA,

[19] Assakkaf IA, Ayybu BM, Hess PE and Atua K (2002a). Reliability-based load and resistance factor design (LRFD) guidelines for stiffened panels and grillages of ship structures. *Naval Engineers Journal*, 114(2): 89-111.

[20] Assakkaf IA, Ayybu BM, Hess PE and Knight DE (2002b). Reliability-based load and resistance factor design (LRFD) guidelines for unstiffened panels of ship structures. *Naval Engineers Journal*, 114(2): 69-88.

[21] Atua K, Assakkaf IA and Ayyub BM (1996). Statistical characteristics of strength and load random variables of ship structures. *7th specialty conference of probabilistic mechanics and structural reliability*, Worcester, Massachusetts, USA.

[22] Ayyub B, Akpan UO, DeSouza GF, Koto TS and Luo X (2000). Risk-based life cycle management of ship structures, *Ship Structure Committee*, Report No. SSC-SR 416, Washington, DC, USA.

[23] Ayyub BM (1998). *Uncertainty modeling and analysis in civil engineering*. CRC Press, Boca Raton, FL USA.

[24] Ayyub BM and McCuen RH (1997). *Probability, Statistics, and Reliability for Engineers*. CRC Press, Boca Raton, FL USA.

[25] Ayyub BM, Akpan UO, Rushton PA, Koko TS, Ross J and Lua J (2002). Risk-informed inspection of marine vessels. *Ship Structure Committee*, Report No .SSC-421, Washington, DC, USA.

[26] Ayyub BM, Beach JE and Sarkani S (2002). Risk Analysis and Management for Marine Systems. *Naval Engineers Journal*, 114(1): 181-206.

[27] Baarholm G and Moan T (2000). Estimation of nonlinear long-term extremes of hull girder loads in ships. *Marine Structures*, 13: 495-515.

[28] Barsa NS and Stanley RF (1978). Survey of structural tolerances in the United States commercial shipbuilding industry. *Ship Structure Committee*, Report No. SSC-273, Washington DC, USA.

[29] Bea RG (1992). Marine Structural Integrity Programs. *Ship Structure Committee*, Report No.SSC-365. Washington, DC, USA.

[30] Bea RG (1993). Reliability-based requalification criteria for offshore platforms. *Proceedings of 12th Conference on Offshore Mechanics and Arctic Engineering (OMAE)*, 2: 351-361, June 1993. Glasgow, Scotland.

[31] Bhattacharya B, Basu R and Ma KT (2001). Developing target reliability for novel structures: the case of the mobile offshore base. *Marine Structures*, 14: 37-58.

[32] Caldwell JB (1972). Design – construction. *De Jngenieur*, 49.

[33] Casella G and Rizzuto E (1998). Second-level reliability analysis of a double-hull oil tanker. *Marine Structures* 11(9): 373-399.

[34] Casella G, Dogliani M and Guedes Soares C (1996). Reliability based design of the primary structure of oil tankers. *Proceedings of the International Offshore Mechanics and Arctic Engineering Symposium (OMAE'96)* 2: 217-224.

[35] Casella G, Dogliani M and Guedes Soares C (1997). Reliability-based design of the primary structure of oil tankers. *Journal of Offshore Mechanics and Arctic Engineering.* 1997: 119: 263-269.

[36] Chen HH, Hsein YJ, Conlon JF and Liu D (1993). New approach for the design and evaluation of double hull tanker structures. *Transactions of the Society of Naval Architects and Marine engineers*, 101: 215-245.

[37] Clifford Cohen A (1965). Maximum-likelihood estimation in the Weibull distribution based on complete and on censored samples. *Technometrics*, 7(4) : 579-588.

[38] Crystal Ball Release 5 (2001). Reference Manual.

[39] Daidola JC and Barsa NS (1980). Probabilistic structural analysis of ship hull longitudinal strength. *Ship Structure Committee*, Report No. SSC-301, Washington DC, USA.

[40] Dalzell JF, Maniar NM and Hsu MW (1979). Examination of service and stress data of three ships for development of hull girder load criteria. *Ship Structure Committee*, Report No. SSC-287, Washington DC, USA.

[41] Davis PG and Rabinowitz P (1975). *Methods of numerical integration*, Academic press, New York, USA.

[42] De Souza GF and Ayyub BM (2000). Risk based inspection planning for ship hull structures. *Association of Scientists and Engineers'2000 Technical Symposium*, USA.

[43] Demsetz LA, Cario R and Schulte-Strathaus R (1996). Inspection of marine structures. *Ship Structure Committee*, Report No. SSC-389, Washington, DC, USA.

[44] Derbanne Q, Leguen JF, Dupau T and Hamel E (2008). Long-term non-linear bending moment prediction. *Proceedings of the International Offshore Mechanics and Arctic Engineering Symposium (OMAE'08)*, Portugal.

[45] DNV (1992). Classification Notes 30.6, *Structural reliability analysis of marine structures*, Det Norsk Veritas, Norway.

[46] DNV (1995). Classification Notes No. 30.1, *Buckling strength analysis*, Det Norsk Veritas, Norway.

[47] DNV (2002). Recommendation practiceRP-C201, *Buckling strength of plated structures*. Det Norsk Veritas, Norway.

[48] Dunn TW (1964). Reliability in shipbuilding. *Transactions of the Society of Naval Architects and Marine engineers*, 72:14-40.

[49] Emi H, Yuasa M, Kumano A, Arima T, Yamamoto N and Umino M (1993). A study on life assessment of ships and offshore structures (3rd report: corrosion control and condition evaluation for a long life service of the ship). *Journal of Naval Architects of Japan*, 174: 735-744.

[50] Farnes KA (1990). *Long-term statistics of response in non-linear marine structures*. PhD Thesis, Department of Marine Structures, Faculity of Marine Technology, Norwegian University of Science and Technology, NTNU, Trondheim.

[51] Farnes KA and Moan T (1994). Extreme dynamic nonlinear response of fixed platforms using a complete long-term approach. *Applied Ocean Research*, 15: 317-326.

[52] Faulkner D (1975). Compression strength of welded grillages, Chapter 21 in *Ship Structural Design Concepts*, Edited by Evans JH, Cornell Maritime Press, 633~712.

[53] Faulkner D and Sadden JA (1979). Toward a unified approach to ship structural safety. *Transactions of the Royal Institution of Naval Architects*, 121: 1-28.

[54] Ferry Borges J and Castanheta M (1971). *Structural Safety*, Laboratório Nacional de Engenharia Civil, Lisboa.

[55] Frankland JM (1940). *The Strength of ship plating under edge compression*. US EMB Report 469.

[56] Frieze PA (2002). *Assessment of ABS SVR results using test database*. ABS Technical Report OTD 2002-05, American Bureau of Shipping, Houston, TX, USA.

[57] Friis-Hansen P and Ditlevsen O (2001). A statistic still water response model. Technical University of Denmark, DK-2800 Kgs. Lyngby, Department of Mechanical Engineering, *Section for Maritime Engineering*, November 13, 2001.

[58] Fujimoto Y (1996). Study on fatigue reliability and inspection of ship structures based on enquete information. *Journal of the Society of Naval Architects of Japan*, 180:601-609.

[59] Galambos TV and Ravindra TV (1978). Properties of steel for use in LRFD. *Journal of the Structural Division*, 104(No. ST9).

[60] Garbatov Y and Guedes Soares C (2001). Cost and reliability based strategies for fatigue maintenance planning of floating structures. *Reliability. Engineering and System Safety (UK)*, 73(3): 293-301.

[61] Garbatov Y, Guedes Soares C and Wang G (2005). Nonlinear time dependent corrosion wastage of deck plates of ballast and cargo tanks of tankers. *25th International Conference on Offshore Mechanics and Arctic Engineering (OMAE'05)*, 12-17 June 2005, Halkidiki, Greece,

[62] Gardiner CP and Melchers RE (2001), Bulk carrier corrosion modeling, *International Offshore and Polar Engineering Conference*, Stavanger, Norway, (IV): 609-615.

[63] Gogliani M (1995). *Guidelines notes on reliability calculations of oil-tankers longitudinal strength*, SHIPREL Report 3,6 R01(1), BRITE EURAM Project BE-4554.

[64] Gran S (1991). *Still-water load statistics*, DnV Technical Report No.91-2043, Det Norsk Veritas, Norway.

[65] Gran S (1992). *Short-term still-water load statistics*, DnV Technical Report No. 92-2070, Det Norsk Veritas, Norway.

[66] Guedes Soares C (1988a). *Design Equation for the compressive strength of unstiffened plate elements with initial imperfection*. NAMES, Technical University of Lisbon, Elsevier Applied Science Publishing Ltd., England.

[67] Guedes Soares C (1988b). Uncertainty modeling in plate buckling. *Structural Safety*, 5: 17-34.

[68] Guedes Soares C (1990a). Stochastic modeling of maximum still-water load Effects in ship structures, *Journal of Ship Research*, 34(3): 199-205.

[69] Guedes Soares C (1990b). Influence of human control on the probability distribution of maximum still water load effects in ships, *Marine Structures*, 3(4): 319-341.

[70] Guedes Soares C (1992). Combination of primary load effects in ship structures. *Probabilistic Engineering Mechanics*, 7: 103-111.

[71] Guedes Soares C and Dogliani M (2000). Probabilistic modeling of time-varying still-water load effects in tankers, *Marine Structures*, 13: 129-143.

[72] Guedes Soares C and Garbatov Y (1996). Reliability of maintained ship hulls subjected to corrosion. *Journal of Ship Research*, 40(3): 235-43.

[73] Guedes Soares C and Garbatov Y (1998). Reliability of maintained ship hulls subjected to corrosion and fatigue. *Structural Safety*, 20: 201-219.

[74] Guedes Soares C and Garbatov Y (1999a). Reliability of maintained ship hulls subjected to corrosion and fatigue under combined loading. *Journal of Constructional Steel Research*, 52: 93-115.

[75] Guedes Soares C and Garbatov Y (1999b). Reliability of maintained, corrosion protected plates subjected to non-linear corrosion and compressive loads. *Marine Structures*, 12: 425–445.

[76] Guedes Soares C and Ivanov LD (1989). Time dependent reliability of the primary ship structure, *Reliability Engineering and System Safety*, 26: 59-71.

[77] Guedes Soares C and Moan T (1982). Statistical analysis of still water bending moments and shear forces in tankers, ore and bulk carriers, *Norwegian Maritime Research*, 3: 33-48.

[78] Guedes Soares C and Moan T (1985). Uncertainty analysis and code calibration of the primary load effects in ship structures. *Proceedings ICOSSAR'85*. II: 501-512, IASSAR, New York, USA.

[79] Guedes Soares C and Moan T (1988). Statistical analysis of still-water load effects on ship structures, *Transactions of the Society of Naval Architects and Marine Engineers*, 96: 129-156.

[80] Guedes Soares C and Moan T (1991). Model uncertainty in the long term distribution of wave induced bending moments for fatigue design of ship structures, *Marine Structures*, 4: 295-315.

[81] Guedes Soares C and Schellin TE (1996). Long-term distribution of non-linear wave induced vertical bending moments on a containership, *Marine Structures*, 9: 333-352.

[82] Guedes Soares C and Soreide TH (1983). Behavior and design of stiffened plates under predominantly compressive loads. *International Shipbuilding Progress*, 30:13~27.

[83] Guedes Soares C and Teixeira AP (2000). Structural reliability of two bulk carrier designs. *Marine Structures*, 13(2): 107-128.

[84] Guedes Soares C, Dias S (1996). Probabilistic models of still-water load effects in containers, Marine Structures, 9: 287-312.

[85] Guedes Soares C, Dogliani M, Ostergaard, C, Parmentier G and Pedersen PT (1996). Reliability based ship structural design. *Transactions of the Society of Naval Architects and Marine Engineers*, 104: 375-389.

[86] Guedes Soares C, Garbatov Y, Zayed A and Wang G (2008). Corrosion wastage model for ship crude oil tanks. *Corrosion Science*, 50: 3095-3106.

[87] Guo J, Perakis AN and Wang G (2009). A study on reliability-based inspection planning – application to deck plate thickness measurement of aging tankers. submitted to *Marine Structures*.

[88] Guo J, Wang G, Ivanov LD and Perakis AN (2008). Time-varying ultimate strength of aging tanker deck plate considering corrosion effect, *Marine Structures*, 21(4): 402-419.

[89] Harada S, Yamamoto N, Magaino A and Sone H (2001). *Corrosion analysis and determination of corrosion margin, Part 1&2,* International Association of Classification Societies, London, UK.

[90] Hart DK, Rutherford SE and Wickham AHS (1985). Structural reliability analysis of stiffened panels. *Transactions of the Royal Institution of Naval Architects,* 128: 293-310.

[91] Harter LH and Moore AH (1965). Maximum-likelihood estimation of the parameters of gamma and Weibull populations from complete and from censored data. *Technometrics,* 7(4): 639–643.

[92] Hess III PE, Bruchman D, Assakkaf IA and Ayyub BM (2002). Uncertainties in material strength, geometric, and load variables. *Naval Engineers Journal,* 2.

[93] Hoadley PW and Yura JA (1985). Ultimate strength of tubular joints subjected to combined loads. *Offshore technology conference (OTC'85),* Houston, TX, USA.

[94] Hogben N, Da Cunha LF and Olliver H N (1986). *Global Wave Statistics,* British Maritime Technology, Brown Union, London, UK.

[95] Hogben N. and Lumb FE (1967). *Ocean wave statistics*. Her Majesty's Stationary Office, London, UK.

[96] Holzman RS (1992). *Advancements in tankship internal structural inspection techniques*. Department of Naval Architecture, University of California, Berkeley.

[97] Horte T, Wang G and White N (2007). Calibration of the hull girder ultimate capacity criterion for double hull tankers. *10th International Symposium on Practical Design of Ships and Other Floating Structures,* 30 September – 5 October 2007, Houston, TX, USA.

[98] Hu Y and Cui W. Time-variant ultimate strength of ship hull girder considering corrosion and fatigue. *9th Symposium on Practical Design of Ships and Other Floating Structures (PRADS'05),* 243-251, Shiffbautechnische Gessellschaft, Luebeck-Travemuende, Germany.

[99] Hu Y, Cui W and Pedersen PT (2004). Maintained ship hull girder ultimate strength reliability considering corrosion and fatigue, *Marine Structures,* 17: 91-123.

[100] IACS (2000). *Recommendations No.34, Standard Wave Data,* International Association of Classification Societies, London, UK.

[101] IACS (2006a) *Longitudinal strength standard, UR S11 Rev.5,* International Association of Classification Societies, London, UK.

[102] IACS (2006b). Background document. Design verification, hull girder ultimate strength. *Common Structural Rules for Double Hull Oil Tankers. Section 9.* International Association of Classification Societies, London, UK.

[103] IACS (2008a). *Scantling requirements, Common structural rules for double hull oil tankers. Section 8.* International Association of Classification Societies, London, UK.

[104] IACS (2008b). *Buckling and ultimate strength, Common structural rules for double hull oil tankers. Section 10.* International Association of Classification Societies, London, UK.

[105] IACS (2009). *Hull surveys of oil tanker, UR Z10.1,* International Association of Classification Societies, London, UK.

[106] Iman RL and Helton JC (1985). *A comparison of uncertainty and sensitivity analysis techniques for computer models.* Technical Report SAND84-1461, Sandia National Laboratories, Albuquerque, NM, USA.

[107] Iman RL, Helton JC and Campbell JE (1981a). An approach to sensitivity analysis of computer models, Part 1. Introduction, input variable selection and preliminary variable assessment. *Journal of Quality Technology,* 13(3): 174-83.

[108] Iman RL, Helton JC and Campbell JE (1981b). An approach to sensitivity analysis of computer models, Part 2. Ranking of input variables, response surface validation, distribution effect and technique synopsis. *Journal of Quality Technology,* 13(4): 232-40.

[109] IMO (2003). *International Convention for the Prevention of Pollution from Ships, 1973, as modified by the Protocol of 1978 relating thereto (MARPOL).* Regulation 13G.2003 Amendments, International Maritime Organization, London, UK.

[110] ISSC (1991). Committee V.1, Applied design (prepared by Frieze PA et al), *International Ship and Offshore Structures Congress*. 1991, Wuxi, China.

[111] ISSC (2006a). Committee V.6, Condition assessment of aged ships (prepared by Paik JK et al), *International Ship and Offshore Structures Congress,* 20-25 August 2006, Southampton, UK.

[112] ISSC (2006b). Committee VI.1, Reliability based structural design and code development (prepared by Moan T et al). *International Ship and Offshore Structures Congress,* 20-25 August 2006, Southampton, UK.

[113] ISSC (2006c). Committee III.1, Ultimate strength (prepared by Yao T et al), *International Ship and Offshore Structures Congress,* 20-25 August 2006, Southampton, UK.

[114] ISSC (2009). Committee V.6, Condition assessment of aged ships and offshore structures (prepared by Wang G, et al), *International Ship and Offshore Structures Congress,* 16-21 August 2009, Seoul, Korea.

[115] IUMI (2008). *Casualty and world fleet statistics*, International Union of Marine Insurance, Zurich, Switzerland.

[116] Ivanov LD (1987). Statistical evaluation of the ship hull cross section geometrical characteristics as a function of her age. *International Shipbuilding Progress*, 198-203.

[117] Ivanov LD and Lynch TJ (2007). Assessment of the level of uncertainty of the hull girder bending stresses, *International Ocean and Polar Engineering Conference (ISOPE-2007)*, July 1- 6, 2007, Lisbon, Portugal.

[118] Ivanov LD and Madjarov H (1975). The statistical estimation of still-water bending moments for cargo ships. *Shipping World & Shipbuilder*, 3908: 759-762.

[119] Ivanov LD and Rousev SG (1979). Statistical estimation of reduction coefficient of ship's hull plates with initial deflections. *Naval Architecture*, 4: 158-160.

[120] Ivanov LD and Wang G (2008a). Incorporated probability that a fleet meets a given permissible value for the hull girder section modulus loss. *Journal of Marine Science and Technology*, 13: 455-464.

[121] Ivanov LD and Wang G (2008b). Probabilistic presentation of the still water loads, which way ahead. *International Conference on Offshore Mechanics and Arctic Engineering (OMAE)*, June 15-20, 2008, Estoril, Portugal.

[122] Ivanov LD, Spencer J and Wang G (2003). Probabilistic evaluation of hull structure renewals for aging ships, *International Marine Design Conference (IMDC)*, 5-8 May 2003, Athens, Greece.

[123] Ivanov LD, Wang Ge and Seah AK (2004). Evaluating corrosion wastage and structural safety of aging ships, *Pacific International Maritime Conference*, February 2-5, 2004, Sidney, Australia.

[124] Iwan WD, Thiel CC, Housner GW and Cornell CA (1993). A reliability-based approach to seismic reassessment of offshore platforms, *International Conference on Structural Safety and Reliability (ICOSSAR)*, August 1993, Innsbruck, Austria.

[125] Jensen JJ and Dogliani M (1996). Wave-induced ship hull vibrations in stochastic seaways. *Marine Structures*, 9: 353-387.

[126] Jensen JJ and Mansour AE (2002). Estimation of ship long term wave induced bending moment using closed form expressions. *Transactions of the Royal Institution of Naval Architects*, 144: 177-191.

[127] Jensen JJ, Petersen JB and Pedersen PT (1990). Prediction of non-linear wave-induced loads on ships. *Proceedings of IUTAM Symposium on Dynamics of Marine Vehicles and Structures in Waves,* Brunel University, London.

[128] Johnson BG and Opila F (1941). Compression and tension tests of structural alloys. *ASTM Proceedings, American Society for Testing and Materials*.

[129] Justus CG, Hargraves WR, Mikhail A and Graber D. Methods for estimating wind speed frequency distributions. *Journal of Applied Meteorology*, 17: 350-353.

[130] Kamenov-Toshkov L, Ivanov LD and Garbatov Y (2008). Design wave-induced bending moment assessment for any given ship's service life. *Ship and Offshore Structures*, 1(2).

[131] Kaminski ML and Krekel M (1995). Reliability analysis of fatigue sensitive joints in FPSO. *Conference on Safety and Reliability,* June, 1995, Gopenhagen, Denmark.

[132] Kaplan M, Benatar M, Bentson J and Achtarides TA (1984). Analysis and assessment of major uncertainties associated with ship hull ultimate failure. *Ship Structure Committee,* Report No. SSC-322, Washington DC, USA.

[133] Kawabe H. and Moan T (2007). Efficient estimation method for design wave-induced load and consideration of the limited wave height effect. *10th Symposium on Practical Design of Ships and Other Floating Structures (PRADS'07),* Houston, TX, USA.

[134] Kim BJ and Kim OH (1995), Design criteria of longitudinal hull girder strength based on reliability analysis. *6th Symposium on Practical Design of Ships and Other Floating Structures (PRADS'95),* September, 1995, Seoul, Korea.

[135] Kim SC, Yoon JH and Fujimoto Y (2000). Optimization for inspection planning of ship structures considering corrosion effects. *Proceeding of the 10th International Offshore and Polar Engineering Conference (ISOPE 2000),* 380-386, Seattle, Washington, USA.

[136] Konami K, Minoshima K and Kim G (1987). Corrosion fatigue crack initiation behavior of 80 kgf/mm2 high-tensile strength steel weldment in synthetic seawater. *Journal of the Society of Materials Science Japan,* 36(401): 141-46.

[137] Kondo Y (1987). Prediction method of corrosion fatigue crack initiation life based on corrosion pit growth mechanism. *Transactions of the Japan Society of Mechanical Engineers,* 53(495): 1983-1987.

[138] Król T (1974). Analysis of the statistical information of the load distribution onboard ships (in Polish), *Politechnika Gdanska*, Institute of Shipbuilding, Gdansk, Poland.

[139] Ku A, Serratella C, Spong R, Basu R, Wang G and Angevine D (2004). Structural reliability applications in developing risk-based inspection plans for a floating production installation. *Proceedings of 23rd rnational Conference on Offshore Mechanics and Arctic Engineering (OMAE'04),* Vancouver, Canada.

[140] Ku A, Spong RE, Serratella C, Wu S, Basu R and Wang G (2005). Structural reliability application in risk-based inspection plans and their sensitivities to different environmental conditions, *Offshore Technology Conference (OTC'05),* 2-5 May 2005, Houston, TX, USA.

[141] Larrabee RD and Cornell CA (1981). Combination of various load processes, *Journal of Structural Division,* 107: 223-238.

[142] Lee AK, Serratella C, Basu R, Wang G and Spong RE (2006). Flexible approaches to risk-based inspection of FPSOs, *Offshore Technology Conference (OTC'06),* 1-4 May 2006, Houston, TX, USA.

[143] Leheta HW and Mansour AE (1997). Reliability-based method for optimal structural design of stiffened panels. *Marine Structures,* 10(5): 323-352.

[144] Lewis EV (1973). Load criteria for ship structural design. *Ship Structure Committee,* Report No. SSC-240, Washington DC, USA.

[145] Løseth R, Sekkeseter G and Valsgård S (1994). Economics of high tensile steel in ship hulls. *Marine Structures,* 7: 31-50.

[146] Lotsberg I (1991). *Target reliability index: a literature survey.* Report No. 91-2023, A.S. Veritas Research, Norway.

[147] Lotsberg I, Sigurdsson G and Wold PT (2000). Probabilistic inspection planning of the asgard a FPSO hull structure with respect to fatigue. *Journal of Offshore Mechanics and Arctic Engineering,* 122(2): 134-140.

[148] Ma KT (1998). Tanker inspection and a risk-based inspection approach. *Proceeding of the 8th International Offshore and Polar Engineering Conference (ISOPE'98),* 4: 504-512, Canada.

[149] Ma KT and Bea RG (1992). *Durability considerations for new & existing ships – design and maintenance procedures to improve the durability of critical internal structural details in oil tankers.* SMP Report 5-1, Department of Naval Architecture, University of California, Berkeley.

[150] Ma KT, Orisamolu IR and Bea RG (1999). Optimal strategies for inspection of ships for fatigue and corrosion damage. *Ship Structure Committee*, Report No. SSC-407. Washington, DC, USA.

[151] Mann NR, Schafer RE and Singpurwalla ND (1974). *Methods for statistical analysis of reliability and life data.* John Wiley and Sons, New York, USA.

[152] Mano H and Kawabe H (1979). Statistical character of the demand on longitudinal strength (third report) – long-term distribution of combined bending moment (in Japanese). *Journal of the Society of Naval Architects of Japan,* 144: 240-248.

[153] Mano H, Kawabe H, Iwakawa K and Mitsumune N (1977). Statistical character of the demand on longitudinal strength (second report) – long term distribution of still-water bending moment (in Japanese). *Journal of the Society of Naval Architects of Japan,* 142: 255-63.

[154] Mansour AE (1972). Probabilistic design concepts in ship structural safety and reliability. *Transactions of the Society of Naval Architects and Marine Engineers,* 80: 64-97.

[155] Mansour AE (1974). Approximate probabilistic method of calculating ship longitudinal strength. *Journal of Ship Research,* 18(3): 201-213.

[156] Mansour AE (1981). Combining extreme environmental loads for reliability-based designs. *Proceedings of the Extreme Loads Response Symposium,* 63-74. Arlington VA, USA.

[157] Mansour AE (1986). Approximate formulation for preliminary design of stiffened plates. *Proceedings of Conference on Offshore Mechanics and Arctic Engineering (OMAE'86),* Tokyo, Japan.

[158] Mansour AE (1990). An introduction to structural reliability theory. *Ship Structure Committee,* Report No. SSC-351, Washington, DC, USA.

[159] Mansour AE (1997). Extreme loads and load combinations. *Journal of Ship Research,* 39(1): 53-61.

[160] Mansour AE and Faulkner D (1973). On applying the statistical approach to extreme sea loads and ship hull strength. *Transactions of the Royal Institute of Naval Architects,* 115.

[161] Mansour AE and Hovem L (1994). Probability based ship structural analysis. *Journal of Ship Research,* 38(4): 329-339.

[162] Mansour AE and Wasson JP. Charts for estimating nonlinear hogging and sagging bending moments. *Journal of Ship Research,* 39(3): 240-249.

[163] Mansour AE and Wirsching PH (1995). Sensitivity factors and their application to marine structures. *Marine Structures,* 8(3): 229-255.

[164] Mansour AE, Jan HY, Zigelman CI, Chen YN and Harding SJ (1984). Implementation of reliability methods to marine structures. *Transactions of the Society of Naval Architects & Marine Engineers,* 92: 353-382.

[165] Mansour AE, Wirsching PH, Lucket MD, Plumpton AM and Lin YH (1997a). Structural safety of ships. *Transactions of the Society of Naval Architects & Marine Engineers,* 105: 61-98.

[166] Mansour AE, Wirsching PH, Luckett M and Plumpton A (1997b). Assessment of reliability of ship structures. *Ship Structure Committee,* Report No. SSC-398, Washington, DC, USA.

[167] Mansour AE. Wirsching P, White G and Ayyub B (1996). Probability-based ship design implementation of design guidelines for ships: a demonstration. *Ship Structure Committee,* Report No. SSC-392, Society of Naval Architects and Marine Engineers, Washington, DC, USA.

[168] Masuda C, Abe T, Hirukawa H and Nishijima S (1986). Corrosion fatigue life prediction for SUS 403 stainless steel in 3% NaCl aqueous solution. *Transactions of the Japan Society of Mechanical Engineers,* 52(480): 1764-69.

[169] Matoba M, Yamamoto N, Watanabe T and Umino M (1994). Effect of corrosion and its protection on hull strength. *Journal of Naval Architects of Japan,* 175: 271-280.

[170] Maximadj AI, Belenkij LM, Briker AS and Neugodov AU (1982). Technical assessment of ship hull girder (in Russian). *Petersburg: Sudostroenie.*

[171] Maximadji AI (1973). Estimation of the still-water bending moments for tankers (in Russian). *Proceedings of the Central Scientific Research Institute of Merchant Fleet,* 169: 16-33. Leningrad, Russia.

[172] McKay MD, Conover WJ and Beckman RJ (1979). A comparison of three methods for selecting values of input variables in the analysis of output from a computer code. *Technometrics,* 21: 239-45.

[173] Melchers RE (1995a). Probabilistic modeling of marine corrosion of steel specimens. *Porceedings Conference ISOPE-95,* June 12-15, 1995, Hauge, Netherlands.

[174] Melchers RE (1995b). Probabilistic modeling of seawater corrosion of steel structures. *Proceedings of the International Conference on Applications Statistics and Probability in Structural and Geotechnical Engineering (ICASP),* 265-270, Paris, France.

[175] Melchers RE (1998). Probabilistic modeling of immersion marine corrosion. In: Shiraishi N, Shinozuka M, Wen YK, editors. *Structural safety and reliability,* 3: 1143-1149. Rotterdam, Balkema.

[176] Melchers RE (1999a). Corrosion uncertainty modeling for steel structures. *Journal of Constructional Steel Research,* 52: 3–19.

[177] Melchers RE (1999b). *Structural reliability analysis and prediction.* John Wiley & Sons, 2nd Edition, UK.

[178] Melchers RE (2003). Probabilistic models for corrosion in structural reliability assessment, Part 2: models based on mechanics. *Journal of Offshore Mechanics and Arctic Engineering,* 125: 272-80.

[179] Melchers RE (2007). Development of new applied models for steel corrosion in marine applications including shipping. *10th International Symposium on Practical Design of Ships and Other Floating Structures (PRADS'07),* September 30-October 5, 2007, Houston, TX, USA.

[180] Moan T (2005). Reliability-based management of inspection, maintenance and repair of offshore structures. *Structure and Infrastructure Engineering: Maintenance, Management, Life-Cycle Design and Performance,* 1(1): 33-62.

[181] Moan T and Ayala-Uraga E (2008). Reliability-based assessment of deteriorating ship structures operating in multiple sea loading climates. *Reliability Engineering and System Safety,* 93: 433-446.

[182] Moan T and Jiao G (1988). *Characteristic still-water load effects for production ships.* Report MK/R 104/88. The Norwegian Institute of Technology, Trondheim, Norway.

[183] Moan T and Vårda OT (2001). Reliability–based requalification of existing offshore platforms. *8th International Symposium on Practical Design of Ships and Other Floating Structures (PRADS'01),* 2: 939-945.

[184] Moan T, Ayala-Uraga E and Wang X (2004). Reliability-based service life assessment of FPSO structures, *SNAME Maritime Technology Conference & Expo,* 30 September – 1 October 2004, Washington DC, USA.

[185] Moan T, Shu Z, Drummen I and Amlashi H (2006). Comparative reliability analysis of ships – considering different ship types and the effect of ship operations on loads. *Transactions of Society of Naval Architects & Marine Engineers,* 114: 16-54.

[186] Moatsos I and Das PK (2005). Time-variant ultimate strength reliability of FPSOs including corrosion and slamming effects. *International Conference on Offshore Mechanics and Arctic Engineering (OMAE'05),* 12-17 June 2005, Halkidiki, Greece.

[187] Moe ET, Holtsmark G and Storhaug G (2005). Measurements of the wave induced hull girder vibration of an ore carrier trading in the North Atlantic. *Conference on Design & Operation of Bulk Carriers, RINA*, London, UK.

[188] Nikolaidis E, Hughes O, Ayybu BM and White GJ (1993). A methodology for reliability assessment of ship structures. *In: Ship Structures Symposium*, 16-17 November 1993, Arlington, VA, USA.

[189] Ochi MK (1981). Principles of extreme value statistics and their application. *Proceedings of the Extreme Loads Response Symposium,* 15-30, Arlington VA, USA.

[190] Onoufriou T (1999). Reliability based inspection planning of offshore structures, *Marine Structures*, 12: 521-39.

[191] Ostergaard C (1991). Partial safety factors for vertical bending loads on containerships. *Proceedings of the International Offshore Mechanics and Arctic Engineering Symposium (OMAE'91)*, 221-228.

[192] Paik JK and Frieze PA (2001). Ship structural and reliability. *Progress in Structural Engineering and Materials,* 3:198-210.

[193] Paik JK and Kim DH (1997). An analytical method for predicting ultimate compressive strength of stiffened panels, *Journal of the Research Institute of Industrial Technology*, 52(6): 215-230.

[194] Paik JK and Thayamballi AK (2003). *Ultimate limit state design of steel-plated structures.* John Wiley & Sons, Ltd.

[195] Paik JK, Kim SK and Lee SK (1998). Probabilistic corrosion rate estimation model for longitudinal strength members of bulk carries. *Ocean Engineering,* 25(10): 837-860.

[196] Paik JK, Kim SK, Yang SH and Thayamballi AK (1998). Ultimate strength reliability of corroded ship hulls. *Transactions of the Royal Institution of Naval Architects,* 140.

[197] Paik JK, Lee JM, Hwang JS, Park Y (2003). A time-dependent corrosion wastage model for the structures of single- and double-hull tankers and FSPs and FPSOs. *Marine Technology*, 40(3): 201-217.

[198] Paik JK, Melchers RE (2008). *Condition assessment of aging structures*. Woodhead Publishing Ltd.

[199] Paik JK, Thayamballi AK, Kim SK and Yang SH (1998). Ship hull ultimate strength reliability considering corrosion. *Journal of Ship Research*, 42(2): 154-165.

[200] Paik JK, Thayamballi AK, Park YI and Hwang JS (2003). A time-dependent corrosion wastage model for bulk carrier structures. *International Journal of Maritime Engineering, Royal Institution of Naval Architectures,* 61-87.

[201] Paik JK, Thayamballi AK, Park YI, Hwang JS (2004). A time-dependent corrosion wastage model for seawater ballast tank structures of ships. *Corrosion Science*, 46: 471-486.

[202] Paik JK, Wang G, Thayamballi AK and Lee JM (2003). Time-variant risk assessment of aging ships accounting for general / pit corrosion, fatigue cracking and local dent damage, *SNAME annual meeting,* San Francisco, CA, USA.

[203] Parunov J, Senjanovic I and Guedes Soares C (2007). Hull-girder reliability of new generation oil tankers. *Marine Structures,* 20: 49-70.

[204] Pastoor W (2001). Nonlinear reliability based sea-keeping performance on naval vessels. *Proceedings of FAST 2001,* 213-223, Southampton UK.

[205] Qin S and Cui W (2002). A discussion of the ultimate strength of ageing ships, with particular reference to the corrosion model. *Journal of Engineering for the Maritime Environment,* 216(M2): 155-160.

[206] Qin S and Cui W (2003). Effect of corrosion models on the time-dependent reliability of steel plated elements. *Marine Structures,* 16: 15-34.

[207] Rice SO (1954). *Selected papers on noise and stochastic processes*. Wax, N.,Editors, Dover publications.

[208] Rizzo CM and Lo Nigro A (2008). A review of ship surveys practices and of marine casualties partly due to aging effects. *International Conference on Offshore Mechanics and Arctic Engineering,* 15-20 June 2008, *E*storil, Portugal.

[209] Rizzo CM, Paik JK, Brennan FB, Carlsen CA, Daley C, Garbatov Y, Ivanov L, Simonsen BC, Yamamoto N and Zhuang HZ (2007). Current practice and recent advances in condition assessment of aged ships. *Journal of Ships and Offshore Structures,* 2(3): 261-271.

[210] Rizzuto E (2009). Stochastic model of the still water bending moment of oil tankers. *MASTRACT,* 16-18 March 2009, Lisbon, Portugal.

[211] Serratella C, Wang G and Tikka K (2008). Risk-based inspection and maintenance of aged structures. *Condition Assessment of Aging Structures*, 487-519, Woodhead Publishing Ltd.

[212] Shetty NK, Gierlinski JT, Smith JK and Stahl B (1997). Structural system reliability considerations in fatigue inspection planning. *In Behavior of Offshore Structures.* 161-175. Vugts, JH Editor, Delft University of Technology.

[213] Shi WB (1992). In-service assessment of ship structures: effects of general corrosion on ultimate strength. *Spring Meeting of the Royal Institution of Naval Architects,* 4.

[214] Shi WB and Frieze PA (1993) Time variant reliability analysis of a mobile offshore unit. *Proceedings of the Ship Structure Symposium, SSC/SNAME,* Arlington VA USA.

[215] Shu S and Moan T (2006). Effect of avoidance of heavy weather on wave-induced loads on ships. *25th International Conference on Offshore Mechanics and Arctic Engineering (OMAE'06),* 4-9 June 2006, Hamburg, Germany.

[216] Sipes JD (1990). *Report on the Trans-Alaska Pipeline Service (TAPS) tanker structural failure study.* Office of Marine Safety, Security and Environmental Protection, United States Coast Guard (USCG), Washington, DC, USA.

[217] Sipes JD (1991). *Follow-up report on the Trans-Alaska Pipeline Service (TAPS) tanker structural failure study.* Office of Marine Safety, Security and Environmental Protection, United States Coast Guard (USCG), Washington, DC, USA.

[218] Skjong R (1985). Reliability based optimization of inspection strategies. *Proceedings of ICOSSAR'85,* 3: 614-618.

[219] Sőding H (1979). The prediction of still-water wave bending moments in containerships. *Schiffstechnik,* 26: 24-48.

[220] Southwell CR, Bultman JD and Hummer CW Jr (1979). Estimating service life of steel in seawater. In: Schumacher M, editor. *Seawater corrosion handbook,* 374-387, Noyes Data Corporation, New Jersey, USA.

[221] St. Denis M and Pierson WJ (1953). On the motion of ships in confused seas. *Annual meeting of the Society of Naval Architects and Marine Engineering.* New York, USA.

[222] Stevenson J and Moses F (1970). Reliability analysis of frame structures. *Journal of Structural Engineering,* 96(ST11): 2409-2427.

[223] Stiansen SG et al (1980). Reliability methods in ship structures. *Transactions of Royal Institution of Naval Architects*, 122: 381-397.

[224] Sun H and Bai Y (2000). Reliability assessment of a FPSO hull girder subjected to degradations of corrosion and fatigue, *Proceedings of the 10th International*

Conference of Offshore and Polar Engineering, 355-363, Seattle, Washington, USA.

[225] Sun H and Bai Y (2001). Time-variant reliability of FPSO hulls. *Transactions of Society of Naval Architects and Marine Engineers,* 109: 341-366.

[226] Sun H and Bai Y (2003). Time-variation Reliability Assessment of FPSO's Hull Girders, *Marine Structures,* 7: 219-253.

[227] Sun H and Guedes Soares C (2003). Reliability-based structural design of ship-type FPSO units. *Journal of Offshore Mechanics and Arctic Engineering*, 125: 108-113.

[228] Sun H and Guedes Soares C (2006). Reliability-based inspection of corroded ship-type FPSO hulls. *Journal of Ship Research,* 50(2): 171-180.

[229] Teixeira AP, Guedes Soares C and Wang G (2005). Reliability based approach to determine the design loads for the remaining lifetime of ships. *Proceedings of the 11th International Congress of the International Maritime Association of the Mediterranean (IMAM 2005),* 1611-1619, 26-30 September 2005, Lisbon, Portugal.

[230] Thayamballi AK, Chen YK and Chen HH (1987). Deterministic and reliability retrospective strength assessments of ocean-going vessels. *Transactions of the Society of Naval Architects and Marine Engineers*, 95: 159-187.

[231] Thayamballi AK, Kuttl and Chen YN (1986). Advanced strength and structural reliability assessment of the ship's hull girder. *Advances in Marine Structures,* 136-151. In: Smith CS and Clarke JD (eds). Elsevier Applied Science, London.

[232] Thuanboon S, Tordonato DS, Navidi W, Olson DL, Mishra B and Wang G (2006), A statistical analysis of corrosion wastage of transverse members in single hull tankers, *25th International Conference on Offshore Mechanics and Arctic Engineering (OMAE'06)*, 4-9 June 2006, Hamburg, Germany.

[233] Trafalski W (1967). Cargo loads of general cargo ships (preliminary study) (in Polish), *Ship Design and Research Center, Strength Analysis Division*, 3(67). Gdansk, Poland.

[234] Truhin BV (1970). Determination of the margin of safety of ships (in Russian), *Proceedings of the Gorky Institute for Water Transport Engineers,* 88: 248-283, Gorky, Russia.

[235] TSCF (1986). *Guidance manual for the inspection and condition assessment of tanker structures.* Tanker Structure Cooperative Forum.

[236] TSCF (1992). *Condition evaluation and maintenance of tanker structures,* Tanker Structure Cooperative Forum, Witherby & Co. Ltd, London, UK.

[237] TSCF (1995). *Guidelines for the inspection and maintenance of double hull tanker structures.* Issued by Tanker Structure Cooperative Forum in association with International Association of Classification Societies, Witherby & Co. Ltd, UK.

[238] Turkstra CJ (1970). Theory of structural safety. *Solid Mechanics Division,* University of Waterloo, Waterloo, Ontario, Canada.

[239] Videiro P and Moan T (1999). Efficient evaluation of long term distributions. *Proceedings of the International Offshore Mechanics and Arctic Engineering Symposium (OMAE'99),* St. John, Newfoundland, Canada.

[240] Walden H (1964). *The characteristics of sea waves in the North Atlantic* (in German), Report No. 41, Deutscher Wetterdienst Seewetteramt, Hamburg, Germany.

[241] Wang G, Lee AK, Ivanov LD, Lynch TJ, Serratella C and Basu R (2008). A statistical investigation of time-variant hull girder strength of aging ships and coating life. *Marine Structures,* 21: 240-256.

[242] Wang G, Lee M, Serratella C and Kalghagti S (2008). Chapter 1 Condition assessment of ship structures, *Condition assessment of aging structures*, Woodhead Publishing Ltd.

[243] Wang G, Spencer J and Elsayed T (2002). Estimation of corrosion rates of oil tankers, *22nd International Conference on Offshore Mechanics and Arctic Engineering (OMAE'03),* 8-13 June 2003, Cancun, Mexico.

[244] Wang G, Spencer J and Sun H (2003). Assessment of Corrosion Risks to Aging Oil Tankers, *22nd International Conference on Offshore Mechanics and Arctic Engineering (OMAE'03),* 8-13 June 2003, Cancun, Mexico.

[245] Wang G, Spencer S, Olson D, Mishra B, Saidarasamoot S and Thuanboon S (2005). Chapter 25 Tanker Corrosion. *Handbook of Environmental Degradation of Materials,* edited Kutz M, William Andrew Publishing, Norwich, NY, USA.

[246] Wang X and Moan T (1994). Reliability analysis of production ships. *International Journal of Offshore and Polar Engineering,* 4(4): 302-311.

[247] Wang X and Moan T (1996). Stochastic and deterministic combinations of still water and wave bending moments in ships. *Marine Structures,* 9: 787-810.

[248] Wang X, Jiao G and Moan T (1996). Analysis of oil production ships considering load combination, ultimate strength and structural reliability. *Transactions of the Society of Naval Architects and Marine Engineers,* 104: 3-30.

[249] Watson GS (1954). Extreme values in samples from m-dependent stationary stochastic processes. *Annals of Mathematical Statistics,* 25: 798-800.

[250] Wen YK (1977). Statistical combination of extreme loads. *Journal of the Structural Division,* 103(ST5): 1079-1093.

[251] Whitman R (1984). Evaluating calculated risk in geotechnical engineering. *Journal of Geotechnical Engineering,* 110(2):145-188.

[252] Wierzchowski EP (1971). *Statistical investigation of the sectional dimensions of ship structural members (in Polish).* In: Research Report No. 018-BR/BW3-71, Ship Design and Research Center, Gdansk, Poland.

[253] Wirsching PH, Ferensic J and Thayamballi AK (1997). Reliability with respect to ultimate strength of a corroded ship hull. *Marine Structures,* 10(7): 501-518.

[254] www.cedre.fr

[255] www.itopf.com/information-services/data-and-statistics/statistics/index.html

[256] www.lloydsmiu.com

[257] Xu T, Bai Y, Wang M and Bea RG (2001). Risk based optimum inspection for FPSO hulls. *Proceedings of the Annual Offshore Technology Conference (OTC'01),* 115-124, Houston, TX, USA.

[258] Yamamoto N and Ikegami K (1996). A study on the degradation of coating and corrosion of ship's hull based on the probabilistic approach. *Proceedings of the International Offshore Mechanics and Arctic Engineering Symposium (OMAE'96)* 2: 159-66.

[259] Yamamoto N and Ikegami K (1998). A study on the degradation of coating and corrosion of ship's hull based on the probabilistic approach, *Journal of Offshore Mechanics and Arctic Engineering,* 120: 121-128.

[260] Yao T, Fujimoto M, Yanagihara D, Varghese B and Niho O (1998). Influences of welding imperfections on the buckling/ultimate strength of ship bottom plating subjected to combined bi-axial thrust and lateral pressure, *2nd International Conference on Thin-Walled Structures,* 425-432.